H24/3622

MONASH UNIVERSITY

THESIS ACCEPTED IN SATISFACTION OF THE
REQUIREMENTS FOR THE DEGREE OF
DOCTOR OF PHILOSOPHY

ON..... 23 March 2004 .....

.....[redacted].....

Sec. Research Graduate School Committee

H124/3622

Page 54, Section 2.12.2, following 2nd paragraph
Insert '45 µl of the soluble fraction and 6.25 µl of the insoluble fraction were loaded onto the gel'.
These volumes represent equal proportions of these samples and therefore Pf332 is both soluble and insoluble in TX100.

Page 83, Figure 3.3, Panel B and C.
The smaller bands are likely to be breakdown products of the full length fusion protein. These bands are detected with both Coomassie Brilliant Blue staining and immunoblot analysis using an anti-MBP antisera and are likely to consist of MBP plus varying portions of the PfEMP3 fusion. The bottom band in lane 1 is likely to be breakdown of the MBP-FIa fusion to the more stable MBP. Without the LacZ portion, which is fused to MBP with expression from pMAL vectors, MBP runs at approximately 43 kDa. This band was therefore not expected to bind IOVs and as shown in Figure 3.4b (lane 3, page 84), binding was not detected.

Page 70, Section 3.6.2, and Figures 3.9, 3.10 and 3.14.
Although there were faint bands detected in lanes 5 and 7 in Figure 3.14, indicating low level binding of PfEMP3Δ29 and Δ45 to spectrin, these bands were not detected consistently across a number of interactions and were not seen in Figure 3.10 for binding of these fragments to IOVs. In addition, the difference in the levels of binding between PfEMP3Δ15, and PfEMP3Δ29 and Δ45 were not consistent with the difference in levels of purified protein seen in Figure 3.9. These points, along with the IAsys data indicate that PfEMP3Δ29 and Δ45 do not bind spectrin.

Page 75, 4th line from the bottom
Insert the word 'of' between 'presence' and 'adjacent'

Page 77, 2nd paragraph
Delete last sentence 'The reproducibility of the results'.Chapter 3. Specificity of the interaction between PfEMP3 and purified spectrin, including discussion of a competition experiment involving a synthetic peptide.
Insert text into Section 3.10, page 77, following 1st paragraph.

A number of experiments performed as part of this study indicate a specific interaction between the spectrin binding domain of PfEMP3. These include the lack of binding to spectrin observed for the BSA negative control and for the different regions of PfEMP3 (Section 3.7.2), along with the ability to delete the spectrin binding domain from a PfEMP3 fragment (Section 3.7.4). In addition, the data obtained using the IAsys system showed an interaction between PfEMP3 and spectrin that is saturable (see Nunomura *et al.*, 1997 for determination of the saturation curves using the IAsys system as referenced in Section 2.20) and binding affinities that are comparable to other interactions at the membrane skeleton (discussed on page 76-77). This, along with the known location of both spectrin and PfEMP3 at the membrane skeleton, was considered strong evidence towards a real and likely specific interaction. A competition experiment with a synthetic peptide was considered worthwhile, as was the addition of a synthetic peptide to infected and uninfected erythrocytes (discussed on page 79), however, it was decided to pursue the identification of the PfEMP3 binding domain within spectrin (Chapter 4) as a higher priority given the limited time available within the time frame of the Australian PhD program.

Chapter 3. Presentation of the PfEMP3 amino acid sequence and discussion of the interacting residues.
Integrate text into Section 3.10, page 78, 4th paragraph.

The amino acid sequence for the PfEMP3 gene is published as part of the chromosome 2 sequence (Gardner *et al.*, 1998, accession number NC_000910). The 60 residue binding domain of PfEMP3 for the erythrocyte membrane skeleton is FTVVKNYNKIDNVYN**IFEIRLKRSLAQVL**GNTRLSSRGVRDPRTKEALKEKQFRDHKRKE where the 14 residue binding domain is represented by the bold type. The 60 residue binding domain contains no regions of hydrophobicity and is non repetitive. The charge of the 14 residue binding domain is discussed briefly on pages 78 and 149. A number of binding domains of malarial proteins have been predicted to form an amphipathic α-helical structure (discussed on page 149), however the 14 residue binding domain of PfEMP3 does not form this structure as shown by the helical wheel or helical network plots (Figure A1). Motif searches with both the 60 and 14 residue binding domains using InterProScan through the European Bioinformatics Institute (www.ebi.ac.uk) (Robert Flegg, Victorian Bioinformatics consortium, personal communication) did not reveal any known motifs within these domains.

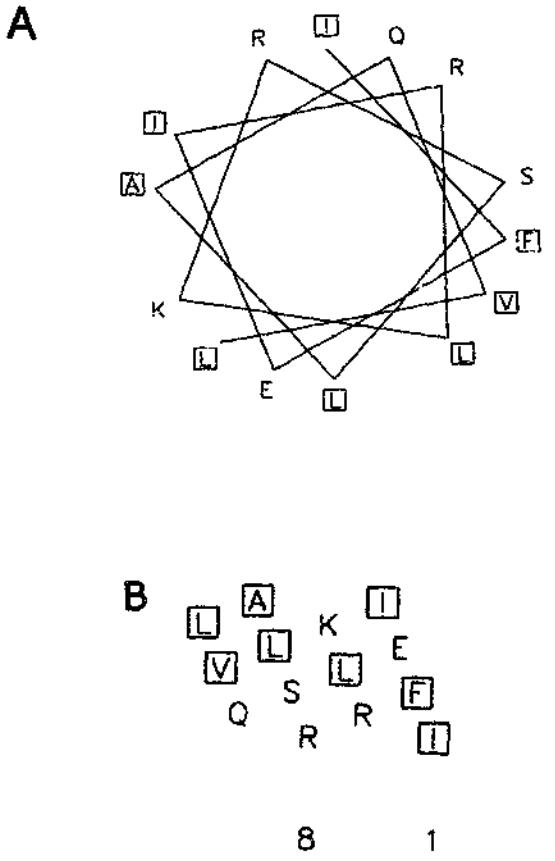

Figure A1. Helical Wheel Plot and Helical Network Plot of the PfEMP3 14 residue binding domain.
Structural proteins can contain amphipathic α-helices, which consist of hydrophobic, non-polar residues on one side of the helix and hydrophilic and polar residues on the other side. Two ways of visualising an amphipathic helix are the helical wheel plot and the helical network plot. The helical wheel gives a view of a helix looking down the axis of the helix, whereas the helical network plot give a view of a helix that has been slit open and folded out flat.

A. The 14 residue binding domain represented as a helical wheel plot. Although one face of the helix appears to consists of majority hydrophobic residues (boxed), the residues of the 14 residue domain do not arrange with the hydrophobic residues all on one side and the hydrophilic residues on the opposing side.

B. The 14 amino acid domain represented as a helical network plot. The residues do not arrange in diagonal lines (/ direction) as either hydrophobic residues (boxed) or hydrophilic residues, indicating that each face of the helix formed by the 14 residue binding domain would not be either exclusively hydrophobic or hydrophilic.

Together these plots indicate that the PfEMP3 14 residue binding domain does not form an amphipathic α-helical structure.

Chapter 4. Degradation of GST-Spectrin fusion proteins.
Insert text into Section 4.8, page 108, following 1st paragraph.

The degradation products in the purified GST-Spectrin protein preparations are not thought to interfere with the identification of binding domains for malarial proteins. Although pure, full length fusion proteins would be ideal, it is our experience that some proteins express poorly. Due to the large number of proteins expressed during the course of this study, it was not feasible to repeatedly repurify proteins to obtain a higher proportion of full-length protein. Experience has shown us that binding can be demonstrated using protein preparations that contain a low proportion of full length protein. For example, Chapter 3 identified a binding domain for spectrin within MBP-PfEMP3-FI (Figure 3.1a, lane 2) and Waller *et al.*, 1999 showed binding of GST-KAHRP-F1 to VARC, although both of these protein preparations showed low proportions of full length protein. In the past, following their identification, binding fragments were commonly sub-fragmented to further define the binding domain. These sub-fragments often purify with a large proportion of full length protein, thereby eliminating any concern over the degradation products. This was not performed in this study due to the wide spread binding of the spectrin fragments.

Figure 5.3.
Page 137, Replace figure.

Figure 5.3. Triton X-100 Extraction of Pf332 from Parasitised Erythrocytes
Immunoblot analysis of Triton X-100 samples detected using anti-Pf332 antiserum. Samples are 3D7 (lane 1), Triton X-100 insoluble (lane 2) and Triton X-100 soluble (lane 3). In each sample a band thought to be Pf332 (arrow) resolved at well above the 250 kDa marker. A number of smaller products are also detected.

Chapter 5. Referencing.
Integrate into the text in Section 5.2.1, page 119.

Accession number M55282 referenced to **Kun, J., Hesselbach, J., Schreiber, M., Scherf, A., Gysin, J., Mattei, D., Pereira da Silva, L., Muller-Hill, B.** (1991) Cloning and expression of genomic DNA sequences coding for putative erythrocyte membrane-associated antigens of *Plasmodium falciparum*. *Research in Immunology*, **142**, 199-210.

Page 123, line 10
Replace word 'lightly' with 'slightly'.

Page 123, line 11
Replace 'lane 20' with 'lane 10'.

Page 123, 4th line from the bottom
Replace 'E3' with 'E1'.

Chapter 5. Hydrophopic regions
The N-terminal hydrophobic region of Pf332 is 23 amino acids and the C-terminal hydrophobic region is 15 amino acids. Therefore replace the following text.

Page 128, 8th line from the bottom, replace "approximately 10-20" with "23 amino acids". Page 128, 2nd line from the bottom, replace "small region" with "15 amino acid region".

Page 137, Figure 5.3.
The band well above the 250 kDa marker in lane 3, which has no equivalent in lanes 1 and 2, is thought to be a cross reactive protein that is only found in the insoluble pellet. It may be that the TX100 solublisation led to the concentration of this protein and therefore clear visualisation within this sample. Alternatively, this protein may be a soluble breakdown product that is formed during the manipulations required for solublisation and is therefore not present in the 3D7 sample (lane 1).

Interactions of *Plasmodium falciparum* Proteins at the Membrane Skeleton of Infected Erythrocytes

Lisa Marie Stubberfield

BSc (Biomedical) (Hons)

A thesis submitted as a requirement for the degree of Doctor of Philosophy under the supervision of

Prof. R. L. Coppel

and

Dr. B. M. Cooke

Department of Microbiology
Monash University
Melbourne, Australia
October 2003

Table of Contents

List of Tables and Figures

Chapter 1 – Introduction

Chapter 2 – Materials and Methods

Chapter 3 - Mapping Domains in PfEMP3 That Bind to the Erythrocyte Membrane Skeleton

Chapter 4 - Mapping the Spectrin Domains that Bind PfEMP3

Chapter 5 - Mapping the Domains of Pf332 that Bind to the Erythrocyte Membrane Skeleton

Statement of Authorship

This thesis contains no material that has been accepted for the award of any other degree or diploma in any University and, to the best of my knowledge and belief, contains no material previously published or written by another person, except where due reference is made in the text of this thesis.

[redacted]

Lisa Marie Stubberfield

Summary

P. falciparum infected erythrocytes undergo cellular, mechanical and adhesive modifications known to be associated with the pathogenesis of malaria. During parasite development, parasite proteins are exported to the erythrocyte membrane where they become inserted into the membrane or associated with the membrane skeleton. A complete characterisation of these proteins and the erythrocyte proteins with which they interact is important for a better understanding of the molecular basis for these modifications and for a more complete understanding of the pathogenesis of malaria. This thesis describes the interactions of two *P. falciparum* exported proteins, PfEMP3 and Pf332, with the erythrocyte membrane skeleton.

Prior to this study, virtually nothing was known of the function of either PfEMP3 or Pf332 and no specific interactions involving these proteins with the erythrocyte membrane skeleton had been described. Here, we have shown for the first time that a 14 residue domain encoded near the N-terminus of PfEMP3 is responsible for binding to the erythrocyte membrane skeleton through specific interactions with spectrin and actin. An additional domain encoded near the C-terminus of PfEMP3 is also mediates binding to the erythrocyte membrane skeleton, however, the erythrocyte protein responsible for this interaction has not yet been identified. Quantification by resonant mirror detection showed strong interactions when compared to previously described interactions for erythrocyte proteins and other well characterised exported malaria proteins.

To date, a number of interactions with malaria proteins have been described that involve spectrin, including KAHRP, RESA, PfEMP1 and MSP1. However, the domains in spectrin responsible for mediating binding to these proteins have yet to be identified. Here we describe the interaction between PfEMP3 and the CH2 domain of β-spectrin and the repeat regions of both α- and β-spectrin. Quantitative and qualitative analysis of these interactions depicts a complex interaction involving multiple binding domains within the spectrin molecule.

Using membranes prepared from infected erythrocytes as a tool, we have identified the first reported malaria protein that appears to bind poorly to the erythrocyte membrane from uninfected erythrocytes, but is able to bind membranes prepared from infected erythrocytes. The interaction identified between Pf332 and membranes purified from infected erythrocytes is mediated by two binding domains encoded near either end of the protein, each containing one of the two hydrophobic regions of Pf332. Analysis of the protein composition of pIOVs prepared in this study show the presence of proteins of parasite origin, including exported malaria proteins

and proteins contained within the parasite itself, making it difficult to speculate on the interacting partner for Pf332 in the infected erythrocyte.

Overall our studies have led to a better understanding at the molecular level of how the membrane skeleton in malaria infected erythrocytes is modified. Additionally, we have identified novel protein-protein interactions in malaria-infected erythrocytes that may offer previously unthought of targets that could be the basis of novel antimalarial therapeutic strategies.

Acknowledgments

I would like to extend my sincere gratitude to my supervisors, Ross Coppel and Brian Cooke. Thankyou for always challenging me and instilling a sense of independence and self-belief. I appreciate the opportunities that you have provided to me and wish to thank you for your scientific input and encouragement.

To Tony Mason and Biota Holdings Ltd., thankyou for having enough faith in my abilities to fund this project. To my collaborator Wataru Nunomura, thankyou for the fantastic data and to Xuili An, thankyou for answering my constant questions and for the speedy and constant supply of clones

To my unofficial supervisor, Karena Waller, I wish to extend my heartfelt thanks. Your input from New York was often the easiest to obtain and for this, I thankyou. Your help and contribution, especially over the past six months, has been invaluable and your friendship over the past five years has made the science just a little easier.

Thankyou to Fiona Glenister for the walks and the talks and most importantly, thanks for being on my side, unconditionally. It takes a very special person to give that sort of support and I hope that I can give you a fraction of the support you have given me.

I wish to thank Sheena McGowan for her unwavering patience over the past five years. Your ability to listen to my problems, when you had problems of your own, did not go unnoticed. Thankyou for helping to broaden my horizons by sharing a fantastic holiday with me and just for being the greatest friend.

To Vicki Adams, thankyou for the extensive conversations and for telling it like it is. Both personally and scientifically, your support has been unwavering.

I would like to extend deepest my gratitude to the morning tea crew, both past and present, in particular Milena Awad, Dena Lyras, Lina Laskos, Ishara Gunesekere, Natasha Pincus, Kylie Farrow, Grant Jenkin, Jackie Cheung, Priscilla Johanesen and Catherine Ryan. Thankyou for letting me into your lives and giving me advice on everything from food and clothes to DNA and proteins. I look forward to more weddings, christenings, house warmings and lunches at Chady. You know it has been lovely!

I would also like to thank the members of the Coppel Lab, both past and present for your friendship and support. Also to other members of the department who have made contributions to this project. This wouldn't have happened without the assistance of you all.

I also wish to thank my undergraduate friends. This extended group has always been there, often experiencing all the same ups and downs. I am looking forward to sharing the process of 'getting on with the rest of our lives' with you guys, it is going to be great!

I would also like to thank my family. Mum for the long phone conversations and for always knowing what was going on, and to Dad, Jude and Mike, and Michael and Jodie for supporting me by having no idea what was going on. I have needed support in all kinds of ways and the escape 'home' has been one of my greatest comforts. To my lovely Grandma and Granma, I haven't cured it yet, but we may have got a little closer. To my dearest Grandad and Poppy, I know you would have been so proud.

Finally, I need to thank my strongest supporter. Thankyou Mick for always being there, for being understanding when I wasn't home and I put my PhD first and that I was constantly grumpy. I love you babe.

Acronyms and Abbreviations

α	alpha
A_{260nm}	Absorbance at 260 nm
A_{600nm}	Absorbance at 600 nm
aa	amino acid
ABRA	acidic basis repeat antigen
AE1	Anion exchange protein 1; band 3
Ag332	Antigen 332, Pf332
ATP	Adenosine Triphosphate
β	beta
bp	base pair
BSA	Bovine Serum Albumin
ddH_20	double distilled water
cAMP	cyclic adenosine monophosphate
cbd3	cytoplasmic domain of band 3
CD36	Cluster Determinant 36
cDNA	complimentary Deoxyribonucleic Acid
CH	calponin homology
CIDR	Cysteine-rich Inter-Domain Region
Clag	Cytoadherence-Linked Asexual Gene
cm	centimetre
$CPDA_1$	Citrate Phosphate Dextrose Adenine
°C	degrees Celsius
Δ	delta, indicates deletion of a specific region of DNA
DBL	Duffy Binding-Like
DEAE	diethylaminoethyl
DNA	Deoxyribonucleic Acid
dNTP	Deoxynucleotide Triphosphate
dsDNA	double stranded Deoxyribonucleic Acid
DTT	Dithiothreitol
EBA-140	Erythrocyte Binding Antigen-140
EBA-175	Erythrocyte Binding Antigen-175
EDTA	Ethylenediaminetetra-acetic acid
ER	Endoplasmic reticulum
G3PD	glyceraldehyde-3-phosphate dehydrogenase
G6PD	glucose-6-phospahte dehydrogenase
GST	Glutathione S-Transferase
GPA	Glycophorin A
GPB	Glycophorin B
GPC	Glycophorin C
GPD	Glycophorin D
GPE	Glycophorin E
GPC/D	Glycophorin C/D
HE	Hereditary Elliptocytosis
HEPES	N-2-hydroxyethylpiperazine-N'-2-ethanesulfonic acid
HPP	Hereditary Pyropoikilocytosis
hr	hour
HRP	Horseradish peroxidase
HRPII	
HS	Hereditary Spherocytosis
ICAM-1	Intercellular Adhesion Molecule-1
IgM	Immunoglobulin M
IOV(s)	Inside-out vesicle(s)
IPTG	Isopropyl-1-thio-β-galactopyranoside
KAHRP	Knob-Associated Histidine-Rich Protein
kb	kilobase
K_a	association rate constant
K_d	dissociation rate constant
$K_{(D)kin}$	dissociation constant by kinetic analysis
$K_{(D)Scat}$	dissociation constant by Scatchard analysis

kDa	kilodalton
kPa	kilopascal
λ	bacteriophage lambda
l	litre
***lac*Z**	β-galactosidase gene
LB	Luria-Bertani medium
M	molar
$M^{-1}sec^{-1}$	per Mole per second
MAGUKs	Membrane-Associated Guanylate Kinase Homologues
MESA	Mature-parasite-infected Erythrocyte Surface Antigen
µg	microgram
µl	microlitre
µM	micromolar
mg	milligram
mm	millimeter
ml	millilitre
mM	millimolar
min	minute
mRNA	messenger Ribonucleic Acid
MSP1	Merozoite Surface Protein 1
ND	not determined
ng	nanogram
NIH	National Institutes of Health
nm	nanometre
O/N	overnight
PAGE	Polyacrylamide Gel Electrophoresis
PBS	Phosphate Buffered Saline
PCR	Polymerase Chain Reaction
PDZ	PSD-95/Discs large/ZO-1
PEG	Polyethylene Glycol
Pf332	*P. falciparum* antigen 332
PfEMP1	*P. falciparum* Erythrocyte Membrane Protein 1
PfEMP3	*P. falciparum* Erythrocyte Membrane Protein 3
pH	log $[H^+]$ at 25 °C
PMSF	Phenyl methyl sulfonyl fluoride
PVDF	Polyvinylidene Diflouride Transfer Membrane
PVM	Parasitophorous vacuolar membrane
RESA	Ring-infected Erythrocyte Surface Antigen
rif	repetitive interspersed family gene family
RNA	Ribonucleic Acid
RT	room temperature
s	second
SAB	Spectrin-actin binding
SAO	Southeast Asian Ovalocytosis
ssDNA	single stranded Deoxyribonucleic Acid
sec^{-1}	per second
SDS	Sodium dodecyl sulphate
SH3	scr Homology 3 domain
TAE	Tris acetate ethylenediaminetetra-acetic acid buffer
TBS	Tris-buffered saline
TEMED	N,N,N',N'-tetramethylethylenediamine
Tris	Tris [hydroxymethyl] aminomethane
TVM	Tubovesicular Membrane network
Tween 20	Polyoxyethylene(20) sorbitan monolurate
var	variant genes encoding PfEMP1
v/v	volume per volume
w/v	weight per volume
WEHI	Walter and Eliza Hall Institute of Medical Research
g	gravity
X-gal	5'-Bromo-4-chloro-3-indolyl-β-D-galactopyranoside

Chapter 1 - Introduction

1.1 Malaria

1.1.1 Epidemiology of Malaria

Malaria is a blood borne disease caused by infection with protozoan parasites of the genus *Plasmodium* and is transmitted by the female *Anopheles* mosquito. Four species of *Plasmodium* infect humans; *P. falciparum, P. vivax, P. malariae* and *P. ovale*. Of these four species, *P. falciparum* causes the most severe disease and accounts for almost all the mortality associated with human malaria infection. In addition to the *Plasmodium* species that infect humans, many more species infect a variety of other hosts. A number of these, such as the murine and monkey malarias are used as animal models of human infections (for reviews see Landau and Gautret, 1998; Gysin, 1998). The development of *in vitro* culture methods for *P. falciparum* (Trager and Jensen, 1976; Trager and Jensen, 1978) has facilitated extensive research on these parasites during the last 25 years.

More than 40% of the world's population is at risk of malarial infection, with mainly those in the world's poorest countries affected. Malaria causes between 10-300 million cases of acute illness and up to 2.5 million deaths annually (Breman, 2001). It is estimated that well over 75% of these deaths occur in young children in sub-Sahara Africa (Breman, 2001).

1.1.2 Clinical features of Malaria

Uncomplicated malaria is characterised by headache, muscular discomfort, weakness and malaise, and periodic fever and chills. Severe complications of *P. falciparum* infection include cerebral malaria, jaundice, anaemia and enlargement of both the spleen and the liver, often resulting in death (for review see White and Ho, 1992).

1.1.3 Control of Malaria

The control and treatment of malaria relies on drugs, to which resistance is rapidly emerging. Resistance to chloroquine, sulfadoxine-pyrimethamine, mefloquine and quinine has developed, with multi-drug resistance emerging. Due to the problem of increasing drug resistance, certain drugs are being used selectively in areas, whereas others are using combination therapy in an effort to

reduce the development of resistance (for reviews see Trigg and Kondrachine, 1998; Winstanley, 2000).

Vector control programs are also vital in the control of malaria. Pesticide-treated mosquito nets have been shown to be successful at reducing transmission and along with other methods of vector control, may help to reduce the incidence of malaria (for review see Hougard *et al.*, 2002).

1.2 *The Lifecycle of* P. falciparum

P. falciparum undergoes a complex life cycle in both the mosquito vector and the human host (Figure 1.1). Sexual reproduction occurs in the mosquito, whereas the asexual reproduction occurs in the liver and erythrocytes of the human host. *P. falciparum* gametocytes are taken up by the mosquito when taking a blood meal. Following fertilisation, gametocytes attach to the mosquito gut wall and develop into an oocyst. Subsequently, sporogony results in the production of many thousands of sporozoites that migrate to the salivary glands of the mosquito. When taking the next blood meal, infected mosquitos inject haploid sporozoites into the peripheral blood of the human. These migrate immediately to the liver where they invade hepatocytes and develop into liver schizonts. After approximately fourteen days, liver schizonts rupture and release merozoites into the circulation where they invade circulating erythrocytes.

The erythrocyte stage of the life cycle consists of repeating cycles of asexual reproduction, each lasting 48 hours. Following invasion, merozoites develop into ring stage parasites. Over the following 24 hours, ring stage parasites mature into larger pigmented trophozoites parasites. During the next 12 hours, trophozoites develop into schizonts that lyse the erythrocyte releasing 8 to 32 merozoites into the blood stream. These merozoites invade other erythrocytes and continue the erythrocytic life cycle. During this part of the life cycle, merozoites can also differentiate into gametocytes by a complex and not fully understood process. Upon taking the blood meal, a mosquito ingests these gametocytes and the cycle between mosquitos and humans continues.

1.3 *The Normal Human Erythrocyte*

The human erythrocyte has been studied extensively and a great deal is known of its biochemical composition, structure and mechanical properties. Erythrocytes are biconcave discs 8 μm in diameter that must pass multiple times through capillaries that are only 2-3 μm in diameter, and therefore, must be able to reversibly deform (for review see Mohandas and Chasis, 1993). The erythrocyte membrane consists of a lipid bilayer and underlying membrane skeleton (Figure

1.2). The membrane skeleton is made up of many proteins, that can be divided into integral and peripheral proteins (for review see Lux and Palek, 1995). Features, interactions and organisation of some of the major integral and peripheral proteins are discussed below, including their importance in malaria infection.

1.3.1 Integral Membrane proteins

The major integral membrane proteins are band 3 and a group of proteins collectively termed glycophorins.

1.3.1.1 Band 3

Band 3, also known as the anion exchange protein 1 (AE1), is one of the most abundant proteins of the erythrocyte membrane, present at approximately 10^6 copies/cell (Steck, 1978). It is composed of two functionally and structurally independent domains (Lux *et al.*, 1989) and is able to form dimers, tetramers and higher order oligomers in solution (Casey and Reithmeier, 1991).

The C-terminal membrane domain consists of 12 to 14 transmembrane domains and is responsible for anion exchange (Kopito and Lodish, 1985). The N-terminal cytoplasmic domain (cdb3) is responsible for binding haemoglobin (Walder *et al.*, 1984), glycolytic enzymes (for review see Lux and Palek, 1995) and the membrane skeletal proteins ankyrin (Bennett and Stenbuck, 1980a; Hargreaves *et al.*, 1980), protein 4.1 (Pasternack *et al.*, 1985) and protein 4.2 (Korsgren and Cohen, 1986). cdb3 is a highly flexible domain, with a proposed 'hinge' region that is thought to facilitate pH-dependent conformational changes (Low *et al.*, 1984; Thevenin *et al.*, 1994). Recent crystal structure analysis of this domain revealed 11 β-strands and 10 α-helices, collectively forming a large globular domain and dimerisation arm connected by a short helix and loop segment (Zhang *et al.*, 2000).

Ankyrin (see Section 1.3.2.4) predominantly binds to the tetrameric form of band 3 and has been reported to bind to a number of regions within cdb3 (Willardson *et al.*, 1989). Recent studies suggest that the binding domain for ankyrin is confined primarily to a β-hairpin loop encoded by residues 175 to 185 of cdb3 and that blocking of ankyrin binding to band 3 by antibodies to the N-terminus of cdb3 is a result of steric hindrance (Chang and Low, 2003). Crystal structure analysis of cdb3 reveals proximity within the band 3 tetramer of the β-hairpin loop from one dimer, with the N-terminal from the second dimer (Zhang *et al.*, 2000). This suggests binding of ankyrin to both proposed regions within cdb3 (Zhang *et al.*, 2000) and steric hindrance of ankyrin binding to the β-hairpin loop by antibodies to the N-terminus, are both feasible hypotheses (Chang and Low, 2003).

Protein 4.1 (see Section 1.3.2.3) binds to band 3 through the I/LRRRY motif within cdb3 (Jons and Drenckhahn, 1992). Dissociation of protein 4.1 by synthetic IRRRY peptides results in a decrease in membrane deformability of the erythrocyte membrane, indicating a role for this interaction in the modulation of membrane properties (An *et al.*, 1996). Other studies have suggested binding of protein 4.1 to the N-terminus of cdb3 (Lombardo *et al.*, 1992). Crystal structure analysis indicates simultaneous binding of protein 4.1 to the I/LRRRY motif and the N-terminus of cdb3 is feasible in both monomers and dimers (Zhang *et al.*, 2000), however, it has been reported that the binding of protein 4.1 is predominantly to the tetramic form of band 3 (von Ruckmann *et al.*, 1997). Interactions with the band 3 tetramer is likely to result in competition with the ankyrin binding site (Zhang *et al.*, 2000). In support of this, competition between the binding of ankyrin and protein 4.1 has been reported in previous biochemical studies (Lombardo *et al.*, 1992; An *et al.*, 1996).

Less well characterised interactions involve the interaction of cdb3 and protein 4.2 (see Section 1.3.2.6.5) and the interaction of band 3 and glycophorin A (see Section 1.3.1.2). The interaction between protein 4.2 and cdb3 is thought to strengthen the band 3-membrane skeleton linkage (Rybicki *et al.*, 1996) and may be modulated by the presence of ankyrin (Rybicki *et al.*, 1995a). The interaction of glycophorin A and band 3 has not been mapped to a specific domain of band 3 (Bruce *et al.*, 1995; Nigg *et al.*, 1980), however this interaction is thought to be involved in both trafficking of these proteins to the membrane and the anion transport activities of band 3 (Young *et al.*, 2000; Young and Tanner, 2003; Hassoun *et al.*, 1998).

Band 3 is modified and may undergo changes in levels of phosphorylation in erythrocytes infected with malaria parasites (Section 1.4.1.4) (Crandall and Sherman, 1991; Crandall and Sherman, 1994; Murray and Perkins, 1989). In addition, band 3 has recently been identified as a receptor for merozoite protein 1 (MSP1), an interaction that is important in merozoite invasion of erythrocytes (Goel *et al.*, 2003) and for acidic basic repeat antigen (ABRA), which associates with the merozoite surface at the time of schizont rupture (Kushwaha *et al.*, 2002)

1.3.1.2 Glycophorins

Five glycophorins (GP) have been described in erythrocytes, GPA, GPB, GPC, GPD and GPE. Glycophorins each consist of a single transmembrane domain with an exterior N-terminal domain and interior C-terminal domain (for review see Chasis and Mohandas, 1992). The erythrocyte glycophorins can be divided into two subgroups. The first group includes the GPA and GPB, which are present in the

erythrocyte at $9x10^6$ and $3x10^5$ copies/cell, respectively. This group is thought to arise from a common ancestral gene and share large regions of homology. This group also includes GPE, but as yet, no evidence exists for protein translation of the GPE gene. The second group includes GPC and GPD ($1x10^5$ and $0.2x10^5$ copies/cell, respectively), which are encoded by a single gene and show no structural homology to GPA, GPB and GPE. GPD contains a truncated N-terminal domain but is otherwise identical to GPC (for review see Chasis and Mohandas, 1992). Glycophorins contribute 60% of the overall negative charge of the erythrocyte surface due to their high sialic acid content and are involved in minimising the agglutination of erythrocytes by electrostatic repulsion (for review see Chasis and Mohandas, 1992).

GPA is involved in ligand binding and modulation of erythrocyte membrane mechanical properties (Chasis *et al.*, 1988; Chasis *et al.*, 1991). GPA is thought to bind band 3 (Bruce *et al.*, 1995; Nigg *et al.*, 1980) resulting in a number of physiological consequences. These include enhancing the trafficking of band 3 to the membrane by the C-terminal cytoplasmic domain of GPA and the increase in specific anion transport activities of band 3, facilitated by the interaction of residues 68-70 within the extracellular domain (Young and Tanner, 2003). Glycophorin A also binds protein 4.1, providing a link to the cytoskeleton (Anderson and Lovrien, 1984; Anderson and Marchesi, 1985).

GPC is thought to play a role in the regulation of cell shape and membrane mechanical properties however, little is known of the function of GPD. It has been established that the cytoplasmic domain of GPC and GPD (GPC/D) binds protein 4.1 though a 12 residue region near the N-terminus (Marfatia *et al.*, 1994) and binds p55 Section 1.3.2.5) through residues 112-128 (Marfatia *et al.*, 1995).

Glycophorins are important in binding of ligands responsible for mediating invasion of erythrocytes by malaria parasites. GPA, GPC and GPB are thought to mediate invasion of erythrocytes in a sialic acid-dependent manner. GPA is able to mediate invasion through an interaction with the *P. falciparum* erythrocyte binding antigen 175 (EBA-175) (Sim *et al.*, 1994), whereas GPC is able to mediate invasion through an interaction with a homologue of EBA-175; EBA-140 (Maier *et al.*, 2003; Lobo *et al.*, 2003). GPB is also thought to mediate invasion through an interaction which does not involve EBA-175, however as yet, the malarial ligand involved in this interaction has not been identified (Dolan *et al.*, 1994).

1.3.2 Cytoskeletal Proteins

The cytoskeletal proteins of the membrane are responsible for much of the deformability and elasticity of the erythrocyte. The cytoskeletal proteins form a

meshwork under the lipid bilayer and interact at what is termed the junctional complex. Cytoskeletal proteins form links with the bilayer through interactions with integral membrane proteins (Figure 1.2). Features of the major cytoskeletal proteins of the erythrocyte; spectrin, actin and protein 4.1, along with many of the minor proteins are described below.

1.3.2.1 Spectrin

Spectrin is the major component of the erythrocyte membrane skeleton, present at approximately 10^5 tetramers/cell (Marchesi, 1974; Bennett, 1985) and consists of two structurally similar but functionally distinct polypeptide chains; α-spectrin and β-spectrin. The α- and β- subunits associate in a side-to-side, antiparallel manner to form heterodimers, which can associate in a head to head manner to form tetramers and higher order oligomers (Ralston *et al.*, 1977). The majority of each α- and β- polypeptide chain consists of 106 amino acid repeats, each forming a triple α-helical arrangement and interspersed with non-helical regions (Speicher and Marchesi, 1984; Yan *et al.*, 1993). The triple helical arrangement is due to formation of a hairpin by helices A and B, followed by a reverse turn of helix C to form the helical bundle. This structure is stabilised by both hydrophobic interactions and salt bonds formed between charged residues (Yan *et al.*, 1993).

α-spectrin is found only in erythrocytes, whereas β spectrin is also found in the brain and muscle. Two other spectrin-like genes have been found in humans; these encode α- and β-fodrin. Fodrin is found in most cells throughout the body with the exception of the erythrocyte (for review see Winkelmann and Forget, 1993). Also included in the spectrin superfamily are dystrophin and α-actinin which contain 106 amino acid repeats and N- and C- terminal regions found in spectrin and fodrin (for review see Dhermy, 1991).

1.3.2.1.1 α-spectrin

α-spectrin is encoded by a gene that spans 80 kb and encodes 52 exons whose sizes range from 18 bp to 684 bp. The size and the location of these exons do not correspond to the junctions between the 106 amino acid spectrin repeats (Kotula *et al.*, 1991). The translated polypeptide is 2429 residues in length and can be divided into 22 segments (Figure 1.3). Segments 1-9 and segments 11-19 are imperfect 106 amino acid spectrin repeats, whereas segment 10 shows sequence homology to *src* homology 3 (SH-3) domains. The N-terminus of the protein consists of an unpaired helix C involved in formation of tetramers, whereas the C-

terminus contains a region with similarity to the potential calcium-binding EF hands (Sahr *et al.*, 1990).

1.3.2.1.2 β-Spectrin

β-spectrin is encoded by a gene that consists of 32 exons ranging in size from 49 bp to 871 bp. As for α-spectrin, the exon boundaries of β-spectrin do not correspond to the 106 amino acid spectrin repeat junctions (Winkelmann *et al.*, 1990). The encoded polypeptide of 2137 residues consists of three distinct domains (Figure 1.3). The N-terminal domain is a 272 residue domain that consists of two calponin homology (CH) domains (Castresana and Saraste, 1995), so named after smooth muscle actin binding protein calponin. This region contains the actin binding domain (Karinch *et al.*, 1990) and shows homology to actin binding domains of α-actinin and dystrophin (Karinch *et al.*, 1990; Winkelmann *et al.*, 1990). The protein 4.1 binding domain is also within this region (Becker *et al.*, 1990; Cohen *et al.*, 1980).

The central domain consists of 17 imperfect 106 amino acid spectrin repeats (Winkelmann *et al.*, 1990), the 15th of which contains the ankyrin binding domain (Kennedy *et al.*, 1991). The first and second repeats, along with the N-terminal domain is involved in spectrin binding to adducin (Li and Bennett, 1996). It has also been reported that the first repeat has a role in the binding of spectrin to actin (Li and Bennett, 1996). The C-terminal domain contains four sites at which β-spectrin is phosphorylated (Harris and Lux, 1980). Phosphorylation of the β-spectrin chain can act to modulate membrane mechanical stability. Increased phosphorylation by membrane bound casein kinase decreases membrane mechanical stability, whereas decreased phosphorylation increases membrane mechanical stability (Manno *et al.*, 1995).

1.3.2.1.3 Formation of Spectrin Heterodimers, Tetramers and Oligomers

The assembly of spectrin in a side-to-side, antiparallel manner is facilitated by nucleation sites at the C-terminus of α-spectrin and the N-terminus of β-spectrin. The nucleation sites were initially mapped to the 106 amino acid repeats α18 to α21 and β1 to β4 (Speicher *et al.*, 1992). Not only do these repeats show highest similarity to four spectrin-like repeats within α-actinin, but three of these repeats contain an 8 bp insertion which is thought to be involved in the nucleation process (Speicher *et al.*, 1992; Viel and Branton, 1994). More recent evidence suggests that amino acid repeats α20 to α21 and β1 to β2 are sufficient for nucleation (Begg *et al.*, 2000).

Newly formed heterodimers exist in an open form, where the longer end of α-spectrin is free. The heterodimer can also exist in a closed form through the formation of a hairpin loop by interaction between α- and β-spectrin chains within the heterodimer, or through self association in a head to head fashion to form heterotetramers (Speicher *et al.*, 1993; DeSilva *et al.*, 1992). Both associations involve a coiled-coil association (Mehboob *et al.*, 2001) between the helix C at the N-terminal of α-spectrin and helices A and B of the β17 repeat at the C-terminal of β-spectrin (Speicher *et al.*, 1993).

Tetramers are the predominant form of spectrin present in the erythrocyte membrane skeleton (Ungewickell and Gratzer, 1978), where approximately 45-50% of the spectrin eluted from erythrocyte ghosts exists as tetramers, 5-10% as heterodimers and the remainder as oligomers and complexes of spectrin, actin, protein 4.1 and dematin (Liu *et al.*, 1984). It is thought that tetramers predominate over higher order oligomers due to a higher association rate required for formation of oligomers (Shahbakhti and Gratzer, 1986; Lofvenberg and Backman, 2001)

Spectrin tetramers exist in the cell as a coil. The 200 nm tetramers (Shotton *et al.*, 1979; Vertessy and Steck, 1989) condense by twisting around themselves to form an end-to-end distance of 76 nm (Vertessy and Steck, 1989). The native spectrin tetramer consists of a coil with 10 turns with a pitch of 7 nm and a diameter of 5.9 nm (McGough and Josephs, 1990). This coiling, along with local disassociation of tetramers to dimers accounts for much of the elasticity of the erythrocyte membrane skeleton (McGough and Josephs, 1990; An *et al.*, 2002).

1.3.2.1.4 Spectrin and Malaria

Upon infection of an erythrocyte with *P. falciparum*, spectrin undergoes changes in the level of phosphorylation (Murray and Perkins, 1989) and is able to be cleaved by plasmepsin II (Magowan *et al.*, 1998; Le Bonniec *et al.*, 1999) (Section 1.4.1.4). In addition, spectrin is able to bind ring-infected erythrocyte surface antigen (RESA/Pf155) (Foley *et al.*, 1991; Foley *et al.*, 1994), *Plasmodium falciparum* erythrocyte membrane protein 1 (PfEMP1) (Oh *et al.*, 2000), knob associated histidine rich protein (KAHRP/PfHRP1) (Kilejian *et al.*, 1991) and MSP1 (Herrera *et al.*, 1993). To date, the spectrin binding domains for these proteins have not been identified.

1.3.2.2 Actin

Erythrocyte actin is approximately 43 kDa and is present at about $5x10^5$ copies/cell (Branton *et al.*, 1981). Erythrocyte actin has many similarities to actin

found in non-erythroid cells (Tilney and Detmers, 1975; Nakashima and Beutler, 1979). In erythrocytes, globular actin (G-actin) polymerises to form short, defined actin filaments (filamentous actin (F-actin)) of approximately 13 monomers in length, visualised as 37 nm rod structures (Byers and Branton, 1985). Many actin binding proteins have been identified within the erythrocyte. These include spectrin (Karinch *et al.*, 1990), protein 4.1 (Becker *et al.*, 1990; Morris and Lux, 1995), dematin (Section 1.3.2.6.2) (Azim *et al.*, 1995) and tropomyosin (Fowler and Bennett, 1984; Mak *et al.*, 1987). The actin filament is capped at the slow growing end by tropomodulin and at the fast growing end by adducin, thus regulating filament length (Weber *et al.*, 1994; Kuhlman *et al.*, 1996).

Within malaria infected erythrocytes, actin is believed to bind KAHRP (Kilejian *et al.*, 1991), *P. falciparum* histidine-rich protein II (HRPII) (Benedetti *et al.*, 2003) and PfEMP1 (Oh *et al.*, 2000).

1.3.2.3 Protein 4.1

Protein 4.1 exists as either a 78 kDa or 80 kDa protein with approximately $2x10^5$ copies/cell (Branton *et al.*, 1981). Protein 4.1 contains four structural domains identified by proteolysis; 30 kDa, 16 kDa, 10 kDa and 22/24 kDa domains (Leto and Marchesi, 1984). There are two forms of protein 4.1 present in the erythrocyte, protein 4.1a and protein 4.1b (corresponding to the 78 kDa and 80 kDa polypeptides). Protein 4.1a is found in higher abundance in older erythrocytes as it is derived from protein 4.1b by gradual deamidation within the 22/24 kDa domain (Inaba *et al.*, 1992).

Protein 4.1 binds both spectrin and actin in the main ternary interaction within the erythrocyte membrane skeleton. This ternary interaction increases the strength of the otherwise weak interaction between spectrin and actin (Ungewickell *et al.*, 1979; Cohen and Foley, 1982; Ohanian *et al.*, 1984). The spectrin-actin binding region (SAB) within protein 4.1 has been mapped to the 10 kDa domain (Correas *et al.*, 1986), which is encoded by an alternatively spliced exon encoding the N-terminal 21 residues and a constitutive exon encoding the C-terminal 59 residues (Conboy *et al.*, 1988). The protein 4.1 binding domain for spectrin has been mapped to the N-terminal 14 residues encoded by the alternatively spliced exon and residues 37 to 43 of the constitutive exon (Gimm *et al.*, 2002; Horne *et al.*, 1993; Discher *et al.*, 1993; Schischmanoff *et al.*, 1995). An 8 residue region encoded by the constitutive exon is essential for binding of protein 4.1 to actin (Gimm *et al.*, 2002).

The interaction of protein 4.1 with spectrin and actin is modulated in several ways. Firstly, phosphorylation of protein 4.1 by either protein kinase C or cAMP-

dependent kinase results in both reduced promotion of spectrin binding to actin and reduced protein 4.1 binding to spectrin (Ling *et al.*, 1988; Eder *et al.*, 1986). In addition to this, the phosphorylation of SAB region of protein 4.1 by tyrosine kinase reduces the ability of protein 4.1 to promote the formation of the protein 4.1/spectrin/actin complex (Subrahmanyam *et al.*, 1991).

Furthermore, protein 4.1 30 kDa domain binds calmodulin in a Ca^{2+} independent manner. This complex is able to confer Ca^{2+} dependent sensitivity to the actin cross-linking activity of spectrin (Tanaka *et al.*, 1991). Interestingly, two binding sites for calmodulin have been identified, one of which is Ca^{2+} independent and the other Ca^{2+} dependent (Nunomura *et al.*, 2000b).

Protein 4.1 also interacts with the membrane to serve as an attachment site for spectrin. It is thought that attachment of protein 4.1 to the membrane is facilitated by a ternary interaction between protein 4.1, p55 and GPC/D. Protein 4.1 binds to p55 and to GPC/D within the 30 kDa domain (Marfatia *et al.*, 1995; Hemming *et al.*, 1995). The binding domain for p55 has been mapped to a 33 residue region encoded by exon 10 and the binding domain for GPC/D to a 73 residue region encoded by exon 8 (Nunomura *et al.*, 2000a). GPC/D also binds to p55 (Marfatia *et al.*, 1995; Hemming *et al.*, 1995), resulting in a ternary interaction. This ternary interaction is modulated by the binding of calmodulin to protein 4.1 in a Ca^{2+} dependent manner. In addition, the binding of protein 4.1 to p55 modulates the formation of the p55/GPC interaction (Nunomura *et al.*, 2000a). Protein 4.1 has also been shown to bind GPA (Anderson and Lovrien, 1984; Anderson and Marchesi, 1985).

Protein 4.1 also interacts with band 3 (Pasternack *et al.*, 1985) through a 5 residue region, LEEDY, at position 37-41 within the 30 kDa domain (Jons and Drenckhahn, 1992). It has been suggested that this interaction is not involved in attachment of the junctional complex to the lipid bilayer, rather it is involved in the modulation of band 3 binding to ankyrin (An *et al.*, 1996; Workman and Low, 1998). This interaction is modulated by the phosphorylation of protein 4.1 by protein kinase C, but not by the phosphorylation by cAMP-dependent kinase (Danilov *et al.*, 1990).

The crystal structure of the 30 kDa domain has been determined and consists of a cloverleaf-like architecture. Each lobe of the cloverleaf contains the binding domain for one of p55, GPC or band 3, whereas the central region contains the calmodulin binding domains (Han *et al.*, 2000). Within the malaria infected erythrocyte, mature parasite infected erythrocyte surface antigen (MESA) binds to protein 4.1 (Lustigman *et al.*, 1990; Coppel, 1992; Bennett *et al.*, 1997). The protein 4.1 binding domain for MESA overlaps with the p55 binding domain and

in vitro can interfere with the protein 4.1-p55 interaction (Waller *et al.*, 2003). Protein 4.1 can also be cleaved by the parasite protease, falcipain-2 and possibly plasmepsin II (Raphael *et al.*, 2000; Dua *et al.*, 2001; Deguercy *et al.*, 1990) and is additionally phosphorylated within the malaria infected erythrocyte (Lustigman *et al.*, 1990; Chishti *et al.*, 1994; Magowan *et al.*, 1998).

1.3.2.4 Ankyrin

Erythrocyte ankyrin is a 210 kDa protein that is present at approximately 10^5 copies/cell (Lux and Palek, 1995). Ankyrin interacts with band 3 (Bennett and Stenbuck, 1980a; Hargreaves *et al.*, 1980) and with the β-subunit of spectrin (Luna *et al.*, 1979; Yu and Goodman, 1979; Bennett and Stenbuck, 1979), linking the membrane skeleton with the lipid bilayer. Ankyrin is also able to bind protein 4.2 (Korsgren and Cohen, 1988). Ankyrin consists of three domains, a 89 kDa band 3-binding domain (Davis and Bennett, 1990) which consists of 24 consecutive 33 residue ANK repeats (Lux *et al.*, 1990; Lambert *et al.*, 1990), a 62 kDa spectrin binding domain (Davis and Bennett, 1990) and a C-terminal regulatory domain, that can be alternately spliced to enhance or diminish binding of ankyrin to Band 3 and possibly to spectrin (Davis *et al.*, 1992).

The N-terminal 70 residues of the 62 kDa domain are crucial for spectrin binding (Davis and Bennett, 1990), however a more recent report suggests that this region is not sufficient for binding and that residues 1101-1192 are important for ankyrin binding to spectrin (Platt *et al.*, 1993). The band 3 binding domain has been localised to repeats 7-12 and repeats 13-24 of the 89 kDa domain (Michaely and Bennett, 1995). Within malaria infected erythrocytes, KAHRP has been shown to bind ankyrin within both the 89 kDa band 3 binding domain and the 62 kDa spectrin binding domain (Magowan *et al.*, 2000). In addition, ankyrin is able to bind two members of the *P. falciparum* acyl-CoA synthetase (PfACS) family (Tellez *et al.*, 2003). Ankyrin may also undergo changes in levels of phosphorylation (Murray and Perkins, 1989) and can be cleaved by falcipain-2 in malaria infected erythrocytes (Raphael *et al.*, 2000; Dua *et al.*, 2001).

1.3.2.5 p55

p55 was originally co-purified with dematin from erythrocytes (Husain-Chishti *et al.*, 1989) and was subsequently discovered to be a member of the family of signalling and cytoskeletal proteins termed membrane-associated guanylate kinase homologues (MAGUKs) (Ruff *et al.*, 1991). p55 is present at $8x10^4$ copies/cell (Lux and Palek, 1995) and contains multiple domains. These include a

PDZ (PSD-95/Discs large/ZO-1) domain (Kim *et al.*, 1996), a domain containing a SH-3 motif (Ruff *et al.*, 1991) and a guanylate kinase-like domain (Goebl, 1992).

Within the erythrocyte, p55 forms a ternary complex with protein 4.1 and GPC/D (Alloisio *et al.*, 1993). The GPC/D binding domain within p55 is located within the PDZ domain (Marfatia *et al.*, 1997), whereas the protein 4.1 binding site has been mapped to a 39 residue motif located between the SH-3 and guanylate kinase-like domains (Marfatia *et al.*, 1994; Marfatia *et al.*, 1995). Within the malaria parasitised erythrocyte, the binding domain of MESA for protein 4.1 overlaps with the binding domain for p55 and interferes with the interaction of p55 with protein 4.1 (Waller *et al.*, 2003).

1.3.2.6 Other Erythrocyte Cytoskeletal Proteins

A number of additional proteins are found within the membrane skeleton. These proteins have not been reported to interact with any malaria proteins in infected erythrocytes. However, they are important in maintenance of the structure of the membrane skeleton and will be discussed briefly in terms of their function and protein interactions.

1.3.2.6.1 Adducin

Adducin is located at spectrin-actin junctions (Derick *et al.*, 1992) and was originally discovered as a calmodulin binding protein in erythrocytes (Gardner and Bennett, 1986) and a substrate for protein kinases A and C (Waseem and Palfrey, 1988; Ling *et al.*, 1986). It has been shown to bind both spectrin and actin, and promote the formation of the spectrin-actin complex (Gardner and Bennett, 1987; Mische *et al.*, 1987; Li and Bennett, 1996). Phosphorylation of adducin by protein kinase A, modulates the formation of spectrin-actin-adducin complexes in what is thought to be a complex relationship involving the binding of calmodulin (Matsuoka *et al.*, 1996).

Adducin is a 200 kDa heterodimer made up of α and β subunits and is present at $3x10^4$ heterodimers/cells (Lux and Palek, 1995). These polypeptides can be divided into three domains; a N-terminal protease-resistant core region and a C-terminal protease-sensitive tail region, connected by a small neck domain (Joshi and Bennett, 1990; Joshi *et al.*, 1991). Although the N-terminal core regions contain a sequence with similarity to actin binding domains (Joshi *et al.*, 1991), they are not sufficient for binding to spectrin-actin complexes or to actin alone (Joshi and Bennett, 1990). However, the C-terminal tail domains of both α- and β-

adducin are sufficient to not only bind spectrin-actin complexes, but also to promote the formation of these complexes (Hughes and Bennett, 1995).

Recent evidence suggests that adducin is involved in capping the fast growing ends of actin filaments. The ability of adducin to block elongation and depolymerisation of actin filaments is down regulated by the Ca^{2+} dependent binding of calmodulin (Kuhlman *et al.*, 1996).

1.3.2.6.2 Dematin/Protein 4.9

Dematin exists in the erythrocyte as a trimer consisting of two 48 kDa subunits and one 52 kDa subunit (Azim *et al.*, 1995) and is present at approximately 10^6 trimers/cell (Lux and Palek, 1995). The dematin trimer can bind actin and bundle actin filaments into cables (Siegel and Branton, 1985). This bundling activity is abolished by phosphorylation by cAMP-dependent protein kinase (Husain-Chishti *et al.*, 1988). Two actin binding sites in each subunit has been identified, one in the headpiece region and one in the N-terminal domain (Azim *et al.*, 1995).

1.3.2.6.3 Tropomyosin

Tropomyosin is well characterised in skeletal muscle where it self-associates along groves of actin filaments. Tropomyosin has been identified in erythrocytes as a 60 kDa heterodimer which consists of a 27 kDa and a 29kDa subunit (Fowler and Bennett, 1984) and binds tropomodulin (Fowler, 1987; Fowler, 1990). Erythrocyte tropomyosin resembles other tropomyosins in both size and structure (Fowler and Bennett, 1984), however differs in its ability to self-associate (Mak *et al.*, 1987). Tropomyosin is present at approximately $7x10^4$ dimers/cell (Lux and Palek, 1995).

1.3.2.6.4 Tropomodulin

Tropomodulin is a 43 kDa protein that was identified from its ability to bind tropomyosin (Fowler, 1987) and is present at approximately $3x10^4$ copies/cell (Lux and Palek, 1995). Purified tropomodulin binds to one of the ends of tropomyosin and is a non-competitive inhibitor of tropomyosin binding to actin (Fowler, 1990). Tropomodulin is able to bind directly to actin at the pointed end of the actin protofilament and has been shown to block elongation and depolymerisation of tropomyosin containing actin filaments (Weber *et al.*, 1994). This evidence suggests possible roles for tropomodulin in regulation of tropomyosin-actin interactions and as a capping protein for the pointed, slow growing ends of actin filaments (Weber *et al.*, 1994; Fowler, 1990).

1.3.2.6.5 Protein 4.2/Pallidin

Protein 4.2 is a 72 kDa protein that shows homology to guinea pig liver transglutaminase and human coagulation factor VIII, especially across the active sites of both these enzymes (Korsgren and Cohen, 1991). Protein 4.2 is present at approximately $2.5x10^5$ dimers or trimers/cell (Lux and Palek, 1995). Protein 4.2 has been shown to bind the cytoplasmic domain of band 3 (Korsgren and Cohen, 1988; Korsgren and Cohen, 1986) and to ankyrin in solution, however it has been difficult to show binding of protein 4.2 to ankyrin when it is attached to band 3 (Korsgren and Cohen, 1988). In contrasting results, the binding domain of protein 4.2 for band 3 has been mapped to two different regions; residues 187 to 211 and residues 63 to 75 (Bhattacharyya *et al.*, 1999; Rybicki *et al.*, 1995b). Protein 4.2 has also been shown to bind spectrin within a region encompassing residues 470-492 of protein 4.2 (Golan *et al.*, 1996; Mandal *et al.*, 2002).

1.3.3 Organisation of the Erythrocyte Membrane Skeleton

The above descriptions of the components of the erythrocyte membrane skeleton highlight many binary and ternary interactions that are involved in its complex organisation. Table 1.1 lists these interactions, including known binding affinities. This includes the major ternary interactions of spectrin/actin/protein 4.1, band 3/ankyrin/protein 4.2 and protein 4.1/GPC/p55, as well as other binary interactions observed. A model of the erythrocyte has evolved with the mapping of these interactions, along with the visualisation of the membrane skeleton using electron microscopy.

Electron Microscopy revealed junctional complexes consisting of actin protofilaments (Ursitti and Fowler, 1994), protein 4.1, adducin, dematin (Derick *et al.*, 1992), tropomodulin and tropomyosin (Ursitti and Fowler, 1994), linked by spectrin dimers and tetramers (Liu *et al.*, 1987; Byers and Branton, 1985). These findings correspond to the above descriptions of the individual interactions for each protein.

The major ternary interaction within this complex is between spectrin, actin and protein 4.1. These proteins interact in a 1:2:1 ratio of spectrin dimer:actin monomers:protein 4.1 (Pekrun *et al.*, 1989) and form the basis of the junctional complex. Most junctional complexes crosslink five or six spectrin tetramers, to form what has been described as a hexagonal lattice (Liu *et al.*, 1987; Byers and Branton, 1985). The minor proteins bind to form the remainder of the junctional complex (Figure 1.2).

Tropomyosin is found within the erythrocyte in a ratio of one tropomyosin heterodimer to 7-8 actin monomers (Fowler and Bennett, 1984), consistent with one tropomyosin molecule laying down each of the two actin filament groves (Pinder and Gratzer, 1983; Gilligan and Bennett, 1993). Tropomodulin binds both tropomyosin (Fowler, 1987) and actin (Fowler, 1990) and is present at a ratio of approximately 1-2 tropomodulin molecules per actin protofilament (Fowler *et al.*, 1993), consistent with a role in capping the slow growing end of the actin filament (Weber *et al.*, 1994). Adducin is a candidate for capping fast growing ends of actin filaments and is a protein that is able to not only bind, but also to promote the formation of the spectrin/actin complex (Gardner and Bennett, 1987, Mische *et al.*, 1987). Adducin is found in the erythrocyte at one dimer per actin protofilament (Mische *et al.*, 1987), however evidence of an adducing tetramer (Joshi *et al.*, 1991) would halve the amount of adducin available for binding actin (Gilligan and Bennett, 1993). Dematin is another actin binding protein that is found within the junctional complex that is present in a 1:1 ratio with actin (Gilligan and Bennett, 1993).

The junctional complex is linked to the lipid bilayer through interactions between cytoskeletal proteins and integral membrane proteins. Ankyrin has been visualised as a globular protein found near the midregion of the spectrin molecule, consistent with the known ankyrin binding site (Liu *et al.*, 1987; Byers and Branton, 1985). Ankyrin is in turn able to bind to band 3 (Bennett and Stenbuck, 1980a; Hargreaves *et al.*, 1980), linking spectrin to the bilayer. Both ankyrin and band 3 are further involved in a possible ternary interaction involving protein 4.2 (Korsgren and Cohen, 1988; Korsgren and Cohen, 1986). Another set of interactions strengthening the link between the junctional complex and the bilayer is the ternary interaction involving p55, GPC and protein 4.1 (Nunomura *et al.*, 2000a; Marfatia *et al.*, 1995; Hemming *et al.*, 1995).

1.3.4 Genetic Disorders of Erythrocytes

Protein-protein interactions between cytoskeletal proteins within the membrane skeleton and between integral and cytoskeletal proteins that link the membrane skeleton to the bilayer are important in both the structure and function of erythrocytes. It is, therefore, important to discuss erythrocyte disorders resulting from defects and deficiencies in both integral and cytoskeletal proteins. These disorders fall into two main categories; hereditary spherocytosis, and hereditary elliptocytosis (HE) and hereditary pyropoikilocytosis (HPP). These, along with Southeast-Asian ovalocytosis and Gerbich-negativity will be discussed briefly, in particular, in terms of their importance to malaria.

Hereditary spherocytosis (HS) is characterised by the presence of spherocytes in peripheral blood with varying degrees of splenomegaly and haemolysis. Erythrocytes become more fragile and this can lead to vesicularisation, resulting in destruction by the spleen. HS is caused by defects in erythrocyte proteins involved in interactions between the erythrocyte membrane skeleton and the lipid bilayer (for review see Tse and Lux, 1999; Delaunay, 2002). These defects are most commonly due to deficiencies in spectrin and/or ankyrin, band 3 or protein 4.2 (for review see Tse and Lux, 1999; Delaunay, 2002). HE and HPP are a group of disorders with a wide range of clinical presentations. The basic defect underlying this group of disorder is a failure of spectrin to self associate into tetramers (for review see Tse and Lux, 1999; Delaunay, 2002).

A number of studies have looked at the rates of invasion and growth of *P. falciparum* parasites in HS and HE erythrocytes. These studies have found decreased rates of invasion and/or decreased growth, dependent on the deficiency involved, with some contrasting results between studies (Schulman *et al.*, 1990; Chishti *et al.*, 1996; Magowan *et al.*, 1995; Facer, 1995). However, the extent of protein deficiency correlates with the observed decrease in rates of parasite invasion and growth in these erythrocytes (Schulman *et al.*, 1990; Facer, 1995). In addition to alterations to invasion and/or growth, infection of HE/protein 4.1 deficient erythrocytes with *P. falciparum* parasites, results in aberrant development of parasites (Magowan *et al.*, 1997).

Ovalocytes were orininally thought to be resistant to invasion by the malaria parasite (Mohandas *et al.*, 1984). More recent evidence suggests SAO does not prevent parasite invasion or reduce parasitaemia *in vivo*, but acts to prevent cerebral malaria (Allen *et al.*, 1999).

Erythrocytes negative for the Gerbich blood group antigen are characterised by a deletion of exon 3 of the gene encoding GPC (Serjeanson *et al.*, 1994). In malaria infection, Gerbich-negative individuals show no apparent differences in rates of infection (Patel *et al.*, 2001), however *P. falciparum* parasites are unable to bind GPC in Gerbich-negative erythrocytes and can not invade erythrocytes via the EBA140-GPC pathway (Maier *et al.*, 2003).

A number of other genetic defects including sickle cell anaemia, thalassaemia and glucose-6-phosphate dehydrogenase (G6PD) deficiency have also been associated with resistance to malaria infection and protection from severe disease complications (for review see Nagel and Roth, 1989; Nagel, 1990).

1.4 *The* P. falciparum *Infected Erythrocyte*

1.4.1 *Structural, Functional and Biochemical Alterations to Erythrocytes infected with* P. falciparum

Invasion by *P. falciparum* parasites results in many alterations to the erythrocyte (for reviews see Coppel *et al.*, 1998, Haynes, 1993, Howard, 1988; Cooke *et al.*, 2001). Some of these changes, including cellular, mechanical and adhesive properties are discussed below.

1.4.1.1 *Alteration of Cellular Properties*

Alterations include the formation of a parasitophorous vacuole, the formation of Maurer's clefts, the tubovesiclular membrane network and trafficking pathways, and the deposition of parasite proteins at the erythrocyte membrane skeleton, resulting in structural modification of the erythrocyte including the formation of knobs.

1.4.1.1.1 Parasitophorous Vacuole

The parasitophorous vacuole develops during invasion of the merozoite where the contact point between the merozoite and the erythrocyte invaginates, leading to the complete engulfment of the merozoite. The parasitophorous vacuole becomes the space that surrounds the merozoite and is separated from the cytoplasm of the erythrocyte by the parasitophorous vaculolar membrane (PVM). This membrane is thought to contain lipids from the erythrocyte membrane and proteins and lipids derived from the invading parasite. Measurement on the loss of surface area of newly infected erythrocyte suggest that erythrocyte membrane material internalised for the formation of the PVM is minimal (Dluzewski *et al.*, 1995).

1.4.1.1.2 Trafficking Pathways

Although still poorly understood, trafficking pathways within the malaria infected erythrocyte are essential for the survival and maturation of the parasite. Evidence exists in support of the involvement of a classical secretory pathway involving the transport of proteins from the endoplasmic reticulum (ER) to the Golgi apparatus in a similar manner to that seen in other eukaryotes. Evidence supporting this pathway includes firstly, the discovery of a number of homologues within *Plasmodium* of proteins known to be involved in the classical secretory pathway (for reviews see Foley and Tilley, 1998; Taraschi *et al.*, 2001). Secondly,

Brefeldin A, a fungal metabolite known to inhibit the formation of vesicles involved in trafficking between the ER and golgi apparatus, is able to block transport of a number of parasite proteins including KAHRP, PfEMP1, *Plasmodium falciparum* erythrocyte membrane protein 3 (PfEMP3) (Wickham *et al.*, 2001) and *Plasmodium falciparum* antigen 332 (Pf332) (Hinterberg *et al.*, 1994). Thirdly, the existence of possible signal sequences within a number of parasite proteins (for review see Nacer *et al.*, 2001). There is also evidence to suggest a non-classical secretory pathway that is Brefeldin A insensitive (Elmendorf *et al.*, 1992, Mattei *et al.*, 1999) and an additional Brefeldin A sensitive pathway that involves the diversion of proteins to a ER-like compartment and operates in parallel with the classical secretory pathway (Wiser *et al.*, 1999; Wiser *et al.*. 1997; Cortes *et al.*, 2003).

1.4.1.1.3 Tubovesiclular Membrane Network, Maurer's Clefts and Secretory Vesicles

Microscopy studies of infected erythrocytes have identified a number of membranous structures thought to be involved in protein trafficking and solute transport. The tubovesicular network (TVN) which extends from the PVM to the erythrocyte membrane (Elmendorf and Haldar, 1994; Elford *et al.*, 1995), is thought to be involved predominantly in transport of nutrients into the parasite (for review see Haldar *et al.*, 2001). Maurer's clefts appear as flattened lamellar membranes, which are associated with the exported proteins Pf332, PfEMP3, PfEMP1 and KAHRP and are involved in the assembly of the cytoadherence complex (Wickham *et al.*, 2001; Hinterberg *et al.*, 1994). Recent evidence suggests the existence of smaller, electron dense, possibly coated vesicles, which are associated with PfEMP1 and PfEMP3 and are proposed to be involved in vesicle mediated trafficking from the PVM to Maurer's clefts (for review see Taraschi *et al.*, 2001).

1.4.1.1.4 Knobs

Erythrocytes infected with mature forms of *P. falciparum* are characterised by the development of electron-dense protrusions on the erythrocyte membrane surface; termed knobs (Trager *et al.*, 1966). Knobs are essential for sequestration (Langreth and Peterson, 1985), vascular obstruction (Raventos-Suarez *et al.*, 1985) and adhesion under flow conditions (Crabb *et al.*, 1997). Many studies have been undertaken to determine the topography of knobs (Langreth *et al.*, 1978; Nagao *et al.*, 2000; Gruenberg *et al.*, 1983). The most recent of these estimates the height of knobs to be 22 nm and the width to be 83 nm (Nagao *et al.*, 2000). This study also concluded that knob volume remains constant throughout parasite maturation and that the number of knobs increases continuously throughout the maturation

process (Nagao *et al.*, 2000). Because of their role in malaria pathogenesis, the composition of knobs has also been of great interest (Kilejian, 1979). A protein varying from 80–108 kDa, depending on the parasite line examined, was consistently identified as the main component of knobs (Leech *et al.*, 1984a; Gritzmacher and Reese, 1984; Kilejian, 1984). This protein, known as KAHRP, is essential for knob formation (Crabb *et al.*, 1997).

1.4.1.2 Alteration of Membrane Mechanical Properties

Normal erythrocytes are able to repeatedly deform when subjected to an applied force however, infection with malaria parasites reduces this ability dramatically. Filtration techniques were originally used to demonstrate reduced deformability of parasitised monkey erythrocytes (Miller *et al.*, 1971). These studies lead to the use of a rheoscope, and more recently analytical micropipettes to confirm this observation in *P. falciparum* infected erythrocytes (Cranston *et al.*, 1984; Nash *et al.*, 1989; Glenister *et al.*, 2002). Erythrocytes infected with ring stage parasites have a slight degree of impaired deformability, whereas erythrocytes infected with more mature stage parasites completely lose their ability to deform (Cranston *et al.*, 1984; Nash *et al.*, 1989).

1.4.1.3 Alterations to Erythrocyte Adhesive Properties

There are three main changes in adhesive properties of the erythrocyte following parasite invasion, these are cytoadherence, rosetting and autoagglutination.

1.4.1.3.1 Cytoadherence

During *P. falciparum* infection parasitised erythrocytes sequester in many organs including the heart, kidney, lungs, liver, placenta and the brain. Sequestration results from the ability of infected erythrocytes to cytoadhere to the endothelial cells that line the vasculature and it is this accumulation of parasitised erythrocytes in brain capillaries that is a major factor in the development of cerebral malaria (MacPherson *et al.*, 1985; Pongponratn *et al.*, 1991).

A number of possible cytoadherence ligands have been identified for *P. falciparum*, including PfEMP1 (Section 1.4.2.1.1), cytoadherence linked asexual gene 9 (Clag9) (Section 1.4.2.1.3) (Trenholme *et al.*, 2000), rifins (Section 1.4.2.1.2) (Fernandez *et al.*, 1999) and modified band 3 (Section 1.4.1.4.2) (Crandall and Sherman, 1994). The majority of research has focused on PfEMP1 and its binding to the endothelial cell-expressed receptors CD36, thrombospondin and intercellular adhesion molecule 1 (ICAM-1) (Baruch *et al.*, 1996), and also to

chondroitin sulphate A in the placenta (Buffet *et al.*, 1999; Reeder *et al.*, 1999; Cooke *et al.*, 1996). A synergistic model for binding of *P. falciparum* to ICAM-1 and CD36 has also been proposed (McCormick *et al.*, 1997; Gray *et al.*, 2003).

A 179 residue binding site for CD36 has been identified in the cysteine-rich interdomain region of PfEMP1 (Baruch *et al.*, 1997) and a recombinant peptide encompassing this region subsequently demonstrated to block and reverse adhesion under physiologically relevant flow conditions (Cooke *et al.*, 1998). A number of other erythrocyte receptors have been identified, however the importance of adhesion to these receptors *in vivo* is unclear (for review see Cooke *et al.*, 2001).

1.4.1.3.2 Rosetting

Rosetting is another form of adhesion and is described as the binding of two of more uninfected erythrocytes to a single infected erythrocyte (Udomsangpetch *et al.*, 1989b). Rosetting has been reported to be associated with disease severity (Carlson *et al.*, 1992b; Ringwald *et al.*, 1993; Rowe *et al.*, 1995), however contrasting data have been seen in other studies (al-Yaman *et al.*, 1995). The function of rosette formation in disease is not clear however, rosettes formed in *P. falciparum* infection show strong cell-cell attachments that are able to withstand arterial flow stresses (Nash *et al.*, 1992; Chotivanich *et al.*, 2000), suggesting a possible role in microvascular obstruction (Udomsangpetch *et al.*, 1992; Chotivanich *et al.*, 2000). Rosettes do not appear to play a role in the enhancement or targeting of parasite to invasion of uninfected erythrocytes (Clough *et al.*, 1998b).

Rosetting requires divalent ions, is favoured at a slightly acidic pH and is frequently sensitive to heparin (Carlson *et al.*, 1990; Carlson *et al.*, 1992a) and other sulphated glycoconjugates (Rowe *et al.*, 1994). Evidence also suggests a requirement for serum components for formation of rosettes, in particular IgM (Clough *et al.*, 1998a; Treutiger *et al.*, 1999; Somner *et al.*, 2000). Rosetting has been demonstrated in both *Plasmodium* species that sequester, such as *P. coatneyi* (Udomsangpetch *et al.*, 1991), and in species such as *P. vivax* that do not appear to cytoadhere and do not cause cerebral malaria (Udomsangpetch *et al.*, 1995). Both PfEMP1 and Rifins have been implicated as rosetting ligands (Helmby *et al.*, 1993; Rowe *et al.*, 1997). Much of the recent evidence suggests PfEMP1 as the ligand responsible for rosetting. Multiple erythrocyte ligands have been identified for PfEMP1 binding, including complement receptor 1 (Rowe *et al.*, 1997), heparin sulphate or a heparin sulphate-like glycosaminoglycan (Chen *et al.*, 1998; Chen *et*

al., 2000; Barragan *et al.*, 2000; Barragan *et al.*, 1999) and the ABO blood group antigens (Chen *et al.*, 2000; Carlson and Wahlgren, 1992)

1.4.1.3.3 Autoagglutination

The ability of parasitised erythrocytes to adhere to each other (autoagglutination) has been shown to occur in both laboratory lines and clinical isolates (Roberts *et al.*, 2000; Cooke *et al.*, 1993). Autoagglutinates appear to be more common in children with severe malaria than those with more mild disease, however autoagglutinates are not always seen with severe malaria (Roberts *et al.*, 2000).

1.4.1.4 Biochemical Alteration of Erythrocyte Proteins

Maturation of the malaria parasite within the erythrocyte is known to lead to alterations of normal erythrocyte proteins. The most notable of these alterations are phosphorylation of integral and cytoskeletal proteins, modification of band 3 and cleavage of membrane skeletal protein by proteases.

1.4.1.4.1 Phosphorylation of Erythrocyte Proteins

Changes in the level of phosphorylation is thought to occur in many proteins, including spectrin, ankyrin, band 3 and protein 4.1 (Murray and Perkins, 1989; Chishti *et al.*, 1994; Lustigman *et al.*, 1990; Magowan *et al.*, 1998). The most notable of these is the phosphorylation of protein 4.1. Although not originally thought to be additionally phosphorylated (Murray and Perkins, 1989), protein 4.1 has been identified as the novel phosphoprotein of 80 kDa that co-precipitates with the parasite protein MESA in erythrocytes infected with mature forms of *P. falciparum* (Chishti *et al.*, 1994; Lustigman *et al.*, 1990). Phosphorylation of erythrocyte proteins is likely to be of importance to the erythrocyte structure and mechanical properties following *P. falciparum* invasion and maturation. This is most evident from studies showing that phosphorylation of protein 4.1 reduces its affinity for spectrin binding and ability to promote the formation of the spectrin/actin/protein 4.1 complex (Ling *et al.*, 1988; Eder *et al.*, 1986; Subrahmanyam *et al.*, 1991) and that increased phosphorylation of spectrin decreases mechanical stability of erythrocytes (Manno *et al.*, 1995).

1.4.1.4.2 Modification of Band 3

During *P. falciparum* infection, band 3 has been described as undergoing truncation and covalent modification to produce a novel 65 kDa protein (Crandall and Sherman, 1991). These modifications are thought to expose cryptic residues

of band 3 and contribute to cytoadherence (Crandall and Sherman, 1994). Both synthetic peptides and monoclonal antibodies that recognise only band 3 in infected erythrocytes were shown to block binding of the infected erythrocyte to C32 amelanotic melanoma cells (Winograd and Sherman, 1989; Crandall *et al.*, 1993; Crandall *et al.*, 1994). More recent studies suggest that the receptor molecule for binding is thrombospondin (Lucas and Sherman, 1998; Eda *et al.*, 1999). The precise role of thrombospondin in adhesion remains controversial.

1.4.1.4.3 Cleavage of Erythrocyte Proteins by Parasite Proteases

Proteases of the cysteine protease, aspartic protease, metalloprotease and aminopeptidase families have been identified within malaria parasites (for review see Rosenthal, 2002). These proteases are responsible for the hydrolysis of membrane skeletal proteins during invasion and rupture by the parasite and for the hydrolysis of haemoglobin for a source of amino acids which are incorporated into parasite proteins (Rosenthal, 2002). To date, two proteases have been described that are able to hydrolyse erythrocyte membrane skeletal proteins. These are the cysteine protease falcipain-2 (Shenai *et al.*, 2000) and the aspartic protease plasmepsin II (Le Bonniec *et al.*, 1999).

Falcipain-2 was originally purified by affinity chromatography and it was shown that both native and recombinant forms of the protein were able to hydrolyse haemoglobin (Shenai *et al.*, 2000). This protease was subsequently shown to cleave both ankyrin and protein 4.1 at neutral pH. This cleavage results in an increased rate of membrane fragmentation, which is proposed to modulate parasite release (Dua *et al.*, 2001; Raphael *et al.*, 2000). Cleavage of protein 4.1 occurs after lysine 437, which is within the SAB and possibly causes instability of the membrane skeleton (Hanspal *et al.*, 2002). The cleavage of ankyrin occurs after arginine 1210 and interestingly, a 10-mer peptide containing the cleavage site is able to block late stage parasite development (Dhawan *et al.*, 2003).

Plasmepsin II is an aspartic protease that is thought to be responsible for the cleavage of spectrin within the SH-3 domain (Le Bonniec *et al.*, 1999) and the hydrolysis of haemoglobin (Gluzman *et al.*, 1994). Initially, a 37 kDa protease was described in both *P. falciparum* and *P. berghei* that was able to cleave spectrin and protein 4.1 (Deguercy *et al.*, 1990). Subsequently, the proteolytic activity of a 35-40 kDa protease able to cleave α-spectrin within the SH-3 domain was shown to be inhibited by pepstatin A (Le Bonniec *et al.*, 1996). Recent studies have shown that a recombinant form of a 37 kDa aspartic protease, plasmepsin II, is able to cleave both purified spectrin and spectrin contained within ghosts, suggesting that plasmepsin II is this previously described protease (Le Bonniec *et al.*, 1999).

1.4.2 P. falciparum *Proteins Exported to the Erythrocyte Membrane*

During *P. falciparum* infection, parasite encoded proteins are present at the erythrocyte membrane and are major contributing factors in the alterations to the structure and function of normal erythrocytes. Proteins known to be exported to the erythrocyte membrane include those that are found in association with the membrane skeleton, and those inserted into the membrane and exposed to the external surface of the erythrocyte (Figure 1.4). Many of these proteins have been studied in detail (for recent review see Cooke *et al.*, 2001), although our functional understanding of most of these proteins remains incomplete.

1.4.2.1 *Proteins Exposed to the Surface*

1.4.2.1.1 PfEMP1

PfEMP1 is encoded by the *var* gene family (Smith *et al.*, 1995; Baruch *et al.*, 1995; Su *et al.*, 1995). Recent annotation reveals approximately 70 *var* genes can be identified in the genome of *P. falciparum* (Robert Heustis, Victorian Bioinformatics Consortium (VBC), personal communication). *Var* genes are distributed on all chromosomes, most predominantly in a subtelomeric location (Rubio *et al.*, 1996; Fischer *et al.*, 1997). The structure of the *var* gene has been determined and consists of two exons. The longer 5' exon encodes the variable extracellular region that consists of a variable number of Duffy binding ligand (DBL) domains and cysteine-rich inter domain regions (CIDR). The shorter 3' exon encodes the conserved intracellular domain that has been shown to be anchored to the erythrocyte membrane skeleton through interactions with KAHRP (Waller *et al.*, 2002; Waller *et al.*, 1999; Voigt *et al.*, 2000), spectrin and actin (Oh *et al.*, 2000). PfEMP1 is widely thought to be the major binding ligand for infected erythrocytes and has been shown to bind a number of receptor molecules through different defined regions of the extracellular domain. For example, the CIDR of a number of different PfEMP1 molecules have been shown to bind to CD36 (Baruch *et al.*, 1997; Smith *et al.*, 1998), whereas, binding sites for chondroitin sulphate A appear to reside in DBL3 (Buffet *et al.*, 1999; Reeder *et al.*, 1999), DBL7 (Buffet *et al.*, 1999) or CIDR1 domains (Reeder *et al.*, 1999; Degen *et al.*, 2000), depending on the particular PfEMP1 expressed.

1.4.2.1.2 Rifins

Rifins are encoded by the *rif* gene family that are found in multiple copies near the telomers of *P. falciparum* chromosomes (Gardner *et al.*, 1998; Bowman *et al.*, 1999). This family of proteins, formerly known as rosettins, are clonally

variant, surface expressed proteins that range in size from 30-45 kDa (Fernandez *et al.*, 1999; Kyes *et al.*, 1999). It has been suggested that the size of this family, along with their location and clonal variation may indicate a role in antigenic variation seen in *P. falciparum* infection.

1.4.2.1.3 Clag 9

Clag9 was identified by chromosome nine spontaneous deletions and is encoded by a gene that consists of 9 exons. The protein is expressed in blood stages and is predicted to contain transmembrane domains (Trenholme *et al.*, 2000). Clag9 is essential for binding to CD36 via both targeted gene knockout (Trenholme *et al.*, 2000) and antisense RNA approaches (Gardiner *et al.*, 2000). Interestingly, the high molecular mass rhoptry protein, RhopH1, is encoded by a member of the clag gene family, suggesting this family encodes proteins of similar structure with divergent locations (Kaneko *et al.*, 2001).

1.4.2.2 Proteins Associated with the Erythrocyte Membrane Skeleton

Proteins found in association with the erythrocyte membrane skeleton include KAHRP, MESA, RESA, PfEMP3 and Pf332. Of particular relevance to this study are PfEMP3 and Pf332, which are described in detail below (Sections 1.4.2.3 and 1.4.2.4).

1.4.2.2.1 KAHRP

KAHRP is encoded by a gene found on chromosome 2 (Ellis *et al.*, 1987; Gardner *et al.*, 1998) in *P. falciparum* and consists of two exons, with three repeat regions present in the second exon (Triglia *et al.*, 1987; Sharma and Kilejian, 1987)(Figure 1.5a). Sequence comparison from various clones indicates conservation of overall structure, with some variation within the 3′ repeat region (Kant and Sharma, 1996; Hirawake *et al.*, 1997). KAHRP was shown through targeted gene disruption to be essential for the formation of knobs and the ability of parasitised erythrocytes to bind to CD36 under physiologically relevant flow conditions (Crabb *et al.*, 1997).

The three repeat regions of KAHRP all individually interact with the conserved intracellular domain of PfEMP1 (Waller *et al.*, 1999; Waller *et al.*, 2002; Oh *et al.*, 2000; Voigt *et al.*, 2000) whereas, a 271 residue region containing the 5′ repeat region interacts with both spectrin and actin (Kilejian *et al.*, 1991) and the 5′ repeat region alone is responsible for binding to the band 3 and spectrin binding domains of ankyrin (Magowan *et al.*, 2000). KAHRP is transcribed mainly in ring stage parasites (Pasloske *et al.*, 1994) and is detected in mature stage parasites

where it is associated with Maurer's clefts before association with knobs at the erythrocyte membrane skeleton (Wickham *et al.*, 2001). Recent studies have shown the first 60 residues of KAHRP, including the proposed hydrophobic signal sequence, are sufficient for trafficking of KAHRP into the secretory system and to the parasitophorous vacuole. Addition of the 63 residues encoding the histidine rich region, enabled trafficking across the PVM and into the erythrocyte cytoplasm (Wickham *et al.*, 2001) (Figure 1.5a).

1.4.2.2.2 MESA

MESA is encoded by a two exon gene on chromosome five of *P. falciparum* The second exon of MESA contains repeat regions (Coppel, 1992) (Figure 1.5b). MESA is a phosphoprotein of 250-300kDa that is synthesised in late ring stage parasites through to late schizony (Coppel *et al.*, 1988). It is associated with the erythrocyte membrane skeleton (Coppel *et al.*, 1988), however is not required for the formation of knobs or cytoadherence *in vitro* (Petersen *et al.*, 1989). It has been shown to interact with protein 4.1 (Lustigman *et al.*, 1990) through a 19 residue region near the N-terminus of MESA (Bennett *et al.*, 1997). Recently the binding region within protein 4.1 for MESA was mapped to a 51 residue region within the 10 kDa domain of protein 4.1 encoded by exon 10 (Waller *et al.*, 2003). Interestingly, this region overlaps the 33 residue region that binds to p55 (Nunomura *et al.*, 2000a) and the binding of MESA to this region within protein 4.1 is able to inhibit the binding of p55 to protein 4.1 when tested *in vitro* (Waller *et al.*, 2003). Although the precise function of MESA in infected erythrocytes is unknown, expression of MESA in erythrocytes deficient in protein 4.1 results in accumulation of MESA and leads to poor parasite survival (Magowan *et al.*, 1995).

1.4.2.2.3 RESA

RESA is encoded by a two exon gene on chromosome one of *P. falciparum* (Favaloro *et al.*, 1986). RESA is synthesised in mature parasites and is stored in vesicles, possibly micronemes, until released at the time of merozoite invasion (Brown *et al.*, 1985). Following invasion, RESA becomes associated with the erythrocyte membrane (Brown *et al.*, 1985) where it interacts with spectrin (Foley *et al.*, 1991) via a 48 residue region located between two blocks of repeats (Foley *et al.*, 1994) (Figure 1.5c). This interaction has been proposed to stabilise spectrin, as seen by decreased heat denaturation of spectrin in the presence of RESA fragments and the increased heat-induced fragmentation of erythrocytes infected with RESA negative parasites (Da Silva *et al.*, 1994). This protection may occur

through the prevention of irreversible denaturation of spectrin by the DnaJ-type motif in RESA (Da Silva *et al.*, 1994; Bork *et al.*, 1992) (Figure 1.5c).

1.4.2.3 PfEMP3

PfEMP3 is a protein of approximately 315 kDa which is localised at the erythrocyte membrane skeleton of *P. falciparum* infected erythrocytes (Pasloske *et al.*, 1993). PfEMP3 is associated with Maurer's clefts during ring stages (Wickham *et al.*, 2001) before being distributed at the erythrocyte membrane skeleton (Pasloske *et al.*, 1993). PfEMP3 trafficking from the parasite to the erythrocyte is thought to be via the classical secretory pathway, as treatment with brefeldin A results in accumulation of PfEMP3 in the parasite (Wickham *et al.*, 2001). PfEMP3 has also been identified on the surface of *P. falciparum* sporozoites and in the cytoplasm of mature hepatic stage parasites (Gruner *et al.*, 2001).

The gene encoding PfEMP3 is located adjacent to the gene encoding KAHRP on chromosome two (Pasloske *et al.*, 1994; Gardner *et al.*, 1998);(Lanzer *et al.*, 1994; Gardner *et al.*, 1998). The gene has a two exon structure and contains three discernible regions of repeats (Figure 1.6). The first repeat region starts approximately 600 residues from the N-terminus of PfEMP3 and consists of 3 imperfect repeats of the sequence EYEKGHVSREYQLDNEVRDELP, 6 imperfect repeats of the sequence EYDQTELAKGKDVTNKPHESVD and 13 imperfect repeats of the sequence EYNETDLAKGKEVTNKAHENLE. The second repeat region starts at approximately 1080 residues from the N-terminus of PfEMP3 and consists of 14 imperfect repeats of the sequence KNKELQNKGSEGLKENAEL. The third and most extensive set of repeats starts approximately 1315 residues from the N-terminus of PfEMP3 and consists of 81 repeats of the sequence QQNTGLKNTPSEG. Of these 81 repeats, 38 are perfect and 43 are imperfect, with the majority of the changes within the final five residues of each repeat. The N-terminal 592 residues and C-terminal 78 residues contain no repeat regions, however predictions of coiled-coil domains has revealed coiled-coils across contiguous 1000 residue domain that shows 27% identity and 48 % similarity to Uso1p, a tethering protein in yeast (Waterkeyn *et al.*, 2000).

Sub-telomeric deletions of chromosome two, involving the loss of both KAHRP and PfEMP3 are associated with the inability to form knobs (Culvenor *et al.*, 1987) and to cytoadhere under conditions of flow (Cooke *et al.*, 2002), originally indicated that PfEMP3 may be involved in the formation of knobs. However, subsequent targeted gene disruption of PfEMP3 has shown that PfEMP3 is in fact not essential for either the formation of knobs or adhesion of infected erythrocytes under flow conditions *in vitro* (Waterkeyn *et al.*, 2000). This parasite line was

shown to have reduced membrane rigidity compared to the parental line containing the intact PfEMP3 gene (Glenister *et al.*, 2002). A truncated PfEMP3 parasite line, generated in the same study, showed a small reduction in adhesion of infected erythrocytes, which may be due to the accumulation of truncated PfEMP3 in vesicle structures, and subsequent blockage of the transfer of PfEMP1 to the external surface of the infected erythrocytes (Waterkeyn *et al.*, 2000).

Another interesting feature of PfEMP3 is the ability of PfEMP3 specific antisera to cross react with sporozoites from *P. vivax*, *P. yoelii yoelii* and *P. berghei*. In invasion studies with these antisera, inhibition was observed at more than 77% for both *P. yoelii yoelii* and *P. berghei*, presenting PfEMP3's potential as a vaccine candidate (Gruner *et al.*, 2001).

1.4.2.4 Pf332

Pf332 is a large protein of approximately 750 kDa (Mattei and Scherf, 1992a; Wiesner *et al.*, 1998). The gene encoding Pf332 is found in the subtelomeric region of chromosome 11 of *P. falciparum* and is approximately 20 kb in size (Mattei and Scherf, 1992a). This gene encodes a region of highly degenerate glutamic acid-rich repeats with a period of 10-11 residues (Mattei and Scherf, 1992b) and shows restriction length polymorphism in various isolates of *P. falciparum* (Mattei and Scherf, 1992a; Fandeur *et al.*, 1996). Pf332 was initially observed as a 2.5 MDa protein on SDS-PAGE (Mattei and Scherf, 1992a; Mattei and Scherf, 1992b), however was more recently shown to be closer to the predicted size of 750 kDa by polyacrylamide-agarose composite gels (Wiesner *et al.*, 1998).

Pf332 is found in trophozoite stages in the parasitophorous vacuole and in vesicle like structures in the erythrocyte cytoplasm. Within schizont stages, Pf332 is found in large vesicles in the erythrocyte cytoplasm and in association with the erythrocyte membrane. In more mature schizonts, Pf332 is located at the membrane of the erythrocyte (Hinterberg *et al.*, 1994). Experiments utilising Brefeldin-A treatment have lead to the proposal that the large vesicles in which Pf332 is found are Maurer's clefts and that transport of Pf332 from the parasitophorous vacuole, through the erythrocyte cytosol and to the erythrocyte membrane occurs via the classical secretory pathway (Hinterberg *et al.*, 1994).

Pf332 was originally thought to be surface exposed due to the ability of antibodies specific to sequences within Pf332 to inhibit parasite growth *in vitro* (Udomsangpetch *et al.*, 1989a; Ahlborg *et al.*, 1993; Ahlborg *et al.*, 1996). However, more recent evidence suggests that Pf332 is only exposed on the surface in very late schizonts (Hinterberg *et al.*, 1994) and this may allow antibodies to inhibit new ring development through the formation of abnormal schizonts (Ahlborg

et al., 1996). Alternatively, antisera specific to sequences in Pf332 have been shown to cross react with the glutamic acid rich repeats of RESA and Pf11.1, which may account for the reactivity to Pf332 antisera to the surface of infected erythrocytes (Udomsangpetch *et al.*, 1989a).

1.5 Protein-Protein Interactions at the Membrane Skeleton in Parasitised Erythrocytes

As indicated in Section 1.4.2, a number of the parasite proteins that are exported to the erythrocyte membrane skeleton interact with not only erythrocyte proteins but also with other parasite proteins. Interactions have been described between KAHRP, PFEMP1, and the erythrocyte proteins spectrin and actin. Waller *et al.* (1999) showed that the repeat regions within KAHRP interact with PfEMP1 with a moderate affinity (Histidine-rich repeats; $K_{(D)kin}=1x10^{-7}$, 5' repeats; $K_{(D)kin}=3.3x10^{-6}$, 3'repeats; $K_{(D)kin}=1.3x10^{-5}$). These interactions have been proposed to have an additive affect, resulting in a stronger overall interaction. Evidence supporting this was recently published showing a stronger binding affinity of full length KAHRP ($K_{(D)Scat}=1.07x10^{-8}$) (Oh *et al.*, 1997) than that previously published for individual fragments. This cooperative model was substantiated by the mapping of multiple regions within the PfEMP1 intracellular domain that are able to bind the KAHRP repeat regions (Waller *et al.*, 2002). It has been proposed that many of these interactions are due to electrostatic forces (Waller *et al.*, 1999; Waller *et al.*, 2002) and this is supported by the observed interaction of PfEMP1 intracellular domain with other basic, unrelated proteins and the pH dependence of the PfEMP1/KAHRP interaction (Voigt *et al.*, 2000).

The importance of KAHRP's ability to anchor PfEMP1 to the erythrocyte membrane skeleton is demonstrated in the targeted gene knockout of KAHRP. This line of *P. falciparum* lacks knobs and shows a reduced ability to adhere to CD36 under physiologically relevant flow conditions (Crabb *et al.*, 1997). PfEMP1 is still present at the surface of the infected erythrocyte in this knockout line and is able to bind CD36 in static conditions, but it is proposed that without the anchoring by KAHRP, PfEMP1 is lost from the membrane under flow conditions (Crabb *et al.*, 1997). The residual ability of PfEMP1 to remain anchored at the erythrocyte membrane under static conditions may be attributed to the interaction between the PfEMP1 intracellular domain with both spectrin and actin (Oh *et al.*, 2000). Given that the interaction between PfEMP1/F-actin and PfEMP1/KAHRP are both in the nM range (Oh *et al.*, 2000), it is interesting that the spectrin and actin interactions are not sufficient for PfEMP1 to retain ability to bind CD36 under flow conditions in the

absence of KAHRP. It may be that there is an additive affect of interactions involving a number of proteins that allow PfEMP1 to retain its binding properties.

The anchoring of PfEMP1 via KAHRP is an incomplete picture without the subsequent anchoring of KAHRP to the erythrocyte membrane skeleton. This is thought to occur through interactions with the spectrin-actin junction. Reports have showed an interaction of a 271 residue region containing the 5' repeats of KAHRP with spectrin and actin (Kilejian *et al.*, 1991). In addition to this, KAHRP is thought to be further anchored by an interaction of the 5' repeat regions with ankyrin (Magowan *et al.*, 2000).

Although no interactions have yet been mapped for PfEMP3, its involvement in this complex set of interactions is of great interest. The truncation, but not the knockout of this protein results in an accumulation of PfEMP1 in vesicle like structures under the erythrocyte membrane and subsequent loss of binding to CD36 under both static and flow conditions. This suggests that although PfEMP3 is not essential for PfEMP1 trafficking, it is able to block the transport of PfEMP1 to the surface of infected erythrocytes when present in a truncated form. It has been suggested that truncation of PfEMP3 may have resulted in the loss of a binding domain required for correct sorting and trafficking (Waterkeyn *et al.*, 2000).

Other interactions within the infected erythrocyte involve the parasite proteins MESA and RESA. MESA has been shown to bind erythrocyte protein 4.1 in a moderate affinity interaction (Bennett *et al.*, 1997; Waller *et al.*, 2003). This interaction is important due to the ability of protein 4.1 to stabilise the interaction between spectrin and actin, and to anchor the junctional complex to the membrane. The ability of the MESA-protein 4.1 interaction to inhibit the interaction between p55 and protein 4.1 (Waller *et al.*, 2003) may act to modulate the protein 4.1-GPC-p55 interaction and therefore, modulate the ability of protein 4.1 to anchor the junctional complex to the membrane. The role that this interaction plays with respect to the other interactions of protein 4.1 in the normal erythrocyte and the additional phosphorylation of protein 4.1 seen in the infected erythrocyte is of great interest.

RESA is known to interact with spectrin (Foley *et al.*, 1991; Foley *et al.*, 1994). Again, the role which this plays in the infected erythrocyte in respect to the earlier timing of expression of RESA compared with other exported parasite proteins and the many interactions within the infected erythrocyte involving spectrin, may prove invaluable to our complete understanding of the structural and functional alterations caused by malaria proteins infected erythrocytes.

1.6 Aims of this Thesis

During parasite development within the infected erythrocyte, proteins are exported to the erythrocyte membrane where they become inserted into the membrane or are associated with the membrane skeleton. These proteins are involved in protein-protein interactions that are responsible for many modifications of the infected erythrocyte. Work over the last few years describing protein-protein interactions between parasite proteins and both other parasite proteins and erythrocyte proteins, have started to reveal a complicated picture of the organisation of proteins at the membrane. Due to the complicated nature of these interactions including the changes in phosphorylation levels of erythrocyte proteins within the infected erythrocyte and the cleavage of erythrocyte proteins by parasite proteases, much more knowledge is needed before the picture is complete.

A number of recent publications describing targeted gene knockout of parasite proteins have provided insight into the function of these proteins (Crabb *et al.*, 1997; Waterkeyn *et al.*, 2000; Reed *et al.*, 2000; Trenholme *et al.*, 2000). However, these studies have also raised a number of questions concerning the role of protein-protein interactions in the precise function of these proteins (Waterkeyn *et al.*, 2000).

The work described in this thesis is aimed at answering some of these questions by investigating protein-protein interactions at the erythrocyte membrane skeleton, especially those interactions between the erythrocyte membrane skeletal proteins and exported parasite proteins. During this investigation, we have looked specifically at the interactions involving both PfEMP3 and Pf332 with the erythrocyte membrane skeleton. No interactions involving either PfEMP3 or Pf332 were published at the time of writing this thesis. Therefore we aimed to;

- Clone, express and purify recombinant fragments of these proteins
- Interact these proteins with the erythrocyte membrane skeleton
- Identify binding partners for these proteins in the erythrocyte membrane skeleton
- Map the binding domains within these proteins involved in these interactions

By identifying and mapping interactions involving PfEMP3 and Pf332 and the erythrocyte membrane skeleton, we may begin to assign function to these proteins. Mapping of protein-protein interactions may, in the longer term, reveal regions of these proteins that may prove useful in design of novel targets for drug therapy. The ongoing annotation of the recently sequenced *P. falciparum* genome, along

with improved technologies for targeted gene disruption and methods for studying protein-protein interactions, is enabling us to more quickly and accurately model the infected erythrocyte membrane skeleton and ultimately better understand the pathogenesis of *P. falciparum* infection.

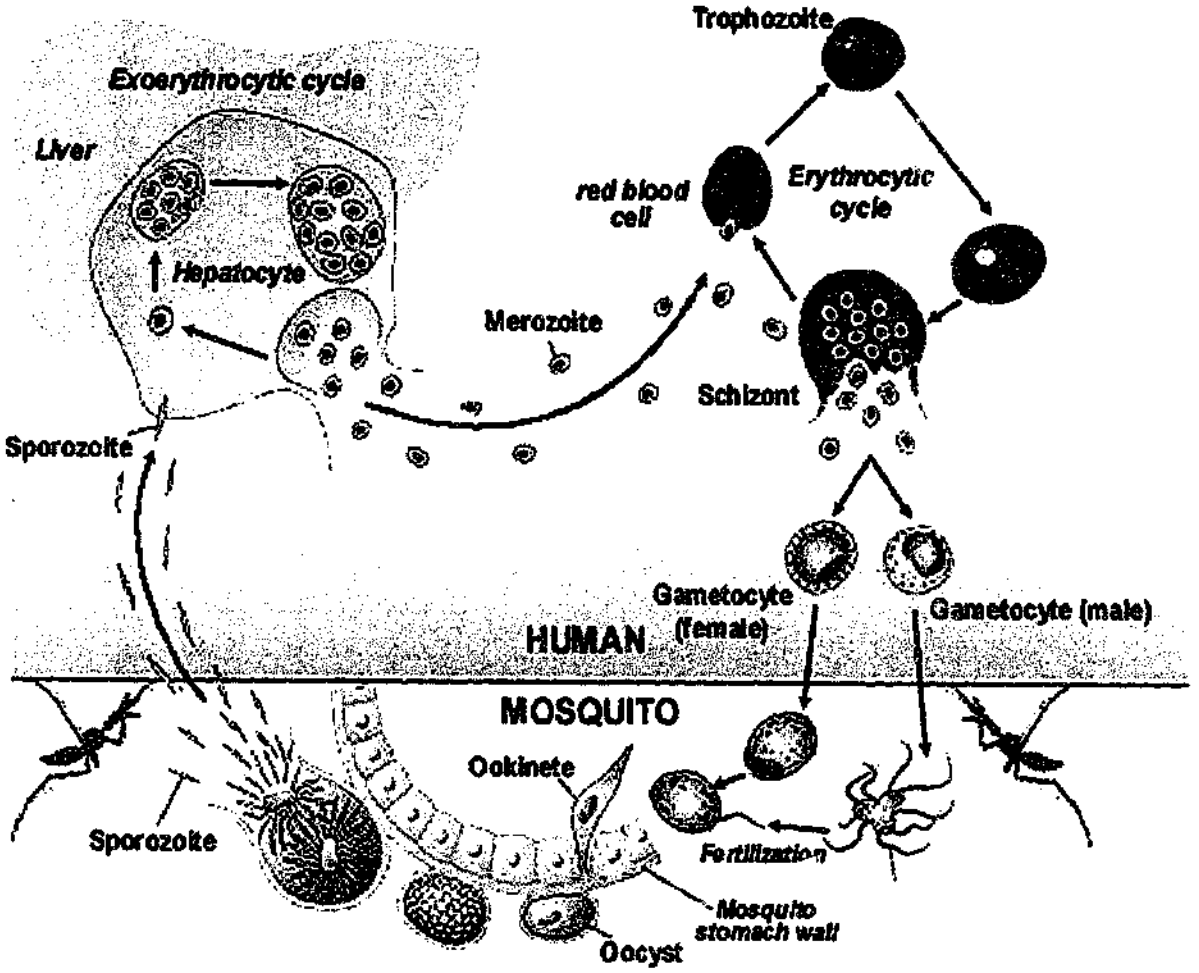

Figure 1.1 Life Cycle of *Plasmodium* in the Mosquito and Humans (*From Scientific American Medicine OnLine, http://www.samed.com)*

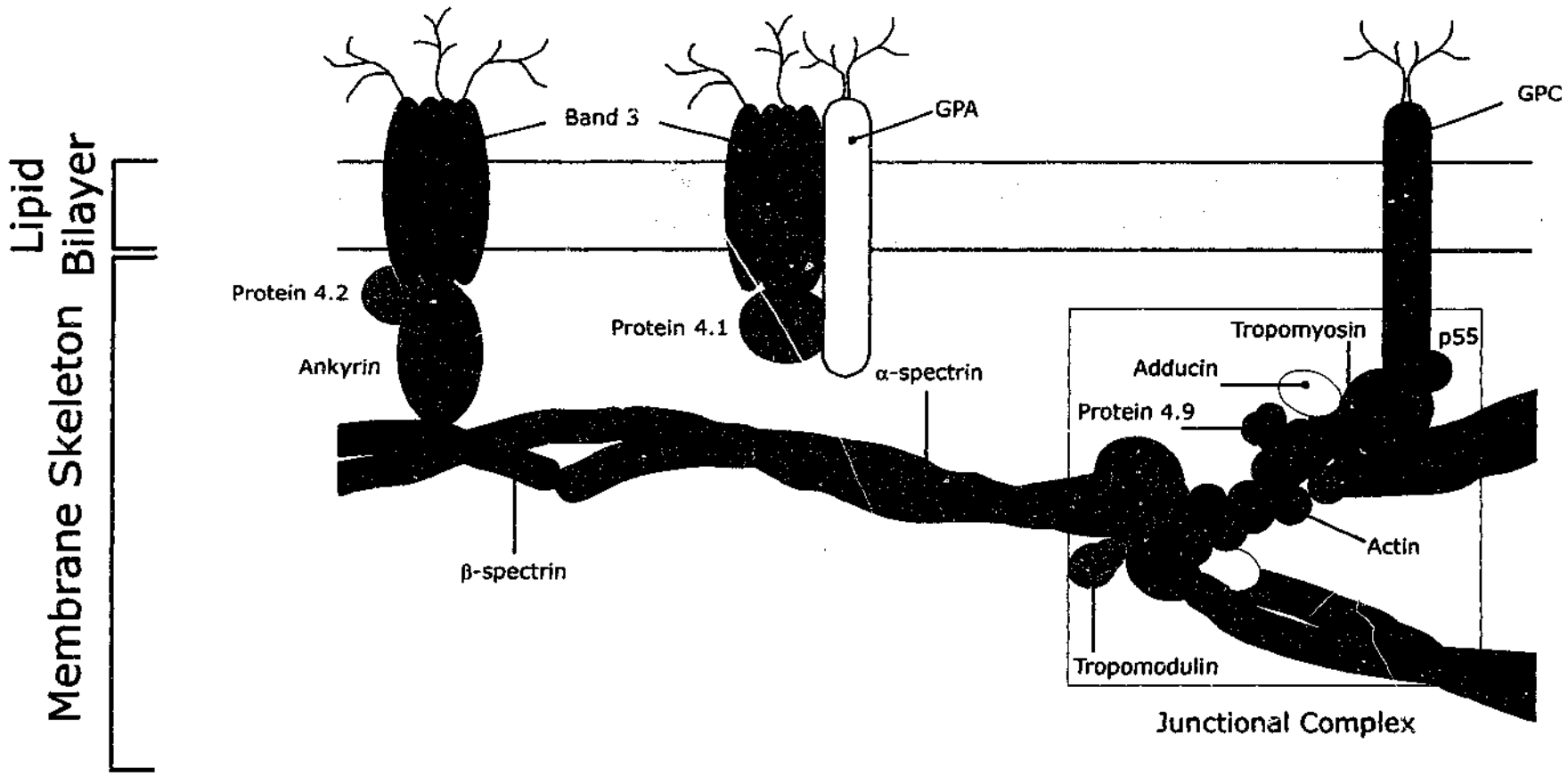

Figure 1.2. Schematic of the Erythrocyte Membrane Skeleton Showing Important Protein-Protein Interactions

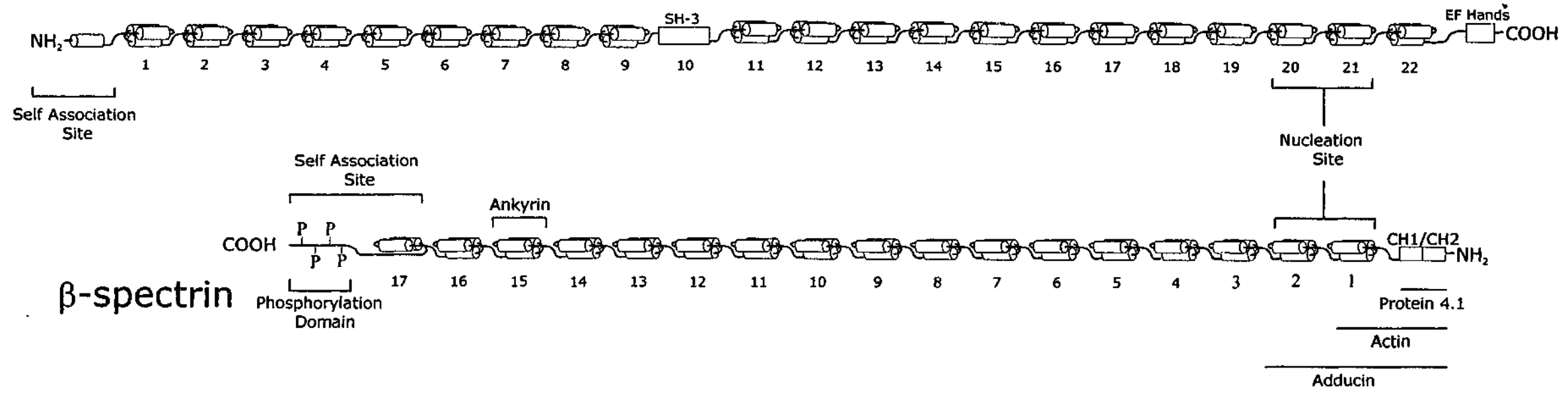

Figure 1.3. Schematic of α- and β-Spectrin

The 106 amino acid spectrin repeats are numbered from the N-terminusl and are represented by a triple helix. The SH-3 domain and EF Hands within the α-chain and the CH1/CH2 domains and phosphorylation domain within the β-chain are labelled. The α- and β-chains are aligned antiparallel and the nucleation site is indicated. Also indicated are the self association sites and protein binding domains (Adapted from Lux and Palek, 1995).

Interacting Proteins	Binding constants (nM)*	Reference
Spectrin/Actin/Protein 4.1		
Spectrin/Actin	$5x10^3$	(Ohanian *et al.*, 1984)
Spectrin/Actin in presence of protein 4.1	$1x10^{12}$	(Ohanian *et al.*, 1984)
Spectrin/Protein 4.1	100	(Tyler *et al.*, 1980)
Protein 4.1/Actin	10^4-10^6	(Morris and Lux, 1995)
Protein 4.1/GPC/p55		
Protein 4.1/GPC	90	(Nunomura *et al.*, 2000a)
Protein 4.1/p55	100	(Nunomura *et al.*, 2000a)
p55/GPC	1600	(Nunomura *et al.*, 2000a)
p55/GPCin the presence of protein 4.1	2400	(Nunomura *et al.*, 2000a)
Band 3/Ankyrin/Protein 4.2		
Band 3/Ankyrin	8-13	(Bennett and Stenbuck, 1980a); (Thevenin and Low, 1990)
Band 3/Protein 4.2	200-800	(Korsgren and Cohen, 1988); (Bhattacharyya *et al.*, 1999)
Ankyrin/Protein 4.2	100-350	(Korsgren and Cohen, 1988)
Spectrin/Ankyrin	100	(Tyler *et al.*, 1980)
Protein 4.1/Band 3	580	(Siegel and Branton, 1985)
Actin/Dematin	ND	(Siegel and Branton, 1985)
Actin/Tropomyosin	ND	(Mak *et al.*, 1987)
Actin/Tropomodulin	ND	(Weber *et al.*, 1994)
Tropomyosin/Tropomodulin	ND	(Fowler, 1987)
Protein 4.2/spectrin	ND	(Mandal *et al.*, 2002)
Spectrin-actin complex/Adducin	ND	(Hughes and Bennett, 1995)
Glycophorin A/Band 3	ND	(Nigg *et al.*, 1980)
Glycophorin A/Protein 4.1	ND	(Anderson and Lovrien, 1984)

Table 1.1 Interactions of Erythrocyte Membrane Proteins
*Binding constants are disassociation constants (K_D or K_d) measured in nM, except for spectrin/actin and protein 4.1/actin, and spectrin/actin in the presence of protein 4.1, which are association constants measured in M^{-1} and M^{-2}, respectively.
ND=Not Determined

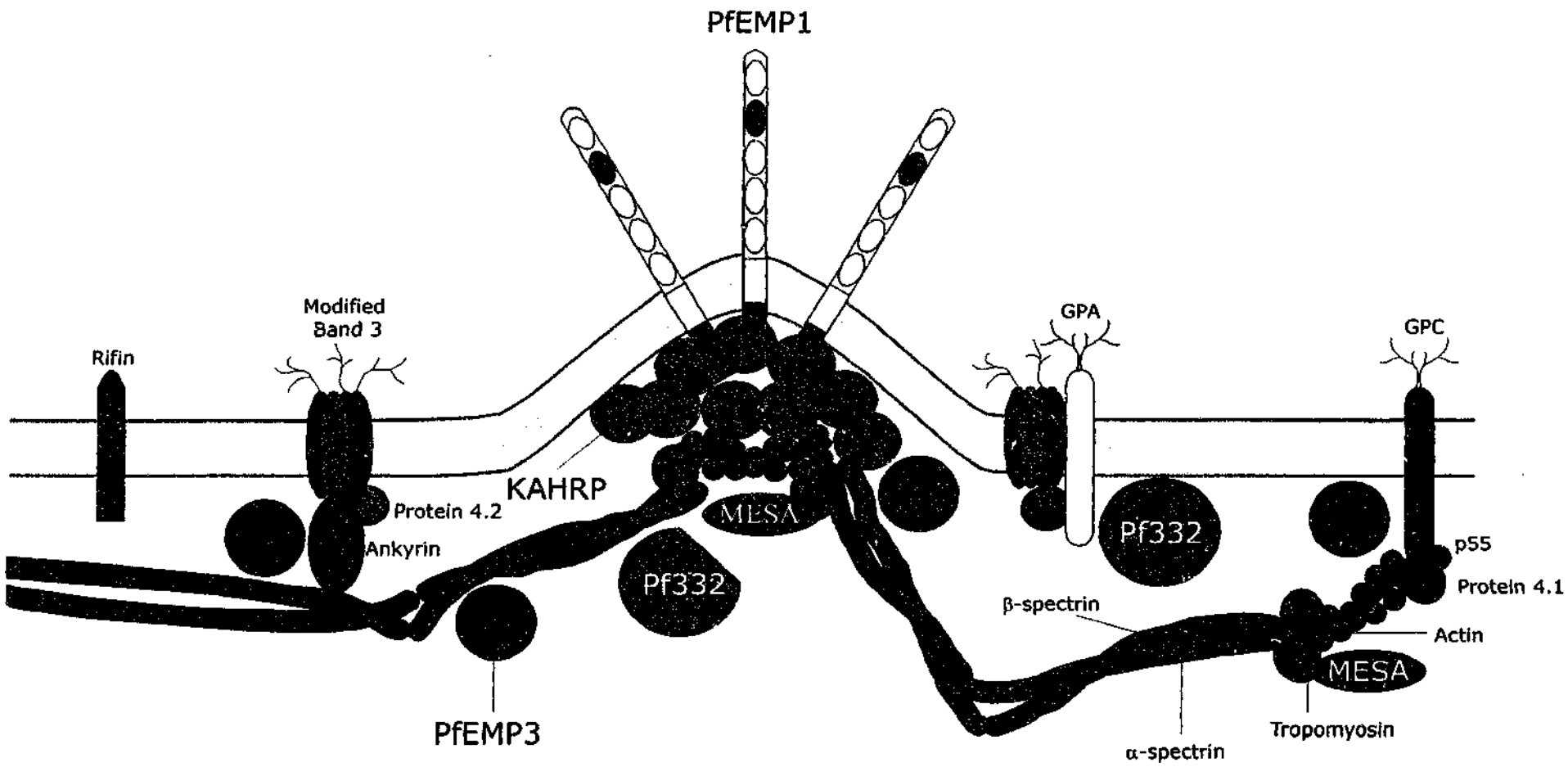

Figure 1.4. Schematic of the Erythrocyte Membrane Skeleton Following Infection with *P. falciparum* Showing Parasite Proteins and their Interactions with the Erythrocyte Membrane

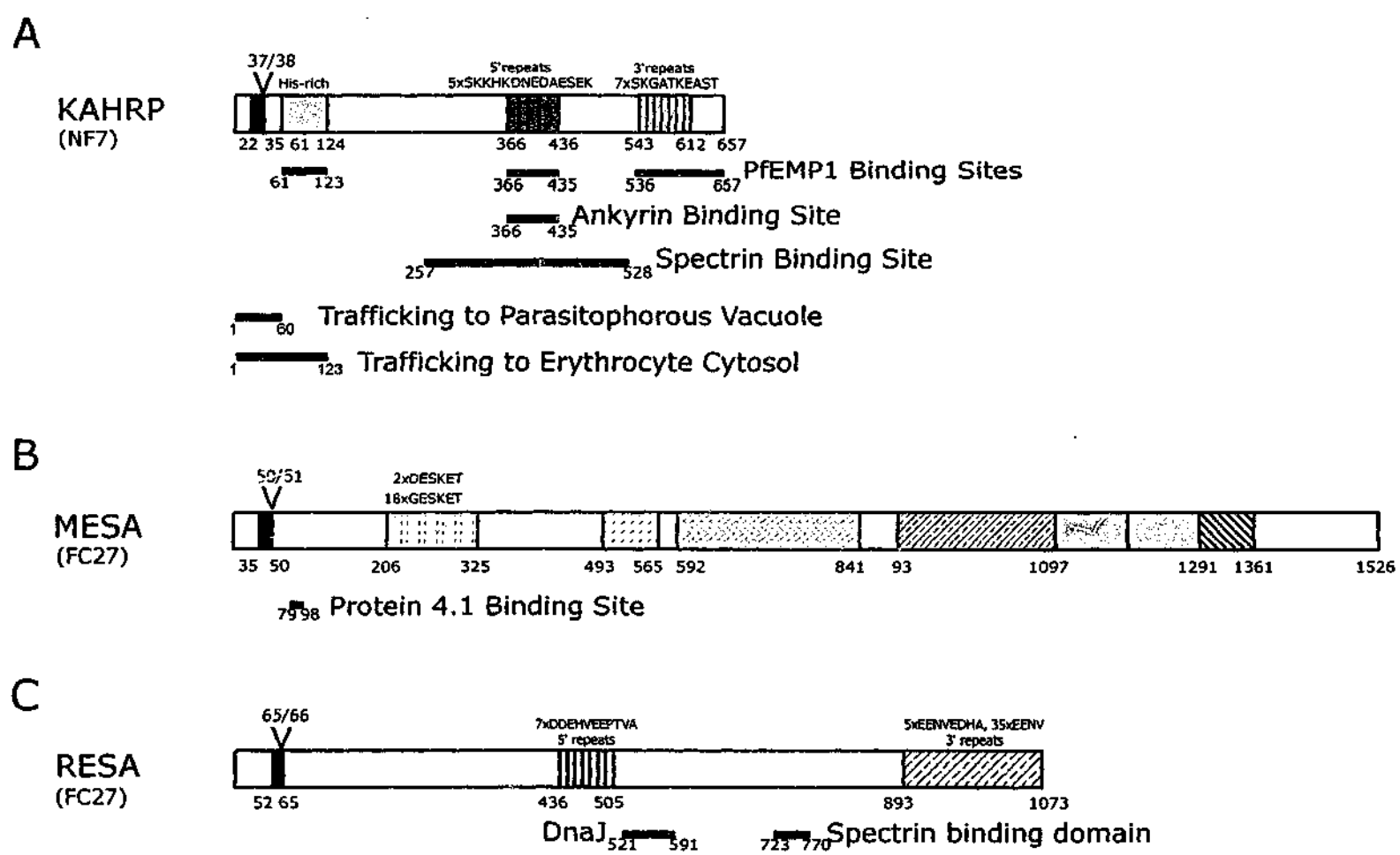

Figure 1.5. Schematic of the Proteins Encoded by the KAHRP, MESA and RESA Genes

Hydrophobic regions and repeat regions are shown as solid and shaded boxes respectively. Intron splice sites are represented as (V), nuber represent amino acid residues and binding domains and sequence motifs are indicated below each schematic (Adapted from Cooke *et al.*, 2001).

Figure 1.6. Schematic of PfEMP3

Repeat regions are shown as coloured boxes and non-repeat regions shown as open boxes. Amino acid residue numbers are indicated above the schematic and the gene intron splice site is indicated by the line at position 37.

Chapter 2 – Materials and Methods

2.1 *Enzymes, Reagents and Media*

All enzymes were purchased from Roche Molecular Biochemicals, Promega Corporation, Progen Industries Ltd., New England Bio-labs and Life Technologies.

All chemicals and media components were purchased from Sigma-Aldrich Co., BDH Laboratory Supplies, Roche Molecular Biochemicals, BioRad Laboratories, Oxoid, Gibco BRL, Baxter Healthcare, Ophthalmic Laboratories, Pharmacia & Upjohn and Amresco Inc.

2.2 Escherichia coli *Strains and Culture Conditions*

All *Escherichia coli* strains used in this study are listed in Appendix 1. Liquid *E. coli* stains were cultured in either Luria-Bertani (LB) broth (Sambrook *et al.*, 1989) or Superbroth (3.5% (w/v) Tryptone, 2% (w/v) yeast extract, 0.5% (w/v) NaCl, 0.1% (v/v) 5M NaOH) supplemented with ampicillin (100 μg/ml), kanamycin (50 μg/ml) or chloramphenicol (30 μg/ml) when required. LB containing 1.5% (w/v) agar was used for solid culture. When "blue-white" selection was required, 40 μl of 20 mg/ml 5-bromo-4-chloro-3-indolyl-β-D-galactopyranoside (X-gal) (Roche), dissolved in dimethylformamide was spread onto solid media. All media were autoclaved prior to addition of supplements and use in bacterial culture.

E. coli strains were stored in glycerol storage broth (3.7% (w/v) Brain Heart Infusion broth, 50% (v/v) glycerol) at -20°C and -70°C.

2.3 *Recombinant Plasmids and Cloning Vectors*

Routine cloning experiments were carried out using the *E. coli* vector pUC18 (Yanisch-Perron *et al.*, 1985) (Invitrogen). The donor vector pDONR201 (Life Technologies) was used to create entry clones when using GATEWAY™ Cloning Technology. pMAL-c2 (Ausubel *et al.*, 1994) (NEB), and the pGEX series of plasmids (Guan and Dixon, 1991, Smith, 1988) (Amersham Pharmacia Biotech) were used to facilitate the overexpression and purification of recombinant MBP and GST fusion proteins, respectively. All plasmids used in this study are shown in Appendix 2.

2.4 *Culture of* P. falciparum in vitro

2.4.1 *Culture Media for* P. falciparum

All culture procedures for *P. falciparum* were carried out under aseptic conditions. All solutions were filter sterilised (0.22 μm filter) or autoclaved before use.

Incomplete RPMI media was prepared by using sterile water for irrigation (Baxter Healthcare) supplemented with 10x RPMI-1640 (Gibco BRL), sodium bicarbonate (14 mM) (Pharmacia & Upjohn), gentamicin sulphate (40 μg/ml) (Pharmacia & Upjohn), glucose (11 mM) (Ophthalmic Laboratories), glutamine (1 mM) (Sigma-Aldrich), HEPES (N-2-hydroxyethylpiperazine-N'-2-ethanesulfonic acid) (25 mM) (Gibco BRL) and hypoxanthine (200 μM) (Sigma-Aldrich). The pH was adjusted to 7.4 with 2 M NaOH.

Complete RPMI media was prepared by supplementing incomplete RPMI media with AlbuMAX II (0.5% w/v) (Gibco BRL) and re-adjusting the pH to 7.4 with 2 mM NaOH. Complete and incomplete RPMI media were stored at 4°C for a maximum of one month.

2.4.2 *Preparation of Human Erythrocytes for* P. falciparum *Culture*

Venous blood was collected from healthy individuals into the anticoagulant $CPDA_1$ (89 mM trisodium citrate dihydrate, 17 mM citric acid monohydrate, 16 mM sodium dihydrogen phosphate monohydrate, 177 mM dextrose, 2 mM adenine, pH 5.6-5.8; 0.14 ml $CPDA_1$ per ml of whole blood). Whole blood was stored at 4°C for maximum of one month.

Washed erythrocytes were prepared by the centrifugation of whole blood at 2000 *g* for 5 minutes (min). The upper plasma and buffy coat layers were removed, the erythrocytes washed in sterile phosphate buffered saline (PBS) (Oxoid) and centrifuged for a further 5 min at 2000 *g*. Erythrocytes were then resuspended to 50% haematocrit (where haematocrit is the volume of packed erythrocytes in relation to the total volume of a solution) with complete RPMI media and stored at 4°C for a maximum of one week.

2.4.3 P. falciparum *parasites and culture* in vitro

The parasite line 3D7 was used in this study (Walliker *et al.*, 1987). Parasites were maintained in continuous culture using standard procedures (Trager and Jensen, 1976; Trager and Jensen, 1978) in complete RPMI media (Cranmer *et al.*, 1997).

Parasites were cultured in 25 cm^2 or 75 cm^2 tissue culture flasks and maintained at 2-6% parasitaemia (number of parasitised erythrocytes per 100 erythrocytes expressed as a percentage). Culture media was replaced every 1-2 days to meet nutritional requirements of the parasites and washed erythrocytes added every 2-4 days to maintain fresh erythrocytes for merozoite reinvasion. The headspace of the flasks were gassed with 1% O_2, 5% CO_2 and 94% N_2 (BOC gases) prior to incubation in a dry 37°C incubator.

2.4.4 Determination of Parasitaemia and Stage of Parasite Maturation

The parasitaemia and stage of maturation was determined every 1-2 days by taking a sample from each flask and making a thin smear. A single drop of culture was placed onto a microscope slide and smeared with a second slide. The smears were air dried and methanol fixed for 2 min, then stained for 5 min with Giemsa Staining Solution (BHD) diluted 1:9 with Sorrensen's buffer (0.3 % (w/v) Na_2HPO_4, 0.06% (w/v) KH_2PO_4, pH 7.2). Thin smears were viewed on a bright field microscope (Leica) using a x100 oil immersion objective lens.

2.4.5 Synchronisation of Parasite Cultures Using Gelatine Flotation

During continuous culture, *P. falciparum* lines become asynchronous and may lose their knobby phenotype (Langreth *et al.*, 1979) due to spontaneous chromosome deletions (Culvenor *et al.*, 1987). Gelatine flotation (Goodyer *et al.*, 1994; Waterkeyn *et al.*, 2001) separates knobby, mature stage parasites from non-parasitised erythrocytes, ring stage parasites and knobless parasites, and leads to synchronisation of cultures. This procedure was carried out no less than once every two weeks to maintain knobby parasites.

When the parasite cultures were predominantly late stages, cultures were centrifuged at 400 *g* for 5 min and supernatant removed. The parasitised erythrocytes were resuspended to 50% haematocrit in incomplete RPMI media and 2 volumes of 1% (w/v) 175 bloom gelatin was added. The suspension was mixed and incubated at 37°C for 10–20 min, until two layers could be seen clearly. The resulting supernatant, containing knobby, mature parasites was transferred into 6 ml of incomplete RPMI media and centrifuged for 5 min at 650 *g*. The supernatant was removed and the parasite pellet resuspended with washed erythrocytes to a parasitaemia of 1-4% for continued culture.

2.4.6 Purification of Mature Stage Parasites by Percoll Density Gradient Purification

Synchronised, mature stage parasitised erythrocyte cultures were isolated at ≥99% parasitised erythrocytes using a Percoll density gradient. Initially a 10x RPMI supplemented with 250 mM Hepes solution was used to make a 90% Percoll stock solution (90% (v/v) Percoll™ (Density 1,130g/ml) (Amersham Pharmacia Biotech), 10% (v/v) 10x RPMI-Hepes). These stock solutions was used to make a 80% Percoll solution (80% (v/v) Percoll, 4% (w/v) sorbitol solution in 1x RPMI-Hepes), a 60% Percoll solution (60% (v/v) Percoll, 4% (w/v) sorbitol solution in 1x RPMI-Hepes) and a 40% Percoll solution (40% (v/v) Percoll, 4% (w/v) sorbitol solution in 1x RPMI-Hepes). 2 ml of 80% Percoll was placed in a 10 ml tube and 2 ml of the 60% Percoll layered carefully on top. 2 ml of 40% Percoll was layered on top of the 60% Percoll and up to 3 ml of 50% haematocrit parasitised erythrocytes were then layered on top of 40% Percoll. Gradients were spun at 2000 *g* for 10 min. Following centrifugation the top suspended layer contains free merozoites, the second suspended layer contains the erythrocytes infected with mature stage parasites and the bottom suspended layer and the pellet contain the erythrocytes infected with ring stage parasite and the uninfected erythrocytes. The layer containing the mature stage parasites was harvested and placed in a 10 ml tube. Complete media was added to the parasites drop wise, to avoid osmotic shock and the parasites were spun at 650 *g* for 5 min. A second wash in complete media was performed and a sample smeared to determine the percentage parasitaemia (Section 2.4.4).

2.5 DNA and RNA Purification and Manipulation

2.5.1 Preparation of Plasmid DNA from E. coli

Plasmid DNA was routinely isolated from liquid *E. coli* cultures using small scale alkaline lysis as detailed by Ausubel *et al.*, 1994.

Plasmid DNA for use in nucleotide sequencing reactions was precipitated in 0.1 volumes of 4 M NaCl and 2 volumes of 13% (w/v) PEG_{8000} for 30 min at -70°C. Plasmid DNA was recovered by centrifugation at 12,000 *g* for 15 min at 4°C and the resultant pellet washed in 70% (v/v) ethanol. The pellet was dried in a Savant Speed Vac Concentrator for 5 min and resuspended in ddH_2O.

2.5.2 Agarose Gel Electrophoresis

DNA fragments were resolved in 0.8-1% (w/v) agarose gels using MINI SUB™ DNA cell (BioRad). 1 x TAE (2 mM EDTA, 0.1% (v/v) glacial acetic acid, 40 mM Tris-HCl, pH 8.5) was used as the electrophoresis buffer. Electrophoresis was performed at 80-120 volts for 1-2 hour (hr). 500 ng of λ bacteriophage DNA digested with *Hin*dIII and *Eco*RI was loaded simultaneously as molecular size and concentration standards. Gels were stained with 5 μg/ml ethidium bromide solution for approximately 5 min and destained in water for approximately 20 min, before visualisation using a Spectroline® Ultraviolet Transilluminator. A Mitsubishi Video Copy Processor was used to take a permanent image of the gel.

2.5.3 Recovery of DNA from Agarose Gels

DNA was recovered from agarose gels using the BRESAclean® DNA purification kit (Bresatec) in accordance with manufacturer's instructions.

DNA fragments below 300 bp were purified by paper elution (Ausubel *et al.*, 1994). Following resolution of a DNA fragment by agarose gel electrophoresis, a piece of DE81 paper cut to size was inserted into the agarose gel below the band to be purified and the gel resolved further to allow the DNA to run into the paper. The paper was incubated in 400 μl of DEAE elution solution (10 mM Tris-HCl, pH 7.9, 1 mM EDTA, pH 8, 1M NaCl) and incubated at 70°C for 2 hr. The paper was removed from the solution and the eluted DNA spun for 15 min at 12,000 *g*. The resulting supernatant was ethanol precipitated (Section 2.5.4).

2.5.4 Precipitation of Plasmid DNA

DNA was recovered from solution by ethanol or isopropanol precipitation. 0.1 volumes of sodium acetate, pH 5.2 and 2.5 volumes of 100% ethanol or 1 volume of isopropanol were added to the DNA solution and incubated for 10 min on ice. The DNA was collected by centrifuging at 12,000 *g* for 10 min, supernatant removed and the DNA pellet was washed in 75% (v/v) ethanol. The pellet was dried in the Savant Speed Vac Concentrator for 5 min and resuspended in ddH_2O.

2.5.5 Phenol/Chloroform Extraction of DNA

When required, DNA was further purified by phenol-chloroform extraction. An equal volume of phenol:chloroform:isoamyl alcohol (25:24:1) was added to the DNA preparation, vortexed vigorously and the phases separated by centrifugation at 12,000 *g* for 1 min at room temperature. The aqueous phase was transferred to a new tube and the DNA isolated by isopropanol precipitation (Section 2.5.4).

2.5.6 Blunt End Modification of DNA fragments

DNA fragments were treated with T4 DNA polymerase 1 and T4 polynucleotide kinase to form blunt ends. DNA was incubated with of 1 mM ATP, 5 mM dNTPs, 10 units T4 Polynucelotide kinase and 1/10 volume of 10 x T4 DNA polymerase 1 buffer (0.5 M Tris-HCl, pH 7.5, 0.1 M $MgCl_2$, 10 mM DTT and 0.5 mg/ml BSA) in a 100 µl total reaction volume and incubated at 37°C for 1 hr. 10 units of T4 DNA polymerase 1 was then added to the reaction and incubated at room temperature for 15 min, before the addition of 1 µl 0.5 mM EDTA, pH 8.0. DNA was purified using a Phenol/Chloroform extraction (Section 2.5.5) and used in ligation reactions (Section 2.6.4).

2.5.7 Determination of DNA and RNA concentration

DNA concentration was calculated by resolution of a known volume by agarose gel electrophoresis and visual comparison of band intensity to a simultaneously resolved lane of DNA standards of known concentration (Section 2.5.2).

Alternatively, the concentration was measured using a CECIL CE 1020 spectrophotometer. The absorbance 260 nm (A_{260}) of the test solution was determined and the concentration of the DNA calculated by the following conversions: for double stranded DNA: A_{260} = 1 for a 50 µg/ml solution, or for oligonucleotides: A_{260} = 1 for a 33 µg/ml solution. RNA concentration was determined using a similar spectrophotometric conversion: A_{260} = 1 for a 40 µg/ml solution.

2.5.8 Restriction Endonuclease Digestion of DNA

Restriction endonuclease digestions were performed in accordance with the enzyme manufacturer's instructions, at the specified temperature and in the presence of the appropriate buffer. Duration of treatment varied from 1-1.5 hr for approximately 100 ng of plasmid DNA. Reactions were terminated by addition of 1/6 volume of 6x stop mix (50% (w/v) sucrose, 10 mM EDTA, 0.5% (w/v) bromophenol blue, pH 7.0).

2.5.9 Cracking Gel Procedure

This procedure enables detection of a shift in plasmid size due to insertion of a DNA fragment compared with a plasmid control, resulting in the identification of potential clones for further analysis. Following transformation, colonies are patched onto solid media and incubated overnight (O/N) at 37°C. Cracking gels were performed on patches no older than 3 days by resuspending colonies from the

patch into 15 µl of ddH_2O. 15 µl of cracking gel buffer (0.5% (w/v) SDS, 0.2M NaOH, 20% (w/v) sucrose plus a few grains of bromcresol green) was added to the resuspended cells and loaded onto agarose gels for resolution (Section 2.5.2).

2.5.10 Isolation of RNA from Malaria Parasites

Messenger RNA (mRNA) was extracted from *P. falciparum* parasites using the Quickprep Micro mRNA Purification Kit (Pharmacia Biotech) according to the manufacturer's instructions.

2.6 Recombinant DNA Techniques

2.6.1 Preparation of Oligonucleotide Primers

Oligonucleotide primers were synthesised using a 392 DNA/RNA Synthesiser (Applied Biosystems). Following synthesis, the oligonucleotides were deprotected by incubation at 55°C for 2 h and dried in a Heto Maxi-Dry Plus vacuum concentrator. Pellets were resuspended in 1 ml of ddH_2O and concentration of oligonucleotide primers was determined (Section 2.5.7). Appendix 3 lists the nucleotide sequences of oligonucleotide primers used in this study.

2.6.2 Annealing of Oligonucleotides

Two oligonucleotides were annealed at equal molar ratios using a PTC-200 DNA Engine (MJ Research). Oligonucleotides were heated to 80°C and cooled 5°C every 3.5 min to 10°C before a 4°C hold.

2.6.3 Polymerase Chain Reactions (PCR)

PCR was used to amplify DNA using a PTC-200 DNA Engine (MJ Research). High fidelity PCR was performed using ProofStart® DNA Polymerase (Qiagen) according to the manufacturer's instructions. Reactions were performed in a 100µl volume containing approximately 60-100ng of genomic DNA or 1-4 ng of plasmid DNA, 1 µM of each primer, 300 µM dNTPs (MBI) and 5 units of enzyme. The temperature program routinely used consisted of an initial Activation step of 5 min at 95°C followed by 10-35 cycles of Denaturation at 94°C for 30 sec, Annealing at 45-55°C for 30 sec (dependent upon annealing temperature of primers used) and Extension at 72°C for 30 sec.

2.6.4 Ligation of DNA Fragments

DNA fragments were ligated for cloning using T4 DNA ligase (Promega) according to the manufacturer's instructions. Routinely, DNA fragments vector and insert were incubated at a ratio of 1:5 with 3 units of T4 DNA polymerase and 0.1 volumes of 10x ligase buffer supplied by the manufacturer. Ligations were carried out at room temperature for 3 hr or O/N at 16°C.

2.6.5 Reverse Transcriptase-PCR (RT-PCR)

Reverse transcriptase was performed with the Superscript II Kit (Gibco BRL) according to the manufacturer's instructions. Briefly, a mixture containing 3 µg of RNA and 0.5 µg of oligo $(dT)_{17}$ was heated to 70°C for 10 min and cooled on ice. 4 µl of 5x first strand buffer (250 mM Tris-HCl, pH 8.3, 375 mM KCl, 15 mM $MgCl_2$), 2 µl of 0.1 M DTT, 2 µl of 5 mM dNTPs and 1 µl of RNase inhibitor (Promega) was added to the mixture and the reaction incubated at 42°C for 2 min. Following the addition of 1 µl of Superscript II RNase H⁻ Reverse Transcriptase (RT), the reaction was incubated at 42°C for a further 50 min. The reaction was inactivated at 70°C for 15 min, boiled for 5 min and diluted to 40 µl with dH_2O before being stored at -20°C. As a negative control, a parallel reaction was set up without the addition of oligo $(dT)_{17}$ and RT. PCR reactions were performed as described in Section 2.6.3 using 1 µl of reverse transcribed complementary DNA (cDNA).

2.7 Site Specific Recombination Using GATEWAY™ Cloning Technology

All reagents used with the GATEWAY™ Cloning Technology were supplied by Life Technologies.

2.7.1 Modification of pMAL vector to GATEWAY™ Destination Vector

pMAL-c2 (NEB) was modified to a GATEWAY™ Destination Vector in accordance with manufacturer's instructions. Firstly pMAL-c2 was digested with *Eco*RI and *Hind*III (Section 2.5.8) and blunt end filled (Section 2.5.6). 50ng of vector and 10 ng of cassette b were ligated (Section 2.6.4) and used to transform DB3.1 heat shock competent cells (Section 5.1.2). Transformations were spread onto LB plates containing chloramphenicol (Section 2.2) and screened using standard techniques (Section 2.9). The resulting pDEST-MAL vector was designated pMC925.

2.7.2 Purification of GATEWAY™ Vectors

GATEWAY™ Vectors were purified using the Concert™ Purification System (Life Technologies) according to the manufacturer's instructions. pDEST-MAL (pMC925) was linearised with *Eco*RI and pDONR201 was checked for majority supercoiled DNA. Preparations were quantified by spectrophotometry (Section 2.5.7) and used for BP and LR Reactions.

2.7.3 Purification of attB PCR Products

100 µl *att*B PCR reactions were resuspended in 150 µl of TE (10 mM Tris, 1 mM EDTA, pH8.0) and 30% PEG 8000/30 mM $MgCl_2$. Reactions were mixed and centrifuged at room temperature for 15 min at 10,000 *g*. The supernatant was removed and the DNA dissolved in 50 µl TE.

2.7.4 Cloning of PCR products via a BP Reaction

BP reactions were performed in accordance with manufacturer's instructions. Briefly, 4 µl of BP Reaction Buffer, up to 500 ng of *att*B-PCR product, 300 ng of pDONR201 vector, 4 µl of BP Clonase Enzyme Mix and TE up to 20 µl were incubated at 25°C for 1 hr. 2 µl of Proteinase K Solution was added and reactions further incubated for 10 min at 37°C. 1 µl of reactions was used to transform DH5α heat shock competent cells (Section 5.1.2) and plated onto LB plates containing kanamycin (Section 2.2). Resulting kanamycin resistant colonies should contain entry clones and were screened using standard techniques (Section 2.9).

2.7.5 Creation of Expression Clones via a LR Reaction

LR reactions were performed in accordance with manufacturer's instructions. Briefly, 4 µl of LR reaction buffer, 100-300 ng Entry Clone, 300 ng destination vector, 4 µl of LR CLONASE Enzyme Mix and TE up to 20 µl volume were incubated at 25°C for 1 hr. 2 µl of Proteinase K Solution was added and reactions further incubated for 10 min at 37°C. 1 µl of the reaction was used to transform DH5α heat shock competent cells (Section 5.1.2) and transformations plated onto LB plates containing ampicillin (Section 2.2). Resulting ampicillin resistant colonies should contain Expression Clones and were screened using standard techniques (Section 2.9).

2.7.6 Cloning of PCR products and Creation of Expression Clones via the "one tube" protocol

PCR products were cloned directly into destination vectors via a two step reaction in a single tube. Briefly, the BP reaction (Section 2.7.4) was performed at 25°C for 3-4 hr and 1 µl of 0.75 M NaCl, 3µl of 150ng/µl Destination vector and 6 µl of LR CLONASE Enzyme Mix added to the reaction. 5 µl of this reaction was removed and incubated with 0.5 µl of proteinase K solution for 10 min at 37°C and 1 µl used to transform DH5α heat shock competent cells (Section 5.1.2) for the recovery of entry clones. The remaining 25 µl of reaction mixture was incubated at 25°C for 1-2 hr. 2.5 µl of Proteinase K Solution was added to the mixture and incubated at 37°C for 10 min before 1 µl was used to transform DH5α heat shock competent cells for the recovery of expression clones. Transformations containing the Entry Clones and Expression Clones were plated onto LB plates containing kanamycin and ampicillin, respectively (Section 2.2).

2.8 Transformation Procedures

5.1.1 Preparation of Heat Shock rubidium chloride-competent E. coli

Rubidium chloride (RbCl)-competent *E. coli* DH5α (Bethesda Research) and BL21 (DE3) (Novagen Inc.) cells were prepared using the method described by Hanahan (1985) . The appropriate *E. coli* strain was subcultured on SOB (10 mM NaCl, 2.5 mM KCl, 2% (w/v) Tryptone, 0.5% (w/v) Yeast Extract) agar and grown at 37°C for 16-20 h. Ten colonies were resuspended in 1 ml of SOB broth, mixed thoroughly by vortexing and subsequently used to inoculate a 2 L flask containing 100 ml of SOB broth, to which 1 ml of a Mg^{2+} solution (1 M $MgCl_2$, 1 M $MgSO_4$) had been added. The cells were grown at 37°C with moderate agitation until the turbidity of the culture at 600 nm was 0.3. The culture was then transferred to sterile 50 ml tubes and chilled on ice for 10-15 min. The tubes were then centrifuged at 12,000 *g* for 15 min at 4°C, the supernatant was discarded and the cell pellet thoroughly drained by inverting the tube. The pellet was resuspended in 0.33 volumes of filter sterilised RF1 (10 mM RbCl, 50 mM $MnCl_2$, 30 mM potassium acetate, 10 mM $CaCl_2$, 15% glycerol, pH 5.8), mixed by moderate vortexing and incubated on ice for 1 h. The cells were centrifuged as before and the resulting cell pellet was resuspended in filter sterilised RF2 (8 mM RbCl, 75 mM $CaCl_2$, 10 mM 3-(N-Morpholino) propane-sulfonic acid (MOPS), 15% glycerol, pH 6.8) to 1/12.5 of

the original volume. The suspension was then incubated on ice for 15 min, dispensed as 100 µl aliquots into pre-chilled microfuge tubes and snap frozen in a dry ice/ethanol bath. The cells were stored at -70°C until use.

5.1.2 Transformation of Heat Shock competent E. coli

DNA was preincubated with the heat shock competent cells for 30 min on ice. Heat shock was performed at 42°C for 90 sec and followed by 2 min on ice. Cells were immediately resuspended in 500 µl of SOC medium and incubated at 37°C for 1 hr. Aliquots of the transformation mix were plated onto antibiotic supplemented solid LB media, with the addition of X-gal as required and incubated at 37°C O/N.

2.9 Screening of Recombinant Bacterial Clones

Appropriate antibiotic resistant bacterial clones were initially screened for plasmid content using the small scale alkaline lysis method of plasmid isolation (Section 2.5.1) and consequent restriction endonuclease digests (Section 2.5.8). After resolution of the digested fragments in an agarose gel and observation of the anticipated size insert, possible clones were selected for further analysis.

In instances were cloning frequency was low, large numbers of antibiotic resistant clones were screened using the cracking gel procedure (Section 2.5.9). Possible clones were confirmed using nucleotide sequencing (Section 2.9.1).

2.9.1 Automated Nucleotide Sequencing

Nucleotide sequencing was performed in accordance with PRISM Ready Reaction DyeDeoxy Terminator Cycle Sequencing Kit (Applied Biosystems). Following thermal cycling, dye terminator products were ethanol precipitated prior to resolution using 373A DNA sequencer STRETCH (Applied Biosystems).

2.9.2 Computer Aided Analysis of DNA sequences

Nucleotide sequence data was analysed using Sequencher™ 3.1.1 (Gene Codes Corporation, Ann Arbor, USA). Oligonucleotide primers were designed with the aid of Amplify 1.2 (William Engels, University of Wisconsin, USA). Nucleotide sequences were compared to sequences in Genbank and The Institute for Genomic Research (TIGR) using BLASTN (Altschul *et al.*, 1997).

2.10 Cloning Procedures for Cloning PfEMP3 fragments

2.10.1 Cloning of PfEMP3 fragments

PCR primers were designed for the cloning of PfEMP3-FI, -FII, -FIII, -FIV and -FV into a pMAL vector. Primers and cloning procedures are outlined in Appendix 3 and 2, respectively and procedures were performed by V. Gatzigiannis and J. Bettadapura (Monash University). Resultant clones were pMC754, pMC755, pMC756, pMC757 and pMC758, respectively.

2.10.2 Cloning of PfEMP3-FI Sub-Fragments

PCR primers were designed for the cloning of PfEMP3-FIa and –FIb into a pMAL vector. Primers and cloning procedures are outlined in Appendix 3 and 2, respectively and procedures were performed by J. Bettadapura (Monash University). Resultant clones were pMC798 and pMC799, respectively.

2.10.3 Cloning of PfEMP3-FIa Sub-Fragments

PCR primers were designed for cloning of four PfEMP3-FIa sub-fragments, PfEMP3-FIa.1, -FIa.2, -FIa.3 and -FIa.4. Forward primers contained a *Bam*HI site and reverse primers contained an *Eco*RI site and a stop codon. Primer pairs for each of the fragments were p766/p994, p995/p996, p997/p998 and p999/p942, respectively (primers designed by K. Waller, Monash University). Using these primers, PCR fragments were amplified from pMC798 and single products resolved by agarose gel electrophoresis. Bands were excised from the gel and purified by the geneclean method. Ends were modified to blunt ends and fragments ligated into *Sma*I pUC18 via a standard ligation reaction (Sections 2.5 and 2.6). *E. coli* DH5α cells were transformed to ampicillin resistance and resultant colonies screened for clones containing an insert of the correct size (Sections 2.8 and 2.9). For each sub-fragment, a single pUC18 clone was chosen, pMC839, pMC841, pMC843 and pMC845 respectively, and digested *Bam*HI/*Eco*RI. Digested DNA was run on an agarose gel, the appropriate band cut from the gel and purified using the geneclean method. Fragments were ligated with modified pMAL vector pMC629 and used to transform *E. coli* DH5α cells to ampicillin resistance. Resultant colonies were screened for the correct size insert using restriction digests and possible clones were used in sequencing reactions to confirm both the sequence and reading frame of the insert.

Clones, pMC840, pMC842, pMC844 and pMC846 were used to transform *E. coli* BL21(DE3) to ampicillin resistance and resultant strains RCM1222, RCM1225, RCM1228 and RCM1231 were used for protein expression and purification (Section 2.16).

2.10.4 Cloning of PfEMP3-Fla.1 Deletion

PfEMP3-FIaΔFIa.1 region was PCR amplified from 3D7 gDNA using primers p995/p942 and cloned into the pMAL modified vector pMC629 using the procedure outlined in Section 2.10.3. The resultant clone, pMC903 was used to transform *E. coli* BL21(DE3) to ampicillin resistance and the resultant strain RCM1222 used for protein expression and purification (Section 2.16).

2.10.5 Cloning of PfEMP3 N-Terminal Deletions

Primers (p1107, p1108 and p1109, respectively) were used in conjunction with reverse primer p1110 for PCR amplification of N-terminal deletions of PfEMP3. All four primers were designed with *att*B sites for use with GATEWAY™ Cloning Technology. For cloning into pMAL with site specific recombination using the GATEWAY™ Cloning Technology, the pMAL-c2 vector was converted to a destination vector (Section 2.7.1), resulting in pDEST-MAL (pMC925).

Following PCR amplification, gene fragments were purified using PEG/$MgCl_2$ (Section 2.7.3) and used to create entry clones via a BP reaction with the pDONR201 vector (Section 2.7.4). Subsequent entry clones, pENTR201-FIaΔ15, pENTR201-FIaΔ29 and pENTR201-FIaΔ45 (pMC932, pMC933 and pMC934, respectively) were used to create expression clones via a LR reaction using the 'one tube protocol' (Section 2.7.6) with pDEST-MAL. Clones, pEXPMAL-FIaΔ15, pEXPMAL-FIaΔ29 and pEXPMAL-FIaΔ45 (pMC941, pMC942 and pMC943, respectively) were used to transform *E. coli* BL21(DE3) competent cells to ampicillin resistance and subsequent strains (RCM1382, RCM1385 and RCM1388, respectively) were used in protein expression and purification as described in Section 2.16.

2.10.6 Cloning of PfEMP3-Fla.1 Sub-Fragments

The pMAL-c2 vector was modified for this cloning procedure to create a stop codon at the end of the multiple cloning site. pMAL-c2 vector was digested *Eco*RI/*Xba*I and then blunt end filled. Blunt ends were then religated, recreating the *Eco*RI site and creating a stop codon directly preceding this site. This new vector is designated pMC910. Oligonuclotides p1211 and p1212 were annealed

(Section 2.6.2) to create a double stranded DNA fragment consisting of the nucleotides of PfEMP3 second exon that encode residues 16-29 and a sticky ended *Eco*RI site at either end. This fragment was ligated into pMC910 and a clone was selected by standard procedures (Section 2.9). PfEMP3-16-45, -16-60 and -1-16 were PCR amplified from pMC798 DNA using the oligonucleotide pairs p1236/p1237, p1236/p1238 and p1245/p1246. PCR product was purified using paper elution and digested with *Eco*RI/*Hin*dIII and ligated into *Eco*RI/*Hin*dIII pMAL-c2 vector. Clones were screened and selected as described in Section 2.9. Clones for PfEMP3-16-29, -16-45, -16-60 and -1-16, designated pMC990, pMC1009, pMC1010 and pMC1011, respectively were used to transform *E. coli* BL21 (DE3) to ampicillin resistance and resultant strains (RCM1457, RCM1483, RCM 1485 and RCM1487, respectively) were used in protein expression and purification as described in Section 2.16.

2.11 Cloning of Pf332 Fragments

For cloning into pMAL vectors, the Pf332 gene was divided into 23 gene fragments. Three fragments from the first exon are designated E1, E2 and E3, where E represents the first exon. Twenty fragments from the second exon are designated 1 through 20. For each of the second exon fragments oligonucleotides primers were designed in the forward and reverse orientation that included an *Eco*RI site and an *att*B site (p1159-p1199). This allowed for site specific recombination using GATEWAY™ Cloning Technology (Section 2.7), as well as the ability to utilise the *Eco*RI site for conventional cloning procedures (Section 2.5 and 2.6). Oligonucleotides were designed for fragment E1, E2 and E3 (p1353/p1354, p1365/p1438 and p1439/p1356, respectively) which included a *Bam*HI site in the forward oligonucleotide and a *Xho*I site in the reverse oligonuclotide for the cloning of these three fragments into a pMAL vector using conventional cloning procedures.

Figure 2.1 shows a flow diagram describing the various cloning procedures as discussed below.

2.11.1 Cloning with Site Specific Recombination Using GATEWAY™ Cloning Technology

Initially fragments from the second exon were PCR amplified from 3D7 genomic DNA and gene fragments purified using PEG/$MgCl_2$. Purified gene fragments were used to create entry clones via a BP reaction with the pDONR201 vector. Entry clones were obtained for fragments 1, 3, 5, 8, 9, 10 and 12

designated pDONR201-Pf332-frag1, pDONR201-Pf332-frag3, pDONR201-Pf332-frag5, pDONR201-Pf332-frag8, pDONR201-Pf332-frag9, pDONR201-Pf332-frag10 and pDONR201-Pf332-frag12 (pMC970-976, respectively). Due to difficulties using the GATEWAY™ Cloning Technology to obtain an entire set of entry clones, conventional procedures were then used to clone the fragments into a pMAL vector

2.11.2 Cloning using Conventional Procedures

Following amplification, products for fragments 2, 4, 6, 7, 11, 13, 14 and 16-19 were run on agarose gels and purified using the geneclean method. Purified fragments were digested with *Eco*RI and repurified with Phenol/Chloroform followed by isopropanol precipitation (Sections 2.5 and 2.6). Resultant fragments were ligated with *Eco*RI pMC901 (pMAL vector modified to contain a stop codon following the *Eco*RI site) (Section 2.10.6). Clones were screened for those with inserts using standard procedures (Section 2.9). Clones with correct size insert were sequenced and subsequent clones designated pMC1053, pMC1055, pMC1057, pMC1058, pMC1062, pMC1064, pMC1065, pMC1068, pMC1069, pMC1070 and pMC1071, respectively.

For fragments 15 and 20, the above method was performed on three occasions and with over 100 colonies screened, no clones containing the correct size insert were isolated. Therefore, fragments were modified to blunt ends (Section 2.5.6) and repurified with Phenol/Chloroform followed by isopropanol precipitation. Resultant fragments were ligated with *Sma*I pUC18 and screened using standard procedures. Resultant clones, pMC1066 and pMC1072 were digested with *Eco*RI and the Pf332 gene fragment purified by geneclean. This fragment was used in a ligation with *Eco*RI pMC910 and resultant clones screened using standard procedures. Clones with correct size insert were sequenced and subsequent clones designated pMC1067 and pMC1073.

In addition to this, entry clones from Section 5.4.1 were used to create clones for fragments 1, 3, 5, 8, 9, 10 and 12 that did not contain sequence from *att* sites. pMC970-976 were digested with *Eco*RI and the resultant Pf332 gene fragment was purified as described above. Gene fragments were ligated with pMC910 and resultant clones screened using standard procedures. Clones for fragments 1, 3, 5, 8, 9, 10 and 12 were designated pMC1052, pMC1054, pMC1056, pMC1059, pMC1060, pMC1061 and pMC1063.

Pf332 fragments E1, E2, and E3 were PCR amplified and fragments purified by geneclean. Fragments were then digested with *Bam*HI and *Xho*I before repurification by Phenol/Chlorophorm and Isopropanol precipitation. Fragments were ligated with pMC629 (pMAL-c2 vector with modified multiple cloning site) and

cloned were screened using standard procedures. Clones for fragments E1, E2 and E3 were designated pMC1189, pMC1191 and pMC1192.

2.12 Sodium Dodecyl Sulphate-Polyacrylamide Gel Electrophoresis (SDS-PAGE)

2.12.1 Preparation of Recombinant Protein Samples

Samples for SDS-PAGE were prepared in reducing 2x sample buffer (20% (v/v) glycerol, 1% (w/v) SDS, 25% (v/v) stacking gel buffer, 0.1 mg/ml bromophenol blue, plus 2% (v/v) 14.3M 2-mercaptoethanol). Dilutions of purified recombinant proteins were prepared and 2 μg of recombinant protein was loaded onto SDS-PAGE for Coomassie Brilliant Blue staining and 50 ng of recombinant protein was loaded onto SDS-PAGE for immunoblot analysis. All samples were boiled for 5 min prior to loading along side Precision markers (BioRad).

2.12.2 Preparation of Samples from P. falciparum Infected Erythrocytes

Both washed erythrocytes and mature parasitised erythrocytes purified by Percoll density gradients (Section 2.4.6) were resuspended 1/10 in reducing 2x sample buffer for resolution on SDS-PAGE.

Alternatively, mature parasitised erythrocytes purified using Percoll density gradients (Section 2.4.6) were extracted with Triton X-100 (t-octylphenoxypolyethoxyethanol) to separate soluble and insoluble proteins. 45 μl of purified infected erythrocytes were extracted in 1.5 ml of 1% (v/v) Triton X-100 in the presence of the Complete, Mini protease inhibitor cocktail (Roche) for 10 min on ice. Samples were spun at 12,000 *g* for 5 min and supernatant transfer to a new tube. Pellet was resuspended 1/10 in reducing 2x sample buffer and supernatant diluted 6/1 in reducing 6x sample buffer (30% (v/v) glycerol, 4% (w/v) SDS, 70% (v/v) stacking gel buffer, 0.3 mg/ml bromophenol blue, plus 2% (v/v) 14.3M 2-mercaptoethanol)

2.12.3 SDS-PAGE

SDS-Page was performed using a Mini-PROTEAN® III CELL (BioRad) in accordance with the manufacturer's instructions in SDS-PAGE running buffer (1% (w/v) SDS, 12.5 mM Tris and 96 mM glycine). Resolving gels of 7.5 % (w/v), 10 % and 12 % polyacrylamide were used in this study. Polyacrylamide gels were poured using the appropriate volume of 40% (w/v) acrylamide stock (37.5:1,

acrylamide:N,N'-methylene-bis-acrylamide) (BioRad), 0.1% SDS, 375 mM Tris-HCl, pH 8.8, 0.1% ammonium peroxodisulfate and 1 µl/ml N,N,N'N'-Tetra-methylethylenediamine (TEMED). Once poured, the resolving gel was overlayed with water-saturated butanol (equal volumes of Tertiary butanol and ddH_2O). Once the resolving gel was set, water saturated butanol was washed away with ddH_2O and a 4% (w/v) polyacrylamide stacking gel poured using the appropriate volume of 40% (w/v) acrylamide stock, 0.1% SDS, 125 mM Tris-HCl, pH 6.8, 0.1% ammonium peroxodisulfate and 1 µl/ml TEMED. Gels were run at 100-200 volts for 1-2 hr or until samples had just run off the gel.

2.12.4 Acrylamide/Agarose Composite SDS-PAGE

Acrylamide/Agarose composite gels were performed for the resolution of large proteins and performed as described by Wiesner *et al.* (1998) with modifications. 0.5% agarose was dissolved in 375mM Tris, pH 8, allowed to cool at 55°C and made up to volume with 3% acrylamide (37.5:1, acrylamide:,N'-methylene-bis-acrylamide), 0.1% SDS, 0.1% Ammonium peroxodisulfate and 1 µl/ TEMED. Gels were poured (without a stacking gel) and run as per Section 2.12.3.

2.13 Coomassie Brilliant Blue Staining of Polyacrylamide Gels

Coomassie Brilliant Blue stain (0.15% (w/v) Coomassie Brilliant Blue, 25% (v/v) isopropanol, 7% (v/v) glacial acetic acid) was used to visualise proteins on polyacrylamide gels. Gels were typically stained in Coomassie Brilliant Blue stain for 30-60 mins and destained in Coomassie destain (10% (v/v) glacial acetic acid and 40% (v/v) methanol). Gels were soaked in water before drying between wet cellophane for permanent storage.

2.14 Immunoblotting

Immunoblotting was used in this study for the detection of specific proteins. The method used was that recommended by NEN™ Life Science Products. Electrophoretic transfer of proteins from SDS-PAGE gels to Polyscreen® PVDF Transfer Membrane (NEN™) was achieved using a Trans Blot® Cell (BioRad) containing transfer buffer (0.19 M glycine, 10% (v/v) methanol and 25 mM Tris-HCl, pH 8.3) at 75-100 volts for 1-4 hr at 4°C, in accordance with the manufacturer's instructions. For large proteins 0.01-0.02% SDS was added to the transfer buffer. The membrane was then placed a blocking buffer of 5% (w/v) skim milk powder in TBS-Tween 20 (0.15 M NaCl, 0.05 M Tris-HCl, pH 7.4 containing 0.05% (v/v) Tween-20 (Polyoxyethylene-20-Sorbitan Monolaurate) (Amresco)). Blocking was conducted for 1h at room temperature or O/N at 4°C.

Detection of immunoblots was in accordance with manufacturer's instructions using *Renaissance*® Western Bot Chemiluminescence Reagent (NEN™). Fuji Medical X-ray film was exposed to the membrane (5 seconds to 1 hr) and the film developed using a Fuji FPM-100A Film Processor.

2.15 Antisera

Antisera used in immunoblotting (Section 2.14) were diluted in 3% (w/v) BSA/TBS-Tween 20. Uses, dilutions and the source of antisera are detailed in Appendix 4.

2.16 Recombinant Protein Expression

2.16.1 Expression and Purification of MBP Fusion Proteins

pMAL plasmid constructs were used for the large scale expression and purification of MBP fusion proteins as described by Ausubel *et al.*, 1994.

Starter cultures of Superbroth were inoculated with the BL21 (DE3) strain containing the appropriate pMAL plasmid construct and incubated O/N at 37°C with shaking. Superbroth cultures were inoculated 1/10 with starter cultures and incubated for 1.5 hr or until A_{600} = 0.5-0.6. Following induction of cultures with 0.1-1mM IPTG, cultures were incubated for a further 3 hr at 37°C or O/N at 16°C. The cells were then centrifuged at 10,000 *g* for 10 min, at 4°C, in a RC5 Sorvall centrifuge using a GSA rotor. Following a wash with 1x Column buffer (20mM Tris, 0.2M NaCl, 1mM EDTA, pH 7.4), the pellet was frozen at -70°C O/N.

Thawed cells were resuspended in Column Buffer before disruption using a French Pressure Cell with between 8000-9000LBS/square inch. Lysate was centrifuged at 17,000 *g*, for 15 min, at 4°C in a RC5 Sorvall centrifuge with an SS34 rotor. Supernatant was transferred to a new SS34 tube and re-centrifuged before binding to Amylose Resin.

Amylose Resin was prepared by taking 2ml of the Amylose Resin Slurry (NEB) and performing 3x washes in Column Buffer with centrifugation at 600 *g* for 5 min at 4°C. Recombinant MBP Fusion Proteins were bound to the Amylose resin by incubation of the supernatant from French Pressure Cell lysate with the Amylose Resin for 1 hr at 4°C with rotation.

Following 3x washes with Column buffer with centrifugation as above, the Amylose Resin was allowed to settle in a 2.5x10cm column. Once settled, excess Column Buffer was allowed to flow through the column. Recombinant MBP fusion proteins were eluted with 10ml Column Buffer/10mM Maltose. 10x 1 ml fractions

were collected and purified proteins resolved using SDS-PAGE and proteins visualised with Coomassie stain.

2.16.2 Expression and Purification of GST Fusion Proteins

Large scale expression and purification of GST fusion proteins was carried out on pGEX plasmid constructs as outlined for MBP fusion proteins (Section 2.16.1). PBS (10 mM NA_2HPO_4/NaH_2PO_4, pH 7.4, 0.15 M NaCl) was used instead of Column buffer and Glutathione Agarose were used to bind the GST fusion proteins. GST fusion proteins were eluted in 10 ml of 50 mM reduced glutathione and 100 mM Tris, pH 9.4.

2.16.3 Dialysis of Recombinant Proteins

Following purification, peak fractions of recombinant proteins were pooled and then dialysed against 1x PBS. The appropriate dialysis tubing was chosen given the protein molecular weight and volume of solution. Tubing was then pre-soaked in H_2O for 15 mins. One end of the tubing was sealed and the tubing checked for leaks, before the addition of protein and sealing of the second end. Dialysis was carried out with an O/N incubation, followed by a change in buffer and a further 3 hr incubation.

2.16.4 Concentration of Recombinant Proteins

Recombinant proteins were concentrated through an Ultrafree®-15 Centrifugal Filter Device (Millipore Corporation) with a 30 K Nominal Molecular Weight Limit by centrifugation at 2000 *g* at 4°C. Proteins were concentrated down to between 100 µl and 2 ml, dependent on the amount of protein in solution. Total protein concentration was determined using the Bradford Assay (BioRad) as per the manufacturer's instructions.

2.17 Preparation of Inside-out Vesicles (IOVs)

Inside-out Vesicles were prepared by the vesiculation and resealing of ghosts prepared from human erythrocytes, adapted from the procedure described by Steck & Kant, 1974.

Approximately 5ml of packed whole blood collected from healthy individuals was resuspended to 10 ml in incomplete RPMI media and centrifuged at 2000 *g* for 5 min. Plasma supernatant and the buffy coat layer were removed and discarded.

The pelleted erythrocytes were resuspended once again to 10 ml with Incomplete RPMI Media and centrifuged at 1000 *g* for 5 min. Supernatant and remaining buffy coat were removed and discarded and the wash repeated twice

more. Pelleted erythrocytes were finally washed in 1x PBS and centrifuged for 5 min at 650 *g* and the supernatant discarded.

Approximately 1 ml of washed erythrocytes were transferred to a glass Corex tube and lysis initiated by the addition of 20 ml of ice cold 5 mM Phosphate Buffer, pH 8.0. Erythrocytes were resuspended by inversion ten times and centrifuged in a RC5 Sorvall centrifuge at 12,000 *g* in a SS34 rotor, for 10 min, at 4°C. The supernatant was discarded and the lysis step was repeated three times or until all haemoglobin depleted and ghosts were a creamy white colour.

Once the ghosts were clean, the membranes were transferred to a new glass Corex tube leaving behind the contaminating protease pellet that forms under the membranes upon centrifugation. The membranes were rewashed in 20 ml of ice cold 5 mM Phosphate Buffer, pH 8.0 and supernatant discarded.

To vesicularise the membranes are diluted in 20 ml ice cold 0.5 mM Phosphate Buffer, pH 8.0 and incubated on ice for 30 min. The membranes were then centrifuged at 12,000 *g* for 30 min at 4°C and vesicularised by passing through a 21 gauge needle fairly aggressively 10 times.

10 ml of ice cold 0.5 mM Phosphate Buffer, pH 8.0 was added to vesicularised membranes, mixed by inversion and centrifuged at 12,000 *g* for 20 min at 4°C. The supernatant was discarded and the pelleted IOVs resuspended in 2 ml of ice cold Incubation Buffer (IB) (183 mM NaCl, 5 mM KCl, 6 mM Na_2HPO_4, 5 mM glucose). IOVs were stored at 4°C and used within one week. For Protein Interaction Assays, IOV preparations were then diluted 1/5 in IB.

2.17.1 *Preparation of IOVs from* P. falciparum *Parasitised Erythrocytes (pIOVs)*

Mature infected erythrocytes were isolated by Percoll gradient (Section 2.4.6) at more than 99% parasitised erythrocytes and used for preparation of pIOVs. pIOVs were typically prepared as described for normal IOVs (Section 2.11) from approximately 100 µl of parasitised erythrocytes. The resultant pIOVs remained brown in colour and could not be separated from the contaminating pellet. pIOVs were diluted in 200 µl of ice cold IB, stored at 4°C and used within one week. For protein interaction assays, pIOV preparations were diluted 1/5 in IB.

2.18 Solid Phase Microtitre Plate IOV Interaction Assay

The IOV Interaction Assays were performed as previously described by Kun *et al.*, 1999 and as briefly described below (Figure 2.2). All O/N incubations were performed in a humidified box at 4°C.

2.18.1 Coating of Wells with IOVs

A 96-well microtitre plate was firstly prelabelled with the contents of each set of triplicate wells. To the corresponding wells, 50 µl of IOVs (diluted 1/5) was added to the first triplicate of wells and 50 µl Blocking Buffer (5% (w/v) BSA in IB) added to the next triplicate set of wells before incubation O/N.

2.18.2 Blocking of Wells with Blocking Buffer

Aliquots of IOVs and BSA were aspirated and discarded. Into each well, 200 µl of Blocking Buffer was added and the plate incubated O/N.

2.18.3 Addition of Recombinant Fusion Protein to the Wells

Aliquots of Blocking Buffer were removed from each well and each well was washed twice with IB. 2-5 µg of interacting protein diluted to 50 µl of IB/0.05% (v/v) Tween-20, was added to the appropriate wells and the plate incubated O/N.

2.18.4 Elution of Bound protein from Wells

Aliquots of protein were removed from the wells and each well washed 5x with 200 µl of IB. Each triplicate set of interactions were eluted from the wells in a total of 50 µl of pre-warmed (70°C) reducing 2x sample buffer, resolved using SDS-PAGE (Section 2.12.3), transferred to PVDF membrane and detected using the appropriate antibody in immunoblot analysis (Section 2.14).

2.19 Solid Phase Microtitre Plate Spectrin Interaction Assay

Spectrin interaction assay was performs as per IOV interaction assay (Section 2.18). PBS was used instead of IB and 100-200ng of purified spectrin from human erythrocytes (Sigma) was used to coat the wells of the microtitre plate.

2.19.1 Competition Solid Phase Microtitre Plate Spectrin Interaction Assay

Competition assays were performed as described in Section 2.19. Recombinant fusion protein was preincubated with 10-200 fold molar excess of a competing recombinant fusion protein before addition to the wells for 2 hr at 4°C. Proteins were diluted in either PBS or PBS/0.05% (v/v) Tween 20.

2.20 Interaction Assays using Resonant Mirror Detection Biosensor

Protein-protein interactions were studied using the resonant mirror detection method (Cush *et al.*, 1993; George *et al.*, 1995; Watts *et al.*, 1994) of the IAsys™ (Affinity Sensors, Cambridge, U.K.). The dissociation constant ($K_{(D)}$) was determined by kinetic analysis using results from the binding assay as outlined below (Nunomura *et al.*, 1997). Spectrin and BSA were immobilised on an aminosilane cuvette, which had been activated with *bis*-(sulfosuccinimidyl) suberate (Pierce Chemical Co.) according to the manufacturer instructions, with slight modifications. After immobilisation the cuvette was blocked with 1% (w/v) BSA in PBS. All experimental procedures were carried out in PBS/0.05% Tween 20 at 25°C under constant stirring. The association rate constant (k_a) and the dissociation rate constant (k_d) were measured using the software package FASTfit™ (Affinity Sensors). $K_{(D)kin}$ was calculated from Equation 1 (Cush *et al.*, 1993; George *et al.*, 1995; Watts *et al.*, 1994)

$$K_{(D)kin} = k_d/k_a \qquad \text{(Eq.1)}$$

Dissociation constants by scatchard analysis ($K_{(D)Scat}$) were also derived from the binding data. The maximal extent of binding (R_{eq}) at various concentrations of [B] were derived from the binding curves.

$$K_A(R_{max} - R_{eq}) = R_{eq}/[B] \qquad \text{(Eq. 2)}$$

The slope of the plot of R_{eq} verses Req/[B] provides the value of $-K_A$. $K_{(D)Scat}$ is then calculated.

$$K_{(D)Scat} + 1/-K_A \qquad \text{(Eq. 3)}$$

At least two cuvettes were used to determine the various binding constants, and the derived values differed by less than 10% between the two measurements. The cuvettes were reused after cleaning with HCl. Original binding curves could be replicated after HCl washes, implying that the washing procedure did not denature the bound ligand.

2.21 GST Pull Down Assays

GST pull down assays were used to identify proteins that bound to particular GST fusion proteins. The GST fusion protein and a secondary protein were preincubated at equal molar ratios (5 μM) and allowed to bind at room temperature O/N with rotation in PBS/Complete, Mini protease inhibitor cocktail (Roche). Proteins were allowed to bind 50 μl of Glutathione Agarose beads for 1 hr at 4°C, the beads pelleted and the supernatant retained as the unbound supernatant sample. The beads were washed in 3 times with 1 ml PBS and both the beads and

the unbound supernatant sample resuspended 1/2 in 2x reducing sample buffer. Samples were boiled and equivalent amounts of supernatant and bead samples loaded onto 10% SDS-PAGE (Section 2.12.3) for use in immunoblot analysis (Section 2.14)

2.22 *Actin Interaction Assays*

Monomeric actin (from platelets) (Cytoskeleton) was polymerised to 0.4 mg/ml in the presence of 50 mM KCl, 2 mM $MgCl_2$, 1 mM ATP for 1 hr at room temperature. F-actin (5 μM) and recombinant MBP fusion proteins (5 μM) were incubated in PBS for 30 min at room temperature and then centrifuged at 25°C for 10 min at 313000 *g* in a Beckman Optima™ TLX ultracentrifuge using a TLA 120.2 rotor. The pellet was reconstituted into twice the original sample volume and equal volumes of pellet and supernatant were run on SDS-PAGE (Section 2.12.3). Gels were stained with Coomassie Brilliant Blue (Section 2.13) or transferred to PVDF for immunoblot analysis (Section 2.14).

Immunoblots were analysed by densitometry performed on a Macintosh computer using the public domain NIH Image program (developed at the U.S. National Institutes of Health and available on the Internet at http://rsb.info.nih.gov/nih-image/). The percentage protein in the pellet was adjusted for reactions containing recombinant fusion protein alone as negative controls. Each interaction was performed in at least two independent experiments.

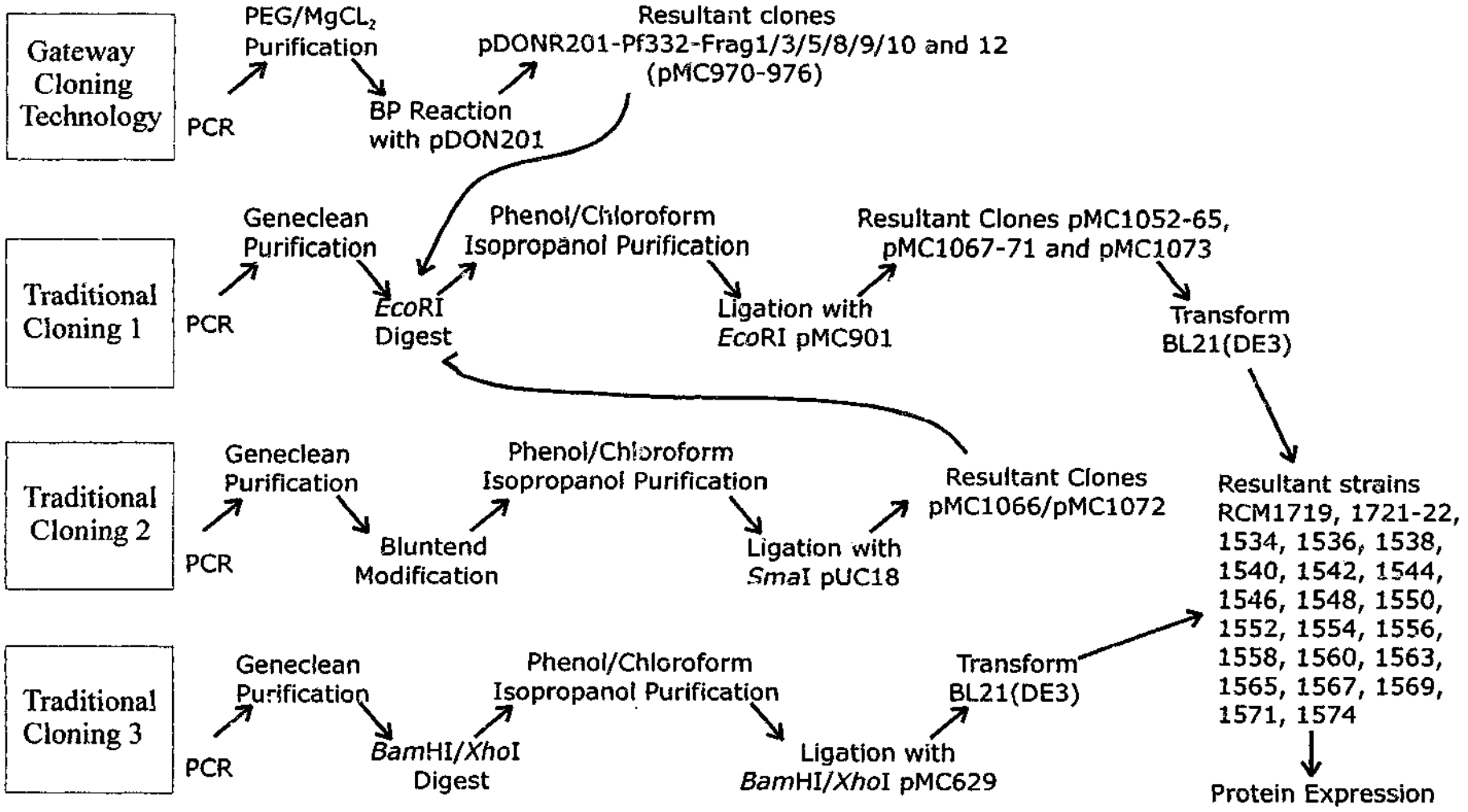

Figure 2.1. Flow Chart Detailing the Cloning Procedures used for Pf332

Four procedures were used for cloning of Pf332 fragments into pMAL vectors. Initially GATEWAY Cloning Technology was used to create entry clones. Due to the inability to obtain a full set of entry clones for Pf332, conventional cloning methods were then utilised. Conventional cloning method 1 described cloning of PCR products directly into pMAL utilising *Eco*RI sites present in the original *att*B primers. Conventional cloning method 2 describes the cloning blunt end into pUC18 before shuttling of the fragment into *Eco*RI pMAL. Conventional cloning method 3 describes the cloning of PCR products directly into pMAL utilising *Bam*HI/*Xho*I site present in the exon 1 fragments. DNA from all clones was used to transform *E. Coli* BL21 (DE3) cells to ampicillin resistance for use in expression and purification as MBP fusion proteins.

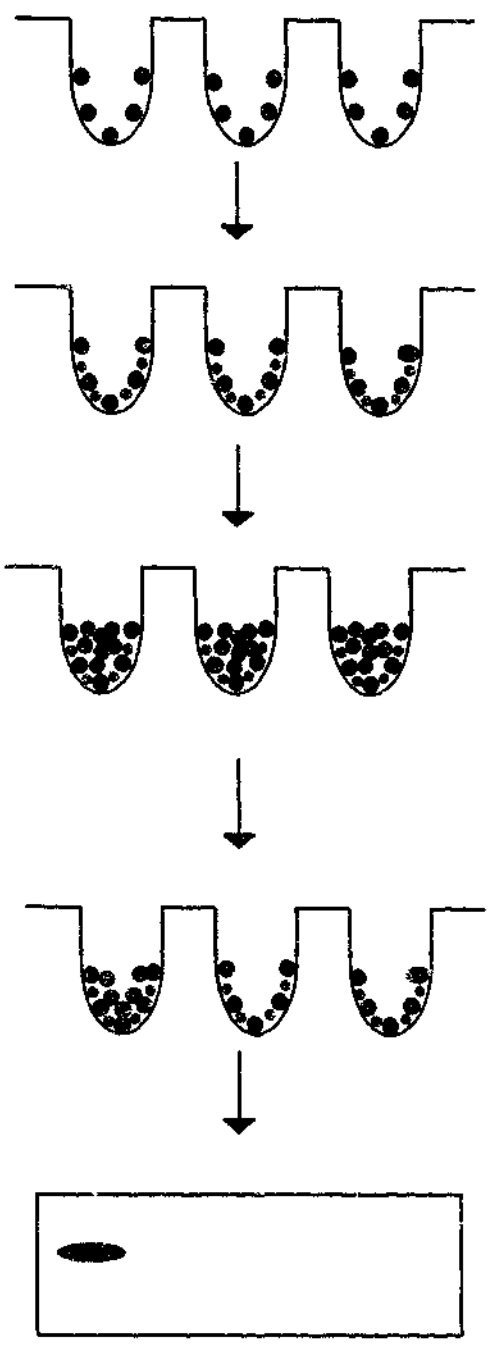

Figure 2.2. Schematic Representation of the Solid Phase Microtitre Plate Interaction Assay

Chapter 3 – Mapping Domains in PfEMP3 That Bind to the Erythrocyte Membrane Skeleton

3.1 Introduction

A number of interactions between parasite proteins and the erythrocyte membrane skeleton are important in the pathogenesis of *P. falciparum* malaria. To date, more than 10 parasite proteins have been described that are exported to the erythrocyte membrane where they can interact with both erythrocyte membrane proteins and with other exported parasite proteins (for a recent review see Cooke *et al.*, 2001). The most studied set of interactions involves the anchoring of PfEMP1 in the erythrocyte membrane skeleton via an interaction with KAHRP (Waller *et al.*, 1999; Oh *et al.*, 2000; Waller *et al.*, 2002). This, and other interactions between KAHRP and spectrin, actin (Kilejian *et al.*, 1991) and ankyrin (Magowan *et al.*, 2000) have been implicated in the ability of parasites to cytoadhere under flow conditions (Crabb *et al.*, 1997). Another important interaction occurs between MESA and protein 4.1 (Lustigman *et al.*, 1990; Coppel, 1992; Bennett *et al.*, 1997; Kun *et al.*, 1999). This interaction may modulate the protein 4.1-p55 interaction (Waller *et al.*, 2003) and subsequent linking of the lipid bilayer to the membrane skeleton through the protein 4.1-p55-glycophorin C ternary interaction (Marfatia *et al.*, 1995).

PfEMP3 is a 315 kDa parasite protein (Pasloske *et al.*, 1993) that is trafficked via Maurer's clefts to the membrane skeleton of parasitised erythrocytes (Wickham *et al.*, 2001). Here, PfEMP3 is distributed around the erythrocyte membrane skeleton (Pasloske *et al.*, 1993). To date, no function has been assigned to PfEMP3, however, erythrocytes infected with parasites in which the gene encoding PfEMP3 had been disrupted showed a reduced degree of erythrocyte membrane rigidification (Glenister *et al.*, 2002) and a slight reduction in the ability to cytoadhere (Waterkeyn *et al.*, 2000). Furthermore, parasites expressing a truncated form of PEMP3, show reduced expression of PfEMP1 on the erythrocyte surface, suggesting a role for PfEMP3 in trafficking of PfEMP1 to the erythrocyte membrane (Waterkeyn *et al.*, 2000).

Prior to this study, proteins at the parasitised erythrocyte membrane skeleton with which PfEMP3 interacts were not known, however, it has been suggested that C-terminal truncation of PfEMP3 may result in the loss of a domain necessary for binding (Waterkeyn *et al.*, 2000). The aim of this study was to investigate the interaction of PfEMP3 with the erythrocyte membrane skeleton and determine the precise domains within PfEMP3 that are responsible for mediating

binding. Furthermore, using solid phase and kinetic binding assays, we aimed to identify specific proteins at the erythrocyte membrane skeleton with which PfEMP3 interacts.

3.2 Identification of Domains Within PfEMP3 that Bind to the Erythrocyte Membrane Skeleton

3.2.1 Cloning PfEMP3 Fragments into pMAL Vectors

To study interactions between PfEMP3 and the erythrocyte membrane skeleton, recombinant fragments of PfEMP3 were created. The second exon of PfEMP3 contains five defined regions, three repeat regions and two non-repeat regions (Figure 3.1a). Due to the difficulty in cloning large *P. falciparum* gene fragments containing repeat regions (Coppel and Black, 1998), PfEMP3 was not cloned as full-length gene. Instead, specific primers were designed for use in PCR and resulting fragments used in cloning of the PfEMP3 second exon as five defined regions. The first region (PfEMP3-FI) encompasses the 5' region of the second exon and is non-repetitive. The next three regions (PfEMP3-FII, PfEMP3-FIII and PfEMP3-FIV) each encompass one of the three repeat regions of PfEMP3. The fifth region (PfEMP3-FV) encompasses the 3' region of the gene and is non-repetitive. All fragments were cloned separately into pMAL-c2 or modified pMAL vector pMC629 by V. Gatzigiannis and J. Bettadapura (Monash University) as detailed in Section 2.10.1. pMAL *E. coli* cloning vectors are used in creating fusions between the cloned gene and the *E. coli malE* gene, which encodes maltose binding protein (MBP). Constructs can be used in the expression and purification of MBP fusion proteins, utilising the ability of MBP to bind amylose (Ausubel *et al.*, 1994). Both PfEMP3-FII and -FIV were cloned as representative repeat fragments due to difficulty in design of unique primers for the regions and subsequent difficulty in amplification of distinct full length PCR products.

3.2.2 Expression and Purification of MBP-PfEMP3 fusion proteins

E. coli BL21(DE3) was transformed to ampicillin resistance using pMAL-c2, pMC754, pMC755, pMC756, pMC757 and pMC758 for the expression and purification of MBP, MBP-PfEMP3-FI, -FII, -FIII, -FIV and -FV, respectively. Bacterial strains were grown in superbroth and protein expression induced with 1mM IPTG. Proteins were purified, dialysed extensively against PBS, concentrated in centrifugal concentrators and protein concentration determined using the

Bradford assay as described in Section 2.16. Approximately 2 µg and 50 ng of protein were resolved on 10% polyacrylamide gels and visualise either by Coomassie Brilliant Blue staining or transferred to PVDF for immunoblot analysis detected using anti-MBP antiserum (Figure 3.1b and 3.1c) (as described in Section 2.12). Recombinant protein was purified from all five strains and in addition to the predicted full-length protein, a number of smaller molecular mass MBP fusion proteins were co-purified. Full-length MBP resolved just below the predicted size of 50.8 kDa (Figure 3b and 3c, lane 1). MBP-PfEMP3-FI showed only a small proportion of full-length protein at the predicted size of approximately 108 kDa (Figure 3.1b, lane 2). The full-length protein could be transferred and detected using anti-MBP antiserum, however longer exposures than that shown in Figure 3.1c (lane 2) were required for visualisation by immunoblot (data not shown). MBP-PfEMP3-FII purified as predominantly full-length protein and resolved at approximately 105 kDa (Figure 3b and 3c, lane 3), well above the predicted size of approximately 80 kDa. This phenomenon is often see with malaria proteins and is thought to be a consequence of charged repeat regions (Coppel *et al.*, 1994). MBP-PfEMP3-FIII, -FIV and -FV were purified as predominantly full-length proteins that resolved approximately at their predicted size of 71 kDa, 55 kDa and 51 kDa, respectively (Figure 3b and 3c, lanes 4, 5 and 6, respectively).

3.2.3 Binding of PfEMP3 Fragments to IOVs

MBP-PfEMP3 fusion proteins were incubated with IOVs to determine their ability to bind to the erythrocyte membrane skeleton. IOVs were prepared from human erythrocytes (Section 2.17), coated onto the wells in triplicate and following blocking, 4 µg total protein of each MBP-PfEMP3 fragments (MBP-PfEMP3-FI, -FII, -FIII, -FIV and -FV) were added and allowed to bind. Bound protein was eluted from the wells (Section 2.18), resolved on 10% polyacrylamide gels, transferred to PVDF and detected by immunoblot analysis using anti-MBP antiserum (Section 2.12). Initial interaction assays were performed by V. Gatzigiannis and J. Bettadapurra (Gatzigiannis, 1999). These assays were repeated and confirmed in this study. A representative immunoblot is shown in Figure 3.2b. A binding domain within PfEMP3-FI was detected as seen by elution of bound MBP-PfEMP3-FI from wells coated with IOVs (lane 3). As described for the purified MBP-PfEMP3-FI protein (Section 3.2.2), full-length fusion protein was only detected following overexposure of the immunoblots (data not shown). A low intensity band was also detected for MBP-PfEMP3-FV binding to wells coated with IOVs (lane 11). MBP, MBP-PfEMP3-FII, -FIII and -FIV did not bind wells coated with IOVs (lanes 1, 5, 7, and 9,

respectively). None of the proteins bound to wells coated with BSA (lanes 2, 4, 6, 8, 10 and 12).

These data indicated a specific interaction between the erythrocyte membrane skeleton and the 551 residues encoded by the 5′ region of the second exon of PfEMP3 (PfEMP3-FI). These data also indicated a possible interaction between the erythrocyte membrane skeleton and the 74 residues encoded by the 3′ region of the second exon of PfEMP3 (PfEMP3-FV). This interaction was always detected, but was consistently of lower intensity.

3.3 Identification of Binding Sub-Fragments Contained Within PfEMP3-FI

3.3.1 Cloning, Expression and Purification of PfEMP3-FIa and PfEMP3-FIb

To further define the binding domain within PfEMP3-FI, the fragment was divided into two sub-fragments (PfEMP3-FIa and PfEMP3-FIb) (Figure 3.3a). Fragments encompassing this region were cloned into a modified pMAL vector pMC793 to create pMC798 and pMC799 by J. Bettadapura (Monash University) (Section 2.10.2). *E. coli* BL21(DE3) was transformed to ampicillin resistance by pMC798 and pMC799 and used in protein expression and purification as described in Section 3.2.2. Proteins were visualised as described in Section 3.2.2 (Figure 3.3b and 3.3c). Proteins purified from both strains contained only a small proportion of full-length MBP fusion. MBP-PfEMP3-FIa resolved at approximately 75 kDa (Figure 3.3b and 3.3c, lane 1), above the predicted size of approximately 71 kDa. This was also observed for MBP-PfEMP3-FIb, which has a predicted size of approximately 81 kDa and resolved at approximately 100 kDa (Figure 3.3b and 3.3c, lane 2).

3.3.2 IOV Interaction Assay with PfEMP3-FIa and PfEMP3-FIb

MBP-PfEMP3-FIa and MBP-PfEMP3-FIb were incubated with IOVs and bound protein detected as described in Section 3.2.3. A representative immunoblot is shown in Figure 3.4b. MBP-PfEMP3-FIa bound to wells coated with IOVs (lane 3). The banding pattern observed was consistent with that seen for purified MBP-PfEMP3-FIa by immunoblotting (Figure 3.3c, lane1). Neither MBP-PfEMP3-FIb (lane 5) nor MBP (lane 1) was detected to bind to IOVs. None of the proteins bound to

bind to wells coated with BSA (lanes 2, 4 and 6). This was consistent with a binding domain for the erythrocyte membrane skeleton located within the 234 residues encoded by the 5′ end of the PfEMP3 second exon (PfEMP3-FIa).

3.4 Identification of Binding Domain in PfEMP3-FIa

3.4.1 Cloning, Expression and Purification of MBP-PfEMP3-FIa Sub-Fragments

To further map the binding domain within PfEMP3-FIa, four approximately 60 residue sub-fragments were created (PfEMP3-FIa.1, -FIa.2, -FIa.3 and -FIa.4, Figure 3.5a) (Section 2.10.3). Clones, pMC840, pMC842, pMC844 and pMC846 were used to transform *E. coli* BL21(DE3) to ampicillin resistance and resultant strains (RCM1222, RCM1225, RCM1228 and RCM1231) were used for protein expression and purification of MBP-PfEMP3-FIa.1, -FIa.2, -FIa.3 and -FIa.4 respectively, as described in Section 3.2.2. Proteins were visualised as described in Section 3.2.2 (Figure 3.5b and 3.5c). All four purified proteins showed a proportion of full-length MBP fusion protein that resolved at approximately 50 kDa in accordance with the predicted size. MBP-PfEMP3-FIa.1, -FIa.2 and -FIa.4 purified predominantly as full-length protein (Figure 3.5b and 3.5c, lanes 1, 2 and 4, respectively), whereas MBP-PfEMP3-FIa.3 was produced as a major break down product which resolved at approximately 45 kDa (Figure 3.5b and 3.5c, lane 3).

3.4.2 IOV interaction Assay with PfEMP3-FIa.1, PfEMP3-FIa.2, PfEMP3-FIa.3 and PfEMP3-FIa.4

MBP-PfEMP3-FIa.1, -FIa.2, -FIa.3 and -FIa.4 were incubated with IOVs and bound protein detected as described in Section 3.2.3. Initial interaction assays were performed by K. Waller. These assays were repeated and confirmed in this study. A representative immunoblot is shown in Figure 3.6b. Bound protein was detected in wells coated with IOVs for MBP-PfEMP3-FIa.1 (lane 3), but not for MBP (lane 1) or MBP-PfEMP3-FIa.2, -FIa.3 and -FIa.4 (lanes 5, 7 and 9, respectively). None of the proteins bound to wells coated with BSA (lanes 2, 4, 6, 8 and 10). The band detected corresponded to the single band seen for the purified MBP-PfEMP3-FIa.1 on immunoblots at approximately 50 kDa (Figure 3.5c, lane 1). This was consistent with a binding domain for the erythrocyte membrane skeleton located within the 60 residues encoded by the 5′ end of the PfEMP3 second exon (PfEMP3-FIa.1).

3.5 Confirmation of the 60 Residue Binding Region by Domain Deletion

3.5.1 Cloning, Expression and Purification of FIaΔFIa.1

To confirm the 60 residue membrane skeleton binding region of PfEMP3-FIa.1, this region was deleted from the PfEMP3-FIa fragment (PfEMP3-FIaΔFIa.1, Figure 3.7a). The region was PCR amplified and cloned into the pMAL modified vector pMC629 using the procedure outlined in Section 2.10.4. The resultant clone, pMC903 was used to transform *E. coli* BL21(DE3) to ampicillin resistance and the resultant strain (RCM1222) was used for protein expression and purification of MBP-PfEMP3-FIaΔFIa.1 as described in Section 3.2.2. Protein was visualised as described in Section 3.2.2 (Figure 3.7b and 3.7c). MBP-PfEMP3-FIaΔFIa.1 purified with only a small proportion of full-length protein at the predicted size of 64 kDa. The majority of the protein detected was a breakdown product at approximately 50 kDa.

3.5.2 IOV Interaction Assay to confirm FIa.1 as the Erythrocyte Binding Domain

MBP-PfEMP3-FIaΔFIa.1 was incubated with IOVs and bound protein detected as described in Section 3.2.3. A representative immunoblot is shown in Figure 3.8b. No MBP-PfEMP3-FIaΔFIa.1 (lane 5) was detected binding to wells coated with IOVs, however binding to wells coated with IOVs was observed for the MBP-PfEMP3-FIa.1 positive control (lane 3). MBP did not bind wells coated with IOVs (lane 1) and none of the proteins bound to wells coated with BSA (lanes 2, 4 and 6). This assay confirmed that the 60 residue region of PfEMP3-FIa.1 was responsible for binding to the erythrocyte membrane skeleton.

3.6 Defining the Binding Domain by Deletion Analysis

3.6.1 Cloning, Expression and Purification of Deletion Constructs

To further define the binding domain, sequential deletions within the 60 residue binding region were created in PfEMP3-FIa. Forward primers were designed to amplify sequence encoding fragments that started 15 residues, 29 residues or 45 residue from the N-terminus of PfEMP3-FIa (PfEMP3-FIaΔ15, -FIaΔ29, -FIaΔ45,

Figure 3.9a). Primers were designed with *att*B sites for use with GATEWAY™ Cloning Technology (Section 2.7). For cloning into pMAL with site specific recombination using the GATEWAY™ Cloning Technology the pMAL-c2 vector was converted to a destination vector resulting in pDEST-MAL (pMC1342) (Section 2.7.1).

Following PCR amplification, gene fragments were cloned into pDEST-MAL (Section 2.10.5). Clones were used to transform *E. coli* BL21(DE3) competent cells to ampicillin resistance and subsequent strains (RCM1382, RCM1385 and RCM1388, respectively) were used in protein expression and purification as described in Section 3.2.2. Proteins were visualised as described in Section 3.2.2 (Figure 3.9b and 3.9c). All three purified proteins contained only a small proportion of the predicted full-length protein, with a large number of smaller products. MBP-PfEMP3-FIaΔ15, MBP-PfEMP3-FIaΔ29 and MBP-PfEMP3-FIaΔ45 (Figure 3.9b and 3.9c, lanes 1, 2 and 3, respectively) resolved at their predicted sizes of 78 kDa, 76.5 kDa and 75 kDa, respectively.

3.6.2 IOV interaction assay with deletion constructs

MBP-PfEMP3-FIaΔ15, -FIaΔ29 and -FIaΔ45 were incubated with IOVs and bound protein detected as described in Section 3.2.3. A representative immunoblot is shown in Figure 3.10b. MBP-PfEMP3-FIaΔ15 bound to wells coated with IOVs (lane 3). The bands detected corresponded to the banding pattern of purified MBP-PfEMP3-FIaΔ15 on immunoblots (Figure 3.9c, lane 1). Neither MBP-PfEMP3-FIaΔ29 (lane 5), -FIaΔ45 (lane 7) or MBP (lane 1) bound to wells coated with IOVs. None of the proteins bound to wells coated with BSA (lanes 2, 4, 6 and 8). This indicated that the binding domain was not contained within the first 15 residues encoded by the 5′ region of the second exon of PfEMP3 and that residues within the region 16-29 encoded by the PfEMP3 second exon are essential for binding of PfEMP3 to the erythrocyte membrane skeleton.

3.7 Interaction of PfEMP3 with Spectrin

To identify proteins of the erythrocyte membrane skeleton with which PfEMP3 binds, recombinant MBP-PfEMP3 fusion proteins were incubated with spectrin. Purified spectrin was obtained from Sigma Aldrich and contains a mixture of α- and β- spectrin polypeptides. Approximately 200 ng of purified spectrin was coated onto each well of a microtitre plate and treated as described for IOVs (Section 3.2.3). The only modification to the IOV protocol was the use of PBS rather than Incubation Buffer for the dilution of proteins and washing of wells.

3.7.1 Interaction of PfEMP3 Fragments with Spectrin

MBP-PfEMP3-FI, -FII, -FIII, -FIV and -FV were incubated with spectrin and bound protein detected as described in Section 3.2.3. A representative immunoblot is shown in Figure 3.11b. MBP-PfEMP3-FI bound to wells coated with spectrin (lane 3). MBP-PfEMP3-FII (lane 5), -FIII (lane 7), -FIV (lane 9), -FV (lane 11) and MBP (lane 1) did not bind to wells coated with spectrin. None of the proteins bound to wells coated with BSA (lanes 2, 4, 6, 8, 10 and 12). This indicated that the binding domain of PfEMP3 for spectrin was contained within PfEMP3-FI, consistent with the binding of PfEMP3 to IOVs. In contrast to the IOV data, no binding of MBP-PfEMP3-FV to spectrin was detected.

3.7.2 Interaction of PfEMP3-FIa and PfEMP3-FIb with Spectrin

To further define the spectrin binding region within PfEMP3-FI, MBP-PfEMP3-FIa and -FIb were incubated with spectrin and bound protein detected as described in Section 3.2.3. Figure 3.12b shows a representative immunoblot. MBP-PfEMP3-FIa bound to wells coated with spectrin (lane 3), whereas neither MBP-PfEMP3-FIb (lane 5) nor MBP (lane 1) bound spectrin. None of the proteins bound wells coated with BSA (lanes 2, 4 and 6). These results were consistent with those seen for binding of PfEMP3 to IOVs and indicate that the binding region for spectrin was located within the 234 residues encoded by the 5′ end of PfEMP3 second exon (PfEMP3-FIa).

3.7.3 Interaction of PfEMP3-FIa.1, PfEMP3-FIa.2, PfEMP3-FIa.3 and PfEMP3-FIa.4 with Spectrin

To map the spectrin binding region within PfEMP3-FIa, PfEMP3-FIa.1, -FIa.2, -FIa.3 and -FIa.4 were incubated with spectrin and bound protein detected as described in Section 3.2.3. Figure 3.13b shows a representative immunoblot. MBP-PfEMP3-FIa.1 bound to wells coated with spectrin (lane 3), whereas none of MBP-PfEMP3-FIa.2 (lane 5), -FIa.3 (lane7), -FIa.4 (lane 9) and MBP (lane 1) bound to wells coated with spectrin. None of the proteins bound wells coated with BSA (lanes 2, 4, 6, 8 and 10). These data indicated that the binding domain of PfEMP3 to spectrin was contained within the 60 residue region encoded by the 5′ end of the PfEMP3 second exon (PfEMP3-FIa.1). This was once again consistent with results seen for IOVs.

3.7.4 Interaction of PfEMP3-FIaΔFIa.1, PfEMP3-FIaΔ15, PfEMP3-FIaΔ29 and PfEMP3-FIaΔ45 with Spectrin

To confirm the 60 residue spectrin binding domain (PfEMP3-FIa.1) and to further define this binding domain, MBP-PfEMP3-FIaΔFIa.1, -FIaΔ15, -FIaΔ29 and -FIaΔ45 were incubated with spectrin and bound protein detected as described in Section 3.2.3. Representative immunoblots are shown in Figure 3.14b and 14c. MBP-PfEMP3-FIa.1 bound to wells coated with spectrin (Figure 3.14b, lane 4), whereas neither MBP-PfEMP3-FIaΔFIa.1 (lane 5) nor MBP (lane 7) bound wells coated with spectrin. None of the proteins bound to wells coated with BSA (lanes 2, 4 and 6). This confirmed the 60 residue spectrin binding domain (PfEMP3-FIa.1).

Subsequently, bound protein was detected from wells coated with spectrin for MBP-PfEMP3-FIaΔ15 (Figure 3.14c, lane 3), but not for MBP-PfEMP3-FIaΔ29 (lane 5), -FIa.Δ45 (lane 7) or MBP (lane 9), consistent with the binding domain observed for the erythrocyte membrane skeleton. These data showed that the first 15 residues encoded by PfEMP3 second exon were not required for binding to spectrin. In addition, residues 16-29 encoded by the PfEMP3 second exon were essential for binding to spectrin. However, this did not rule out the contribution of residues 30-45 in the PfEMP3-spectrin interaction.

3.7.5 Interaction with Sub-Fragments of PfEMP3-FIa.1

3.7.5.1 Cloning, expression and purification of PfEMP3-FIa.1 Sub-Fragments

To establish involvement of residues 16-29 encoded by the second exon of PfEMP3 and investigate the involvement of residues 30-60 in binding to spectrin, three constructs were made expressing residues 16-29, 16-45 and 16-60 as recombinant MBP fusions (Figure 3.15a). As a control, a small construct was made that would express residues 1-15 as a recombinant MBP fusion protein (Figure 3.15a). Each fragment was cloned into a pMAL vector as described in Section 2.10.6 and clones were used to transform *E. coli* BL21 (DE3) to ampicillin resistance. Resultant strains (RCM1457, RCM1483, RCM1485 and RCM1487) were used in protein expression and purification as described in Section 3.2.2.

Proteins were visualised as described in Section 3.2.2 (Figure 3.15b and 3.15c). MBP-PfEMP3-16-29, -16-45, -16-60 and -1-15 (Figure 3.15b and 3.15c, lanes 1, 2, 3 and 4, respectively) were purified as predominantly full-length product

and were resolved at the predicted sizes of 44 kDa, 46 kDa, 48 kDa and 44 kDa, respectively.

3.7.5.2 Spectrin Interaction Assay with PfEMP3-16-29, -16-45 and -16-60

To further map the binding domain, MBP-PfEMP3-16-29 was incubated with spectrin to see if this region was sufficient for binding. In conjunction with this, MBP-PfEMP3-16-45 and -16-60 were incubated with spectrin to investigate the possibility that amino acids within these regions were required for binding. A representative immunoblot is shown in Figure 3.16. Consistently, this assay showed a very low level of MBP-PfEMP3-16-29 and MBP-PfEMP3-16-45 binding. Low levels of MBP-PfEMP3-16-29 (lane 5) and MBP-PfEMP3-16-45 (lane 7) were detected from wells coated with spectrin in comparison with MBP-PfEMP3-FIaΔ15 positive control (lane 3). No bound protein was detected to wells coated with spectrin for MBP (lane 1) or the any of the wells coated with BSA (lane 2, 4, 6, and 8). Given that PfEMP3-FIaΔ15 encodes residues 16-60 of the binding region, MBP-PfEMP3-16-60 was incubated with spectrin to determine if these residues bound. MBP-PfEMP3-16-60 bound to wells coated with spectrin (lane 9) at slightly higher levels than for those see with MBP-PfEMP3-16-26 and MBP-PfEMP3-16-45. However, the intensity of the band was less than that seen for PfEMP3-FIaΔ15. These data indicated that the microtitre plate assay was unable to showed definitive binding of MBP-PfEMP3 fusions that consisted of a small number of PfEMP3 residues (<60) fused to the relatively large MBP protein (392 residues). Kinetic analysis was performed to further resolve this issue and to define a minimal binding domain.

3.7.6 Kinetic Analysis of PfEMP3 Interaction with Spectrin

A resonant mirror detection method (IAsys™ system) was used to obtain kinetics data for interactions between sub-fragments of PfEMP3 and spectrin. Aminosilane cuvettes were coated with spectrin or BSA, and PfEMP3 proteins were applied in an aqueous solution to determine the association rate constant (K_a), disassociation rate constant (K_d) and subsequent disassociation constant ($K_{(D)}$) of the interaction (Table 3.1). Disassociation constants were obtained by two forms of kinetic analysis resulting in both $K_{(D)kin}$ and $K_{(D)Scat}$ values (Section 2.20) (Nunomura *et al.*, 1997). All kinetic data was performed by W. Nunomura, Tokyo Women's Hospital, Japan.

Binding data confirm the microtitre assay data showing an interaction between spectrin and MBP-PfEMP3 fragments FI, FIa and FIa.1, but not between spectrin and any of the other PfEMP3 sub-fragments. No interaction was observed

with MBP-PfEMP3-F1aΔFIa.1, confirming that the binding region was confined to the 60 residues of PfEMP3-FIa.1. K_D values for the N-terminal deleted forms showed strong interaction of MBP-PfEMP3-F1aΔ15. Quantitative analysis by IAsys™ also revealed binding of MBP fused to the PfEMP3-16-29 residue region, but not of MBP fused to the PfEMP3-1-15 residue regions. These data showed that residues 16-29 encoded by the PfEMP3 second exon were sufficient to confer binding of PfEMP3 to purified spectrin. These data also indicated that small regions of protein fused to a relatively large fusion partner, such as MBP, gave results that although difficult to measure with the solid phase microtitre plate interaction assay, were able to be resolved with resonant mirror detection.

3.8 Interaction of PfEMP3 with F-Actin

To investigate the possibility of a binding domain within PfEMP3 for actin, purified monomeric actin was polymerised in the presence of KCl, $MgCl_2$ and ATP at room temperature and used in high speed centrifugation assays in conjunction with the PfEMP3 fragments (Section 2.22). This assay has previously been used to determine the actin binding ability of a number of proteins at the erythrocyte membrane skeleton including spectrin (Karinch *et al.*, 1990), protein 4.1 (Becker *et al.*, 1990; Morris and Lux, 1995) and adducin (Mische *et al.*, 1987). This method was used, not only because it is accepted as a valid method for identifying interactions with actin, but also due to the ease of experimentation and the ability to show binding of PfEMP3 to F-actin, which is the form present at the erythrocyte membrane skeleton. No previous studies had been performed using a filamentous protein with the microtitre plate method.

Initially, actin was tested for its ability to sediment by centrifugation at high speeds. At 31300 *g* for 10 minutes, polymerised actin (F-actin) pellets, whereas monomeric actin (G-actin) remains in the supernatant. Following high speed centrifugation, equal samples of pellet and supernatant were run on polyacrylamide gels and stained with Coomassie Brilliant Blue. Figure 3.17a shows that following high speed centrifugation, F-actin was found predominantly in the pellet (P), with only a small amount in the supernatant (S). Conversely, G-actin was found predominantly in the supernatant, with only a small amount found in the pellet. This showed that under the polymerisation conditions used G-actin was converted to a form of actin that pelleted under high speed centrifugation, suggesting it was in its filamentous form.

3.8.1 High Speed Centrifugation Actin Pull Down Assay for the identification of Sub-Fragments of PfEMP3 that Bind to Actin

To investigate the ability of F-actin to bind to PfEMP3, MBP-PfEMP3 fragments were subjected to high speed centrifugation in the presence or absence of F-actin. In the absence of F-actin, it was expected that the MBP-PfEMP3 fusions would remain in the supernatant. In the presence of F-actin, PfEMP3 proteins that bound actin would co-sediment and be found in the pellet, whereas proteins that do not bind actin would remain in the supernatant. Following high speed centrifugation, samples from both pellet and supernatant were run on polyacrylamide gels and used for immunoblot analysis using anti-MBP antiserum. Figure 3.17b shows a representative immunoblot for a high speed centrifugation assay using MBP as a negative control and MBP-PfEMP3-FIa.1 in the presence and absence of F-actin. In both the presence and absence of F-actin, MBP was found in the supernatant, indicating that it was unable to bind to and therefore, did not co-sediment with F-actin. In the absence of F-actin, MBP-PfEMP3-FIa.1 was found in the supernatant, whereas in the presence of F-actin, MBP-PfEMP3-FIa.1 was found in both the pellet and the supernatant. This indicated that MBP-PfEMP3-FIa.1 was able to co-sediment with F-actin and suggested that it bound F-actin. To determine the percentage protein in the pellet, densitometry was performed on immunoblots and the percentage protein in the pellet in the presence of F-actin was adjusted for the percentage protein in the pellet in the absence of F-actin. Assays were performed in two independent experiments, and the mean and standard deviation calculated. Figure 3.18 shows the plotted results of the set of MBP-PfEMP3 fusion proteins.

Interestingly, the MBP-PfEMP3 fusion proteins that were found to pellet and therefore to bind F-actin, were consistent with those that were also shown to bind spectrin. Initially it was shown that MBP-PfEMP3-FI was able to bind and therefore co-sediment with F-actin, whereas MBP-PfEMP3-FII, -FII, -FIV and -FV did not co-sediment with F-actin. Subsequent experiments shown that MBP-PfEMP3-FIa and -FIa.1 were able to bind F-actin, whereas the other fragments showed no binding. PfEMP3-FIaΔFIa.1 was unable to bind F-actin confirming the 60 residue region (PfEMP3-FIa.1) as the actin binding domain.

Residues 16-29 were sufficient to confer binding of PfEMP3 to F-actin, however in the presence adjacent residues 30-60, binding could be almost fully restored to FIa.1 levels. This was evident by the binding of MBP-PfEMP3-16-45 and MBP-PfEMP3-FIaΔ15 to F-actin at almost the same levels as the 60 residue actin binding domain (PfEMP3-FIa.1). However, in contrast to the results seen with

spectrin, deletion of residues 1-29 and residues 1-45 appeared to result in low level binding of MBP-PfEMP3-FIaΔ29 and -FIaΔ45. These data indicated that although the 14 residue binding domain (PfEMP3-16-29) was sufficient for binding of PfEMP3 to F-actin, residues in the region 30-60 conferred some additional actin binding activity. Also, that deletion of the 14 residue binding domain (PfEMP3-16-29) did not abolish binding.

3.9 Kinetic Analysis of PfEMP3-FIa.1 binding to Actin

To quantify the interaction between PfEMP3 and F-actin, F-actin was immobilised on an aminosilane coated cuvette and PfEMP3-FIa.1 added in aqueous solution as described in Section 3.7.6. Data showed an interaction with a K_a of $1.0x10^4$ $M^{-1}sec^{-1}$, a K_d of $5.7x10^{-3}$ sec^{-1} and subsequent $K_{(D)kin}$ and $K_{(D)Scat}$ values of $5.7x10^{-7}$ M and $4.5x10^{-7}$ M, respectively.

3.10 Discussion

The results presented here show that a 60 residue region encoded by the 5' end of the second exon of PfEMP3 (PfEMP3-FIa.1) is responsible for binding to the erythrocyte membrane skeleton. In an attempt to identify specific erythrocyte proteins to which PfEMP3 binds, further experiments using spectrin and F-Actin were performed. Mapping experiments showed PfEMP3 binding to spectrin and actin both reside within the same 60 residue region (PfEMP3-FIa.1).

Both the solid phase and quantification methods identified an interaction between spectrin and PfEMP3-FI, PfEMP3-FIa and PfEMP3-FIa.1 indicating that the spectrin binding region is located within the first 60 residues encoded by the PfEMP3 second exon (PfEMP3-FIa.1). Resonant mirror detection method of the IAsys™ system definitively mapped the binding domain to the 14 residues numbered 16-29 encoded by the 5' region of the PfEMP3 second exon (PfEMP3-16-29). We obtained $K_{(D)kin}$ values of $7.0x10^{-8}$ M, $7.5x10^{-8}$ M and $8.5x10^{-8}$ M and $3.8x10^{-7}$ M for PfEMP3-FI, PfEMP3-FIa, PfEMP3-FIa.1 and PfEMP3-16-29, respectively. The small decrease in binding for the 14 residue binding domain (PfEMP3-16-29) could be due to a loss in contributing amino acids, change in conformation of the binding domain or surrounding residues, or due to the change in size of the interacting fragment (Endo *et al.*, 1998). The binding affinities for proteins within the erythrocyte vary from the ankyrin-band 3 interaction ($1.6x10^{-6}$ M) (Bennett and Stenbuck, 1980a) to the p55-GPC interaction ($1x10^{-8}$ M) (Nunomura *et al.*, 2000a). Similar figures have been obtained for interactions within the parasitised erythrocyte, including the protein 4.1-MESA interaction

($2.7x10^{-7}$ M) (Waller *et al.*, 2003), and between parasite proteins, for example between KAHRP and PfEMP1 ($1.1x10^{-8}$ M) (Oh *et al.*, 2000). Our binding kinetics indicate an interaction in the range of the higher affinity interactions seen in the erythrocyte. In fact, for the larger regions, our data shows an interaction between spectrin and PfEMP3 which is up to 8.5 fold higher than those for the most high affinity interactions measured in the erythrocyte to date. Data for $K_{(D)kin}$ and $K_{(D)Scat}$ was closely matched for each of the binding domains. The ability of resonant mirror detection to closely match data for these two forms of kinetic analysis has been described in previous reports (Nunomura *et al.*, 1997; Nunomura *et al.*, 2000b). Given this, more recent reports have found it unnecessary to report $K_{(D)Scat}$ data in support of the $K_{(D)kin}$ data (Nunomura *et al.*, 2000a; Gimm *et al.*, 2002).

The PfEMP3 60 residue binding domain (PfEMP3-FIa.1) binds F-actin with a moderate affinity ($5.7x10^{-7}$ M). The PfEMP3 14 residue binding domain (PfEMP3-16-29) is sufficient to bind actin, however our results also indicate that amino acids within the adjacent 30-60 residue region contained within PfEMP3-16-45 and PfEMP3-FIa.1Δ15, are likely to contribute to binding. These data are consistent with the data presented for spectrin, where a small loss of binding is detected for the 14 residue region (PfEMP3-16-29), when compared with PfEMP3-FIa.1Δ15. In contrast to the data for spectrin, residues within the region 30-60 of PfEMP3 appear to be able to confer binding to actin independent of the presence of the 14 residue binding region (PfEMP3-16-19), as seen by the low level binding detected for PfEMP3-FIaΔ29 and PfEMP3-FIaΔ45. These differences are likely due to variation in either the binding region or contributing amino acids between the PfEMP3 binding domains for spectrin and for actin, or in differences in sensitivities and specificities of the assays. It is important to note that binding of PfEMP3-FIaΔ29 and PfEMP3-FIaΔ45 to actin is only marginally above the binding seen for PfEMP3-FIa.2 and may not represent a significant level of binding above that for negative controls. These experiments were performed on two separate occasions with different preparations of F-actin. The reproducibility of the results

Experiments performed on two separate occasions with different preparations of actin revealed a high degree of variation for MBP-PfEMP3-FIa (38 and 57% associated with F-actin in the pellet) compared to the low degree of variation for MBP-PfEMP3-FIV (1.5 and 2.2 % associated with F-Actin in the pellet). Further data would be required to determine the mean for proteins with high degrees of variation and to draw conclusions about the relevance of the differences seen with the various regions within the 60 residue binding domain (PfEMP3-FIa.1). Additional data obtained with the resonant mirror detection system would also

delineate the contributions to binding for various regions within the 60 residue binding domain (PfEMP3-FIa.1).

Our results indicate that the solid phase microtitre plate assay is useful in defining binding domains of fragments larger than 60 residues fused to MBP fusion proteins. However, once the interacting region created was less than 60 residues, the results were inconclusive, as observed in the use of PfEMP3-16-29, -16-45 and 16-60. This may be due to the size of MBP (392 residues) (Ausubel *et al.*, 1994) in comparison to the interacting region, however this difference in size appeared to cause no problems with ether resonant mirror detection or with high speed centrifugation actin assays. The microtitre plate assay has previously been shown to have a number of disadvantages when compared with resonant mirror detection, however the major advantages of the microtitre plate assay are the low cost, ease of experimentation and lack of expensive, specialised equipment.

Future experiments would involve mapping the domain responsible for binding to PfEMP3 within spectrin and subsequent comparison with known functional domains within spectrin, including those responsible for binding to ankyrin, actin and protein 4.1. This would enable the consequences of PfEMP3 binding on spectrin function to be determined. An example of this approach is for *P. falciparum* protein MESA, which is able to bind a region within protein 4.1 that overlaps with a known binding domain for p55. The MESA-protein 4.1 interaction is able to inhibit the protein 4.1-p55 interaction (Waller *et al.*, 2003). It would be interesting to investigate similar inhibition of interactions of spectrin following PfEMP3 binding, especially given that spectrin-actin-protein 4.1 interactions play a critical role in maintaining the structure of the erythrocyte membrane skeleton. The reduced membrane rigidity of PfEMP3 knockout lines (Glenister *et al.*, 2002) indicated PfEMP3 interaction with spectrin and actin alter reduce flexibility, possibly by altering or interfering with normal interactions.

Mapping the domain within spectrin to which PfEMP3 binds, would also enable us to determine the precise charge of the PfEMP3 binding region within spectrin and speculate on the molecular forces involved in this interaction. The 14 residue PfEMP3 binding domain (PfEMP3-16-29) is positively charged (+1.95) at the pH of the cytoplasm of an infected erythrocyte (7.18 to 7.23) (Wunsch *et al.*, 1997). This positive charge could promote electrostatic interactions with spectrin, which has on overall negative charge at the same pH.

Given that we have shown PfEMP3 to bind both spectrin and actin, it is important to look at the spectrin-actin-PfEMP3 ternary interaction, both in the presence and absence of known interacting proteins, particularly protein 4.1. This may provide insight into the binding domains within spectrin and actin for PfEMP3

and the physiological consequences of this ternary interaction. The addition of peptides to both uninfected and infected erythrocytes has recently been achieved by fusing synthetic peptides to the internalisation domain of Antennapedia homeoprotein (Walsh *et al.*, 2002; Dhawan *et al.*, 2003). An experiment involving the addition of peptides encoding the 14 residue binding domain of PfEMP3 to erythrocytes of uninfected, parental and PfEMP3 knockout lines, following these established methods, may also give insight into the physiological consequences of this interaction.

With the future identification of a PfEMP3 binding region within spectrin, it would be interesting resolve crystal structure of the interacting domains. Again, this would be particularly interesting if the PfEMP3 binding domain within spectrin overlaps with known functional domains. To date, the crystal structure for CH2, EF Hand, phosphorylation and spectrin repeat domains have been determined, whereas the CH1 domain has not. However, the CH1/2 domain for the related dystrophin and utrophin have been solved (for review see Broderick and Winder, 2002). The ability to determine structure of ternary complexes (Jin and Harrison, 2002), also allows us to look more directly at the ternary interactions involving PfEMP3 and spectrin. Crystallographic studies involving the interaction of PfEMP3, spectrin and actin would also enable us to determine the ability of a single PfEMP3 molecule to simultaneously bind spectrin and actin. We have identified a 60 residue region (PfEMP3-FIa.1) which contains both the spectrin and actin binding domains. However, it is unknown wether regions within this binding domain are able to bind both spectrin and actin simultaneously or whether a single PfEMP3 molecule is only able to bind either spectrin or actin.

Previous studies of KAHRP have shown it's ability to bind to multiple erythrocyte proteins and to PfEMP1 (Waller *et al.*, 1999; Magowan *et al.*, 2000; Oh *et al.*, 2000; Voigt *et al.*, 2000). Therefore, identification of additional binding partners for PfEMP3, including both erythrocyte membrane proteins and *P. falciparum* proteins is crucial for a more complete understanding of PfEMP3 function. PfEMP3 has been implicated in the trafficking of PfEMP1, where the truncation of PfEMP3 results in accumulation of PfEMP1 in vesicle-like structures at the erythrocyte membrane. It has been proposed that truncation of PfEMP3 results in the loss of a binding domain, and subsequent inability of vesicle-like structures containing PfEMP1 and PfEMP3 to undergo correct sorting and trafficking (Waterkeyn *et al.*, 2000). Here, we have shown that the proposed binding domain is not responsible for spectrin or actin binding, as binding domains for these proteins are located within the N-terminus of PfEMP3, which is present in the truncated form of PfEMP3. This proposed binding domain might be involved in the

binding of PfEMP3 to an as yet unidentified protein present at the erythrocyte membrane skeleton. The less intense binding seen for MBP-PfEMP3-FV to IOVs, but not seen for spectrin or actin, indicates binding of PfEMP3 to an additional erythrocyte membrane protein. This binding may be to a protein that is less abundant in the erythrocyte membrane skeleton compared with spectrin and actin, for example p55 (which exists as approximately $8x10^4$ copies per cell in comparison to $2.4x10^5$ for each of the spectrin subunits and approximately $5x10^5$ copies for actin (for review see Lux and Palek, 1995)), or to a protein which binds PfEMP3 with an affinity below the sensitivity of this assay.

Alternatively, this suggested binding domain could be responsible for binding to another *P. falciparum* exported protein present at the erythrocyte membrane skeleton. Given the functional link between PfEMP3 and PfEMP1, it would be especially interesting to investigate possible interactions between these two parasite proteins. In addition, given the proposed role for PfEMP3 in trafficking (Waterkeyn *et al.*, 2000) and its location within Maurer's clefts, it would be interesting to look at interactions of PfEMP3 with the proteins involved in *P. falciparum* trafficking, especially those associated with Maurer's clefts, and interactions of PfEMP3 with other proteins known to be associated with Maurer's clefts. In particular, three recently identified proteins MAHRP-1 (Spycher *et al.*, 2003), PfSBP1 (Blisnick *et al.*, 2000) and a putative Sec23 homologue (Wickert *et al.*, 2003), which are associated with Maurer's clefts would be interesting candidates for interactions with PfEMP3.

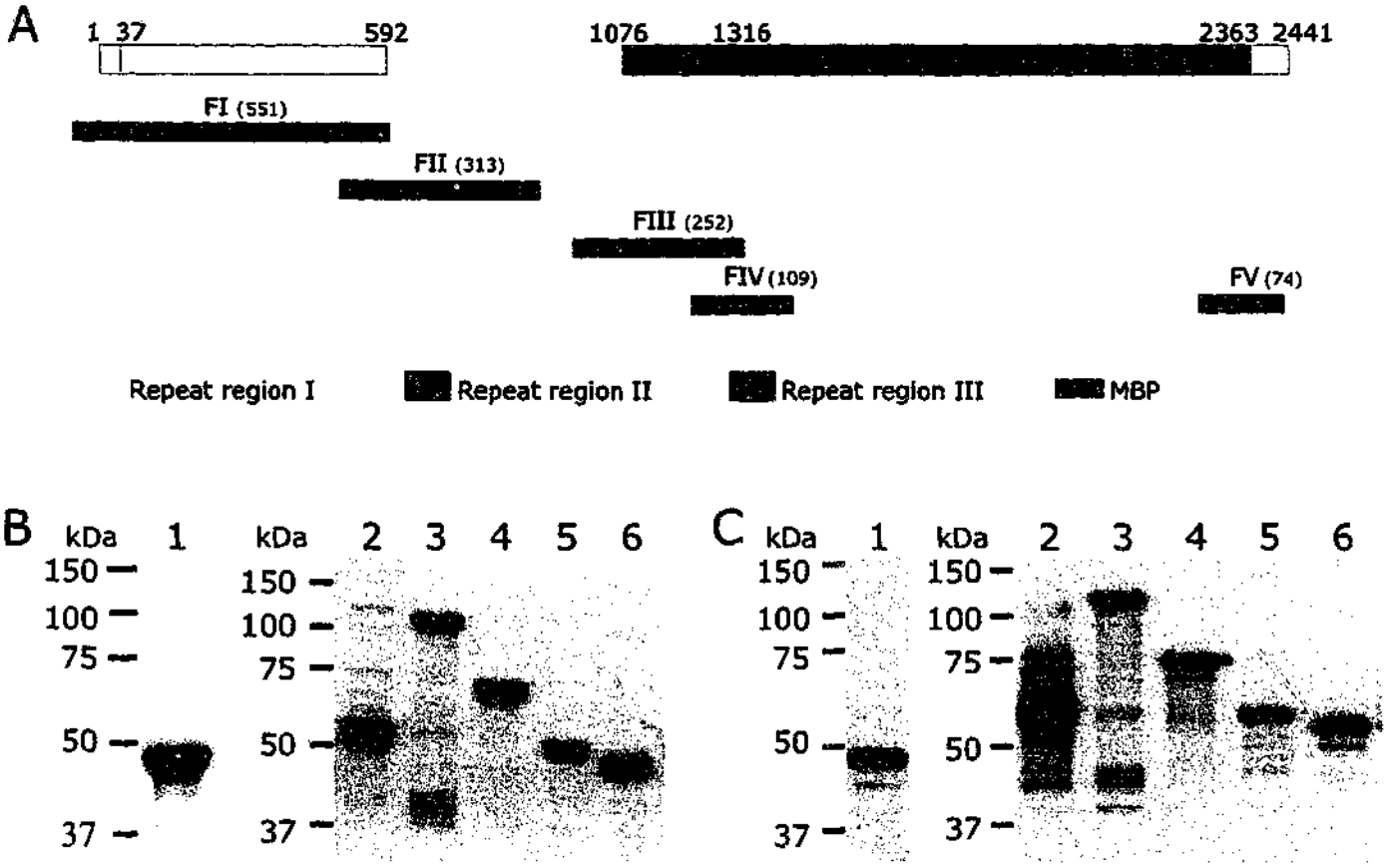

Figure 3.1. Expression and Purification of PfEMP3 Fragments

A. Schematic representation of PfEMP3 and the five fragments, PfEMP3-FI, -FII, -FII, FIV and -FV. Repeat regions are shown as coloured boxes and non-repeat regions shown as open boxes. Amino acid numbers are indicated above the schematic and the amino acid length of each fragment, excluding the MBP fusion is indicated in brackets. The gene intron splice site is indicated by the division at 37 amino acids.

B. Purified MBP-PfEMP3 fusion proteins detected by Coomassie Brilliant Blue staining of SDS-PAGE. 2 μg of each purified protein was resolved on 10% polyacrylamide gels. The protein samples are; MBP (lane 1), MBP-PfEMP3-FI (lane 2), MBP-PfEMP3-FII (lane 3), MBP-PfEMP3-FIII (lane 4), MBP-PfEMP3-FIV (lane 5) and MBP-PfEMP3-FV (lane 6).

C. Immunoblot assay of MBP-PfEMP3 fusion proteins detected using anti-MBP antiserum. 50 ng of each purified protein was resolved on 10% polyacrylamide gels and transferred to PVDF for detection. The protein samples are MBP (lane 1), MBP-PfEMP3-FI (lane 2), MBP-PfEMP3-FII (lane 3), MBP-PfEMP3-FIII (lane 4), MBP-PfEMP3-FIV (lane 5) and MBP-PfEMP3-FV (lane 6).

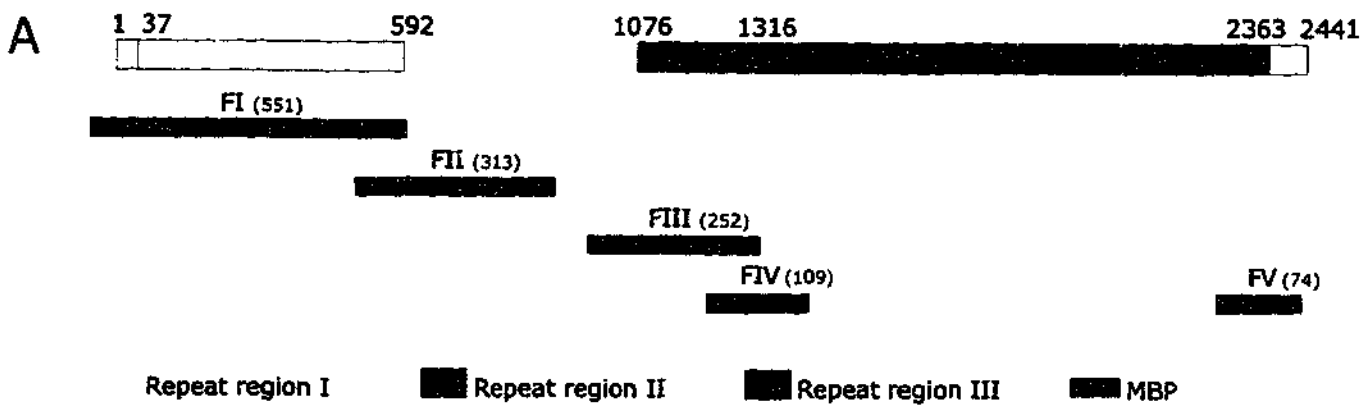

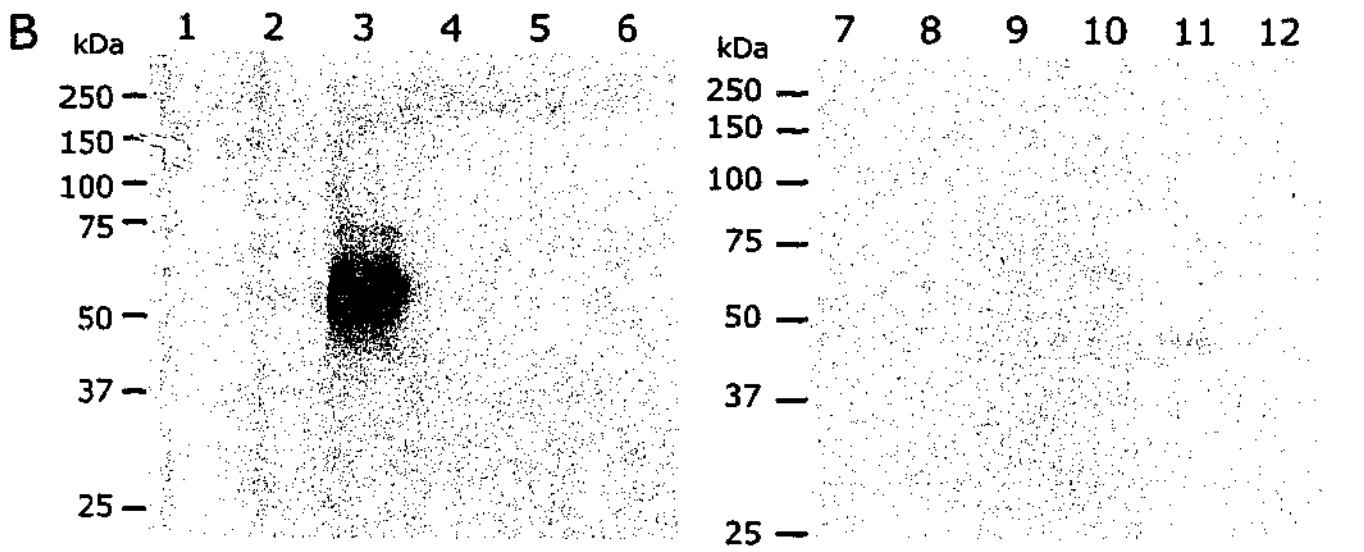

Figure 3.2. IOV Interaction Assay with PfEMP3 Fragments

A. Schematic representation of PfEMP3 and the five fragments, PfEMP3-FI, -FII, -FII, -FIV and -FV.

B. Immunoblot of IOV interaction assay. IOVs (lanes 1, 3, 5, 7, 9 and 11) and BSA (lanes 2, 4, 6, 8, 10 and 12) were coated onto wells of a microtitre plate. MBP (lanes 1 and 2), MBP-PfEMP3-FI (lanes 3 and 4), -FII (lanes 5 and 6), -FIII (lane 7 and 8), -FIV (lanes 9 and 10) and -FV (lanes 11 and 12) were added to the wells and allowed to bind. Bound protein was detected to wells coated with IOVs for PfEMP3-F1 (lane 3) and with a lesser intensity for PfEMP3-FV (lane 11). No bound protein was detected for MBP (lane 1), MBP-PfEMP3-FII (lane 5), -FIII (lane 7) and -FIV (lane 9) to wells coated with IOVs or for any of the proteins to wells coated with BSA (lanes 2, 4, 6, 8, 10 and 12).

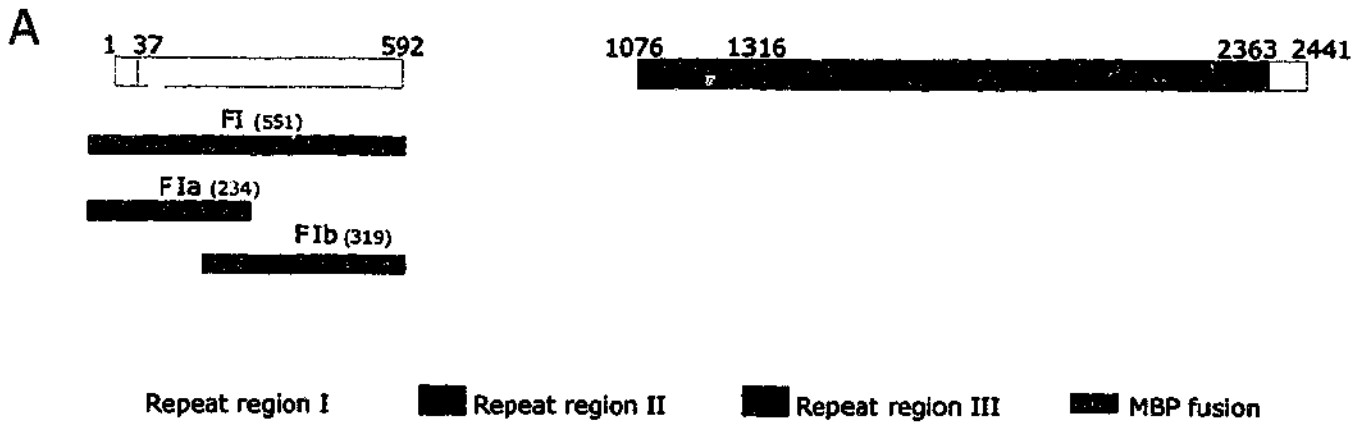

Figure 3.3. Expression and Purification of PfEMP3-FI Sub-Fragments

A. Schematic representation of PfEMP3 and the sub-fragments of PfEMP3-FI; PfEMP3-FIa and PfEMP3-FIb.

B. Purified MBP-PfEMP3 fusion proteins detected by Coomassie Brilliant Blue staining of SDS-PAGE. 2 μg of each purified protein was resolved on 10% polyacrylamide gels. The protein samples are, MBP-PfEMP3-FIa (lane 1) and MBP-PfEMP3-FIb (lane 2),

C. Immunoblot assay of MBP-PfEMP3 fusion proteins detected using anti-MBP antiserum. 50 ng of each purified protein was resolved on 10% polyacrylamide gels and transferred to PVDF for detection. The protein samples are MBP-PfEMP3-FIa (lane 1) and MBP-PfEMP3-FIb (lane 2).

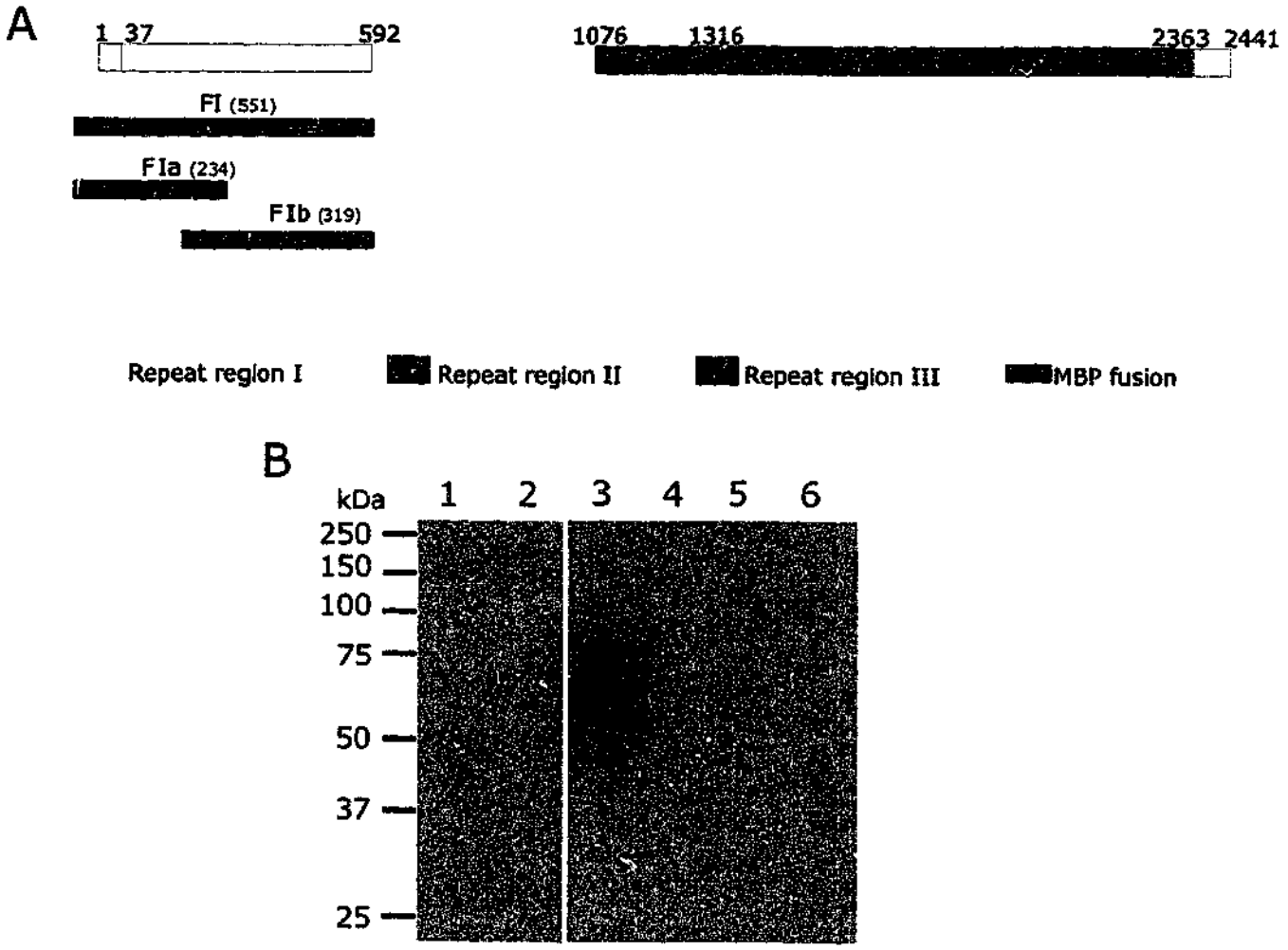

Figure 3.4. IOV Interaction Assay with PfEMP3-FI Sub-Fragments

A. Schematic representation of PfEMP3 and the sub-fragments of PfEMP3-FI; PfEMP3-FIa and PfEMP3-FIb.

B. Immunoblot of IOV interaction assay. IOVs (lanes 1, 3 and 5) and BSA (lanes 2, 4 and 6) were coated onto wells of a microtitre plate. MBP (lanes 1 and 2), MBP-PfEMP3-FIa (lanes 3 and 4) and MBP-PfEMP3-FIb (lanes 5 and 6) were added to the wells and allowed to bind. Bound protein was detected to wells coated with IOVs for MBP-PfEMP3-F1a (lane 3). No bound protein was detected for MBP (lane 1) or MBP-PfEMP3-FIb (lane 5) to wells coated with IOVs or for any of the proteins to wells coated with BSA (lanes 2, 4 and 6).

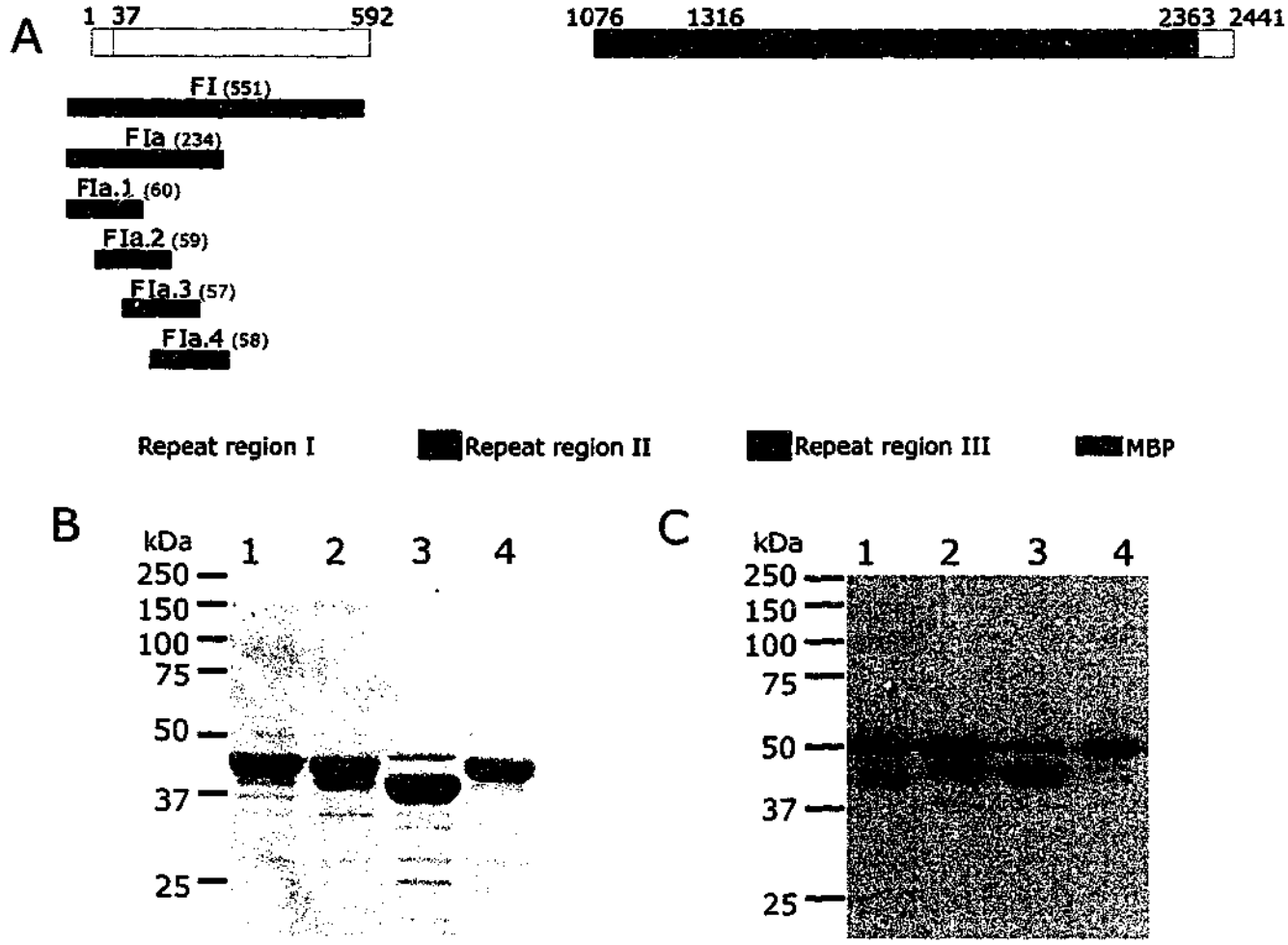

Figure 3.5. Expression and Purification of PfEMP3-FIa Sub-Fragments

A. Schematic representation of PfEMP3 and the sub-fragments of PfEMP3-FIa; PfEMP3-FIa.1, PfEMP3-FIa.2, PfEMP3-FIa.3 and PfEMP3-FIa.4.

B. Purified MBP-PfEMP3 fusion proteins detected by Coomassie Brilliant Blue staining of SDS-PAGE. 2 μg of each purified protein was resolved on 10% polyacrylamide gels. The protein samples are MBP-PfEMP3-FIa.1 (lane 1), MBP-PfEMP3-FIa.2 (lane 2), MBP-PfEMP3-FIa.3 (lane 3) and MBP-PfEMP3-FIa.4 (lane 4).

C. Immunoblot assay of MBP-PfEMP3 fusion proteins detected using anti-MBP antiserum. 50 ng of each purified protein was resolved on 10% polyacrylamide gels and transferred to PVDF for detection. The protein samples are MBP-PfEMP3-FIa.1 (lane 1), MBP-PfEMP3-FIa.2 (lane 2), MBP-PfEMP3-FIa.3 (lane 3) and MBP-PfEMP3-FIa.4 (lane 4).

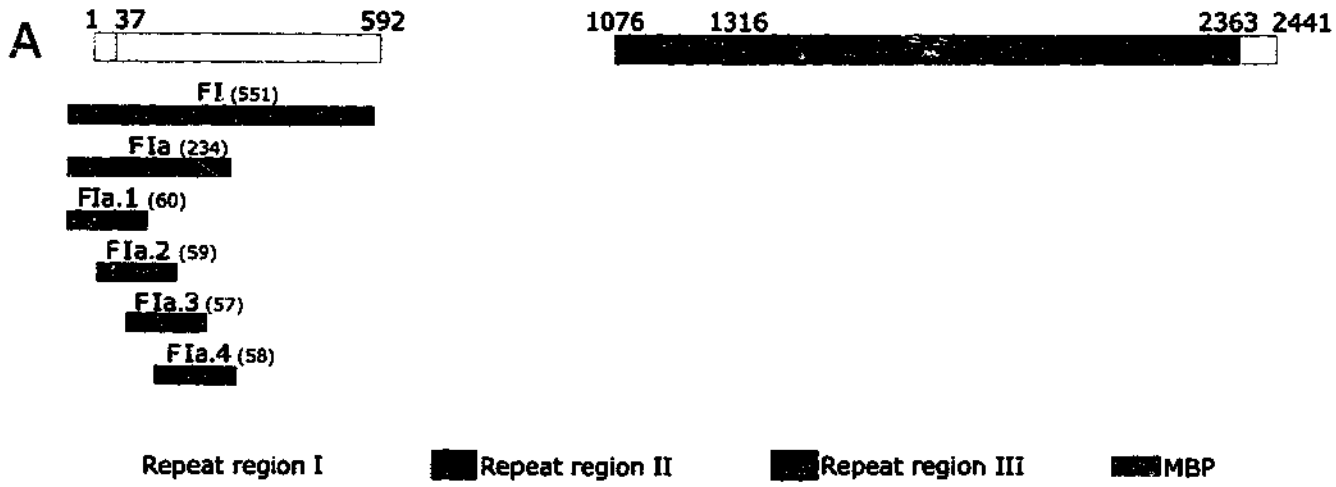

Figure 3.6. IOV Interaction Assay with PfEMP3-FIa Sub-Fragments

A. Schematic representation of PfEMP3 and the sub-fragments of PfEMP3-FIa; PfEMP3-FIa.1, PfEMP3-FIa.2, PfEMP3-FIa.3 and PfEMP3-FIa.4.

B. Immunoblot of IOV interaction assay. IOVs (lanes 1, 3, 5, 7 and 9) and BSA (lanes 2, 4, 6, 8 and 10) were coated onto wells of a microtitre plate. MBP (lanes 1 and 2), MBP-PfEMP3-FIa.1 (lanes 3 and 4), -FIa.2 (lanes 5 and 6), -FIa.3 (lanes 7 and 8) and -FIa.4 (lanes 9 and 10) were added to the wells and allowed to bind. Bound protein was detected for MBP-PfEMP3-F1a.1 (lane 3) to wells coated with IOVs. No bound protein was detected any of the other proteins to wells coated with IOVs (lanes 1, 5, 7 and 9) or for any of the proteins to wells coated with BSA (lanes 2, 4, 6, 8 and 10).

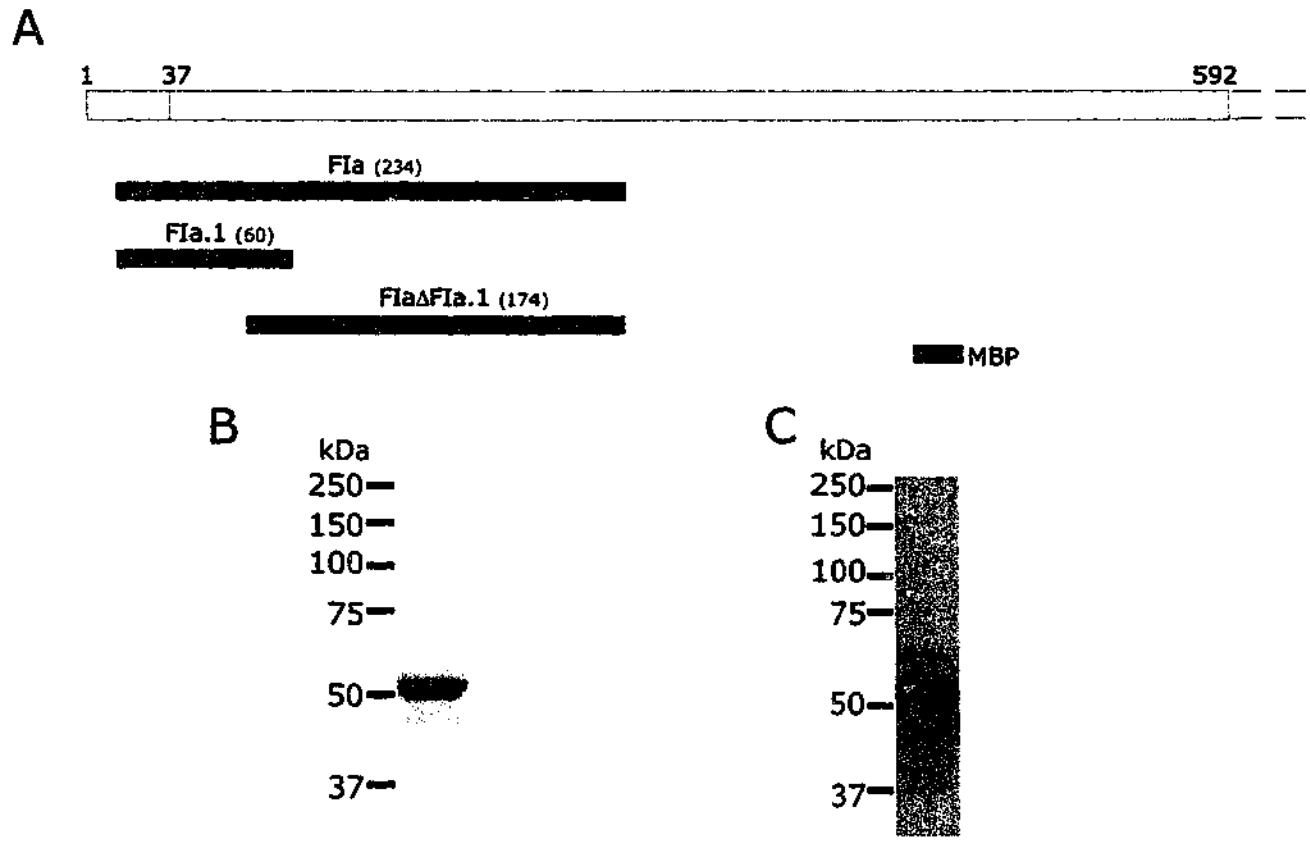

Figure 3.7. Expression and Purification of PfEMP3-FIa.1 Deletion Construct

A. Schematic representation of PfEMP3 and the deletion of PfEMP3-FIa.1; PfEMP3-FIaΔFIa.1.

B. Purified MBP-PfEMP3ΔFIa.1 fusion protein detected by Coomassie Brilliant Blue staining of SDS-PAGE. 2 μg purified MBP-PfEMP3ΔFIa.1 protein was resolved on 10% polyacrylamide gels.

C. Immunoblot assay of MBP-PfEMP3ΔFIa.1 fusion protein detected using anti-MBP antiserum. 50 ng of purified MBP-PfEMP3ΔFIa.1 was resolved on 10% polyacrylamide gels and transferred to PVDF for detection.

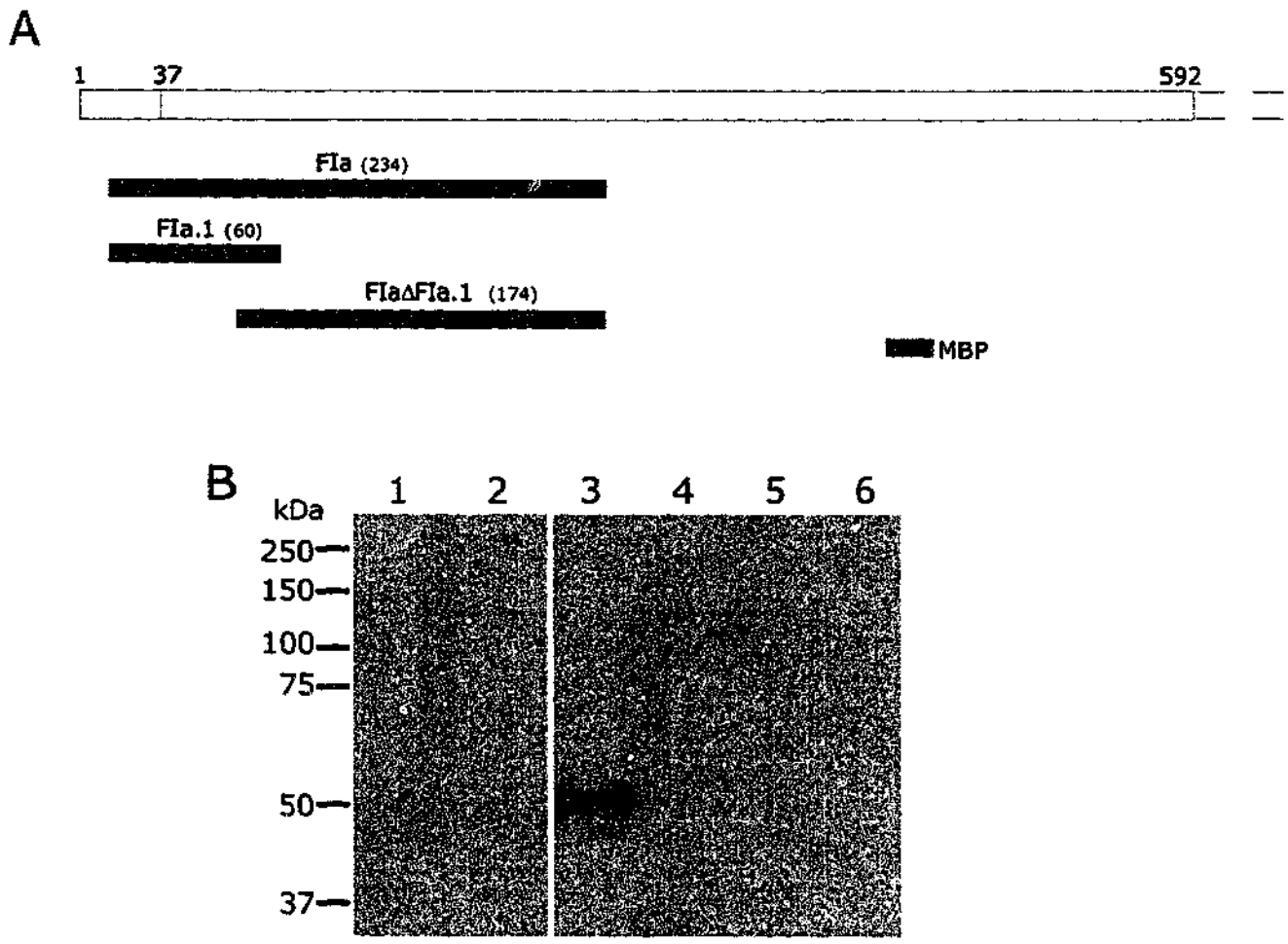

Figure 3.8. IOV Interaction Assay with PfEMP3-FIa.1 Deletion Construct

A. Schematic representation of PfEMP3 and the deletion of PfEMP3-FIa.1; PfEMP3-FIaΔFIa.1.

B. Immunoblot of IOV interaction assay. IOVs (lanes 1, 3 and 5) and BSA (lanes 2, 4 and 6) were coated onto wells of a microtitre plate. MBP (lanes 1 and 2), MBP-PfEMP3-FIa (lanes 3 and 4) and MBP-PfEMP3-FIaΔFIa.1 (lanes 5 and 6) were added to the wells and allowed to bind. Bound protein was detected to wells coated with IOVs for MBP-PfEMP3-F1a.1 (lane 3) but not for either MBP (lane 1) or MBP-PfEMP3-FIaΔFIa.1 (lane 5) or for any of the proteins to wells coated with BSA (lanes 2, 4 and 6).

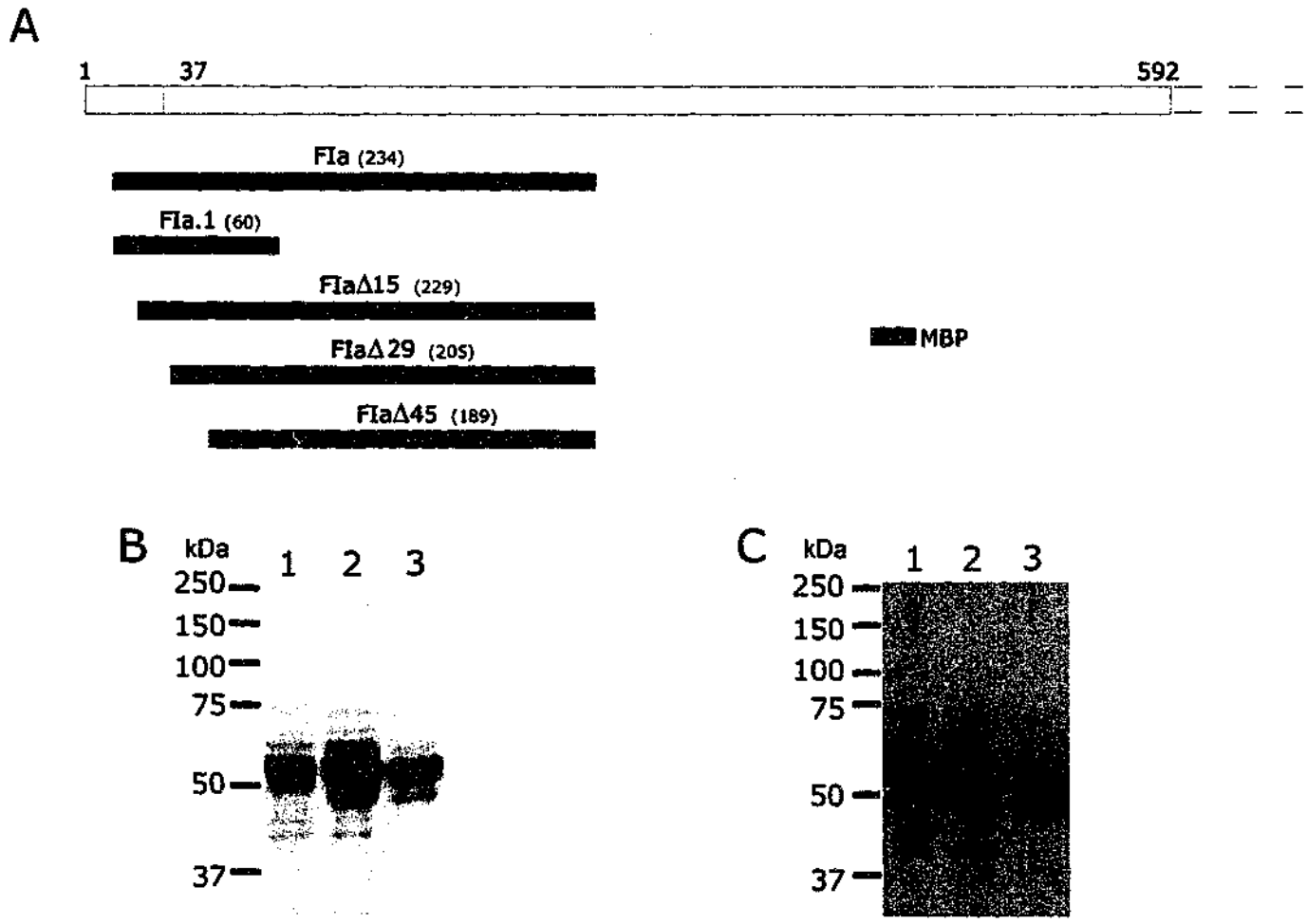

Figure 3.9. Expression and Purification of N-Terminal PfEMP3 Deletions

A. Schematic representation of PfEMP3 and the N-terminal PfEMP3-FIa deletions; PfEMP3-FIaΔ15, PfEMP3-FIaΔ29 and PfEMP3-FIaΔ45.

B. Purified MBP-PfEMP3 fusion proteins detected by Coomassie Brilliant Blue staining of SDS-PAGE. 2 μg of each purified protein was resolved on 10% polyacrylamide gels. The protein samples are; MBP-PfEMP3-FIaΔ15 (lane 1), MBP-PfEMP3-FIaΔ29 (lane 2) and MBP-PfEMP3-FIaΔ45 (lane 3).

C. Immunoblot assay of MBP-PfEMP3 fusion proteins detected using anti-MBP antiserum. 50 ng of each purified protein was resolved on 10% polyacrylamide gels and transferred to PVDF for detection. The protein samples are MBP-PfEMP3-FIaΔ15 (lane 1), MBP-PfEMP3-FIaΔ29 (lane 2) and MBP-PfEMP3-FIaΔ45 (lane 3).

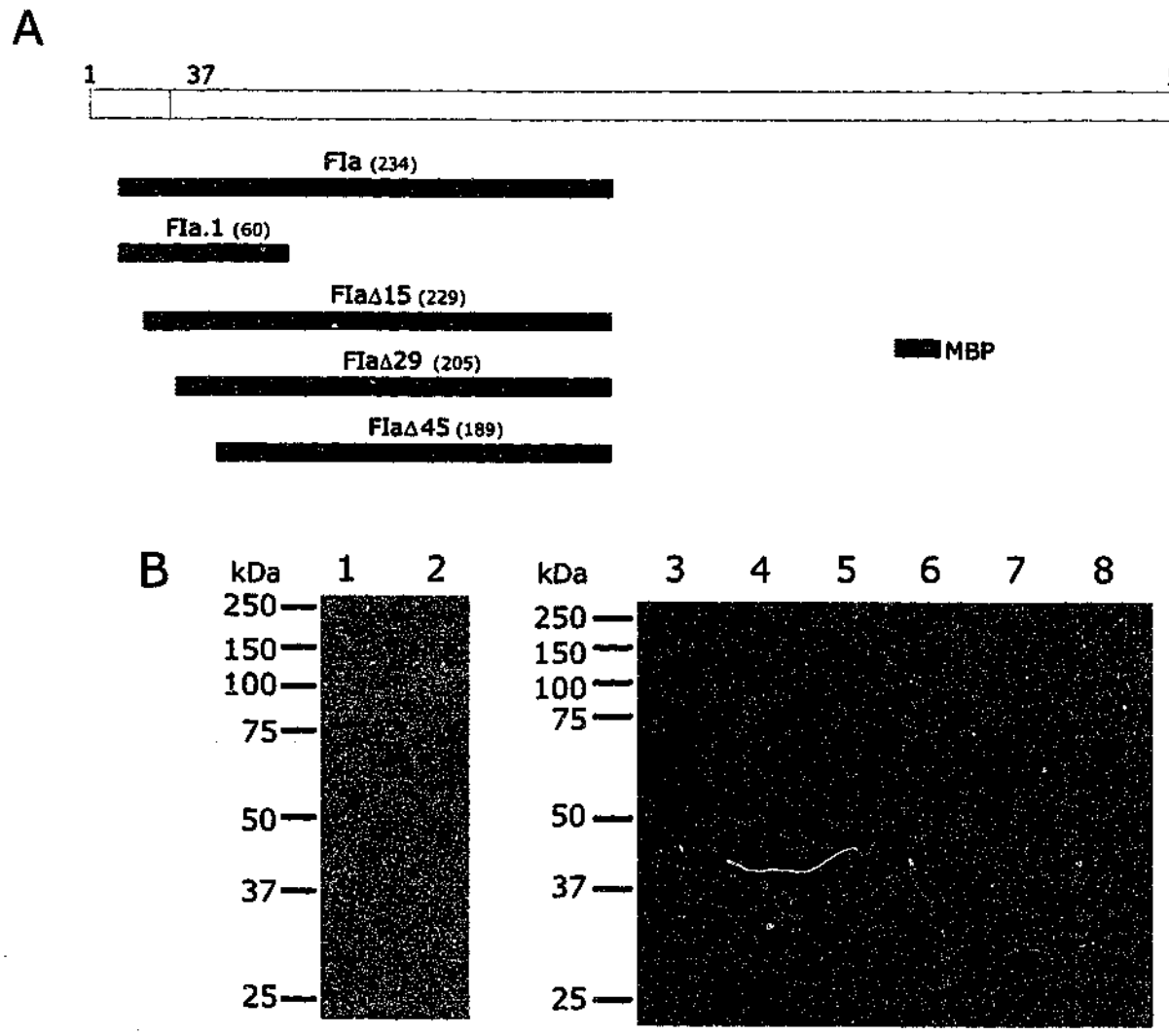

Figure 3.10. IOV Interaction Assay with N-Terminal PfEMP3 Deletions

A. Schematic representation of PfEMP3 and the N-terminal PfEMP3 deletions; PfEMP3-FIaΔ15, PfEMP3-FIaΔ29 and PfEMP3-FIaΔ45.

B. Immunoblot of IOV interaction assay. IOVs (lanes 1, 3, 5 and 7) and BSA (lanes 2, 4, 6 and 8) were coated onto wells of a microtitre plate. MBP (lanes 1 and 2), MBP-PfEMP3-FIaΔ15 (lanes 3 and 4), -FIaΔ29 (lanes 5 and 6) and -FIaΔ45 (lanes 7 and 8) were added to the wells and allowed to bind. Bound protein was detected to wells coated with IOVs for MBP-PfEMP3-FIaΔ15 (lane 3) but not for MBP (lane 1), MBP-PfEMP3-FIaΔ29 (lane 5) or -FIaΔ45 (lane 7), or for any of the proteins to wells coated with BSA (lanes 2, 4, 6 and 8).

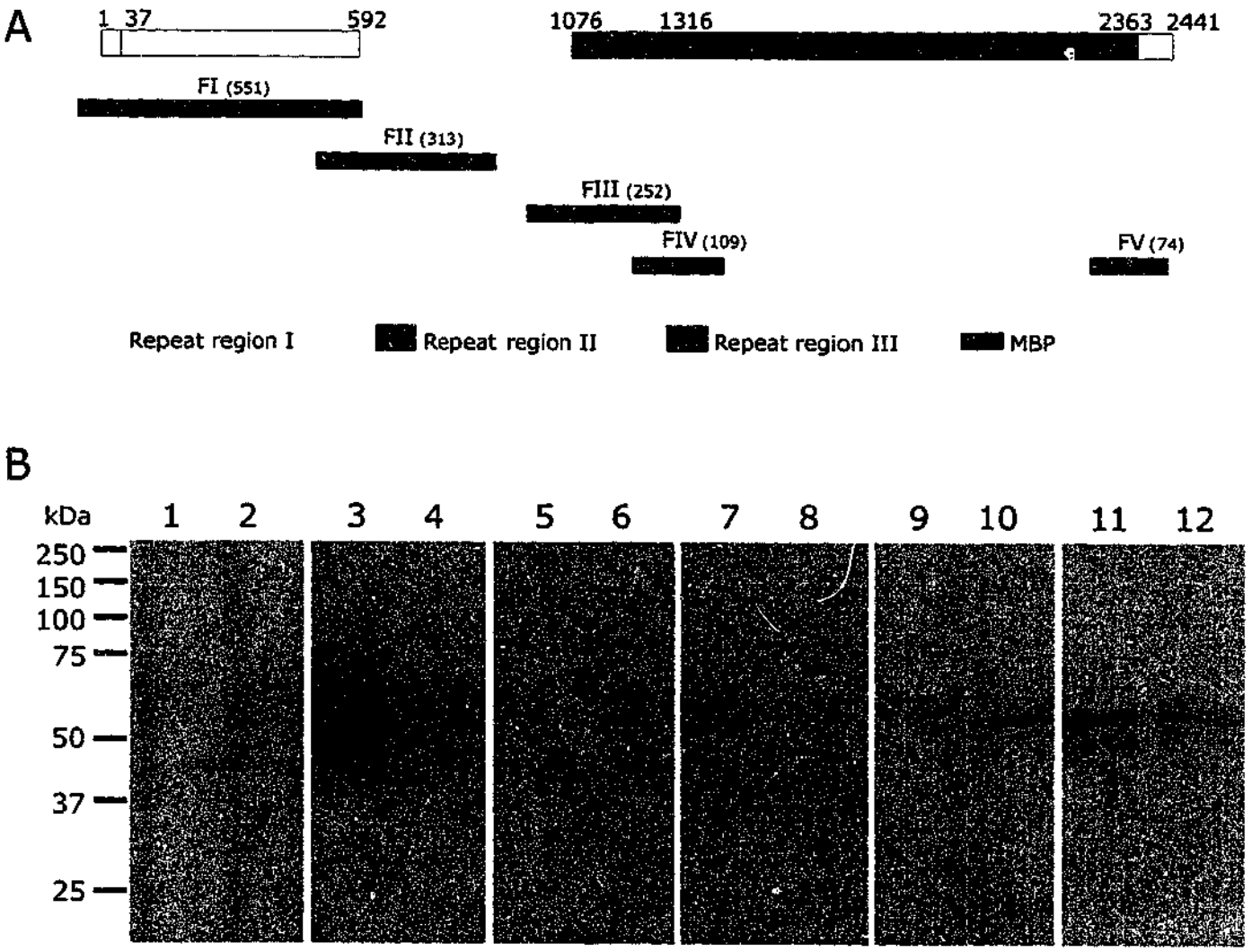

Figure 3.11. Spectrin Interaction Assay with PfEMP3 Fragments

A. Schematic representation of PfEMP3 and the five fragments, PfEMP3-FI, -FII, -FII, -FIV and -FV.

B. Immunoblot of spectrin interaction assay. Spectrin (lanes 1, 3, 5, 7, 9 and 11) and BSA (lanes 2, 4, 6, 8, 10 and 12) were coated onto wells of a microtitre plate. MBP (lanes 1 and 2), MBP-PfEMP3-FI (lanes 3 and 4), -FII (lanes 5 and 6), -FIII (lane 7 and 8), -FIV (lanes 9 and 10) and -FV (lanes 11 and 12) were added to the wells and allowed to bind. Bound protein was detected to wells coated with spectrin for PfEMP3-F1 (lane 3). No bound protein was detected for MBP, MBP-PfEMP3-FII (lane 5), -FIII (lane 7), -FIV (lane 9) or -FIV (lane 11) to wells coated with spectrin or for any of the proteins to wells coated with BSA (lanes 2, 4, 6, 8, 10 and 12).

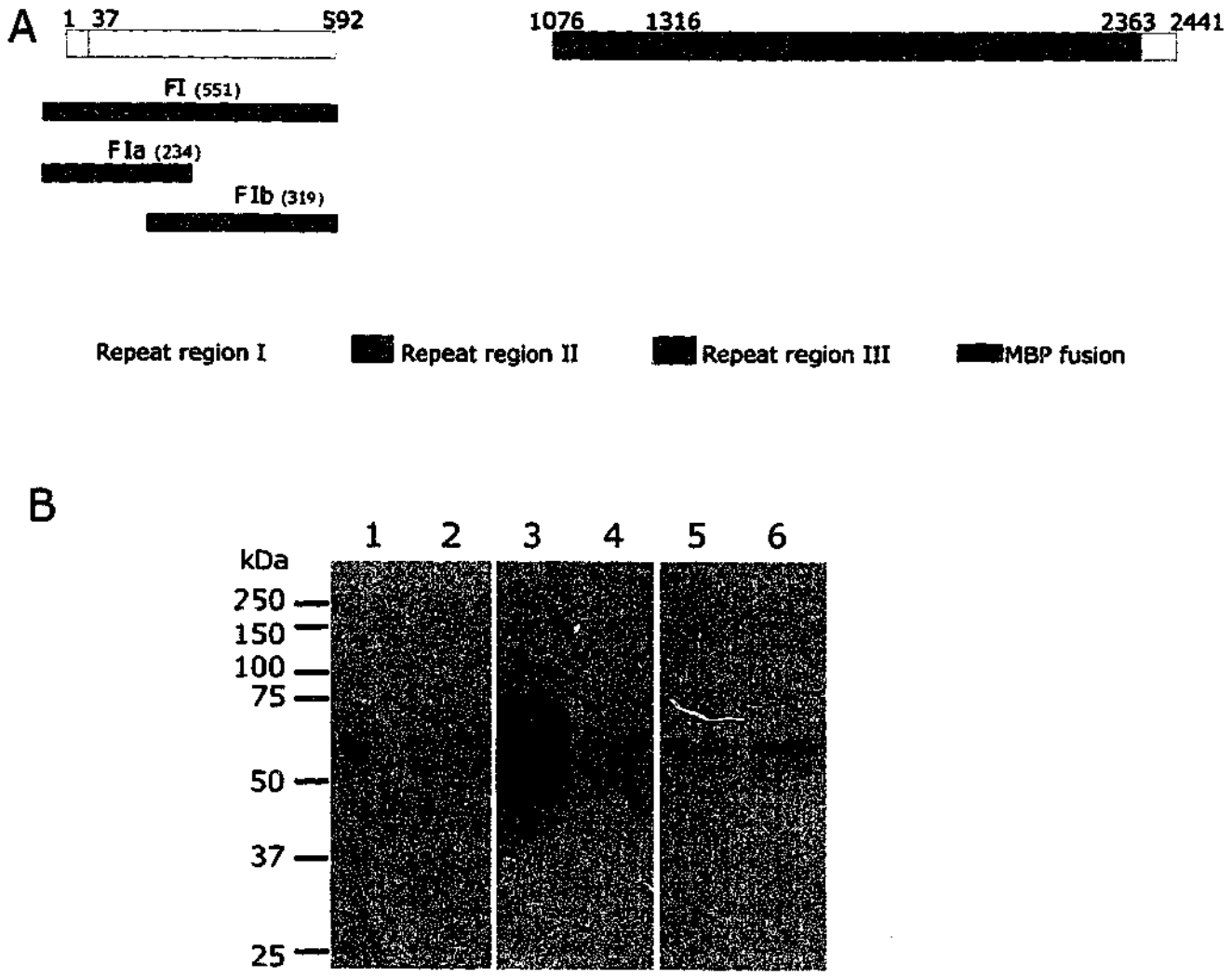

Figure 3.12. Spectrin Interaction Assay with PfEMP3-FI Sub-Fragments

A. Schematic representation of PfEMP3 and the PfEMP3-FI sub-fragments; PfEMP3-FIa and PfEMP3-FIb.

B. Immunoblot of spectrin interaction assay. Spectrin (lanes 1, 3 and 5) and BSA (lanes 2, 4 and 6) were coated onto wells of a microtitre plate. MBP (lanes 1 and 2), MBP-PfEMP3-FIa (lanes 3 and 4) and MBP-PfEMP3-FIb (lanes 5 and 6) were added to the wells and allowed to bind. Bound protein was detected for MBP-PfEMP3-F1a (lane 3) to wells coated with spectrin. No bound protein was detected for MBP (lane 1) or MBP-PfEMP3-FIb (lane 5) to wells coated with IOVs or for any of the proteins to wells coated with BSA (lanes 2, 4 and 6).

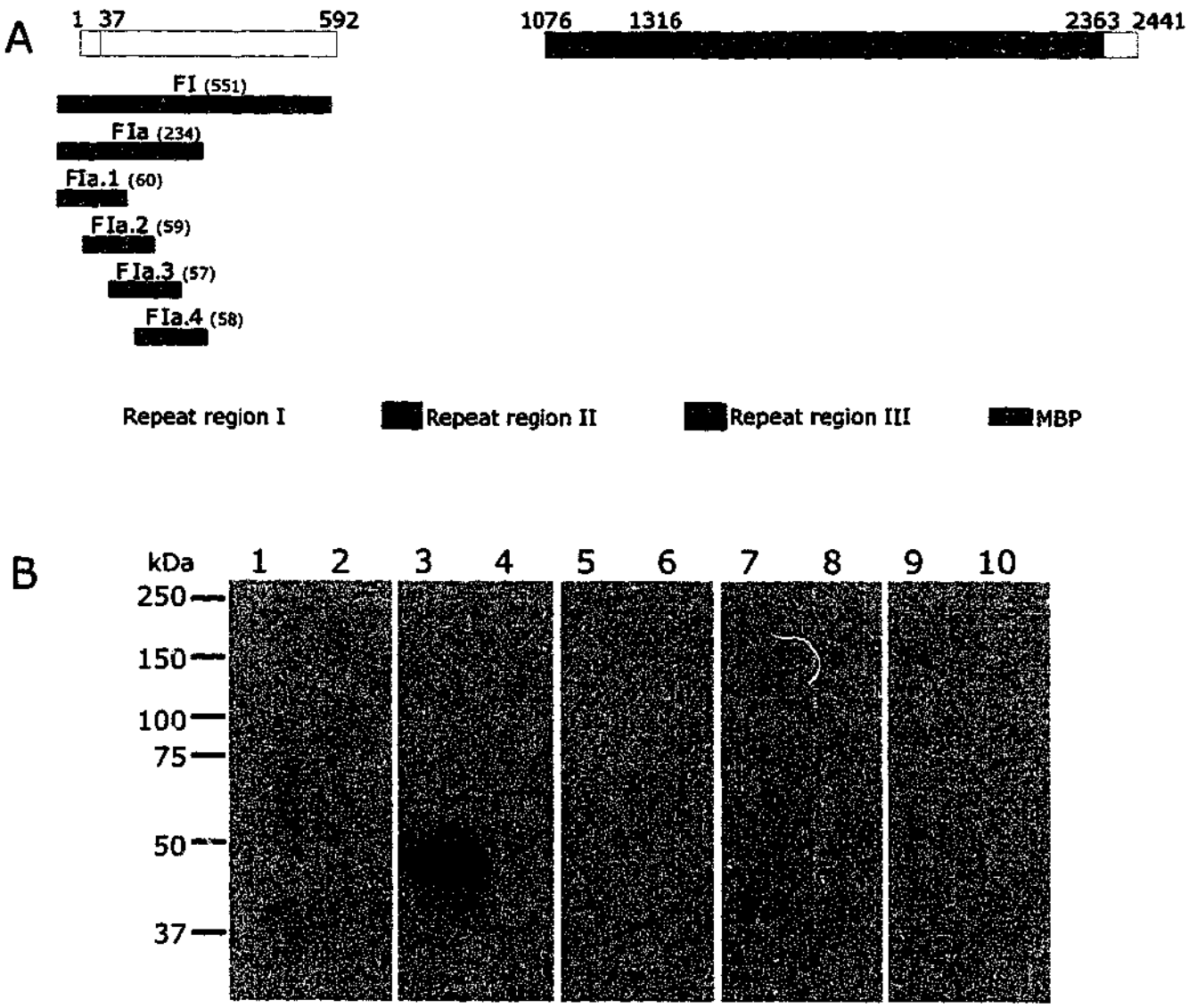

Figure 3.13. Spectrin Interaction Assay with PfEMP3-FIa Sub-Fragments

A. Schematic representation of PfEMP3 and the PfEMP3-FIa sub-fragments; PfEMP3-FIa.1, PfEMP3-FIa.2, PfEMP3-FIa.3 and PfEMP3-FIa.4.

B. Immunoblot of spectrin interaction assay. Spectrin (lanes 1, 3, 5, 7 and 9) and BSA (lanes 2, 4, 6, 8 and 10) were coated onto wells of a microtitre plate. MBP (lanes 1 and 2), MBP-PfEMP3-FIa.1 (lanes 3 and 4), -FIa.2 (lanes 5 and 6), -FIa.3 (lanes 7 and 8) and -FIa.4 (lanes 9 and 10) were added to the wells and allowed to bind. Bound protein was detected for MBP-PfEMP3-F1a.1 (lane 3) to wells coated with spectrin. No bound protein was detected any of the other proteins to wells coated with spectrin (lanes 1, 5, 7 and 9) or for any of the proteins to wells coated with BSA (lanes 2, 4, 6, 8 and 10).

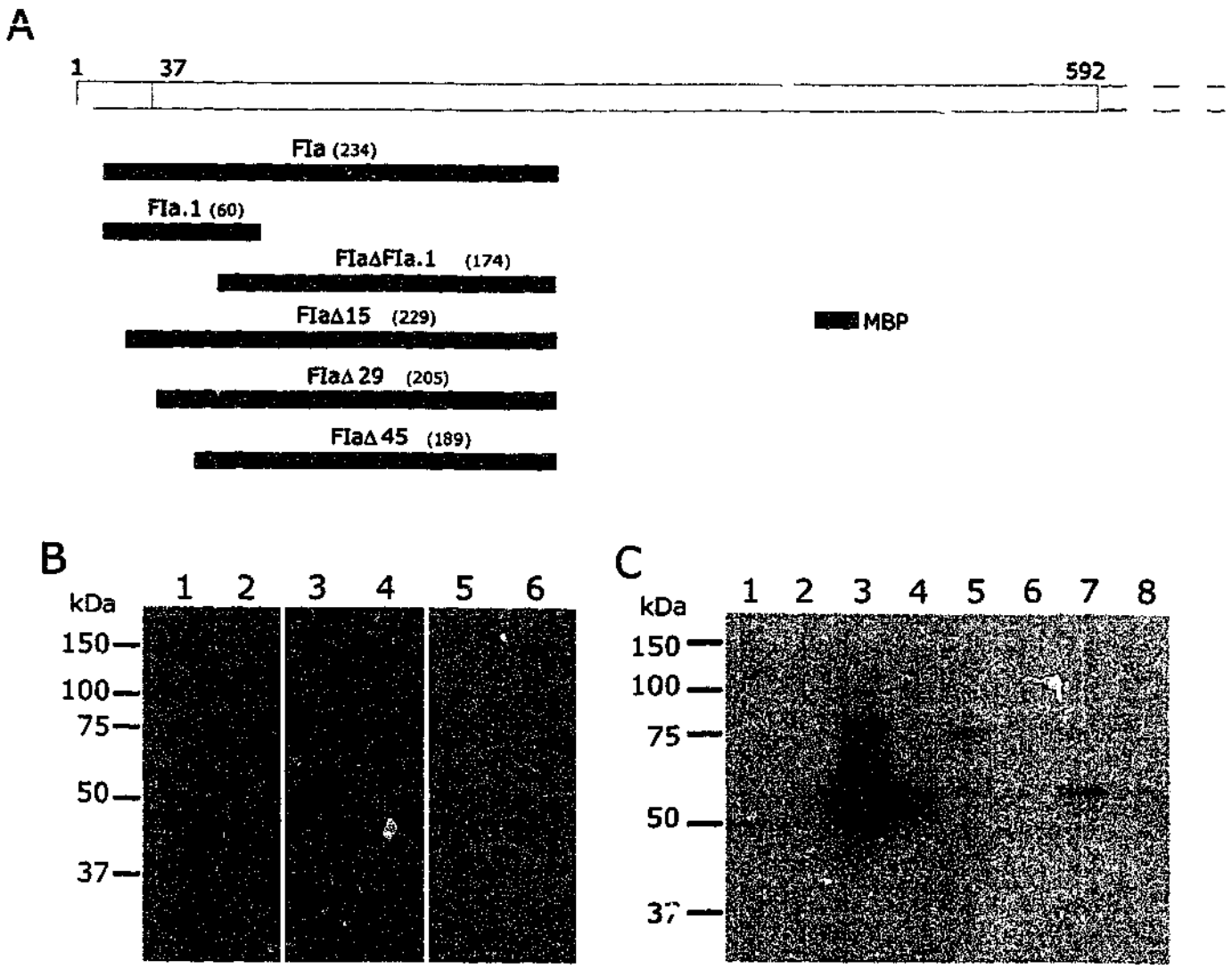

Figure 3.14. Spectrin Interaction Assay with PfEMP3 Deletions

A. Schematic representation of PfEMP3 and the PfEMP3 deletions; PfEMP3-FIaΔFIa.1, PfEMP3-FIaΔ15, PfEMP3-FIaΔ29 and PfEMP3-FIaΔ45.

B. Immunoblot of spectrin interaction assay. Spectrin (lanes 1, 3 and 5) and BSA (lanes 2, 4 and 6) were coated onto wells of a microtitre plate. MBP (lanes 1 and 2), MBP-PfEMP3-FIa (lanes 3 and 4) and MBP-PfEMP3-FIaΔFIa.1 (lanes 5 and 6) were added to the wells and allowed to bind. Bound protein was detected to wells coated with spectrin for MBP-PfEMP3-F1a.1 (lane 3) but not for MBP (lane 1) or MBP-PfEMP3-FIaΔFIa.1 (lane 5) or for any of the proteins to wells coated with BSA (lanes 2, 4 and 6).

C. Immunoblot of spectrin interaction assay. Spectrin (lanes 1, 3, 5 and 7) and BSA (lanes 2, 4, 6 and 8) were coated onto wells of a microtitre plate. MBP (lanes 1 and 2), MBP-PfEMP3-FIaΔ15 (lanes 3 and 4), -FIaΔ29 (lanes 5 and 6) and -FIaΔ45 (lanes 7 and 8) were added to the wells and allowed to bind. Bound protein was detected to wells coated with spectrin for MBP-PfEMP3-F1a.1Δ15 (lane 3) but not for MBP (lane 1) -FIaΔ29 (lane 5) or -FIaΔ45 (lane 7) or for any of the proteins to wells coated with BSA (lanes 2, 4, 6 and 8).

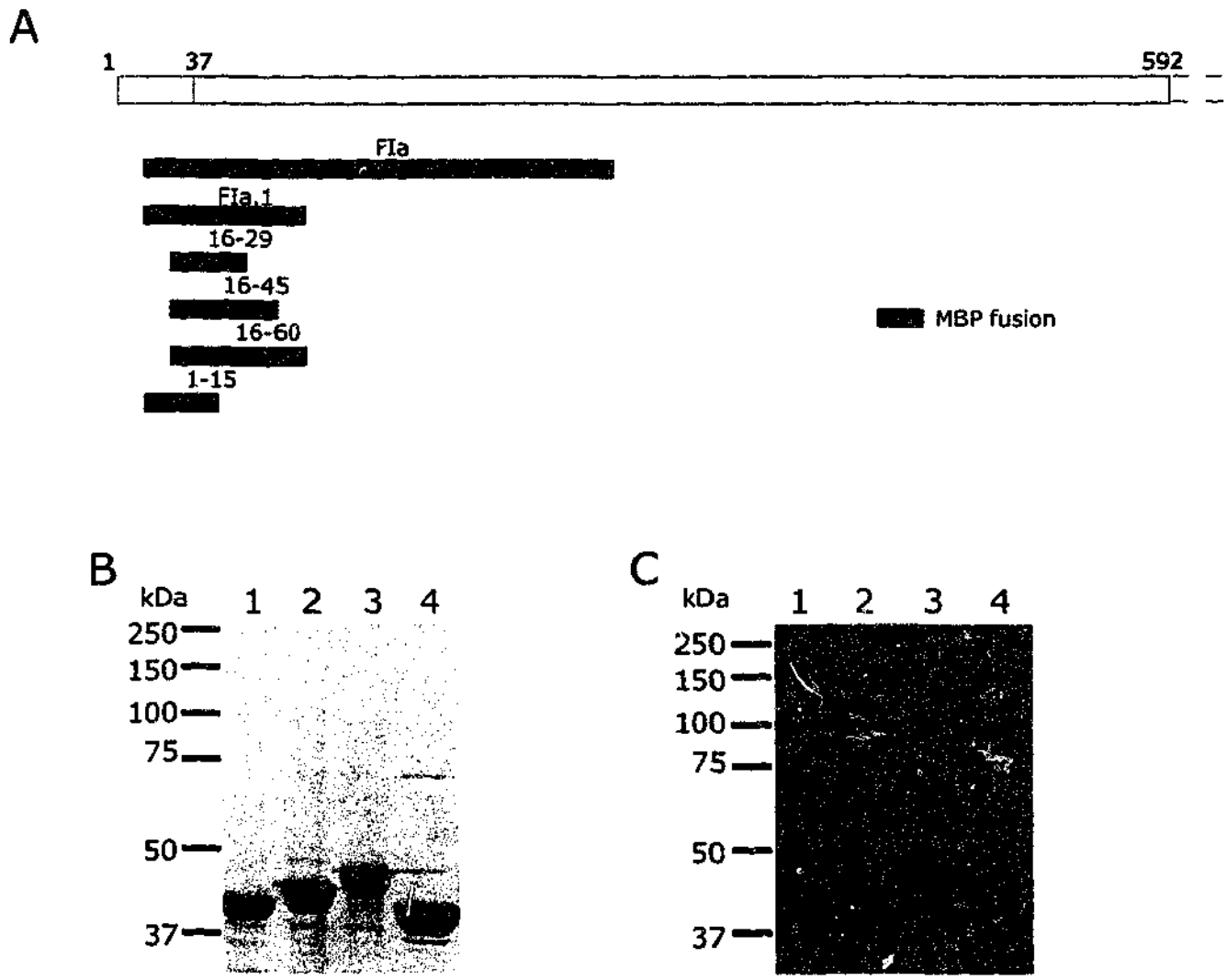

Figure 3.15. Expression and Purification of PfEMP3-FIa.1 Sub-Fragments

A. Schematic representation of PfEMP3 and the PfEMP3-FIa.1 sub-fragments; PfEMP3-16-29, -16-45, -16-60 and -1-15.

B. Purified MBP-PfEMP3 fusion proteins detected by Coomassie Brilliant Blue staining of SDS-PAGE. 2 μg of each purified protein was resolved on 10% polyacrylamide gels. The protein samples are; MBP-PfEMP3-16-29 (lane 1), MBP-PfEMP3-16-45 (lane 2), MBP-PfEMP3-16-60 (lane 3) and MBP-PfEMP3-1-15 (lane 4).

C. Immunoblot assay of MBP-PfEMP3 fusion proteins detected using anti-MBP antiserum. 50 ng of each purified protein was resolved on 10% polyacrylamide gels and transferred to PVDF for detection. The protein samples are MBP-PfEMP3-16-29 (lane 1), MBP-PfEMP3-16-45 (lane 2), MBP-PfEMP3-16-60 (lane 3) and MBP-PfEMP3-1-15 (lane 4).

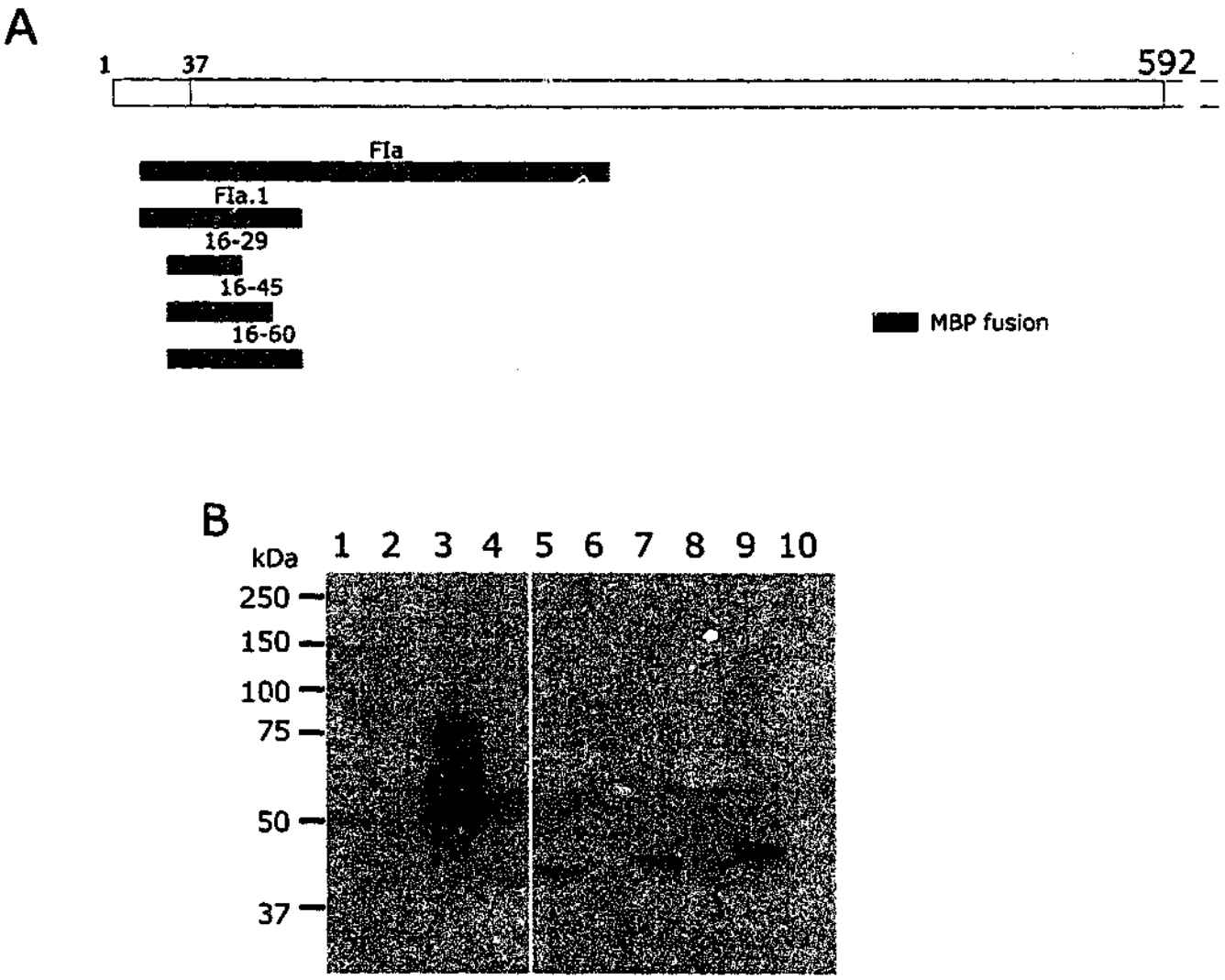

Figure 3.16. Spectrin Interaction Assay with PfEMP3-FIa.1 Sub-Fragments

A. Schematic representation of PfEMP3 and the PfEMP3-FIa.1 sub-fragments; PfEMP3-16-29, -16-45, -16-60 and -1-15.

B. Immunoblot of spectrin interaction assay. Spectrin (lanes 1, 3, 5, 7 and 9) and BSA (lanes 2, 4, 6, 8 and 10) were coated onto wells of a microtitre plate. MBP (lanes 1 and 2), MBP-PfEMP3-FIaΔ15 (lanes 3 and 4), -16-29 (lanes 5 and 6), -16-45 (lanes 7 and 8) and -16-60 (lanes 9 and 10) were added to the wells and allowed to bind. Bound protein was detected to wells coated with spectrin for MBP-PfEMP3-F1a.1Δ15 (lane 3). To a lesser extent, bound protein was detected for MBP-PfEMP3-16-29 (lane 5), -16-45 (lane 7) and -16-60 (lane 9) to wells coated with spectrin. No bound protein was detected for MBP to wells coated with spectrin (lane 1) or for any of the proteins to wells coated with BSA (lanes 2, 4, 6, 8 and 10).

PfEMP3 Fragment	k_a ($M^{-1}sec^{-1}$)	k_d (sec^{-1})	$K_{(D)kin}$ (nM)	$K_{(D)Scat}$ (nM)
FI	$3.0\pm0.1x10^4$	$2.1\pm0.1x10^{-3}$	70	59
FII, FIII, FIV, FV	No binding	No binding	No binding	No binding
FIa	$8.4\pm0.1x10^4$	$6.3\pm0.2x10^{-3}$	75	67
FIb	No binding	No binding	No binding	No binding
FIa.1	$7.9\pm0.2x10^4$	$6.7\pm0.1x10^{-3}$	85	80
FIa.2, FIa.3, FIa.4	No binding	No binding	No binding	No binding
FIaΔFIa.1	No binding	No binding	No binding	No binding
FIaΔ15	$2.4\pm0.2x10^3$	$6.6\pm0.2x10^{-4}$	275	236
FIaΔ29	No binding	No binding	No binding	No binding
1-15	No binding	No binding	No binding	No binding
16-29	$15\pm0.2x10^3$	$5.7\pm0.2x10^{-4}$	380	300
MBP	No binding	No binding	No binding	No binding

Table 3.1. Binding Constants of PfEMP3 Fragments with Spectrin.
The binding assays were carried out in PBS containing 0.05% Tween 20. From the binding curves obtained by resonant mirror detection method, K_a, K_d, $K_{(D)kin}$ and $K_{(D)scat}$ were determined using the software package FASTfit™. Spectrin binding was detected for PfEMP3-FI, PfEMP3-FIa and PfEMP3-FIa.1, but was abolished for PfEMP3-FIaΔFIa.1. Binding was retained following the deletion of the first 15 amino acids (PfEMP3-FIaΔ15), but abolished with the deletion of a further 14 amino acids (PfEMP3-FIaΔ29). Amino acids 16-29 were sufficient to confer spectrin binding (PfEMP3-16-29). The MBP negative control showed no binding to spectrin. No binding is defined as described in Nunomura *et al.*, 2000.

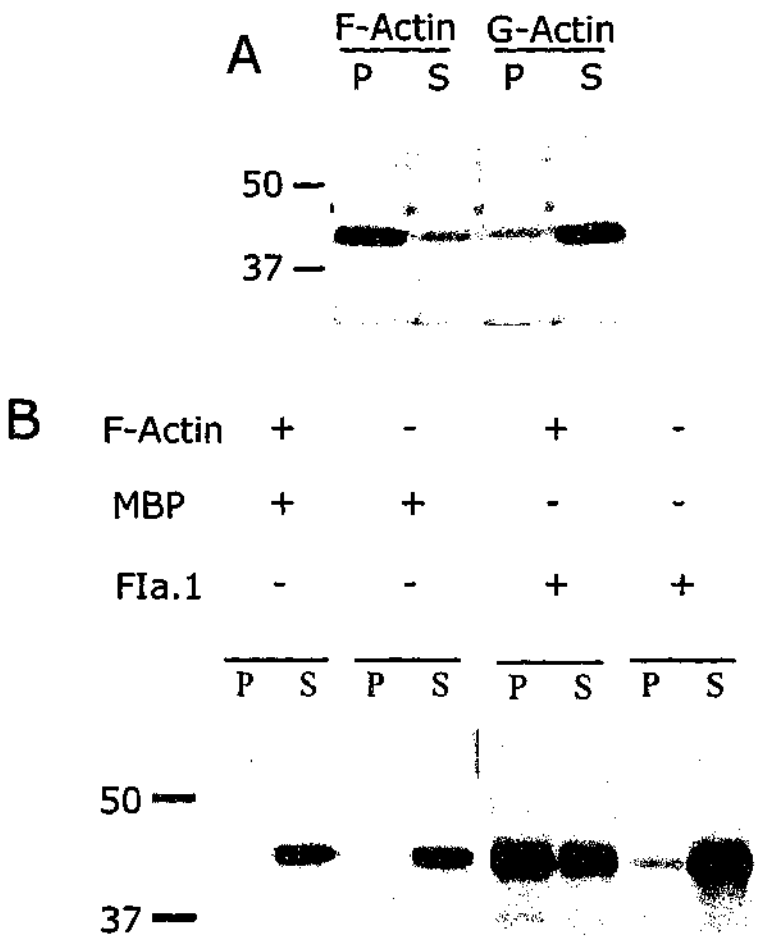

Figure 3.17. High Speed Centrifugation Actin Interaction Assay

A. Actin detected by Coomassie Brilliant Blue staining of SDS-PAGE. Actin samples were subjected to high speed centrifugation and samples from the pellet (P) and supernatant (S) were resolved on 10% polyacrylamide gels. Following polymerisation, actin (F-actin) was found in the pellet (P), with only small amounts detected in the supernatant (S). Without polymerisation, actin (G-actin) was found in the supernatant (S), with only small amounts detected in the pellet (P).

B. Immunoblot of high speed actin centrifugation assays detected using anti-MBP antiserum. In the presence and absence of F-actin, MBP was found in supernatant (S), with no detection of MBP in the pellet (P). In the presence of F-actin, MBP-PfEMP3-FIa.1 was found in both the pellet (P) and the supernatant (S), whereas in the absence of F-actin, PfEMP3-FIa.1 was found in the supernatant (S), with very little protein detected in the pellet (P)

+ = presence of protein

- = absence of protein

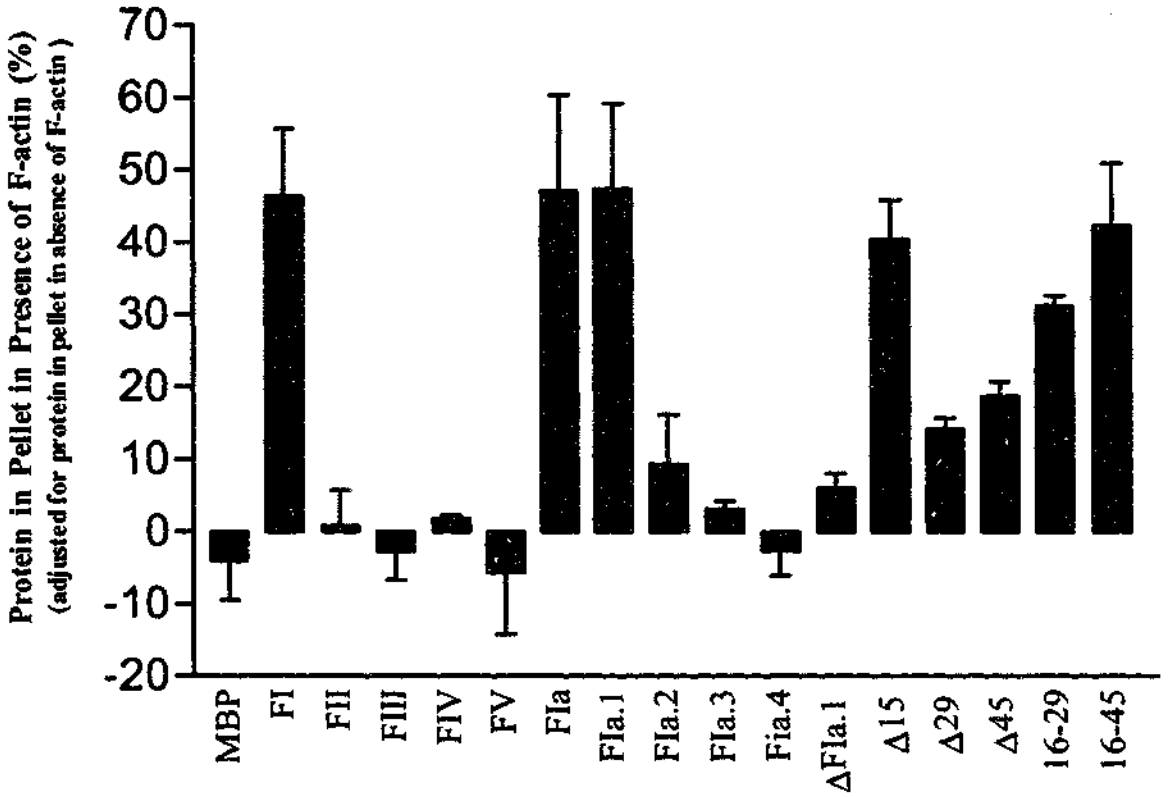

Figure 3.18. High Speed Centrifugation Actin Interaction Assay with PfEMP3 Fragments

High speed actin centrifugation assays were performed with PfEMP3 fragments in both the presence and absence of F-actin. MBP fusion proteins were detected by immunoblot analysis using anti-MBP antiserum. The protein in each lane was measured by densitometry. The percentage protein in the pellet was calculated both in the presence and absence of F-actin. The percentage protein in the pellet in the presence of F-actin was adjusted by subtracting the percentage protein in the pellet in the absence of F-actin. Analyses were performed in two independent experiments and the mean and standard deviation (error bars) are plotted.

The graph shows a clear binding of MBP-PfEMP3-FI, MBP-PfEMP3-FIa and MBP-PfEMP3-FIa.1 to F-actin under the conditions tested. Deletion of the first 15 amino acids (MBP-PfEMP3-FIaΔ15) had little effect on the binding, however deletion of further amino acids reduced, but did not abolished binding (MBP-PfEMP3-FIaΔ29 and MBP-PfEMP3–FIaΔ45). Amino acids 16-29 were sufficient to confer almost all binding of PfEMP3 to actin (MBP-PfEMP3-16-29), however with the addition of amino acids 30-45 (MBP-PfEMP3-16-45) binding increased to almost MBP-PfEMP3-FIa.1 levels.

Chapter 4 – Mapping the Spectrin Domains that Bind PfEMP3

4.1 Introduction

In the previous chapter, we defined a 14 residue domain in PfEMP3 (PfEMP3-16-29) that binds specifically to spectrin. Here, we now define the domains within spectrin, with which PfEMP3 interacts. Although a number of regions within spectrin have been defined that interact with other erythrocyte proteins, domains within spectrin that mediate the binding of parasite proteins have not yet been identified. Interestingly, previous mapping of binding domains for parasite proteins with erythrocyte proteins has revealed overlap of the parasite protein binding domains with the binding domains for other erythrocyte skeletal proteins. For example, the binding domain within ankyrin that mediates binding to KAHRP also mediates binding of band 3 and spectrin (Magowan *et al.*, 2000). Furthermore, the binding site in protein 4.1 for MESA not only overlaps the binding site for erythrocyte p55 in protein 4.1, but also interferes with the interaction between these two important erythrocyte proteins (Waller *et al.*, 2003).

Here, we have attempted to define domains within spectrin to which PfEMP3 binds by studying interactions between recombinant spectrin sub-fragments and the identified erythrocyte binding domain of PfEMP3.

4.2 Expression and Purification of Spectrin GST Fusions

Sub-fragments of spectrin cloned into pGEX vectors were provided by X. An (New York Blood Center, NY, USA). Table 4.1 summarises the important characteristics for each of the sub-fragments and their expressed proteins. Figure 4.1 shows a schematic representation of the cloned fragments in relation to full length α- and β-spectrin polypeptides. Each of the sub-fragments were named according to the domains or the residues which they contain. The α- and β-spectrin polypeptides each contain an N-terminal region, a number of spectrin repeats and a C-terminal region. For each of the sub-fragments the α- or β- polypeptide is indicated, along with the domains included (N, numbers for each of the repeats or C). Where the N-terminal has been divided into smaller regions, residue numbers in subscript are used to define the subdomain. For α-spectrin, pGEX clones containing one of each of four fragments that encompass the entire protein (αN-5, α6-11, α12-16 and α17-C), along with an additional N-terminal region ($\alpha_{1\text{-}154}$) were provided. For β-spectrin, pGEX clones containing one of each of four fragments

that encompass the entire protein (βN-4, β5-9, β10-14 and β15-C), along with a number of N-terminal sub-fragments (βN-2, βN, $\beta_{191-301}$ and β1-2) were provided. DNA from each of these clones was used to transform *E. coli* BL21 (DE3) to ampicillin resistance and the resulting strains (RCM1780, RCM1782, RCM1784, RCM1786, RCM1641, RCM1635, RCM1774, RCM1776, RCM1778, RCM1636, RCM1637, RCM1639 and RCM1640) were used in expression and purification of GST fusion proteins (Section 2.16). Purified recombinant GST protein was supplied by K. Waller (Monash University). Approximately 2 μg and 50 ng of protein were resolved on 12% polyacrylamide gels and visualised by either Coomassie Brilliant Blue staining or immunoblot analysis using anti-MBP antiserum (Figure 4.2). GST spectrin fusion proteins were purified with varying proportions of full length protein. All GST-spectrin fusion proteins resolved at approximately their predicted size. Immunoblot analysis showed similar banding patterns to those seen in Coomassie Brilliant Blue stained gels.

4.3 Interaction of PfEMP3 with Immobilised GST-Spectrin Fragments

To define the PfEMP3 binding domain in spectrin, MBP-PfEMP3-FIa.1 was incubated with the various spectrin sub-fragments. Approximately 0.5 μM of GST, the purified GST-spectrin fusion proteins, 100 ng of purified spectrin or BSA were coated onto wells. Wells were blocked with BSA and approximately 2 μg of MBP or MBP-PfEMP3-FIa.1 was added. Bound protein was eluted from the wells, resolved on 10% polyacrylamide gels, transferred to PVDF and detected by immunoblot analysis using anti-MBP antiserum.

To examine the interaction of the N-terminal regions of spectrin with PfEMP3, MBP-PfEMP3-FIa.1 or MBP were allowed to bind. A representative immunoblot is shown in Figure 4.3. MBP-PfEMP3-FIa.1 was detected binding to wells coated with purified spectrin (lane 1), GST-spectrin βN-4 (lane 2), βN-2 (lane 3), βN (lane 4), $\beta_{191-301}$ (lane 5), β1-2 (lane 6), but not to wells coated with α_{1-154} (lane 7), GST (lane 8) or BSA (lane 9). MBP did not bind to wells coated with purified spectrin (lane 10) or to wells coated with any of the GST-spectrin fusion proteins (lanes 11-16), GST (lane17) or BSA (lane 18). In this particular assay, binding of MBP-PfEMP3-FIa.1 to both purified spectrin (lane 1) and GST-spectrin $\beta_{191-301}$ (lane 5) appeared to be less intense than that to any of the other proteins. This was not consistently observed in a number of similar interaction assays and may have been due to normal variations between assays.

To examine interactions of the eight sub-fragments that encompass the entire α- and β-spectrin polypeptides, wells were coated with GST fusion proteins and MBP-PfEMP3-FIa.1 or MBP allowed to bind. A representative immunoblot is shown in Figure 4.4. MBP-PfEMP3-FIa.1 was detected binding to wells coated with purified spectrin (lane 1), GST-spectrin βN-4 (lane 2), β5-9 (lane 3), β10-14 (lane 4), β15-C (lane 5), αN-5 (lane 6), α6-11 (lane 7), α12-16 (lane 8) and α17-C (lane 9), but not to wells coated with GST (lane 10) or BSA (lane 11). MBP did not bind to wells coated with purified spectrin (lane 12) or to wells coated with any of the GST-spectrin fusion proteins (lanes 13-20, respectively), GST (lane 21) or BSA (lane 22). In this particular interaction, binding of MBP-PfEMP3-FIa.1 to both purified spectrin (lane 1) and GST-spectrin αN-5 (lane 6) appeared to be less intense than that for the other proteins. This was not consistently observed across a number of repeat interactions and again may have been due to normal variations between assays. However, for all of the spectrin fragments tested there was an overall inconsistency of the intensity of the bands observed between repeat assays that was not observed for the binding of PfEMP3-FIa.1 to purified spectrin in Chapter 3.

These assays indicated that the $\beta_{191\text{-}301}$ region and regions within α- and β-spectrin containing spectrin repeats were able to bind PfEMP3. The widespread nature of the binding and the variation between assays made it possible that the binding observed could be artefactual. Accordingly, other binding assays were performed to attempt to confirm these results.

4.4 Interaction of Immobilised PfEMP3 with GST-Spectrin Fragments

Initially we performed a reverse binding assay in which approximately 2 μg of MBP-PfEMP3-FIa.1 or MBP were coated onto the wells, then approximately 0.5 μM of the eight GST spectrin clones, that encompass α- and β-spectrin, were added. Proteins were eluted, resolved on 12% polyacrylamide gels and detected in immunoblot analysis using anti-GST antiserum (Appendix 4). Figure 4.5 shows the immunoblot of this assay.

This experiment was performed only once and following a 4 hour exposure both the GST and MBP fusion proteins were detected at approximately equal intensity with the anti-GST antiserum. Each triplicate consisted of MBP, MBP-PfEMP3-FIa.1 and BSA coated on to the wells, respectively. Proteins added and allowed to bind were GST (lanes 1, 2 and 3), GST-spectrin αN-5 (lanes 4, 5 and 6), α6-11 (lanes 7, 8 and 9), α12-16 (lanes 10, 11 and 12), α17-C (lanes 13, 14 and

15), βN-4 (lanes 16, 17 and 18), β5-9 (lanes 19, 20 and 21), β10-14 (lanes 22, 23 and 24) and β15-C (lanes 25, 26 and 27).

The reactivity visualised on the immunoblot was only achieved following a much longer exposure than was necessary for exposures routinely required to visualise a significant amount of GST fusion protein using the anti-GST antiserum. In addition, the anti-GST antiserum, which was not able to specifically detect MBP fusion proteins, detected the MBP fusion proteins coated onto the wells at levels equal to the interacting GST fusion proteins. Taken together these observations indicated that the levels of GST fusion protein detected were extremely low. The low levels of bound GST fusion protein did not allow for the specific detection of GST fusion proteins above the non-specific detection MBP fusion proteins. This indicated that the GST fusion proteins detected were only background levels and did not represent any real binding. In support of this hypothesis, the intensity of bands detected for interactions of GST-spectrin fragments were no more intense than that detected for the interaction of the GST control. In addition, the intensity of the bands detected for each of the GST-spectrin fragments binding to PfEMP3, was no more intense than that for each binding to MBP or BSA controls. Purified spectrin was not added in solution as a positive control because of the inability of the anti-GST antiserum to detect bound protein and the unavailability of an anti-spectrin antiserum.

4.5 Competitive Binding Assays to Determine the Ability of Spectrin Sub-fragments to Ablate Binding of PfEMP3 to Spectrin

In an attempt to strengthen the results obtained in the PfEMP3 microtitre plate assay, competition experiments were attempted. To determine that preincubation of PfEMP3 with the GST-spectrin fusion proteins could ablate binding of PfEMP3 to spectrin by competing for PfEMP3 binding sites, MBP-PfEMP3 fusion proteins were preincubated with a 10 fold molar excess of GST-spectrin fragment and allowed to bind to wells coated with purified spectrin (Section 2.19.1). Initial experiments with GST-spectrin βN-4 indicated a possible inhibitory effect of PfEMP3 binding to spectrin. Figure 4.6a shows the immunoblot for this interaction. MBP did not bind to wells coated with spectrin (lane 1) or BSA (lane 2). MBP-PfEMP3-FIa.1 preincubated with PBS was detected binding to wells coated with purified spectrin (lane 3), however only background levels were detected binding to wells coated with BSA (lane 4). Preincubation of MBP-PfEMP3-FIa.1 with GST-spectrin

βN-4 greatly reduced the binding of PfEMP3-FIa.1 to purified spectrin (lane 5), consistent with inhibition of PfEMP3 binding to spectrin. MBP-PfEMP3-FIa.1 preincubated with GST-spectrin βN-4 did not bind to wells coated with BSA (lane 6). Preincubation of MBP-PfEMP3-FIa.1 with GST bound to wells coated with spectrin (lane 7) at levels comparable with preincubation with PBS (lane 3), indicating no inhibitory effect of GST. MBP-PfEMP3-FIa.1 preincubated with GST showed only background levels of binding to wells coated with BSA (lane 8). MBP-PfEMP3-FIa.4 preincubated in the presence of either GST-spectrin βN-4 or GST did not bind to wells coated with spectrin (lanes 9 and 11, respectively) or to wells coated with BSA (lane 10 and 12, respectively).

To confirm this initial experiment and to further define the inhibitory region, three subsequent experiments looked at competition through preincubation of MBP-PfEMP3-FIa.1 with each of GST-spectrin βN-2, βN, $\beta_{191\text{-}301}$, β1-2 and $\alpha_{1\text{-}154}$. Preincubation in the presence or absence of Tween-20 and increasing the excess from 10 to 200 fold excess of GST-spectrin fusion, all demonstrated no inhibition of MBP-PfEMP3-FIa.1 (Figure 4.6b). Background levels of bound protein were detected for MBP to wells coated with spectrin (lane 1). In addition, background levels of bound protein were detected for MBP (lane 2) and for MBP-PfEMP3-FIa.1 preincubated with PBS (lane 4), GST-spectrin βN-2 (lane 6), βN (lane 8), $\beta_{191\text{-}301}$ (lane 10), β1-2 (lane 12), $\alpha_{1\text{-}154}$ (lane 14) or with GST (lane 16) to wells coated with BSA. Equal amounts of bound protein were detected for each of the sets of wells coated with spectrin for MBP-PfEMP3-FIa.1 preincubated with PBS (lane 3), GST-spectrin βN-2 (lane 5), βN (lane 7), $\beta_{191\text{-}301}$ (lane 9), β1-2 (lane 11), $\alpha_{1\text{-}154}$ (lane 13), or with GST (lane 15), indicating that none of the GST-spectrin fragments were able to reduce binding of PfEMP3 to spectrin when compared to PBS and GST controls.

Thus, it appears that GST-spectrin βN-4 was able to inhibit binding of PfEMP3 to spectrin, whereas GST-spectrin βN-2 was unable to inhibit binding. These data indicated that β-spectrin repeats 3 and 4 were required for inhibition of spectrin binding to PfEMP3. This would need to be repeated a number of times to be confident of the result. Unfortunately, the inhibition of GST-spectrin βN-4 was not repeated or investigated further due to time constraints.

4.6 GST Pull Down Assays to Identify PfEMP3 Binding Domains in Spectrin

To further strengthen the results obtained in the microtitre plate assay, GST pull down assays were performed. GST pull down assays allow detection of

protein-protein interactions utilising the ability of GST fusions to simultaneously bind Glutathione Agarose and a binding partner. These assays have been used to detected a number of protein-protein interactions including the interaction between α- and β-spectrin resulting in dimerisation (Harper *et al.*, 2001). GST fusions bind the Glutathione Agarose, together with any interacting proteins and following washing these proteins will be found in the bead sample. Unbound proteins will present in the supernatant. Approximately 5 μM GST-spectrin fusion protein and 5 μM MBP-PfEMP3-FIa.1 fusion protein were preincubated, added to Glutathione Agarose and allowed to bind. Samples were spun down to separate beads from the supernatant and beads were washed three times with 20 volumes of PBS (Section 2.21). Figure 4.7 shows a representative immunoblot of equal samples of beads and supernatant, detected using anti-MBP antiserum.

Both MBP and MBP-PfEMP3-FIa.1 were preincubated with each of GST, GST-spectrin βN, βN-4 and β5-9. For all samples, the amount of MBP-PfEMP3-FIa.1 and MBP is distributed evenly between both beads (odd numbered lanes) and supernatant (even numbered lanes). This indicates that either MBP fusions are able to bind non-specifically to glutathione agarose or GST fusion proteins, or that the washing of the samples is incomplete. The immunoblot shows this distribution for MBP preincubated with GST (lanes 1 and 2), GST-spectrin βN (lanes 5 and 6), βN-4 (lanes 9 and 10) and β5-9 (lanes 13 and 14). This is also seen for MBP-PfEMP3-FIa.1 preincubated with GST (lanes 3 and 4), GST-spectrin βN (lanes 7 and 8), βN-4 (lanes 11 and 12), and β5-9 (lanes 15 and 16). There did, however, appear to be less MBP-PfEMP3-FIa.1 following preincubation with GST-spectrin βN in the pellet sample (lane 7), but this was not compensated for in the supernatant sample (lane 8) and was thought to have arisen through a bubble between the polyacrylamide gel and the PVDF membrane during transfer. Due to time constraints and the indication that GST pull down interactions were not likely to confirm or clarify previous results, this interaction was not repeated nor the protocol altered to delineate the equal binding seen for all samples.

4.7 *Kinetic Analysis of Spectrin Sub-Fragments binding to PfEMP3-FIa.1*

In an attempt to confirm interactions identified with the microtitre plate interaction assay between PfEMP3 and the spectrin repeat regions within both α- and β-spectrin and with the N-terminal domain of β-spectrin (Section 3.7.6), resonant mirror detection was used to obtain kinetic data. PfEMP3-FIa.1 was coated onto aminosilane cuvettes and GST-spectrin sub-fragments added in

aqueous solution (as described in Section 3.7.6). Table 4.2 shows the association rate constant (K_a), disassociation rate constant (K_d) and subsequent disassociation constants ($K_{(D)kin}$ *and* $K_{(D)Scat}$) of the interactions (calculated as described in Section 3.7.6). Two additional GST-β-spectrin sub-fragments were used in these assays. These were βN-9 and $\beta_{211\text{-}301}$, encompassing the N-terminal region plus the first 9 repeat regions of β-spectrin and the residues 211-301 contained within the C-terminal end of the N-terminal domain, respectively. Data showed that the N-terminal domain of β-spectrin is able to bind PfEMP3 and confirmed that the region $\beta_{191\text{-}302}$ is sufficient to confer this binding. In addition, resonant mirror detection was able to show binding of $\beta_{211\text{-}301}$ to PfEMP3-FIa.1, identifying a binding domain of 91 residues. Both these sub-fragments conferred binding with a $K_{(D)kin}$ of $4.3\text{x}10^{-7}$ M, which was more than 10 times the $K_{(D)kin}$ of the β-spectrin N-terminal region (βN) in its entirety. The repeat regions β5-9 and β10-14 both showed binding to PfEMP3-FIa.1, however the 5 repeat regions that make up β5-9 ($K_{(D)kin}$ of $6.4\text{x}10^{-8}$ M) conferred binding at over 10 times that conferred by the 5 repeat regions that make up β10-14 ($K_{(D)kin}$ of $2.8\text{x}10^{-7}$ M). The β-spectrin sub-fragment that encompassed the N-terminal region and first 9 repeat regions only conferred binding with a $K_{(D)kin}$ of $1.1\text{x}10^{-6}$ M. This is less than both the 91 residue N-terminal binding domain ($\beta_{211\text{-}301}$) and of β5-9, which are both contained within this sub-fragment. Data also showed that αN-5, α6-11 and α17-C sub-fragments conferred binding with a $K_{(D)kin}$ of $1.7\text{x}10^{-6}$, $1.9\text{x}10^{-6}$ M and $4.5\text{x}10^{-7}$ M, respectively. $\alpha_{1\text{-}154}$ and GST alone showed no binding to PfEMP3-FIa.1 as seen with the microtitre plate assay.

4.8 Discussion

In this chapter, we have attempted to map the PfEMP3 binding domain in spectrin. We have shown that PfEMP3 binds to the $\beta_{191\text{-}301}$ region and to the spectrin repeats of both α- and β-spectrin when GST-spectrin fusion proteins are immobilised in a solid phase microtitre plate interaction assay. Results using this technique were generally inconsistent and in an attempt to further define these interactions, we reversed the immobilised ligand, used competitive assays and GST pull down assays, none of which were able to confirm or clarify these interactions. Resonant mirror detection was able to confirm the interaction of PfEMP3 with both the N-terminal domain of β-spectrin and with the repeat regions of both α- and β-spectrin. This method also defined the binding domain to the 91 residues encompassed by the $\beta_{211\text{-}301}$ sub-fragment.

Previous studies performed in our laboratory using the solid phase microtitre plate assay have shown inconsistencies similar to those seen in this study. For example, in Chapter 3 we showed that small proteins fused to the relatively large MBP protein, resulted in inconsistent and poorly defined binding. This was evident with a binding domain of less than 60 residues fused to MBP. Another example of inconsistent results obtained for this assay, involved mapping the binding domain within protein 4.1 for MESA (Waller, 2000). This inconstancy was resolved with clear and definitive data using a resonance mirror detection method and competitive GST pull down assays (Waller *et al.*, 2003).

It is feasible that there are multiple domains within spectrin to which PfEMP3 binds. Proteins at the erythrocyte membrane are able to bind multiple proteins and to bind a single protein within a number of different domains. For example spectrin, band 3, protein 4.1, ankyrin and p55 have all been shown to interact with multiple proteins (see Section 1.3 and for review see Lux and Palek, 1995) and ankyrin binds specifically to multiple sequences throughout the N-terminal domain of band 3 (Willardson *et al.*, 1989). PfEMP3 may be responsible for the modulation of normal protein-protein interactions between spectrin and its erythrocyte protein binding partners. This may be mediated through interactions with the N-terminal region responsible for the binding of both actin and protein 4.1 or through interactions with the 15th repeat region of β-spectrin, responsible for the binding of ankyrin. Alternatively, PfEMP3 may modulate the formation of heterodimers and of oligomers of α- and β-spectrin through interactions with repeat regions responsible for self association or nucleation. It may also be the case that PfEMP3 binds only to sites within spectrin that contain no functional domain and therefore, remain available for binding. We can speculate that a number of PfEMP3 molecules bind spectrin at multiple sites and lead to the modulation of a number of normal protein-protein interactions at the erythrocyte skeleton.

The protein interactions in this chapter were notably not as consistent as the binding of PfEMP3 to purified spectrin in Chapter 3. This suggests that the sub-fragmentation of spectrin and the expression of these sub-fragments as GST fusions have altered the binding domains for PfEMP3. Previously Winograd *et al.* (1991) have shown that expression of the spectrin repeat α-helical domains as GST fusions resulted in proper folding if boundaries corresponded to folding units. Incorrect folding of these structures may result in either partial or total loss of binding, or may result in binding that would not be seen in the erythrocyte. However, in this study, the spectrin sub-fragments were divided at the junction of repeat regions, so as not to divide any of the structural domains and to retain structure. Circular Dichroism (CD) Spectroscopy, a technique that is able to

determine the presence of secondary structure within a protein, was used to determine that the pGEX-spectrin constructs used in this study are able to produce GST fusions that form α-helical structures (X. An, New York Blood Center, personal communication). However, the actual proteins used in PfEMP3 binding studies were not subjected to CD Spectroscopy. Small differences in composition of the buffers, storage conditions and purification methods may result in changes to the structure of the GST-spectrin sub-fragments and have an effect on the ability of these proteins to bind PfEMP3. The use of CD Spectroscopy to confirm that protein preparations used in this study form α-helical structures would remove one possible area of uncertainty. In addition, data from resonant mirror detection showed that only the interaction between β5-9 and PfEMP3-FIa.1 ($6.4x10^{-8}$ M) was comparable to the interaction of purified spectrin and PfEMP3-FIa.1 ($8.4x10^{-8}$ M) and interestingly that the two sub-fragments that contained the N-terminal residues 1-190 (βN-9 and βN) conferred binding at $K_{(D)kin}$ values of nearly 100 fold less ($1.1x10^{-6}$ M and $1.4x10^{-6}$ M, respectively) than either β5-9 or purified spectrin. This indicates that the tertiary structure of spectrin may be important for the ability of PfEMP3 to bind certain regions of the protein. This could be important within the infected erythrocyte where the binding of other malaria or erythrocyte proteins may effect the ability of PfEMP3 access a binding site within spectrin.

It is also important to consider the quaternary structure of spectrin and the influence this may have on binding. Purified spectrin used in Chapter 3 consists of both α- and β-spectrin which have the ability to form heterodimers, tetramers and higher order oligomers. It is possible that the formation of this quaternary structure contributes to the binding domain within spectrin for PfEMP3. The GST-spectrin clones differ from the native spectrin in a number of ways that may be relevant for binding of PfEMP3. Firstly, the association of the α- and β-spectrin polypeptides to form either dimers or tetramers may result in the formation of a binding domain which is not present in either the individual polypeptides or the fragmented polypeptides. Alternatively, a single binding domain within either α- or β-spectrin is represented multiple times within a tetramer or higher order oligomer. This would result in multiple binding domains within the tetramer or oligomer, compared to the single domain within the monomer, and may result in a higher affinity of binding to purified spectrin when compared to the GST-spectrin fragments. A study by Li and Bennett (1996) investigated the ability of β-spectrin to promote adducin binding to actin. When compared to the native spectrin tetramer, β-spectrin showed reduced ability to stabilise the adducin-actin interaction. However, the heterodimer formation between a β-spectrin fragment and α-spectrin showed no detectable increase in activation, indicating that the

association of α- and β-spectrin has no role in modulating this interaction. This evidence suggests that the additional activity of the spectrin tetramer may be due to the presence of multiple binding domains within the tetramer when compared to a single binding domain within the monomer. This type of approach may be useful in delineating the influence of quaternary structure in the binding of PfEMP3 to spectrin.

It is important, as discussed in Chapter 3, to further investigate these domains in terms of their possible altered function within normal erythrocytes. Further investigation of the interaction between PfEMP3 and spectrin in terms of other interactions such as those with protein 4.1, actin and ankyrin, will be of great interest for future studies.

Fragment	Parent pGEX Plasmid	Size of Inserted Fragment (bp)	Residues Encompassed by Insert	Predicted Molecular Mass of Fusion Protein (kDa)	Approximate Resolved Molecular Mass of Fusion Protein (kDa)
αN-5	4T-2	1752	1-584	95	110
α6-11	4T-2	1821	574-1180	97.5	100
α12-16	4T-2	1602	1181-1714	88.5	95
α17-C	4T-2	2163	1710-2430	110	105
$\alpha_{1\text{-}154}$	3X	462	1-154	45	40
βN-4	3X	2226	1-742	113	115
β5-9	4T-2	1593	743-1273	87.5	95
β10-14	3X	1596	1274-1796	87	95
β15-C	3X	1023	1797-2137	62.5	65
βN-2	3X	1581	1-527	88.5	85
βN	3X	903	1-301	61.5	60
$\beta_{191\text{-}301}$	3X	333	191-301	40	35
β1-2	3X	678	302-527	53.5	48

Table 4.1. Characteristics of pGEX Spectrin Clones

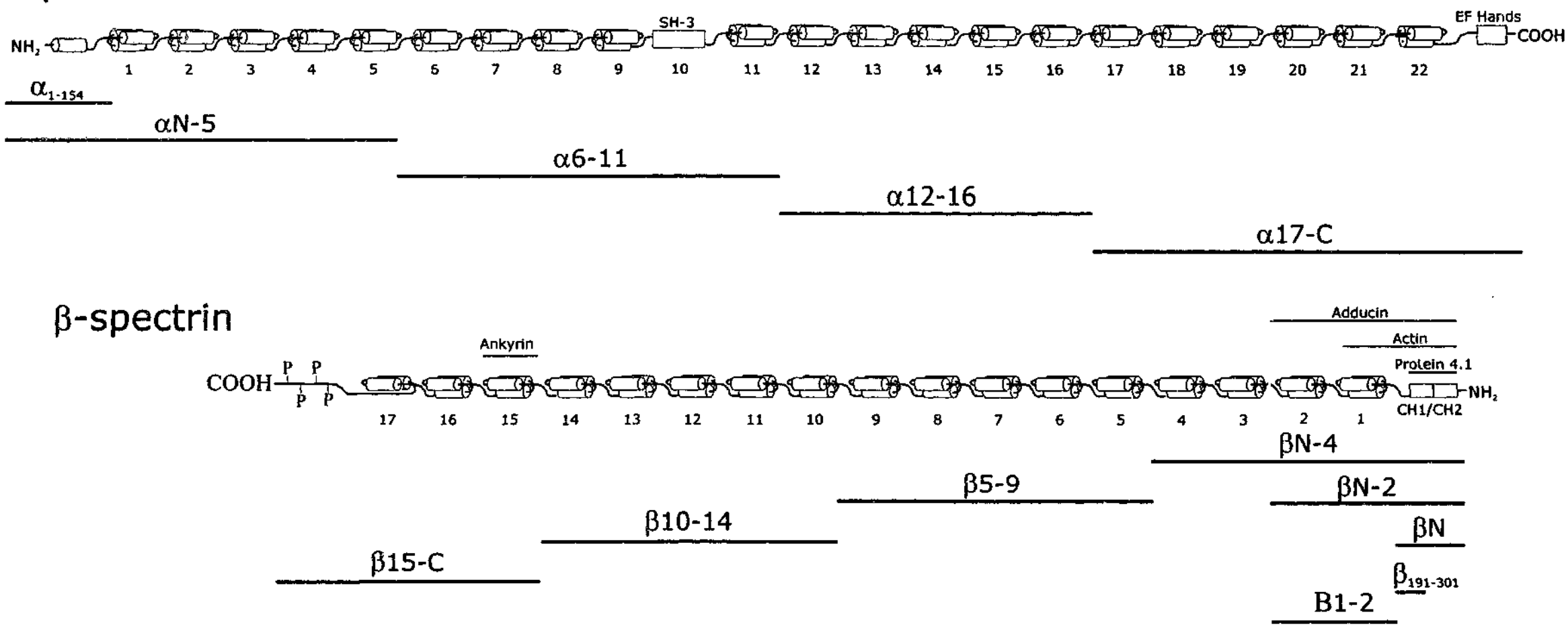

Figure 4.1. Schematic of Spectrin Clones

Schematic representation of α- and β-spectrin showing the regions encompassed within each of the recombinant spectrin fragments. Figure is not to scale and is adapted from Lux and Palek, 1995. Features of the α- and β-spectrin schematic are described in Figure 1.2.

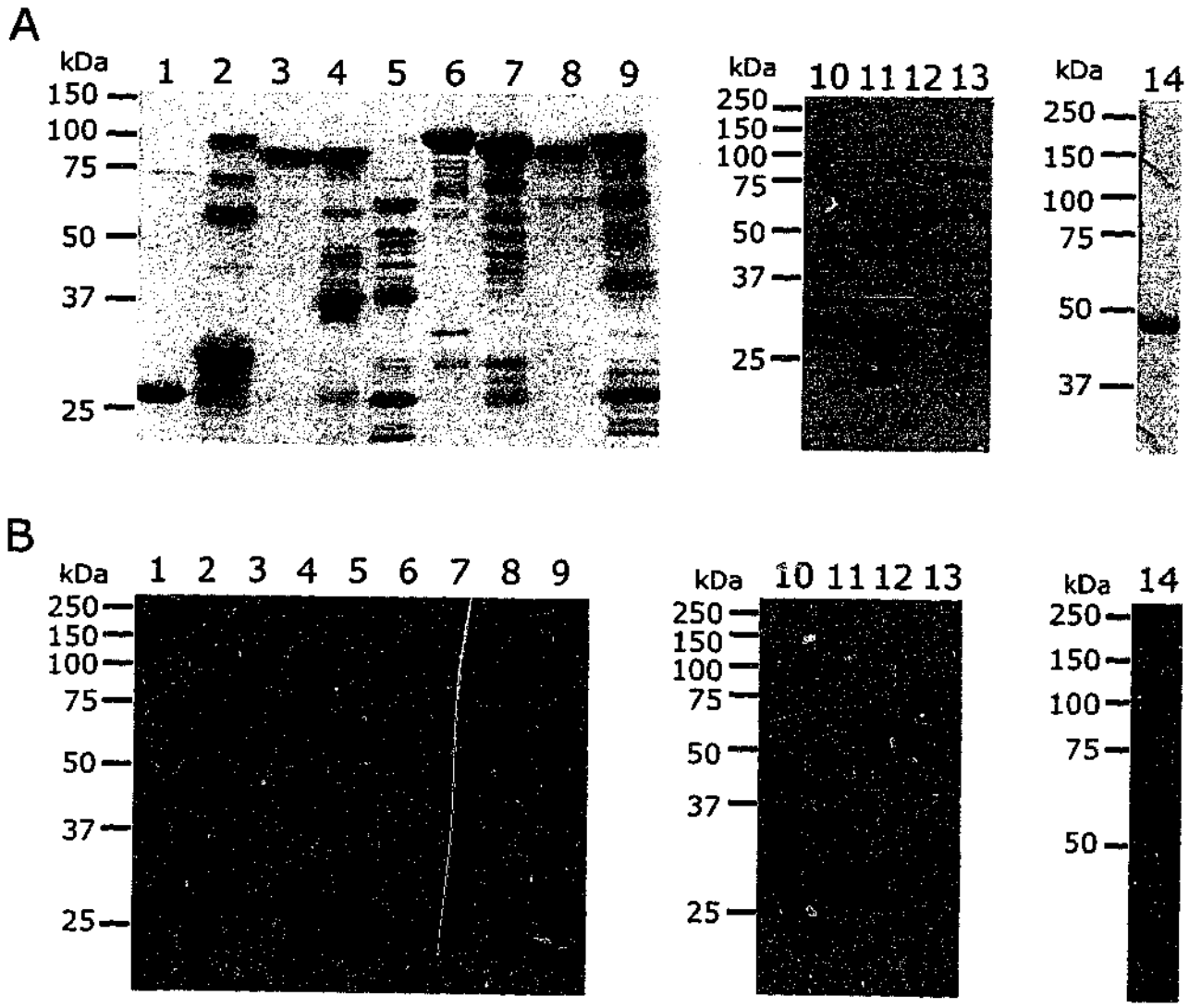

Figure 4.2. Expression and Purification of GST-Spectrin Fragments

A. Purified GST-spectrin fusion proteins detected by Coomassie Brilliant Blue staining of SDS-PAGE. 2 μg of each purified protein was resolved on 12% polyacrylamide gels. GST (lane 1), GST-spectrin βN-4 (lane 2), β5-9 (lane 3), β10-14 (lane 4), β15-C (lane 5), αN-5 (lane 6), α6-11 (lane 7), α12-16 (lane 8), α17-C (lane 9), $\alpha_{1\text{-}154}$ (lane 10), $\beta_{191\text{-}301}$ (lane 11), βN (lane 12), βN-2 (lane 13) and β1-2 (lane 14).

B. Immunoblot assay of GST-spectrin fusion proteins detected using anti-GST antiserum. 50 ng of each purified protein was resolved on 12% SDS-PAGE and transferred to PVDF for detection. GST (lane 1), GST-spectrin βN-4 (lane 2), β5-9 (lane 3), β10-14 (lane 4), β15-C (lane 5), αN-5 (lane 6), α6-11 (lane 7), α12-16 (lane 8), α17-C (lane 9), $\alpha_{1\text{-}154}$ (lane 10), $\beta_{191\text{-}301}$ (lane 11), βN (lane 12), βN-2 (lane 13) and β1-2 (lane 14).

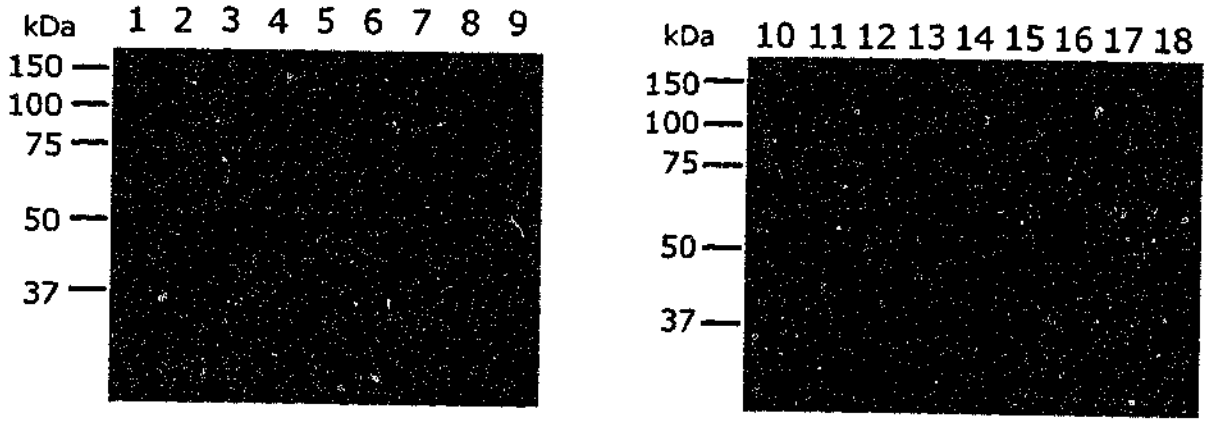

Figure 4.3. Interaction of PfEMP3 with Immobilised Recombinant N-Terminal Spectrin Fragments

Immunoblot of interaction assay with immobilised GST N-terminal spectrin fragments. Purified spectrin (lanes 1 and 10), GST-spectrin βN-4 (lane 2 and 11), βN-2 (lane 3 and 12), βN (lane 4 and 13), $\beta_{191\text{-}301}$ (lane 5 and 14), β1-2 (lane 6 and 15), $\alpha_{1\text{-}154}$ (lane 7 and 16), GST (lane 8 and 17) and BSA (lane 9 and 18) were coated onto wells of a microtitre plate. MBP-PfEMP3-FIa.1 (lanes 1-9) and MBP (lanes 10-18) were added to the wells and allowed to bind MBP-PfEMP3-FIa.1 was detected binding to wells coated with purified spectrin (lane 1), GST-spectrin βN-4 (lane 2), βN-2 (lane 3), βN (lane 4), $\beta_{191\text{-}301}$ (lane 5) and β1-2 (lane 6), but not to wells coated with $\alpha_{1\text{-}154}$ (lane 7), GST (lane 8) or BSA (lane 9). MBP did not bind proteins in any of the wells (lanes 10-18).

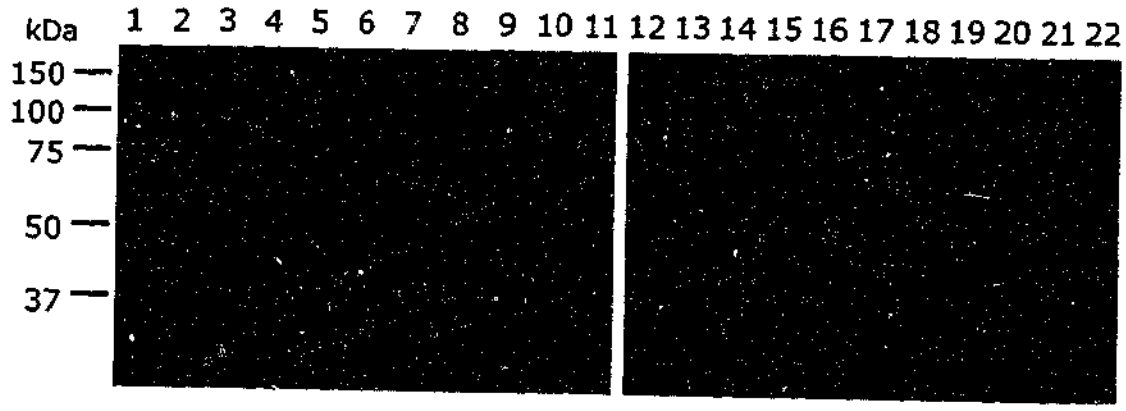

Figure 4.4. Interaction of PfEMP3 with Immobilised GST α- and β-Spectrin Fragments

Immunoblot interaction assay with immobilised GST α- and β-spectrin fragments. Purified spectrin (lane 1 and 12), GST-spectrin βN-4 (lane 2 and 13), β5-9 (lane 3 and 14), β10-14 (lane 4 and 15), β15-C (lane 5 and 16), αN-5 (lane 6 and 17), α6-11 (lane 7 and 18), α12-16 (lane 8 and 19), α17-C (lane 9 and 20), GST (lane 10 and 21) and BSA (lane 11 and 22) were coated onto the wells of a microtitre plate. MBP-PfEMP3-FIa.1 (lanes 1-11) and MBP (lanes 12-22) were added to the wells and allowed to bind. MBP-PfEMP3-FIa.1 was detected to bind wells coated with purified spectrin (lane 1), GST-spectrin βN-4 (lane 2), β5-9 (lane 3), β10-14 (lane 4), β15-C (lane 5),αN-5 (lane 6), α6-11 (lane 7),α 12-16 (lane 8) and α17-C (lane 9), but not to wells coated with GST (lane 10) or BSA (lane 11). MBP did not bind to proteins in any of the wells (lanes 12-22).

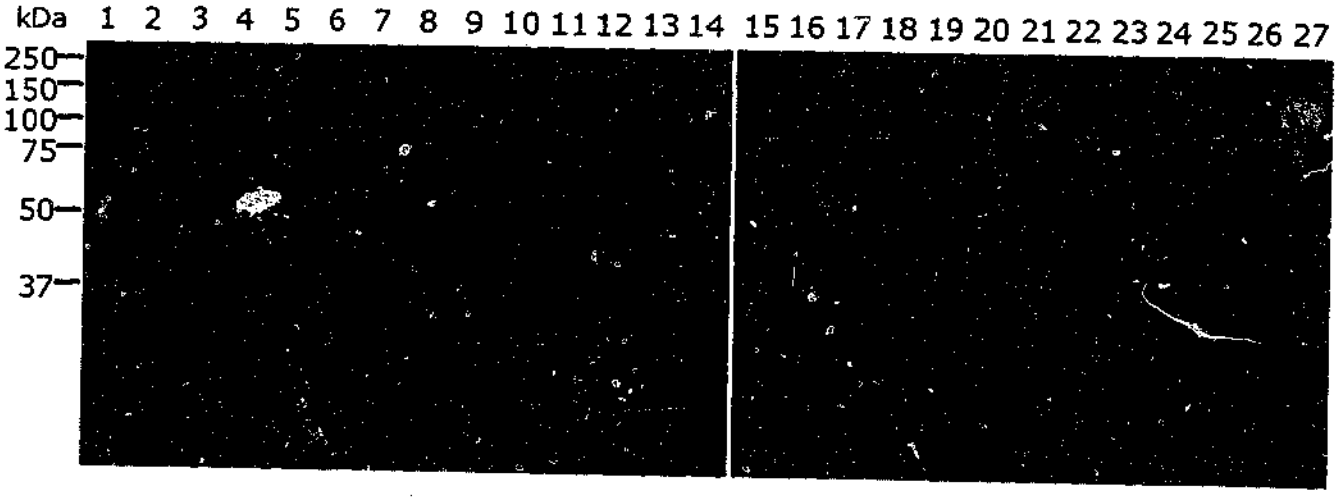

Figure 4.5. Interaction Assay of Immobilised PfEMP3 with GST-Spectrin Fragments

Immunoblot of interaction assay with immobilised PfEMP3 detected using an anti-GST antiserum. MBP (lanes 1, 4, 7, 10, 13, 16, 19, 22 and 25), MBP-PfEMP3-FIa.1 (lanes 2, 5, 8, 11, 14, 17, 20, 23 and 26) and BSA (lanes 3, 6, 9, 12, 15, 18, 21, 24 and 27) were coated onto wells of a microtitre plate. GST (lanes 1, 2 and 3), GST-spectrin αN-5 (lanes 4, 5 and 6), α6-11 (lanes 7, 8 and 9), α12-16 (lanes 10, 11 and 12), α17-C (lanes 13, 14 and 15), βN-4 (lanes 16, 17 and 18), β5-9 (lanes 19, 20 and 21), β10-14 (lanes 22, 23 and 24) and β15-C (lanes 25, 26 and 27) were added to the wells and allowed to bind. Bands detected are of both GST and MBP origin, indicating only background levels of binding for GST-spectrin fusion proteins to immobilised PfEMP3-FIa.1.

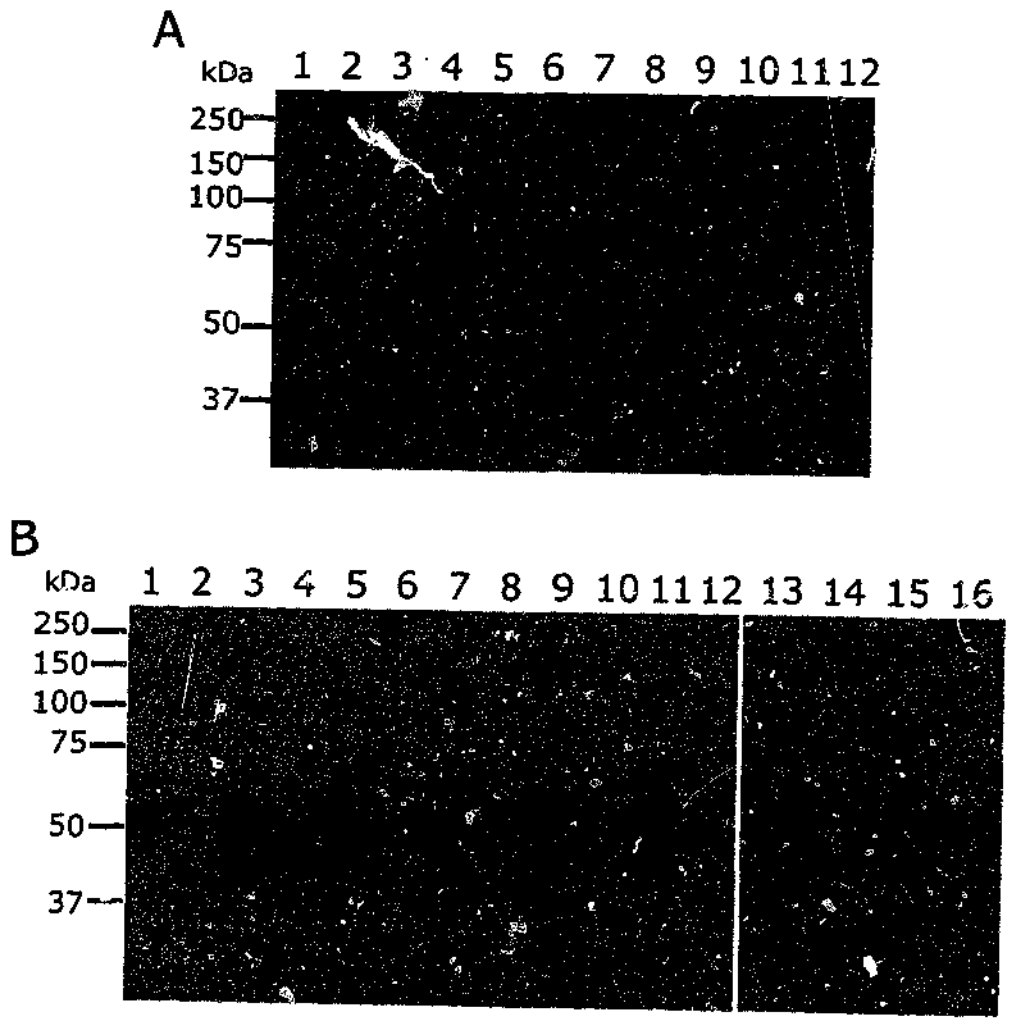

Figure 4.6. Competitive Binding Assays

A. Immunoblot of GST-spectrin βN-4 competitive binding assay. Purified spectrin (lanes 1, 3, 5, 7, 9 and 11) and BSA (lanes 2, 4, 6, 8, 10 and 12) were coated onto the wells of a microtitre plate. MBP (lanes 1 and 2), MBP-PfEMP3-FIa.1 preincubated with PBS (lanes 3 and 4), MBP-PfEMP3-FIa.1 preincubated with GST-spectrin βN-4 (lanes 5 and 6), MBP-PfEMP3-FIa.1 preincubated with GST (lanes 7 and 8), MBP-PfEMP3-FIa.4 preincubated with GST-spectrin βN-4 (lanes 9 and 10) and MBP-PfEMP3-FIa.4 preincubated with GST (lanes 11 and 12) were added to the wells and allowed to bind. Bound protein was detected for MBP-PfEMP3-FIa.1 preincubated with PBS (lane 3) and MBP-PfEMP3-FIa.1 preincubated with GST (lane 7) to wells coated with spectrin. Low levels of bound protein was detected for MBP-PfEMP3-FIa.1 preincubated with GST-spectrin βN-4 (lane 5) to wells coated with purified spectrin.

B. Immunoblot of GST N-terminal spectrin competitive binding assay. Purified spectrin (lanes 1, 3, 5, 7, 9, 11, 13 and 15) and BSA (lanes 2, 4, 6, 8, 10, 12, 14 and 16) were coated onto the wells of a microtitre plate. MBP (lanes 1 and 2), MBP-PfEMP3-FIa.1 preincubated with PBS (lanes 3 and 4), MBP-PfEMP3-FIa.1 preincubated with GST-spectrin βN-2 (lanes 5 and 6), MBP-PfEMP3-FIa.1 preincubated with GST-spectrin βN (lanes 7 and 8), MBP-PfEMP3-FIa.1 preincubated with GST-spectrin $\beta_{191\text{-}301}$ (lanes 9 and 10), MBP-PfEMP3-FIa.1 preincubated with GST-spectrin β1-2 (lanes 11 and 12), MBP-PfEMP3-FIa.1 preincubated with GST-spectrin $\alpha_{1\text{-}154}$ (lanes 13 and 14) and MBP-PfEMP3-FIa.1 preincubated with GST (lanes 15 and 16) were added to the wells and allowed to bind. Background levels of bound protein was detected for MBP to wells coated with spectrin (lane 1) and for all the proteins to wells coated with BSA (lanes 2, 4, 6, 8, 10, 12, 14 and 16). Bound protein was detected for MBP-PfEMP3-FIa.1 preincubated with any of the proteins, to wells coated with spectrin (lanes 3, 5, 7, 9, 11, 13, and 15)

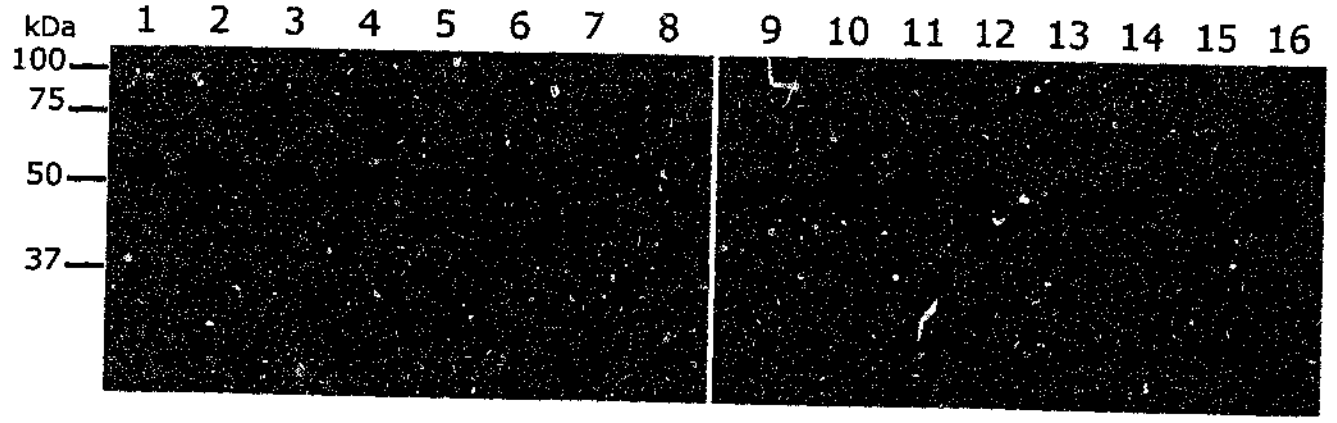

Figure 4.7. GST Pull Down Assays with Spectrin Sub-Fragments and PfEMP3-FIa.1

Immunoblot of GST pull down assays. MBP was preincubated with GST (lanes 1 and 2), GST-spectrin βN (lanes 5 and 6), βN-4 (lanes 9 and 10) and β5-9 (lanes 13 and 14) and added to the beads and allowed to bind. MBP-PfEMP3-FIa.1 was preincubated with GST (lanes 3 and 4), GST-spectrin βN (lanes 7 and 8), βN-4 (lanes 11 and 12), and β5-9 (lanes 15 and 16) and added to the beads and allowed to bind. Equal protein was detected in both the supernatant (lanes 1, 3, 5, 7, 9, 11, 13 and 15) and the pellet (lanes 2, 4, 6, 8, 10, 12, 14 and 16) for each of the proteins.

Spectrin Fragment	k_a ($M^{-1}sec^{-1}$)	k_d (sec^{-1})	$K_{(D)kin}$ (nM)	$K_{(D)Scat}$ (nM)
βN-9	$6.6x10^3$	$7.1x10^{-3}$	1100	1100
βN	$4.2x10^3$	$5.8x10^{-3}$	1400	1400
$\beta_{191-301}$	$1.0x10^4$	$4.3x10^{-3}$	430	320
$\beta_{211-310}$	$1.1x10^4$	$4.9x10^{-3}$	430	320
β5-9	$4.7x10^4$	$3.0x10^{-3}$	64	60
β10-14	$2.0x10^4$	$5.6x10^{-3}$	280	300
α_{1-154}	No binding	No binding	No binding	No binding
αN-5	$4.1 x10^3$	$6.8 x10^{-3}$	1700	1100
α6-11	$3.5x10^4$	$5.9x10^{-3}$	1900	1100
α17-C	$1.3x10^4$	$5.8x10^{-3}$	450	410
GST	No binding	No binding	No binding	No binding

Table 4.2. Kinetics Data for Binding of PfEMP3-FIa.1 to Spectrin Fragments
The binding assays were carried out in PBS containing 0.05% Tween 20. From the binding curves obtained by resonant mirror detection method, K_a, K_d, $K_{(D)kin}$ and $K_{(D)scat}$ were determined using the software package FASTfit™. Binding was detected for MBP-PfEMP3-FIa.1 to all GST-β-spectrin fragments and to all GST-α-spectrin fragments tested. No binding was detected for MBP-PfEMP3-FIa.1 to GST. No binding is defined as described in Nunomura *et al.*, 2000.

Chapter 5 – Mapping the Domains of Pf332 that Bind to the Erythrocyte Membrane Skeleton

5.1 Introduction

Pf332 is a large parasite protein with a predicted size of 700-800 kDa that is found at the erythrocyte membrane and in Maurer's clefts in schizont infected erythrocytes. To date, few studies have focused on Pf332, and until the recent release of the complete genome sequence for *P. falciparum*, the full Pf332 sequence was unknown. Pf332 is one of the largest genes in the *P. falciparum* genome (Robert Huestis, VBC, personal communication) and is 2-3 times larger than other proteins, such as KAHRP, MESA and PfEMP3, that are exported to the erythrocyte membrane skeleton. For these reasons, elucidating the function of Pf332 at the membrane skeleton and its importance in the pathogenesis of malaria is of particular interest.

Due to the large size and repetitive nature of the gene encoding Pf332 and of the encoded protein it was considered unfeasible to clone the entire gene and express it as a full length protein. Therefore, the initial aim of this study was to clone the entire coding region of PfEMP3 as fragments into pMAL vectors for expression as MBP fusion proteins. This would allow us to identify binding domains within Pf332 for the erythrocyte membrane and to identify erythrocyte binding partners for Pf332.

5.2 The Structure of the Pf332 gene

5.2.1 Annotation of the Pf332 Gene

Prior to beginning this project, the sequence and intron-exon structure of the Pf332 gene was unknown. Genbank contained 4 incomplete sequence fragments of the Pf332 gene from the Palo Alto strain, a single incomplete sequence from an unidentified strain and a single incomplete sequence from the strain FCC1/HN (accession numbers AH001084, M69163, A25767 and AF202180).

With the gradual release of genome sequence by The Institute for Genomic Research (TIGR), region of sequence encompassing the Pf332 gene fragments from Genbank that encoded an open reading frame of 16578 bp was identified (Fiona Glenister, Monash University). Upon release of the full chromosome 11 sequence, this open reading frame was later identified as the gene encoding Pf332 (Gardner *et al.*, 2002). Robert Huestis of the VBC has more recently provided a gene model

for Pf332, which differed from that predicted in the released *P. falciparum* genome. The genome consortium prediction was for a single exon gene, whereas the VBC predicted a gene with two exons of 1704 and 16578 bp, separated by a single intron of 235 bp (Figure 5.1). This later prediction represents our current working model for the structure of the full length Pf332 gene.

5.2.2 Confirmation of the Predicted Intron Using RT-PCR

To distinguish between these two predicted Pf332 gene structures, we used RT-PCR to detect differences in the size of amplified products from genomic DNA (gDNA) and complementary DNA (cDNA) templates. Oligonucleotides were designed to amplify across the intron resulting in a 900 bp fragment from gDNA and a 670 bp fragment from cDNA. These primers and resultant products are shown schematically in Figure 5.2a, with the forward oligonucleotide, p1158 binding to sequence within the first exon and the reverse oligonucleotide, p1181 binding to sequence within the second exon. RNA was extracted from parasitised erythrocytes and used in the presence (RT^+) and absence (RT^-) of reverse transcriptase for the synthesis of cDNA. These cDNA samples were provided by Tieqiao Wu (Monash University).

Figure 5.2b shows the RT-PCR products when resolved by agarose gel electrophoresis. RT^+ sample shows a band between the 0.83 kilobase (kb) and 0.56 kb markers (lane 1) corresponding for that expected in cDNA. The band for the RT^+ sample appears to resolve at slightly higher than 670 bp, however sequencing confirmed the size of the product. RT^- shows no amplified products (lane 2) consistent with no contamination of RT samples with gDNA. The gDNA sample shows a band that resolved at approximately the 0.95 kb marker, consistent with the gDNA product containing the VBC predicted intron. The no DNA control showed no amplification product (lane 4) thereby indicating all reagents were free of gDNA contamination. Products from both RT^+ and gDNA were excised from the gel and purified. Purified fragments were sequenced and confirmed the predicted size of the amplified products and boundaries of the intron predicted by Dr. Huestis.

5.3 Cellular Localisation of Pf332 in Parasitised Erythrocytes

5.3.1 Detergent Extraction of Parasitised Erythrocytes

To confirm previous reports that Pf332 was insoluble in Triton X-100 (Mattei and Scherf, 1992a) and, therefore, likely to be associated with the erythrocyte

membrane skeleton (Leech *et al.*, 1984b), 3D7 parasitised erythrocytes were extracted with Triton X-100 and the products analysed to determine Pf332 solubility. *P. falciparum* 3D7 parasite cultures were purified to more than 99% trophozoite infected erythrocytes using Percoll density gradient purification (Section 2.4.6). Parasites were extracted, samples prepared as described in Section 2.12.2 and resolved on acrylamide/agarose composite gels (Section 2.12.4). Proteins were transferred to PVDF and used in immunoblot analysis with anti-Pf332 antiserum (Appendix 4). Figure 5.3 shows a representative immunoblot. Pf332 was detected in 3D7 (lane 1), insoluble (lane 2) and soluble (lane 3) samples as a protein with a molecular mass in excess of 250 kDa. The largest band in this immunoblot for the soluble sample (lane 3) appears to run slightly lower than that of the 3D7 and insoluble samples. This is an artefact of this particular immunoblot and this size difference was not seen consistently across a number of repeat immunoblots. However, slight apparent differences in size were commonly seen for various samples when proteins were resolved on agarose/acrylamide composite gels. The aberrant resolution of bands across samples is most likely due to difficulties in the pouring and handling of these gels. A number of smaller molecular mass proteins were also detected in each of the samples. These proteins could be either breakdown products or cross reactive proteins of either erythrocyte or parasite origin. Previous studies have reported that Pf332 antisera can cross react with other repeat-rich proteins such as RESA and Pf11.1, indicating that a number of these bands were likely to be cross reactive proteins (Udomsangpetch *et al.*, 1989a).

This experiment confirmed that Pf332 was partially insoluble in Triton X-100 and therefore, was most likely associated with the erythrocyte membrane skeleton. It also showed that Pf332 was partially soluble in Triton X-100, possibly indicating that a proportion of Pf332 that was not associated with the erythrocyte membrane skeleton. This may include Pf332 associated with Maurer's Clefts or other membranous structures within the erythrocyte cytoplasm, but it remains unclear at the present time whether such structures are in fact soluble in Triton X-100.

5.4 Cloning Pf332 Fragments

To study the interactions between Pf332 and the erythrocyte membrane skeleton, sub-fragments of Pf332 were cloned into the pMAL vector for expression as MBP fusion proteins. Figure 5.4 shows the division of Pf332 into 23 gene fragments. Three fragments from the first exon were designated E1, E2 and E3, where E represents the first exon. Twenty fragments from the second exon were designated 1 through 20. For each of the second exon fragments oligonucleotide

primers were designed in the forward and reverse orientation that included an *Eco*RI site and an *attB* site (p1159-p1199). This introduced site specific recombination sequences used by GATEWAY™ Cloning Technology (Section 2.7) and an *Eco*RI site used in conventional cloning procedures (Section 2.5 and 2.6). Oligonucleotides were designed for fragment E1, E2 and E3 (p1353/p1354, p1365/p1438 and p1439/p1356 respectively) which included a *Bam*HI site in the forward oligonucleotide and a *Xho*I site in the reverse oligonuclotide for cloning of these three fragments into a pMAL vector using conventional cloning procedures. Cloning procedures are outlined in Section 2.11.

5.5 Expression and Purification of MBP-Pf332 Fusion Proteins

pMAL clones containing each of the 23 fragments were used to transform *E. coli* BL21(DE3) cells to ampicillin resistance and subsequent strains (RCM1719, RCM1721, RCM1722, RCM1534, RCM1536, RCM1538, RCM1540, RCM1542, RCM1544, RCM1546, RCM1548, RCM1550, RCM1552, RCM1554, RCM1556, RCM1558, RCM1560, RCM1563, RCM1565, RCM1567, RCM1569, RCM1571, RCM1574) were used in the protein expression and purification of MBP-Pf332 fragments (Section 2.16). Approximately 2 μg and 50 ng of purified proteins were resolved on 10% polyacrylamide gels and visualised by either Coomassie Brilliant Blue staining or transferred to PVDF for immunoblot analysis using anti-MBP antiserum (Section 2.14) (Figure 5.5a and 5.5b). MBP fusion proteins E1-E3 (lanes 1-3) and 1-20 (lanes 4-24) purified as full length MBP fusion protein in varying yields. Full length fusion protein for each of the purified proteins resolved slightly higher than the predicted size. Table 5.1 summarises the Pf332 gene fragment sizes that were cloned into pMAL vectors and the expected sizes, along with the actual sizes, of proteins resolved on polyacrylamide gels for each of the resultant MBP fusion proteins.

5.6 Interaction of MBP-Pf3332 with IOVs

MBP-Pf332 proteins were incubated with IOVs to determine binding domains for the erythrocyte membrane skeleton within Pf332. MBP-PEMP3-FIa.1 was used as a positive control (Chapter 3) and MBP as a negative control. IOVs (Section 2.17) were coated onto wells, blocked, then approximately 2 μg of MBP-Pf332 fragments were added and allowed to bind. Bound protein was eluted from the wells (Section 2.19), resolved on 10% polyacrylamide gels, transferred to PVDF and for immunoblot analysis using anti-MBP antiserum. A representative immunoblot is shown in Figure 5.6. MBP-PfEMP3-FIa.1 positive control bound to wells coated with

IOVs (Figure 5.6c lane 11). None of MBP-Pf332 fragments E1, E2 (Figure 5.6c, lanes 3 and 5) and 1-18 (Figure 5.6a, lanes 3, 5, 7, 9, 11, 13, 15, 17, 19, 21 and 23, and Figure 5.6b, lanes 1, 3, 5, 7, 9, 11, and 13, respectively) bound to wells coated with IOVs. A small amount of bound protein was detected to wells coated with IOVs for MBP (Figure 5.6a and 5.6c, lane 1) and MBP-Pf332 fragment 20 (Figure 5.6b, lane 15) in this particular interaction, however the intensity of these bands were very low and not consistent across all interactions. Bound protein was detected for MBP-Pf332-fragment 19 (Figure 5.6c, lane 9), but this was far less intense than that detected for the MBP-PfEMP3-FIa.1 positive control (Figure 5.6c lane 11). A lightly less intense band was consistently observed for the binding of MBP-Pf332 fragment 19 to wells coated with BSA (Figure 5.6c, lane 20), indicating that the binding of MBP-Pf332 fragment 19 is only sightly above its negative control. A less intense band was also detected for MBP-Pf332 fragment E3 for wells coated with IOVs (Figure 5.6c, lane 7). This band was consistently only sightly more intense than for MBP-Pf332 fragment E3 binding to wells coated with BSA (Figure 5.6c, lane 8). A small amount of bound protein was detected for MBP-PfEMP3-FIa.1 positive control for wells coated with BSA (Figure 5.6c lane 12). No bound protein was detected for wells coated with BSA for MBP (Figure 5.6a and 5.6c, lane 2) or MBP-Pf332 fragments E1, E2 (Figure 5.6c, lanes 4 and 6), 1-18 and 20 (Figure 5.6 a, lanes 4, 6, 8, 10, 12, 14, 16, 18, 20, 22 and 24, and Figure 5.6b, lanes, 2, 4, 6, 8, 10, 12, 14 and 16).

The presence of background bands seen for MBP binding to IOVs (Figure 5.6a and 5.6c, lane 1) and MBP-PfEMP3-FIa.1 binding to BSA (Figure 5.6c lane 12) may be attributed to the exposure times required to detect the low intensity bands for binding of MBP-Pf332 fragments E3 and 19 to IOVs (Figure 5.6c, lane 7, and Figure 5.6c, lane 9). Whilst still detecting the MBP-PfEMP3-FIa.1 positive control, shorter exposures are not likely detect these background bands, however lesser exposures would fail to detect the binding seen for MBP-Pf332 fragment E3 to IOVs although binding is above binding to the BSA negative control.

These data showed no interaction between the erythrocyte membrane skeleton and MBP-Pf332 fragments E1, E2, 1-18 and 20. MBP-Pf332 fragment 20 appeared to show possible binding in the particular interaction shown here, however fragment 20 was considered a non binding fragment as its binding to IOVs was not consistently detected across a number of repeat interactions. This data also indicated a possible interaction between Pf332 fragments E3 and 19 with the erythrocyte membrane skeleton. The interaction between IOVs and MBP-Pf332 fragments E1 and 19 was always of low intensity and resulted in bands detected which were consistently less intense than the positive control and consistently only

sightly more intense than their BSA control. They were also often only slightly more intense than the MBP negative control. The potential of MBP-Pf332 fragments E3 and 19 to bind to the erythrocyte membrane skeleton led to us investigate the possibility of these regions binding more definitively to erythrocyte membrane following modification by the *P. falciparum* parasite.

5.7 Purification and Characterisation of IOVs from Parasitised Erythrocytes

Proteins at the erythrocyte membrane skeleton are modified following *P. falciparum* infection (for reviews see (Cooke *et al.*, 2001; Haynes, 1993; Coppel *et al.*, 1998; Howard and Gilladoga, 1989). To investigate the possibility of an interaction between Pf332 and the modified erythrocyte membrane skeleton, IOVs were made from parasitised erythrocytes. Parasitised IOVs (pIOVs) were made from 3D7 parasite cultures purified to more than 99% trophozoite infected erythrocytes using Percoll density gradient purification (Section 2.4.6). pIOVs and IOVs were made in parallel using the same method (Section 2.17), before immunoblot analysis and interaction assays were performed.

5.7.1 Coomassie Brilliant Blue Staining and Immunoblot Analysis of pIOVs

Proteins within pIOVs and IOVs were visualised to determine the difference in banding patterns of the proteins present and to equalise for the amounts of the common proteins present (such as spectrin) for immunoblot assays and interaction assays. Figure 5.7 shows 5 µl of both IOVs and pIOVs resolved on 10% polyacrylamide gels and stained with Coomassie Brilliant Blue. Major bands present in both IOVs and pIOVs are indicated as α-spectrin, β-spectrin, band 3, protein 4.1, pallidin, actin and glyceraldehyde-3-phosphate dehydrogenase (G3PD). Numerous additional bands present in pIOVs ranged from more than 250 kDa to less than 37 kDa. No major bands were observed above the stacking gel/resolving gel interface (as indicated, Figure 5.7). It was estimated that the intensity of the α- and β-spectrin bands were approximately equal between IOVs and pIOVs.

To identify additional proteins that co-purified with the erythrocyte membrane in pIOVs, immunoblot analysis was performed on both pIOVs and IOVs. pIOV and IOV samples (2.5 µl), with samples from both normal and 3D7 parasitised erythrocytes (2 µl) (prepared as described in Section 2.12.2), were loaded onto either 10% or 7.5% polyacrylamide gels, resolved and transferred to PVDF for

immunoblot analysis. Antiserum used for detection of each immunoblot is described in Appendix 4.

Figure 5.8a shows an immunoblot using anti-protein 4.1 antiserum. Protein 4.1 exists as 78 and 80 kDa proteins (Leto and Marchesi, 1984) and following resolution on a 7.5% polyacrylamide gel was detected in erythrocyte (lane 1), 3D7 (lane 2), pIOV (lane 3) and IOV (lane 4) samples, as both 78 and 80 kDa products (indicated by the arrows). Smaller molecular mass proteins were detected in all four samples. These could be break down products or cross reactive proteins.

Figure 5.8b shows detection of PfEMP1 using antiserum raised to the conserved intracellular portion of the PfEMP1. PfEMP1 is inserted into the erythrocyte membrane and exposed at the surface of parasitised erythrocytes (Leech *et al.*, 1984b). Therefore, PfEMP1 would be expected to purify with membranes in pIOVs. Samples were resolved on a 10% polyacrylamide gel and the immunoblot showed a feint band present in 3D7 (lane 1) and pIOV (lane 2) samples (indicated by *), but not in IOV (lane 3) or erythrocyte (lane 4) samples. This band was resolved at more than 250 kDa, corresponding to the predicted size of PfEMP1 between 250 and 350 kDa (Leech *et al.*, 1984b). A more intense cross reactive band seen across all four samples was thought to correspond to the spectrin subunits, as it could be resolved as two distinct bands (data not shown).

Figure 5.8c shows detection of KAHRP, which is known to be associated with the erythrocyte membrane skeleton through interactions with membrane skeletal proteins spectrin, actin and ankyrin, and through interactions with other parasite proteins such as PfEMP1 (Kilejian *et al.*, 1991; Magowan *et al.*, 2000; Waller *et al.*, 1999; Voigt *et al.*, 2000; Oh *et al.*, 2000). KAHRP has a predicted size of 85-105 kDa knobs (Leech *et al.*, 1984a; Gritzmacher and Reese, 1984; Kilejian, 1984) and when resolved on 7.5% polyacrylamide gels was detected as a smear in 3D7 (lane 2) and pIOV (lane 3) samples. Although the anti-KAHRP antiserum did not appear to detect a discrete band in ether pIOV or 3D7 samples, there was no reactivity to either erythrocyte (lane 1) or IOV (lane 4) samples. Within the 3D7 and pIOV samples there did appear to be a concentration of signal at around 95 kDa (indicated by the arrow).

Figure 5.8d shows detection of MESA, which is known to interact with protein 4.1 from parasitised erythrocytes (Lustigman *et al.*, 1990; Bennett *et al.*, 1997). Samples were resolved on 7.5% polyacrylamide gels and MESA was detected at more than 250 kDa in both 3D7 (lane 2) and pIOV (lane 3) samples, corresponding with the predicted size of 250-300 kDa (Coppel *et al.*, 1986). (indicated by the arrow). There were many smaller products detected in both

samples that could be due to protein breakdown products or cross reactivity. No bands were detected in either erythrocyte (lane 1) or IOV (lane 4) samples.

Figure 5.8e shows the detection of PfEMP3, which we have shown to interact with the erythrocyte membrane skeleton (Chapter 3). Following resolution on a 10% polyacrylamide gel, a band was detected in 3D7 (lane 2) and pIOV (lane 3) samples at more than 250 kDa corresponding to the predicted size for PfEMP3 of 315 kDa (Pasloske *et al.*, 1993). This band was absent in erythrocyte (lane 1) or IOV (lane 4) samples. A cross reactive band was seen clearly in both IOV and pIOV samples at approximately 250 kDa. This band became more evident in both 3D7 and erythrocyte samples with over exposure of the immunoblot (data not shown), and was therefore likely to have been cross reactivity of the anti-PfEMP3 antiserum with an erythrocyte protein.

Pf332 is thought to be associated with the erythrocyte membrane skeleton due to its insolubility in Triton X-100 (Section 5.3.1) (Mattei and Scherf, 1992a) and presence at the erythrocyte membrane skeleton as visualise by IFA (Hinterberg *et al.*, 1994). For assays looking at the interaction between Pf332 and the modified erythrocyte membrane skeleton, it was important to establish whether Pf332 is present in pIOV preparations. pIOVs and IOVs, along with 3D7 Triton X-100 insoluble (as prepared in Section 5.3.1) and erythrocyte samples were resolved on acrylamide/agarose composite gels (Section 2.12.4). Figure 5.9a shows the immunoblot detection using anti-Pf332 antiserum and reveals the presence of Pf332 in both 3D7 Triton X-100 insoluble (lane 4) and pIOV (lane 2) samples, but not erythrocyte (lane 1) or IOV (lane 3) samples. In contrast to previous acrylamide/agarose composite gels, Phosphorylase b, Cross-Linked SDS Molecular Weight Markers (Sigma) ranging from 97 kDa to 584 kDa were run beside the standard Precision Molecular Weight markers (BioRad), which have a maximum of 250 kDa. Using these markers, the size of Pf332 could be further defined as greater than 600 kDa. The largest protein detected by the anti-Pf332 antiserum is resolved well above the 584 kDa marker and was estimated to have a molecular mass of closer to 900 kDa. No smaller molecular mass products were detected in the erythrocyte (lane 1) or IOV (lane 3) samples, indicating that the products seen for pIOVs (lane 2) and 3D7 samples (lane 4 and Section 5.3.1) were either due to breakdown products or proteins of parasite origin such as RESA and Pf11.1 (as discussed in Section 5.3.1).

Figure 5.9b shows the detection of *P. falciparum* heat shock protein 70 (HSP70). HSP70 is localised within the parasite cytoplasm (Banumathy *et al.*, 2002) and was used as an indicator for the presence of internal parasite material within pIOV preparations. HSP70 was detected in both 3D7 (lane 2) and pIOV

(lane 3) samples, but not erythrocyte (lane 1) or IOV (lane 4) samples. This indicated that although the parasitised erythrocytes were lysed and inverted, parasites were probably still associated with the erythrocyte membrane and were purified with pIOVs. The presence of exported parasite proteins in pIOV samples (as described above) may have been due to their association with the erythrocyte membrane proteins or could be due to the presence of these proteins within the parasite itself, perhaps as part of synthesis and trafficking.

5.8 Interaction of MBP-Pf332 with pIOVs

To establish an interaction between Pf332 and pIOVs, interaction assays were performed with equal amounts of IOVs and pIOVs as described in Section 5.6. Figure 5.10 shows a representative immunoblot of selected interactions. MBP-PfEMP3-FIa.1 positive control bound to wells coated with pIOVs (lane 5) and to a slightly lesser extent, to wells coated with IOVs (lane 4). This difference in binding to pIOV and IOVs was consistent across a number of repeted interactions. MBP-Pf332 fragments E3 (lane 8) and 19 (lane 11) bound to wells coated with pIOV and to a lesser extent, to wells coated with IOVs (lane 7 and lane 12, respectively). The difference in the binding of these fragments to IOVs and pIOVs was greater than the difference for MBP-PfEMP3-FIa.I and was consistent with the low levels of binding seen for these fragments to IOVs in Section 5.6. In contrast with the results seen for IOV interactions (Section 5.6), none of the proteins bound to wells coated with BSA (lanes 3, 6, 9 and 12). No bound protein was detected for MBP to wells coated with IOVs (lane 1) or pIOVs (lane 2). No bound protein was detected for MBP-Pf332-fragments E1, E2, 1-18 or 20 for wells coated with pIOVs, IOVs or BSA (data not shown). These data showed binding of MBP-Pf332-fragments E3 and 19 to pIOVs. This binding appeared to be of greater intensity than that seen for IOVs and similar to the intensity seen for the PfEMP3-FIa.1 interaction.

5.9 Interaction of MBP-Pf332 with Spectrin

To further investigate the interaction of Pf332 with the membrane skeleton, MBP-Pf332 fragments were incubated with purified spectrin. Figure 5.11 shows a representative immunoblot of the interaction between spectrin and MBP-Pf332 fragments E3 and 19, along with MBP negative and MBP-PfEMP3-FIa.1 positive controls (Chapter 3). MBP-PfEMP3-FIa.1 bound to wells coated with spectrin (lane 3), whereas MBP (lane 1) showed no binding. Neither protein bound wells coated with BSA (lanes 2 and 4). Low levels of bound protein were detected for MBP-Pf332 fragments E3 and 19 to wells coated with spectrin (lanes 5 and 7,

respectively) and to an even lesser extent to wells coated with BSA (lanes 6 and 8, respectively). The binding of Pf332-fragments E3 and 19 to purified spectrin was less intense than that seen for the MBP-PfEMP3-FIa.1 positive control. These data were consistent with the results for binding to IOVs (Sections 5.6 and 5.8), where binding of MBP-Pf332-fragments E3 and 19 was consistently detected, however the intensity of the band was lower when compared to the MBP-PfEMP3-FIa.1 positive control and only just above the intensity of the BSA controls. None of the other MBP-Pf332 fragments showed binding to wells coated with spectrin or BSA (data not shown).

5.10 Discussion

This study set out to determine the structure of the Pf332 gene, confirm the association of Pf332 protein to the parasitised erythrocyte and determine its binding partner(s) within the erythrocyte membrane skeleton. By RT-PCR we have confirmed that the Pf332 gene comprises of two exons, in accordance with the VBC prediction. A two exon gene structure is a common feature of *P. falciparum* genes whose products are exported to the membrane skeleton, where a generally short, first exon containing a hydrophobic region is followed by a longer second exon that contains regions of repeats. Genes with these features, KAHRP, MESA, RESA, glycophorin-binding protein (GBP) and PfEMP3 (see Cooke *et al.*, 2001), differ from Pf332, mainly in overall size, however Pf332 has many features in common with these genes. Pf332 has a long first exon, encoding 568 residues, compared to the short first exons encoding 35-65 residues generally seen for these other genes. This however, equates to a first exon of approximately 10% of the total coding region in keeping with 1.5-8% total coding region for these other genes. These genes encode a hydrophobic region near to the 3′ end of the first exon. This hydrophobic region is thought to be the hydrophobic core of a signal sequence (Favaloro *et al.*, 1986; Triglia *et al.*, 1987; Coppel, 1992) and in KAHRP, a region encompassing this hydrophobic core is responsible for trafficking of the protein to the parasitophorous vacuole (Wickham *et al.*, 2001). A hydrophobic region is also present at the 3′ end of the Pf332 first exon and is approximately 10-20 residues in length in keeping with those previously described (for review see Nacer *et al.*, 2001). The second exon of Pf332 contains a large region that encodes glutamic acid rich repeats and extends for approximately 80% of the exon. The sequence for these repeats is degenerate, especially when compared with those described previously for *P. falciparum* proteins such as PfEMP3 (Section 1.4.2.3). A further notable feature, encoded by the second exon, is the small region of hydrophobicity approximately 270 residues from the C-terminus. Hydrophobic regions exist in

other exported proteins, however to date none of these hydrophobic regions have been attributed to binding domains.

In this study we have confirmed, through detergent solublisation, previous findings that Pf332 is located at the erythrocyte membrane skeleton (Hinterberg *et al.*, 1994; Mattei and Scherf, 1992a). In this study we have detailed the first reported *P. falciparum* protein that is localised at the erythrocyte membrane skeleton which appears to bind poorly to non-infected, and therefore unmodified, erythrocyte membranes. We have attempted to examine the hypothesis that parasite proteins that do not bind unmodified erythrocyte membranes may be able to bind erythrocyte membranes after modification by malaria parasites. Erythrocyte membrane proteins are modified through phosphorylation, truncation and covalent modification and by *P. falciparum* protease cleavage. Spectrin, ankyrin, band 3 and protein 4.1 are thought to undergo changes in levels of phosphorylation in infected erythrocytes (Murray and Perkins, 1989; Chishti *et al.*, 1994; Lustigman *et al.*, 1990; Magowan *et al.*, 1998). Spectrin can also be cleaved by Plasmepsin II (Le Bonniec *et al.*, 1999), whereas protein 4.1 and ankyrin can be cleaved by Falcipain-2 (Dua *et al.*, 2001; Raphael *et al.*, 2000). Band 3 is modified by truncation and covalent modification to produce a novel 65 kDa protein (Crandall and Sherman, 1991). Additionally, membranes are altered by the appearance of parasite proteins that bind to the membrane and may become the binding partners of other proteins. Through preparation of IOVs made from parasitised erythrocytes (pIOVs) we have attempted to develop procedures to analyse interactions of proteins that bind to erythrocyte membranes that are modified during *P. falciparum* infection.

Here, we have shown binding of two sub-fragments of Pf332 (E3 and 19) to IOVs made from parasitised erythrocytes (pIOVs), is greater than their binding to IOVs made from uninfected erythrocytes (IOVs) and to purified spectrin. Visualisation of proteins within pIOV preparations with Coomassie Brilliant Blue staining and immunoblot analysis showed that along with the expected presence of erythrocyte proteins, such as protein 4.1, pIOV preparations also contained parasite proteins. These proteins included Pf332, KAHRP, MESA PfEMP1 and PfEMP3, along with HSP70, which is localised in the parasite cytoplasm (Banumathy *et al.*, 2002). The presence of HSP70 indicates that the parasite or remnants of the parasite, possibly including membranes associated with the parasite are likely to have remained attached to the erythrocyte ghosts. Therefore, the interaction between pIOVs and MBP-Pf332 fragments E3 and 19 may involve interaction with modified membrane proteins, exported parasite proteins or other parasite proteins, either within the parasite itself or associated with the various parasite membranes.

Alternatively, MBP-Pf332 fragments may associate with native Pf332 within pIOVs. To date, there have been no reports of parasite proteins that bind to a parasite modified erythrocyte protein, but do not bind the same unmodified erythrocyte protein. Interestingly, MESA co-purifies with protein 4.1, which has been additionally phosphorylated in parasitised erythrocytes (Lustigman *et al.*, 1990; Bennett *et al.*, 1997), however, studies carried out with IOVs and recombinant protein 4.1 have also been able to show binding of MESA to protein 4.1 (Bennett *et al.*, 1997; Waller *et al.*, 2003). These reports indicate that modification of protein 4.1 by the parasite is not necessary for the binding of MESA, although it may lead to increased binding when it does occur.

The binding domains identified for Pf332 (fragments E3 and 19) both contain a hydrophobic region (Figure 5.12). Pf332 fragment E3 encompasses the region encoded by the 3' end of the first exon, which can be compared to the 3' end of the first exon of other exported parasite proteins and encodes a putative hydrophobic signal sequence (for review see Nacer *et al.*, 2001). To the best of our knowledge, no study using recombinant proteins to identify binding domains, have included the first exon. This is most likely due to the small size of the first exon in the majority of the exported proteins and their suggested role as signal sequences. In this study we have included the first exon because, it is much larger than those for previously described exported proteins. However, as there is no data on N-terminal processing of exported parasite proteins, it remains unknown if the E3 region is present in the mature protein. If not, the observed interaction would be artefactual as it could not occur in nature. Pf332 fragment 19 is encoded by a region upstream of the 3' end of the second exon. This region also encodes a region of hydrophobicity. These hydrophobic regions may be responsible for hydrophobic interactions with proteins present in pIOVs. It is also possible that they could interact with the phospholipid bilayer of the erythrocyte membrane, which may be responsible for the low level binding detected for Pf332 fragments to IOVs. It would be interesting to further map the binding domains within Pf332 to see whether the residues responsible for binding are confined to these hydrophobic regions.

Both Pf332 fragments E3 and 19 are negatively charged at the pH of the cytoplasm of parasitised erythrocytes (7.18 to 7.23) (Wunsch *et al.*, 1997). This may indicate electrostatic interactions with a positively charged protein within pIOVs. The binding domains of Pf332 are each a relatively short distance from the either the N- or C-terminal ends of the protein. Pf332 fragment 3 starts 429 residues from the N-terminus of Pf332 and fragment 19 finishes 270 residues from the C-terminus of Pf332 (Figure 5.12). Both these fragments are located outside

the degenerate repeat region of Pf332 that encompasses the majority of the residues encoded by the Pf332 second exon. Identification of binding domains within non repetitive regions is not uncommon within *P. falciparum* exported proteins. A number of binding domains have been identified within non repetitive regions of parasite exported proteins that contains both repeat and non repeat regions. These include the binding domains in MESA for protein 4.1 and in RESA for spectrin (Bennett *et al.*, 1997; Kun *et al.*, 1999; Foley *et al.*, 1994).

Our Pf332-spectrin interaction studies have demonstrated low levels of binding that are comparable to the low levels of binding detected for Pf332 to IOVs, in so far as the levels of binding can be compared across assays with different immobilised proteins. The amount of purified spectrin coated onto wells was not equalised to the spectrin available within IOV studies and therefore it is difficult to compare levels of binding. It may be that Pf332 binding to IOVs can be attributed to the presence of spectrin, and that the increase in binding to pIOVs is due to either a higher binding affinity of Pf332 to parasite modified spectrin or to the presence of an additional binding partner for Pf332 within pIOVs. Alternatively, the spectrin available for binding within IOV assays may be less than that available for binding within spectrin assays, and the Pf332 binding to IOVs may be due to contributions by a number of erythrocyte binding partners.

Here, we have also shown that there is a moderate increase in binding of PfEMP3 to pIOVs when compared to IOVs. Previously, we have shown that PfEMP3 binds to both spectrin and actin within IOVs (Chapter 3), however, the increased binding to pIOVs may indicate the presence of additional binding partners for PfEMP3. These may be modified erythrocyte proteins or parasite proteins purified with pIOVs. A previous study hypothesised that PfEMP3 may be involved in trafficking of parasite proteins to the erythrocyte membrane, possibly involving a binding domain within the C-terminus (Waterkeyn *et al.*, 2000). Evidence presented here points towards additional binding partners for the N-terminus of PfEMP3, however further studies involving interactions of pIOVs with the central and C-terminal regions of PfEMP3 may reveal binding partners within pIOVs for these regions.

Clearly, an attempt quantify this PfEMP3-pIOV interaction and the interactions of Pf332 with IOVs and pIOVs needs to be made. Binding kinetics may define the binding of Pf332 fragments and PfEMP3-FIa.1 to IOVs and pIOVs, and confirm the binding differences identified with the solid phase microtitre assays. Analysis of whole cell binding has been performed using the IAsys™ system (Morgan *et al.*, 1998) and this methodology could be adapted to quantify the binding of Pf332 fragments and PfEMP3-FIa.1 to both IOVs and pIOVs.

Additional future experiments would focus on the alteration of pIOV preparations through the use of modified parasite lines, alterations to the lysis protocols and the additional treatment of pIOVs with reagents that have been shown to selectively strip IOVs of particular proteins. Both our laboratory and others have constructed a number of mutant parasite lines such as those with the genes for PfEMP3 and KAHRP deleted (Waterkeyn *et al.*, 2000; Crabb *et al.*, 1997), and a number of lines that express truncated proteins, including Pf332 (F. Glenister, Monash University, unpublished results). These lines could be used for the purification of modified pIOVs and subsequent interaction assays. Any change in binding profiles could be used to identify a binding partner for Pf332. Of particular interest would be a knockout Pf332 line, which would determine whether the MBP-Pf332 fragments E3 and 19 were binding to native Pf332 within pIOVs. Knocking out the Pf332 gene would also ensure that the sites within binding partners for Pf332 are not obscured by native Pf332 and are available for binding by the MBP-Pf332 fragments E3 and 19. Unfortunately, to our knowledge, this line does not yet exist and wether deletion of such a large gene is not yet known. The truncated Pf332 line produced in our laboratory would be useful given that the Pf332 fragment 19 would be absent from this parasite line. If there was no observed binding between pIOVs purified from this parasite line and MBP-PF332 fragments, we could conclude an interaction between the MBP-Pf332 fragment in the N-terminus of native Pf332. Such a negative interaction with a particular knockout line such as those involving KAHRP or PfEMP3, would suggest a possible binding partner given the parasite protein absent from the parasite line. Unfortunately, positive interactions with these mutant parasite lines would not allow for identification of binding partners for Pf332. Any inferred interactions using these knockout lines would need to by confirmed with the appropriate direct interaction of Pf332 with the proposed binding partner.

Alterations to the pIOV purification protocol may enable us to deplete these preparations of proteins of a particular origin. A number of previous studies have showed depletion of IOVs by alterations to the buffers used to wash the membranes. These treatments result in the depletion of particular proteins from the membranes and resulting membranes have been used to identify binding partners within the erythrocyte membrane skeleton. Initial reports of IOV preparations suggest that incubation of ghosts in low ionic strength buffer completely dissociates spectrin and actin from the membranes (Steck and Kant, 1974). However, results presented here show that under the conditions of 0.5 mM Phosphate Buffer, pH 7.0 a large amount of both spectrin and actin remain in the IOV preparations. Later studies employed low ionic strength buffer treatment

followed by T110 Dextran gradients for the purification of IOVs completely devoid of spectrin and actin (Bennett and Branton, 1977), showing that our findings of residule spectrin and actin in IOVs are not unique. Many other treatments have been employed to deplete ghosts of particular membrane skeletal proteins. For example, Ohanian and Gratzer (1984) showed that treatment of ghosts with concentrated Tris at neutral pH resulted in dissociation of protein 4.1, spectrin, actin and protein 4.9. A study by Bennett and Stenbuck (1980a) showed that treatment of spectrin and actin depleted ghosts with 0.1M acetic acid results in the depletion of protein 4.1, band 6 and ankyrin. Whereas Korsgren and Cohen (1985), showed that following depletion of spectrin and actin, additional proteins can be depleted from IOVs with high pH (pH 11). Moreover, treatment with KCl results in the depletion of ankyrin from ghosts, with the majority of other skeletal proteins remaining in tact (Bennett and Stenbuck, 1980b). Often these depletion methods have been used for the purification of particular proteins, rather than for the purification of IOVs completely devoid of a particular protein. Therefore, the resultant membrane preparations from these procedures need to be analysed to determine contamination of depleted protein/s. Depletion of pIOVs of proteins using modification of such methods may achieve depletion of the parasite material, exported malarial proteins and/or membrane skeletal proteins. Successful application of such techniques would allow identification of the protein or group of proteins to which Pf332 binds, by the absence of binding in particular depleted preparations. Initially, it would be most useful to deplete these preparations of parasite proteins such as HSP70 and other proteins present within the parasite itself. However, depletion of protein exported to the erythrocyte membrane and of erythrocyte membrane proteins could ultimately lead to the identification of binding partners for parasite proteins

The use of alternate methods to lyse the erythrocyte may result in the separation of the parasite and its associated membranes from the erythrocyte membrane skeleton. Blisnick *et al.*(2000) reported the use of a RPMI based hypotonic solution to lyse parasitised erythrocytes, followed by centrifugation at 15,000g. Under these conditions, ghosts are present in the supernatant and parasites in the pellet. Alternatively, extraction of the parasitised erythrocytes with TX100 may result in the separation of the erythrocyte membrane from the parasite. Preparations of pIOV purified with these modifications would require analysis for the presence of parasite proteins prior to use in identification of Pf332 binding domains for proteins within the erythrocyte membrane.

In addition to the use of pIOVs, immunoprecipitation may prove to be useful for identification of binding partners for malaria proteins that show no binding to

IOVs. Previous studies have used immunoprecipitation for identification of protein 4.1 as a binding partner for MESA and for identification of ankyrin as a binding partner for KAHRP (Lustigman *et al.*, 1990; Magowan *et al.*, 2000). Immunoprecipitation of Pf332 with a Pf332-specific antibody and subsequent identification of co-purified protein(s) might be an effective and more efficient way of determining binding partners than the use of mutant lines. Unfortunately, immunoblot analysis of parasites with the Pf332 antiserum used here has shown bands that are most likely due to cross reactivity with other proteins. Cross reactivity has been shown for Pf332 antisera in previous reports to proteins that contain similar glutamic acid rich regions including RESA and Pf11.1 (Ahlborg *et al.*, 1991). Therefore, immunoprecipitation experiments would require the development of more specific antiserum, which was not feasible within in the time frame of this study. In addition, methods and reagents for identification of the co-purified proteins would need to be developed to ensure that this approach is more efficient than using pIOVs.

```
start pf11:1947120w chr11_1.glm_549+550|01jun01 vbc pf332 af202180
exon 1
1947120                                ATG TCT AAT ATA AAT AAC AAA GAC TCT AGT A
1947151  CA GAA TGG AAT TGT AAA GAA GAT GTG GGA TGT GTT CCA CCT AGG AGA CAG
1947201  AAT TTG AAT ATG GAA AGG TTG GAT AAT GAA AAT GAA GAT TCT GTA CCC GA
1947251  T TTC ATG AAG AAA ACT TTT TAT CTT GCT GCT GCT GGA GAA GGA AAG AAG T
1947301  TA CGT GAG AAG CAT GAT GAG AGT TGT GAT GAA TTC TGT GAC GCA TGG AAT
1947351  AGA AGT TTA GCT GAT TAT AAA GAT ATA TTT CAA GGA AAG GAT ATG TGG AA
1947401  T GAT GGG AAA TAT GGT GAA GCG AAA AAT CAT ATT AAG AAT GCT TTT GGT G
1947451  AT ATG AAC AAT AGA AAA ACT ATG TTA AAT GAA ATT GAG AAA GGA ATT AAA
1947501  GAT GAA ACG TTT AGT CGT GAA AAT GGT TTA GAC GTT TGT AAA TCT CAA TG
1947551  T GAG GAA AGA AGT AGA GAT GAC ACA GAA GAT CAA TTT TTG AGG TTT TTT G
1947601  CA GAA TGG GAA GAA GAA TTT TGT GAT GGG TTA AAT AAA CAT GAA GAA CAA
1947651  TTA AAG TCT TGT ACT AAA GAT ATA AAT TGT GAC ATT AAA TGT AGC AAT TT
1947701  T AAA GAT TGG CTT GAA ACT AAA AAA GAT GAA TAT GAT ATT CAA TCG AGG G
1947751  TA TTT GAA AAA AAA TAT GCT AAT GAT AAT AAA TCA AAA CAT TTG AAC TAT
1947801  TTA AAG GAA GGA ATG AAT AAA TGC AAG GTG AAA AAT CCA GAA ATG GTG TT
1947851  T AAA TCA GGA TTT GCA AAC GTA GCT GAA TGT AGA AAT TTG AAT GTA GAA G
1947901  GT GCG GGC AAT AAG AAT TCA AAT AAT TTA AAA GAT TTA GAT AGT AAT TCT
1947951  GAT AAG GAT GGT ATT GTT AGT GAA TCA TAT AAA GCT ACT AAA AAA AAT GG
1948001  T GAG AGT ATT ATG GAT AGA ATT CCT AAA TCT TTT AAT AAA TTA TTC GGT T
1948051  AT TTT AGT GGT TCC CAA GAA GAA GAA CAA AAA GAA AAT GAT GTG TCA CAT
1948101  AGG AAT AAT TAT GAT AAT ATA TTA GTA GAT AAA TTT CAT AGG TCA TCT CT
1948151  A CTG GAT AAA TTA GAT GAC AGA ATG TTT TTT GAT GAA TTA AAT CGT GAT A
1948201  AT ATA ATG GAA GAA GTA TTA TCT AAA ATA CCA GAA CCT ATA ATA CGA GAG
1948251  GCA CCA AAA TAT GTA CCC AAA AAA CCA GTA CCA CCA CAA CAT ATT CCA AG
1948301  A GGT GAT AAT GTA CCA CGA AAT ATT GAT GTA AAC GGA TCA AAA GAT GAA T
1948351  AT TCT CCT GAA ACT GAA AGT GCA AAT TCG AAA ATT AAG CCT ACT TAT GAA
1948401  GAA AAT GAT GAA GAC AAA AGC AAG ATC TCT ATA GAG ACA TCA GAA ATA GA
1948451  T CGT GAT AAA GAA CCA TTT AGA ATA AGT GAA GAG AAA AAA GTT GTA AAA G
1948501  AG GAT GTG CAG GAA TTA GAA AAT ATA GAA TAC GAA TTT GAT GAA ACA TTC
1948551  GAT TTT TTT GAT GAA GAT GCT AAA CGT AAT ATA GAT GAT ATA AGA AAA GA
1948601  T ATA CAG TCA CAA ATT ATG AAA TCC GTA GAA AAT TAT AAT TCA GAA AAG G
1948651  AG GAA TTT AAA AGA AAT ATT GAA ACA CAA CTA ATA GAA TCT GGA GAT GGA
1948701  ATG AAT GCA GGA AAT TAT TCT AGT GCT TTG CAA GAC AAC AGT ACG GAA AT
1948751  A CCA ACA ATG GTG TTA GTA CCA GGA GTA TTA ACA GTA TTT TTG CTT ACT A
1948801  TT ATA TGG GTC TTG GTA TAT AAG
1948823

intron
                                     GTAATAT AATGACGTAT AAATGCACAT
1948851  ATATATATAT ATATATATTT ATTTGTTAAT ATATAAATAT AATATTTTAT
1948901  TGAAAATATT TTTCACATAT AATTTTTTTT TCTTTTTATT ATTAAAATGA
1948951  AAAATTTCTA TTTTTCAACA ATTTTGTTTA TATATAAACT TATATGTAAA
1949001  AAATGTAATA TAATATAATA TAATATAATA TAATATATAT ATATTTTTTA
1949051  ATTTATAG

exon 2
1949059            CAT TCT TTG ATT GAT CGT GTT CAT GGT ACG GGG AAA ACT AAA
1949101  AAG GAA GAG AAA ATG AAA GAA CTA GAA AGT GAA GAA TTT CCA AAA GAG AA
1949151  A TAT AAC ATT GAA GAC ATG GAA GAA ACT GAG AAA GAG AAC GAA ATA GAA A
```

Figure 5.1. Pf332 Gene Structure Prediction
Shows the first exon, intron and the 5′ sequence of the second exon as annotated by R. Huestis, Victorian Bioinformatics Consortium. The second exon extends beyond the sequence shown to nucleotide 1965636 in accordance with the published *P. falciparum* chromosome 11 sequence (Gardner *et al.*, 2002).

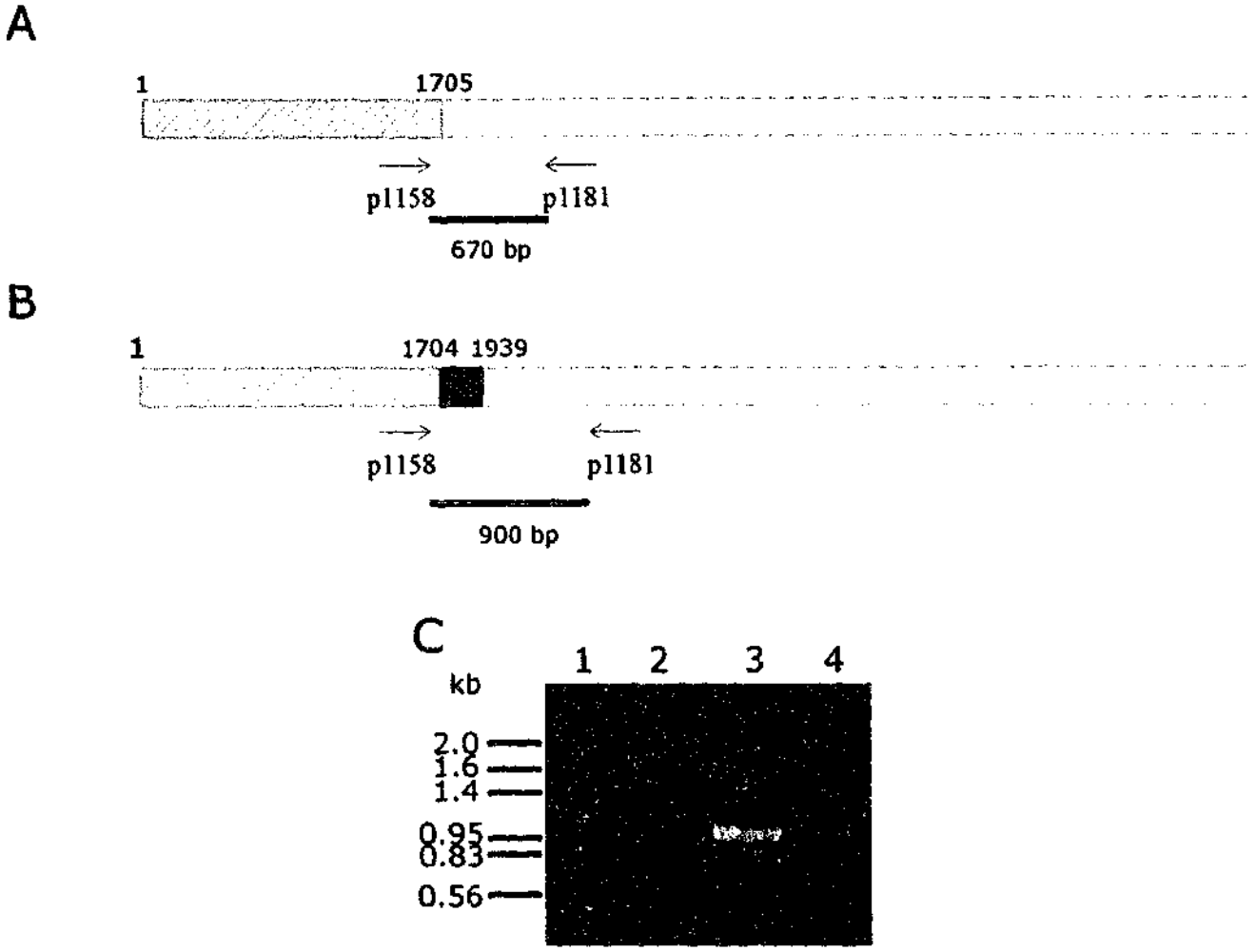

Figure 5.2. RT-PCR to Confirm the Predicted Intron/Exon Structure of Pf332

A. Schematic representation of the RT-PCR product from cDNA. The first exon is represented by the shaded box and the 5' region of the second exon by the open dotted lines. Nucleotide numbers for the boundaries are shown above the gene schematic. The position and orientation of the RT-PCR primers, p1158 and p1181 are indicated by the arrows and the resultant 670 bp product by the blue line.

B. Schematic representation of the RT-PCR product for gDNA. Schematic is as above with the addition of the intron as the coloured box. The resultant 900 bp product is represented by the blue line.

C. RT-PCR products resolved on an agarose gel and stained with ethidium bromide. Samples are RT^+ (lane 1), RT^- (lane 2), gDNA (lane 3) and no DNA (lane 4). The size of the markers is indicated in kilobases (kb). The RT^+ sample showed a band between the 0.83 kb and the 0.56 kb markers. The RT^- (lane 2) and no DNA (lane 4) samples showed no product. The gDNA (lane 3) sample showed a band at approximately 0.95kb (lane 3).

Figure 5.3. Triton X-100 Extraction of Pf332 from Parasitised Erythrocytes
Immunoblot analysis of Triton X-100 samples detected using anti-Pf332 antiserum. Samples are 3D7 (lane 1), Triton X-100 insoluble (lane 2) and Triton X-100 soluble (lane 3). In each sample a band resolved at well above the 250 kDa marker. A number of smaller products are also detected.

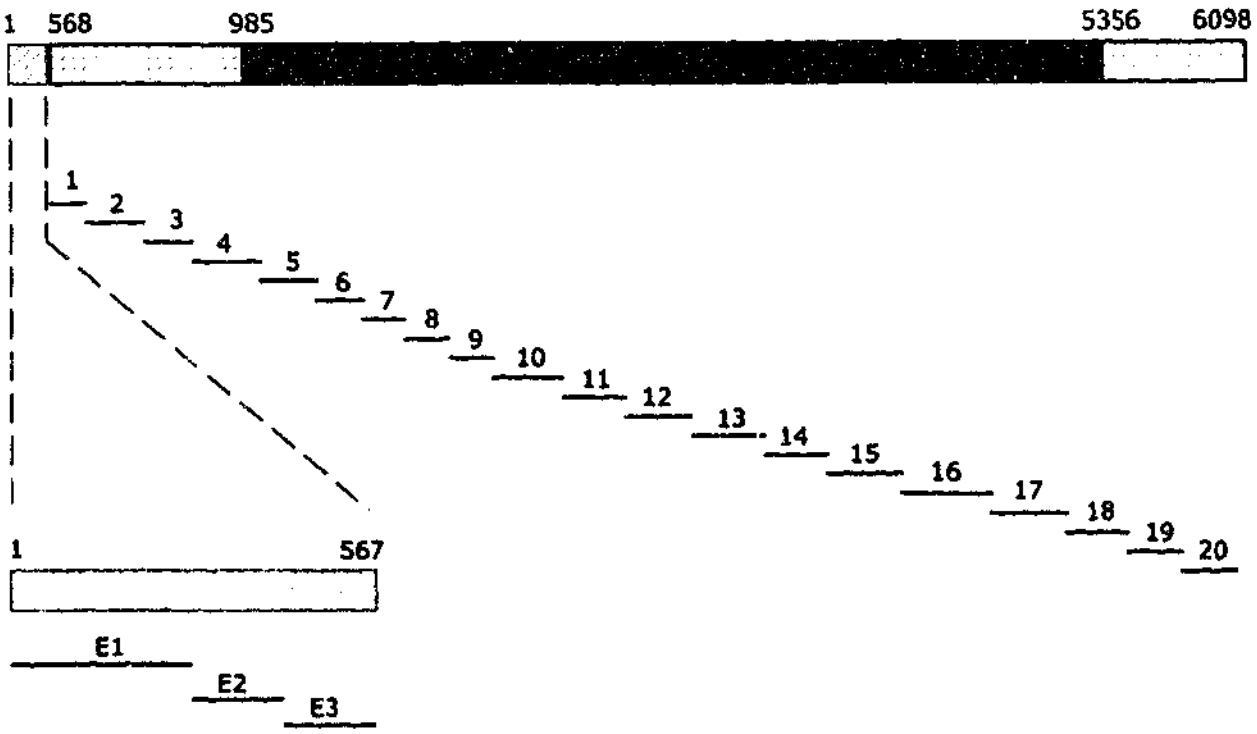

Figure 5.4. Schematic of the Pf332 Fragments

Pf332 was divided into 23 fragments for cloning, expression and purification as MBP fusion proteins. Amino acids 1-567, represented by the shaded orange box, encompass amino acids encoded by the first exon of Pf332. This region is magnified at the bottom of the schematic and the 3 fragments that encompass this region; E1, E2 and E3 are indicated. Amino acids 568-6098, represented by the blue boxes, indicate amino acids encoded by the second exon of Pf332. The shaded blue regions indicate the non-repetitive regions and the solid blue region (amino acids 985-5356) indicates the repetitive region. The second exon is divided into 20 fragments and these are indicated below the protein schematic.

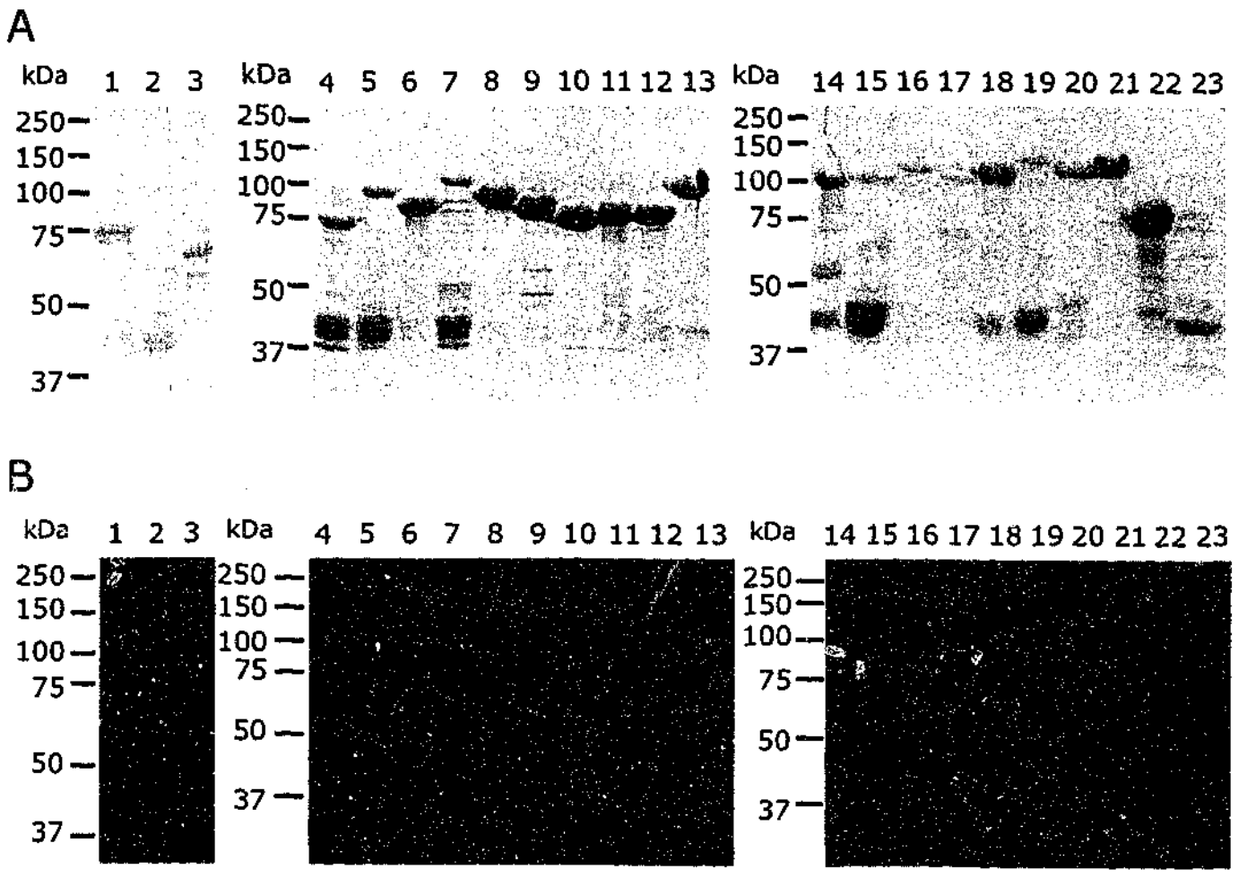

Figure 5.5. Expression and Purification of Pf332 Fragments as MBP Fusion Proteins

A. Purified MBP-Pf332 fusion proteins detected by Coomassie Brilliant Blue staining of SDS-PAGE. 2 μg of each purified protein was resolved on 10% polyacrylamide gels. The proteins are E1, E2, E3 (lanes 1-3, respectively) and 1-10 (lanes 4-13, respectively) and 11-20 (lanes 14-23, respectively).

B. Immunoblot assay of MBP-Pf332 fusion proteins detected using anti-MBP antiserum. 50 ng of each purified protein was resolved on 10% polyacrylamide gels and transferred to PVDF for detection. The protein samples are E1, E2, E3 (lanes 1-3, respectively) and 1-10 (lanes 4-13, respectively) and 11-20 (lanes 14-23, respectively).

Fragment	Approx. Size (kb)	Calculated Molecular Weight as MBP fusion (kDa)	Observed Molecular Weight as MBP Fusion (kDa)
E1	0.85	76	80
E2	0.43	60	60
E3	0.42	59	70
1	0.54	64.3	75
2	0.84	75.1	100
3	0.70	69.3	80
4	0.96	78.9	105
5	0.81	72.7	95
6	0.70	69.7	80
7	0.62	65.9	75
8	0.65	67.4	80
9	0.64	66.9	80
10	1.01	79.8	105
11	0.90	76.4	105
12	0.95	78.6	105
13	1.05	82.1	110
14	0.91	77.2	105
15	1.08	94.1	110
16	1.27	90.7	120
17	1.06	82.1	110
18	0.91	78.2	105
19	0.78	74.3	75
20	0.80	75.2	75

Table 5.1. Characteristics of Pf332 Fragments Used in this Study

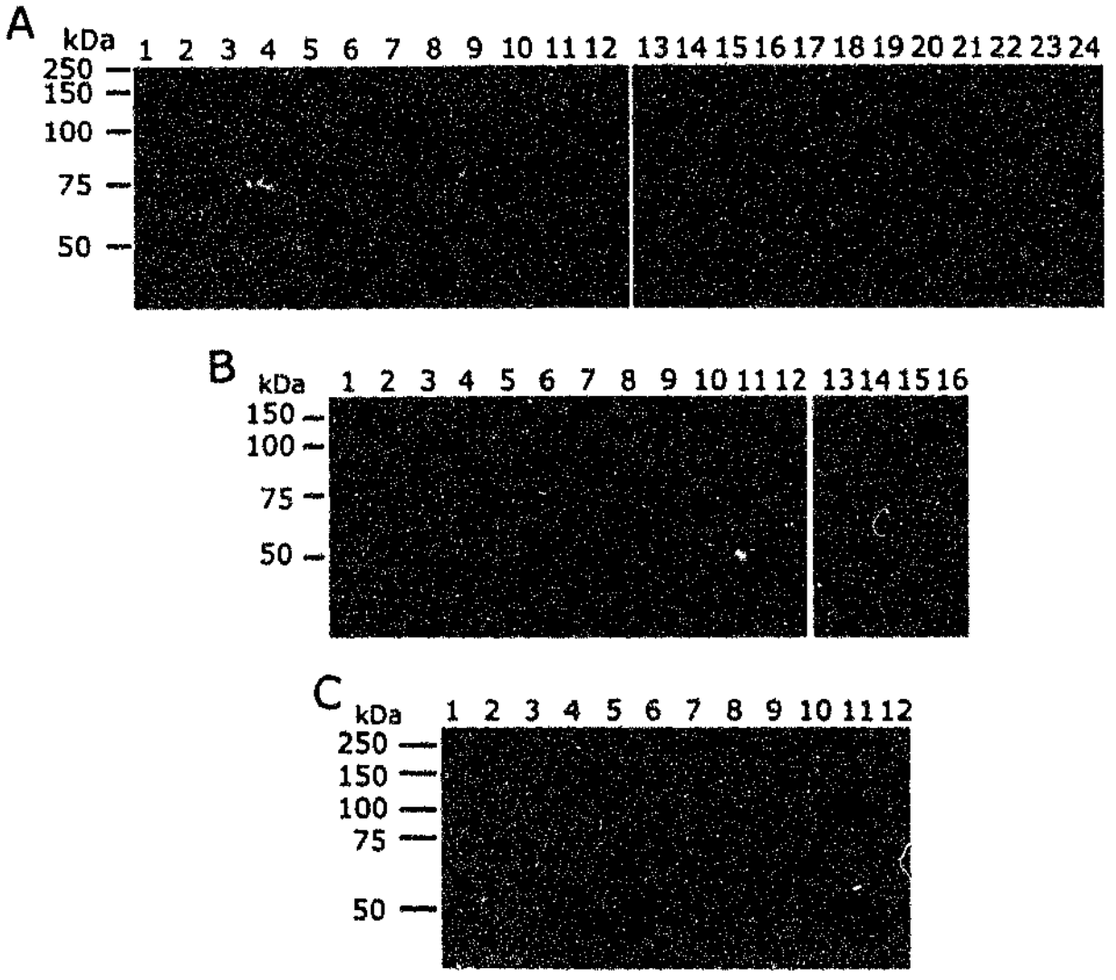

Figure 5.6. Immunoblot of IOV Interaction Assay with Pf332 Fragments

A. IOVs (lanes 1, 3, 5, 7, 9, 11, 13, 15, 17, 19, 21 and 23) and BSA (lanes 2, 4, 6, 8, 10, 12, 14, 16, 18, 20, 22 and 24) were coated onto wells of a microtitre plate. MBP (lanes 1 and 2), MBP-Pf332 fragment 1 (lanes 3 and 4), 2 (lanes 5 and 6), 3 (lanes 7 and 8), 4 (lanes 9 and 10), 5 (lane 11 and 12), 6 (lanes 13 and 14), 7 (lanes 15 and 16), 8 (lanes 17 and 18), 9 (lanes 19 and 20), 10 (lanes 21 and 22) and 11 (lanes 23 and 24) were added to the wells and allowed to bind. Low levels of bound protein were detected for MBP to wells coated with IOVs (lane 1).

B. IOVs (lanes 1, 3, 5, 7, 9, 11, 13 and 15) and BSA (lanes 2, 4, 6, 8, 10, 12, 14 and 16) were coated onto wells of a microtitre plate. MBP-Pf332 fragments 12 (lanes 1 and 2), 13 (lanes 3 and 4), 14 (lanes 5 and 6), 15 (lanes 7 and 8), 16 (lanes 9 and 10), 17 (lane 11 and 12), 18 (lanes 13 and 14) and 20 (lanes 15 and 16) were added to the wells and allowed to bind. Low levels of bound protein were detected for MBP-Pf332 fragment 20 to wells coated with IOVs (lane 15).

C. IOVs (lanes 1, 3, 5, 7, 9, and 11) and BSA (lanes 2, 4, 6, 8, 10 and 12) were coated onto wells of a microtitre plate. MBP (lanes 1 and 2), MBP-Pf332 fragments E1 (lanes 3 and 4) E2 (lanes 5 and 6), E3 (lanes 7 and 8), 19 (lanes 9 and 10) and MBP-PfEMP3-FIa.1 (lanes 11 and 12) were added to the wells and allowed to bind. Low levels of bound protein were detected for MBP to wells coated with IOVs (lane 1) and MBP-PfEMP3-FIa.1 to wells coated with BSA (lane 12). Bound protein was detected for MBP-PfEMP3-FIa.1 to wells coated with IOVs (lane 11). Low levels of bound protein was detected for MBP-Pf332 fragment E3 and 19 to wells coated with IOVs (lanes 7 and 9, respectively). Faint bands were observed for the binding of MBP-Pf332 fragment E3 and 19 to wells coated with BSA (lanes 8 and 10, respectively).

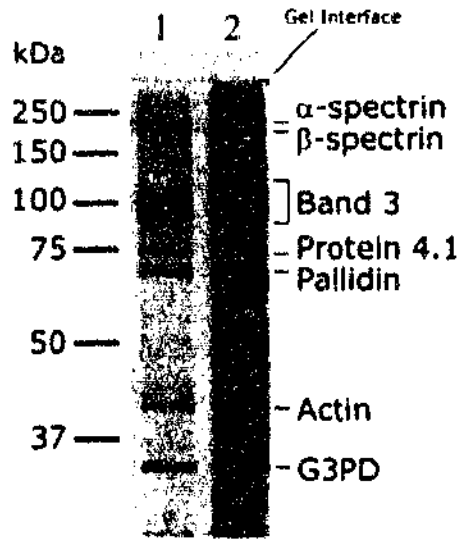

Figure 5.7. Coomassie Brilliant Blue Staining of IOVs and pIOVs

IOVs and pIOVs detected by Coomassie Brilliant Blue staining of SDS-PAGE. 5 μl neat of both IOVs (lane 1) and pIOVs (lane 2) were resolved on 10% polyacrylamide gels. Major bands present in both IOVs and pIOVs are indicated as α-spectrin, β-spectrin, band 3, protein 4.1, pallidin, actin and glyceraldehyde-3-phosphate dehydrogenase (G3PD). Numerous additional bands present in pIOVs range from more than 250 kDa to less than 37 kDa. No major bands are detected above the stacking/resolving gel interface.

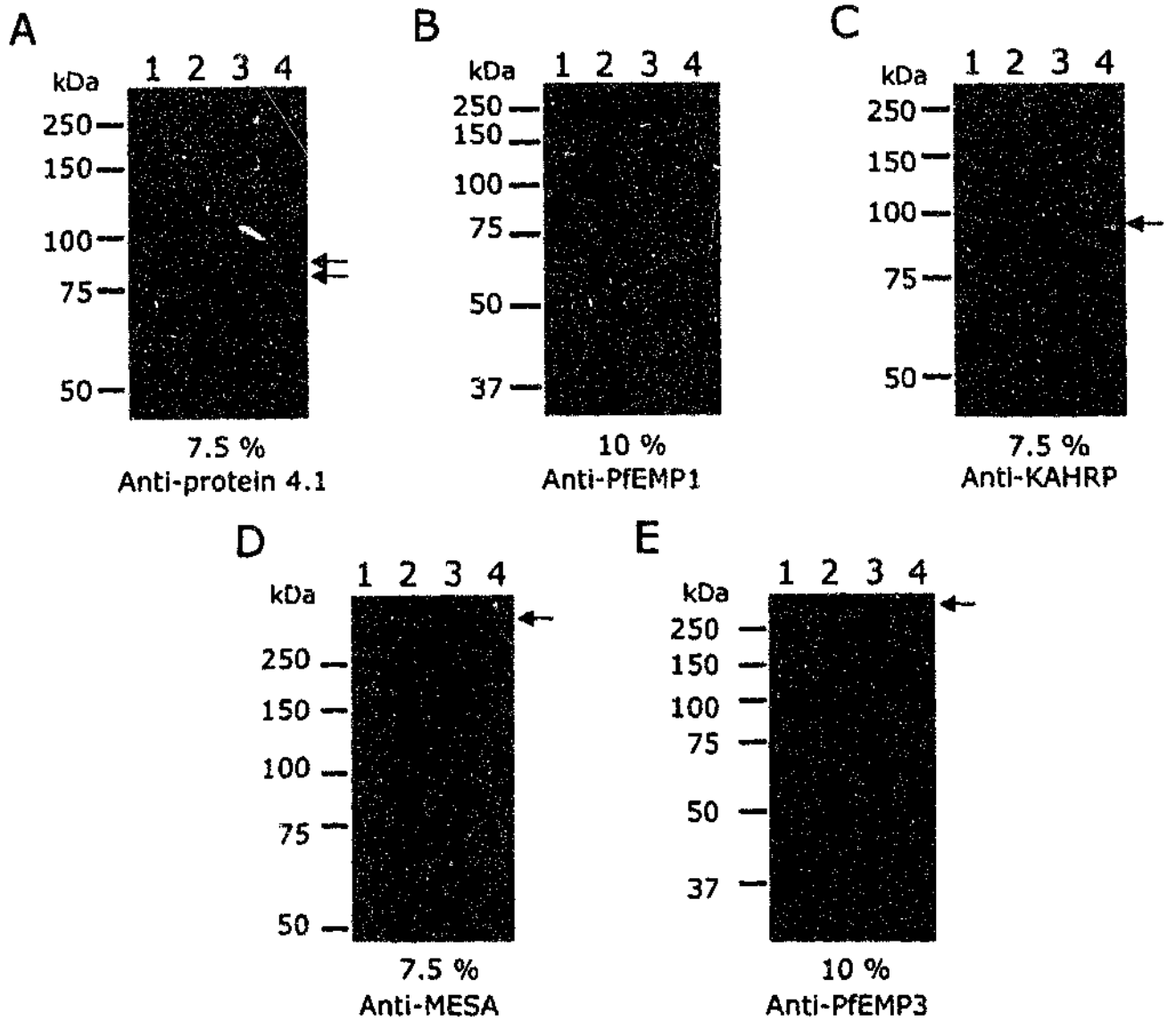

Figure 5.8. Immunoblot Analysis of pIOVs

pIOVs and IOV samples (2.5 µl), along with of erythrocyte and 3D7 samples (2 µl) were resolved on 10% or 7.5% polyacrylamide gels, resolved and transferred to PVDF for immunoblot analysis using the specified antiserum (Appendix 4).

A. Protein 4.1 was detected in erythrocyte (lane 1), 3D7 (lane 2), pIOV (lane 3) and IOV (lane 4) samples as both 78 and 80 kDa products (arrows). Smaller products were also detected in all samples.

B. PfEMP1 was detected in 3D7 (lane 1) and pIOV (lane 2) samples (indicated by the *), but not in IOV (lane 3) or erythrocyte (lane 4) samples. This band resolved at more than 250 kDa. A cross reactive band seen across all samples is thought to correspond to the spectrin subunits

C. KAHRP was not detected as a specific single band. No reactivity was detected to either erythrocyte (lane 1) or IOV (lane 4) samples. 3D7 (lane 2) and pIOV (lane 3) samples showed a concentration of signal at around 95 kDa (arrow).

D. MESA was detected at more than 250 kDa (arrow) in 3D7 (lane 2) and pIOV (lane 3) samples. No protein was detected in erythrocyte (lane 1) or IOV (lane 4) samples. Smaller products were detected in both 3D7 and pIOV samples.

E. PfEMP3 was detected as a band at more than 250 kDa in 3D7 (lane 2) and pIOV (lane 3) samples, but not in erythrocyte (lane 1) or IOV (lane 4) samples. A cross reactive band was seen in both IOV and pIOV samples at approximatey 250 kDa and in 3D7 and erythrocyte samples with over exposure of the immunoblot (data not shown).

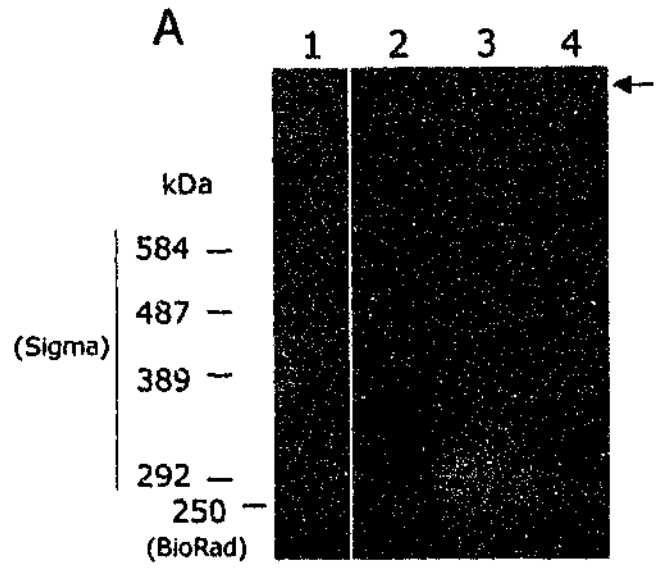

Figure 5.9. Immunoblot Analysis of pIOV

A. Detection of Pf332. pIOV and IOV samples (2 μl), along with 3D7 Triton X-100 insoluble and erythrocyte samples were run on acrylamide/agarose composite gels, transferred to PVDF and used in immunoblot analysis. Detection using anti-Pf332 antiserum shows a band in both 3D7 Triton X-100 insoluble (lane 4) and pIOV (lane 2) samples (arrow), but not erythrocyte (lane 1) or IOV (lane 3) samples. Phosphorylase b, Cross-Linked SDS Molecular Weight Markers (Sigma) and Precision Molecular Weight markers (BioRad) are indicated adjacent to the gel.

B. Detection of HSP70. PIOV and IOV samples (2.5 μl), along with 3D7 and erythrocyte samples (2 μl) were loaded onto 10% polyacrylamide gels, resolved and transferred to PVDF for immunoblot analysis. Anti-HSP70 antiserum detected HSP70 in 3D7 (lane 2) and pIOV (lane 3) samples, but not erythrocyte (lane 1) or IOV (lane 4) samples.

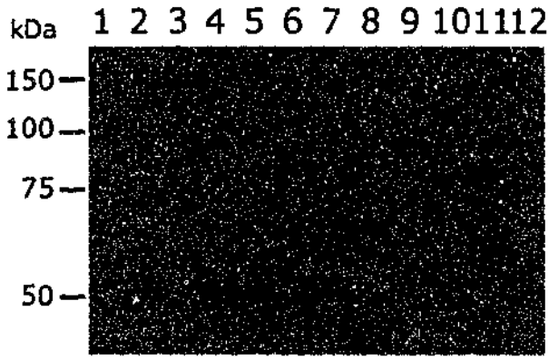

Figure 5.10. pIOV Interaction Assay with Pf332 Fragments

Immunoblot of pIOV interaction assay. IOVs (lanes 1, 4, 7 and 10), pIOVs (lanes 2, 5, 8 and 11) and BSA (lanes 3, 6, 9 and 12) were coated onto wells of microtitre plates. MBP (lanes 1, 2 and 3), MBP-PfEMP3-FIa.1 (lanes 4, 5 and 6), MBP-Pf332 fragments E3 (lanes 7, 8 and 9) and 19 (lanes 10, 11 and 12) were added to the wells and allowed to bind. PfEMP3-FIa.1 positive control bound to wells coated with pIOVs (lane 5) and to a slightly lesser extent to wells coated with IOVs (lane 4). Bound protein was detected for wells coated with pIOV for Pf332 fragments E3 (lane 8) and 19 (lane 11). To a lesser extent, bound protein was detected for both Pf332-fragments E3 (lane 7) and 19 (lane12) to wells coated with IOVs.

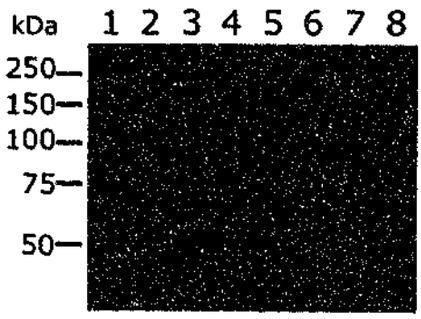

Figure 5.11. Spectrin Interaction Assay with Pf332 Fragments

Immunoblot of spectrin interaction assay. Spectrin (lanes 1, 3, 5 and 7) and BSA (lanes 2, 4, 6 and 8) were coated onto the wells of a microtitre plate. MBP (lanes 1 and 2), MBP-PfEMP3-FIa.1 (lanes 3 and 4), MBP-Pf332 fragments E3 (lanes 5 and 6) and 19 (lanes 7 and 8) were added to wells and allowed to bind. Bound protein was detected for MBP-PfEMP3-FIa.1 to wells coated with spectrin (lane 3). Bound protein was detected at a lesser intensity for MBP-Pf332 fragments E3 and 19 to wells coated with spectrin (lanes 5 and 7, respectively) and to BSA (lanes 6 and 8, respectively).

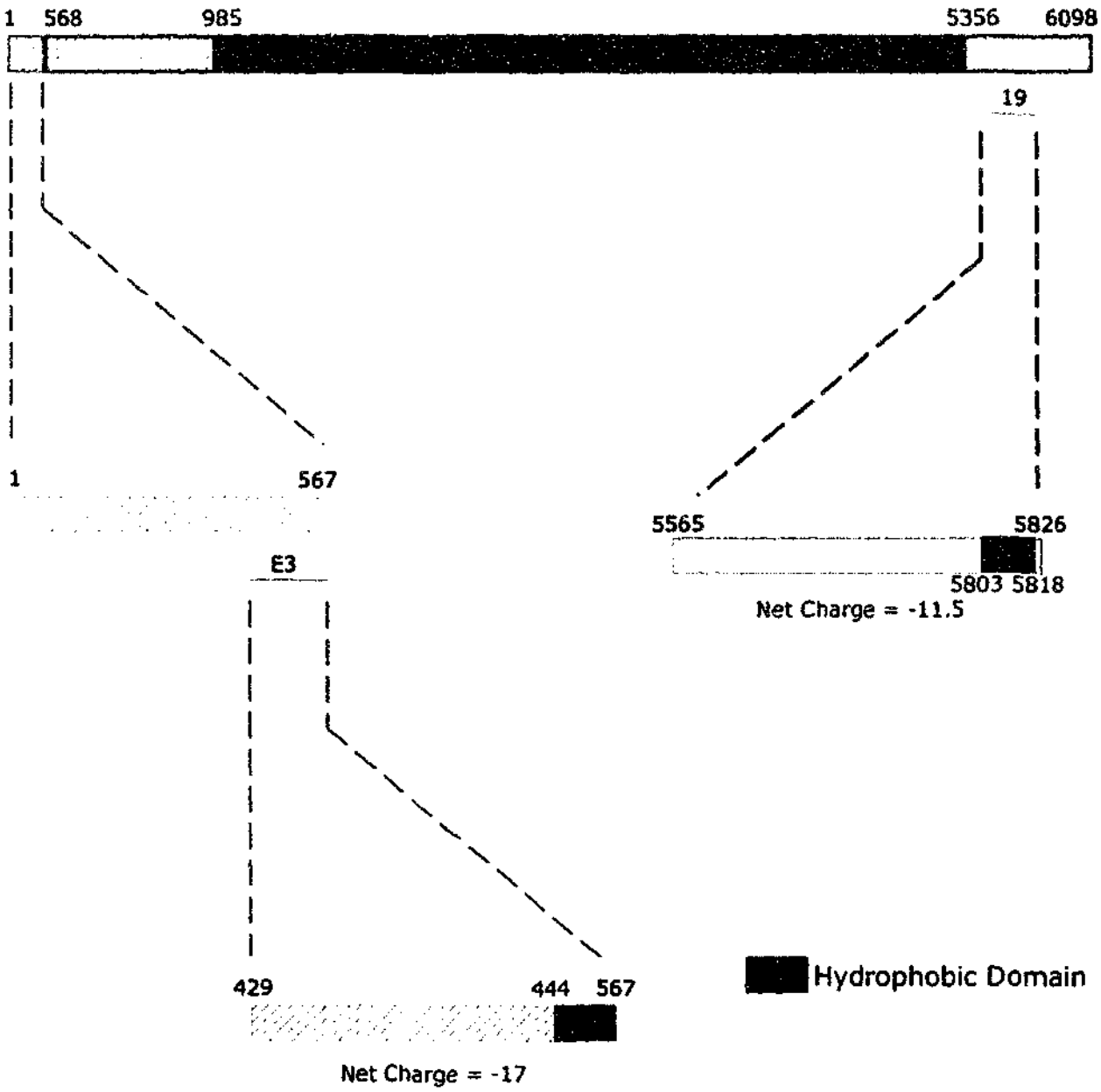

Figure 5.12. Schematic of the Pf332 Binding Fragments E3 and 19.
The overall charge at the pH of the infected erythrocyte and the hydrophobic regions are indicated. The numbers above the protein fragments represent the amino acids.

Chapter 6 – General Discussion

The results presented in this thesis describe novel interactions between the malaria proteins PfEMP3 and Pf332 and the erythrocyte membrane skeleton. Interactions involving these two malaria proteins have not been studied before now and provide useful insights into the structural changes that occur at the membrane skeleton in parasitised erythrocytes.

We have described an interaction between spectrin and a 14 residue binding domain within the N-terminal region of PfEMP3. The affinity of this interaction, as measured by resonant mirror detection, is considered a strong interaction when compared to other protein-protein interactions, both in normal and parasitised erythrocytes. We have also identified binding domains within the N-terminus of β-spectrin and the spectrin repeats within both α- and β-spectrin for PfEMP3 using a solid phase microtitre plate assay. These interactions could not be confirmed using competitive binding assays or GST pull down assays, however, resonant mirror detection confirmed multiple binding domains within spectrin for PfEMP3.

In addition to the PfEMP3-spectrin interaction, we identified a moderate affinity interaction between the 14 residue PfEMP3 binding domain and F-actin, indicating a complex set of interactions between PfEMP3 and the erythrocyte membrane skeleton. The complexitiy of the interaction of PfEMP3 is supported by the possibility of an additional interaction of the C-terminus of PfEMP3 with an as yet, unidentified erythrocyte membrane protein. This interaction was observed using IOVs, but not with either spectrin or actin. In addition, the interaction of PfEMP3 with pIOVs was consistently more intense than that with IOVs when viewed on immunoblots, indicating that PfEMP3 may interact with additional or modified proteins present only in pIOVs.

The interaction of Pf332 with the membrane skeleton also appears to be highly complex, possibly involving an erythrocyte membrane protein, which has been previously modified by the parasite. Pf332 showed low intensity interactions with both IOVs and spectrin. These interactions were substantially more intense when pIOVs were used in place of IOVs. This suggests that infection of the erythrocyte with malaria parasites results in modification of the erythrocyte membrane skeleton that enhances binding of Pf332. Unfortunately, since immunoblot analysis revealed that exported parasite proteins and other parasite parasite proteins such as HSP70 were present in these pIOVs preparations, we can not rule out the possibility that Pf332 may be binding to parasite proteins still resident within these preparations.

6.1 Characteristics of Binding Domains

The binding domains identified in this study have a number of notable features. The 14 residue binding domain of PfEMP3 is positively charged at the pH of the infected erythrocyte, whereas the two binding domains of Pf332 are negatively charged at the same pH. This indicates that the PfEMP3 and Pf332 binding domains may be involved n electrostatic interactions with proteins of opposing charge. Interacting domains with opposing charge have been reported previously for the interaction of KAHRP-PfEMP1 (Waller *et al.*, 1999). Additionally, the binding domains within Pf332 encompass the only two relatively hydrophobic regions within the protein, indicating a possible contribution of hydrophobic interactions with proteins at the erythrocyte membrane skeleton.

It is also interesting to note the position of the binding domains within the proteins and in particular, their position relative to the repeat structures of these proteins. The PfEMP3 14 residue binding domain encompasses a region commencing at residue 16 of the second exon. This region begins 52 residues from the N-terminus of PfEMP3 and is within a non-repetitive domain. The binding domains of Pf332 are also a relatively short distance from end of the protein. Pf332 fragment 3 starts 429 residues from the N-terminus of Pf332 and fragment 19 finishes 270 residues from the C-terminus of Pf332. Both of these binding domains are outside of the large degenerate repeat region encoded by the second exon of Pf332. In previous studies, binding domains within malaria proteins that are exported to the erythrocyte membrane have been identified in defined regions throughout the entire length of the protein. For example, within KAHRP, binding domains have been identified within fragments encompassing each of the repeat regions (Waller *et al.*, 1999). These repeat regions begin 61 residues, 366 residues and 543 residues from the N-terminus of the 657 residue protein, with the third repeat region finishing at residue 612. Therefore, it can be seen that the binding domains are spread throughout the protein. For RESA, the spectrin binding domain is found within a non repetitive region just C-terminal to the middle of the protein (Foley *et al.*, 1994). MESA contains a binding region that is locationally similar to binding domains identified within PfEMP3 and Pf332. The MESA-protein 4.1 binding domain is located 79 residues from the N-terminus of MESA and is not contained within one of the numerous repetitive regions found within MESA (Bennett *et al.*, 1997). In addition, it has been proposed that binding domains for MESA to protein 4.1 and of MSP1 to spectrin may form amphipathic α-helical structures, whereas the binding domain for RESA to spectrin does not (Bennett *et al.*, 1997). Our analysis indicates that the 14 residue binding domain of PfEMP3 does not form an

amphipathic α-helical structure and although the Pf332 binding domains show regions of poccible helical structure (Robert Flegg, VBC, personal communication), until the precise binding residues are mapped, we can not speculate on the possible formation of amphipathic α-helical structures.

These data indicate that binding domains within malaria proteins are difficult to predict based on location within the protein, repetitiveness, charge, hydrophobicity or proposed structure. Therefore, it is likely that screening methods, such as that used in this study, will be required for the future identification of binding domains within malarial proteins.

6.2 Further Studies

Throughout this and previous studies in this laboratory, we have established a number of interaction assay methodologies. We have used the solid phase microtitre plate assay most extensively, however, as outlined in this thesis we have also used GST pull down assays, F-actin high speed centrifugation assays and competitive binding assays. In addition, we have used yeast two hybrid systems (Waller, 2000) and quantitative resonant mirror detection. There are many alternative methods and approaches that may be used to define binding domains within malarial proteins. These alternate interaction methodologies include the use of immunoprecipitation, as mentioned in Chapter 5 and established interaction methodologies such as phage display (Li *et al.*, 2002). Systems such as the surface plasmon resonance of BiaCore may also provide an alternate method of obtaining kinetics data for quantifying interactions of malarial proteins. In the past, we have found that using a number of methodologies for identification and measurement of interactions has allowed us to construct a body of evidence supporting the existence of a particular interaction involving a malaria protein. This evidence, along with the common location of the interacting proteins, has allowed us to identify proteins that not only interact *in vitro*, but are also likely to exert a physiological consequence *in vivo*.

There are a number of ways to further investigate these physiological consequences, including targeted gene knockout technologies and the use of synthetic peptides block putative interactions. The development of transfection and knockout technologies over the last few years has allowed us to create parasite lines that are genetically altered in a specific manner. To date, PfEMP3 has been both truncated and knocked out (Waterkeyn *et al.*, 2000), however, to our knowledge no Pf332 knockout exists. A truncated Pf332 line has been produced within this laboratory (F. Glenister, unpublished results) and it would be of use to create a Pf332 knockout line to use in conjunction with this parasite line. Allelic

exchange, resulting in the removal of specific binding domains from the expressed protein would also be useful in defining the consequences of the identified interactions of PfEMP3, Pf332 and other exported proteins. To date, there have been no reports using this approach to investigate the consequences of protein-protein interactions in infected erythrocytes. Addition of synthetic peptides to infected erythrocytes has recently been described (Dhawan *et al.*, 2003). This allows us to investigate the consequences of protein-protein interactions by the addition of synthetic peptides encoding known binding domains to the parasitised erythrocyte. Subsequent interference of protein-protein interactions and resulting altered pathogenicity, perhaps through reduction of cytoadherence, is a exciting prospect for the development of novel therapeutic drugs.

This study has also identified pIOVs as a possible tool in identifying erythrocyte binding partners. IOVs have long been used to identify binding of malarial proteins to the erythrocyte membrane skeleton. Alterations to IOV purification protocols have resulted in the ability to strip IOVs of particular proteins and to identify possible binding partners or confirm the binding partners within the erythrocyte membrane skeleton. Here we have used the standard IOV purification method to make IOVs from parasitised erythrocytes (pIOVs). These pIOVs contain erythrocyte membrane proteins, which may have been altered by the parasite and proteins of parasite origin. The number of proteins within these preparations and their diversity of origin make it difficult to use pIOVs to identify binding partners. However, alterations to the pIOV purification protocol may enable us to deplete these preparations of proteins of a particular origin. Moreover, alternate methods for lysis of the parasitised erythrocytes may separate the parasite from the modified erythrocyte membrane. These alterations to the pIOV preparations would result in a useful tool for the identification of binding partners for malaria proteins that do not bind or that bind IOVs poorly, as seen for Pf332 in this study.

In addition to the use of alternate protein-protein interaction methodologies, further studies should delineate the overall contribution of these interactions to the infected erythrocyte. For instance, it is important to understand the contribution of PfEMP3 and Pf332 interactions to the normal interactions at the erythrocyte membrane skeleton. We have shown that PfEMP3 interacts with spectrin, possibly within regions that overlap with known binding domains for actin, protein 4.1 and ankyrin, and the domains responsible for self association and nucleation. It is therefore important to establish the interactions between spectrin and its known binding partners in the presence of PfEMP3. It is relevant to not only explore these interactions, but also to investigate the possible interference of normal erythrocyte protein-protein interactions by the interaction of PfEMP3 with spectrin. This is

particularly interesting for the spectrin-protein 4.1-actin interaction, which is considered to be central to the formation of the junctional complex and the overall flexibility of the erythrocyte membrane skeleton.

Future directions also include solving the crystal structures for these interacting proteins. Initially, it would be interesting to look at the binary interaction of spectrin and PfEMP3, but it would also be important to establish a crystal structure that included a number of the spectrin binding partners. These crystal structures are essential in understanding the overall structure of the infected erythrocyte membrane skeleton and the changes that occur due to exported malaria proteins.

Whilst keeping in mind our long term aims to establish a model of how the erythrocyte membrane skeleton is altered in parasitised erythrocytes, it is important to begin to map the binding domain of the many other exported malaria proteins. The availability of the genome and new techniques to study malaria parasites, allows us to understand the complex interactions that are required to not only form the parasitised erythrocyte membrane, but also to perturb erythrocyte membrane mechanical and adhesive properties.

Appendices

Appendix 1
Bacterial Strains

Strain	Description	Source/Reference
DH5α	F^- Φ80dlacZΔM15 Δ(lacZYA-argF)U169 deoR recA1 endA1 hsdR17(r_k^-, m_k^+) phoA supE44 λ^- thi-1 gyrA96 relA1	Life Technologies
BL21(DE3)	E. coli B F^- dcm ompT hsdS)(r_B^- m_B^-) gal λ(DE3)	Statagene, La Jolla, CA, USA
DB3.1	F^- gyrA462 $endA^-$ Δ(sr1-recA) mcrB mrr hsds20(r_B^-, m_B^-) supE44 ara14 galK2 lacY1 proA2 rpsL20(Sm^r) xyl5 λ^-leu mtl1	Life Technologies
RCM1347	DB3.1(pDONR201)	This Study
RCM61	DH5α (pMAL-c2)	This Study
RCM1241	BL21(DE3) (pMAL-c2)	This Study
RCM948	DH5α (pMC629)	J. Bettadapura, Unpublished
RCM1316	DH5α (pMC910)	This Study
RCM1148	DH5α (pMC793)	J. Bettadapura, Unpublished
RCM1342	DB3.1(pMC925)	This Study
RCM1088	DH5α (pMC754)	V. Gatzigiannis, Unpublished
RCM1089	BL21(DE3) (pMC754)	V. Gatzigiannis, Unpublished
RCM1155	DH5α (pMC798)	J. Bettadapura, Unpublished
RCM1157	BL21(DE3) (pMC798)	J. Bettadapura, Unpublished
RCM1220	DH5α (pMC839)	This Study
RCM1221	DH5α (pMC840)	This Study
RCM1222	BL21(DE3) (pMC840)	This Study
RCM1223	DH5α (pMC841)	This Study
RCM1224	DH5α (pMC842)	This Study
RCM1225	BL21(DE3) (pMC842)	This Study
RCM1226	DH5α (pMC843)	This Study
RCM1227	DH5α (pMC844)	This Study
RCM1228	BL21(DE3) (pMC844)	This Study
RCM1229	DH5α (pMC845)	This Study
RCM1230	DH5α (pMC846)	This Study
RCM1231	BL21(DE3) (pMC846)	This Study
RCM1156	DH5α (pMC799)	J. Bettadapura, Unpublished
RCM1158	BL21(DE3) (pMC799)	J. Bettadapura, Unpublished
RCM1090	DH5α (pMC755)	V. Gatzigiannis, Unpublished
RCM1091	BL21(DE3) (pMC755)	V. Gatzigiannis, Unpublished
RCM1092	DH5α (pMC756)	V. Gatzigiannis, Unpublished
RCM1093	BL21(DE3) (pMC756)	V. Gatzigiannis, Unpublished
RCM1094	DH5α (pMC757)	V. Gatzigiannis, Unpublished
RCM1095	BL21(DE3) (pMC757)	V. Gatzigiannis, Unpublished
RCM1096	DH5α (pMC758)	V. Gatzigiannis, Unpublished
RCM1097	BL21(DE3) (pMC758)	V. Gatzigiannis, Unpublished
RCM1300	DH5α (pMC902)	This Study
RCM1301	DH5α (pMC903)	This Study
RCM1302	BL21(DE3) (pMC903)	This Study
RCM1353	DH5α (pMC932)	This Study
RCM1362	DH5α (pMC941)	This Study
RCM1382	BL21(DE3) (pMC941)	This Study
RCM1354	DH5α (pMC933)	This Study
RCM1363	DH5α (pMC942)	This Study
RCM1385	BL21(DE3) (pMC942)	This Study
RCM1355	DH5α (pMC934)	This Study

Strain	Description	Source/Reference
RCM1364	DH5α (pMC943)	This Study
RCM1388	BL21(DE3) (pMC943)	This Study
RCM1456	DH5α (pMC990)	This Study
RCM1457	BL21(DE3) (pMC990)	This Study
RCM1482	DH5α (pMC1009)	This Study
RCM1483	BL21(DE3) (pMC1009)	This Study
RCM1484	DH5α (pMC1010)	This Study
RCM1485	BL21(DE3) (pMC1010)	This Study
RCM1486	DH5α (pMC1011)	This Study
RCM1487	BL21(DE3) (pMC1011)	This Study
RCM1719	DH5α (pMC1189)	This Study
RCM1721	DH5α (pMC1191)	This Study
RCM1722	DH5α (pMC1192)	This Study
RCM1422	DH5α (pMC970)	This Study
RCM1533	DH5α (pMC1052)	This Study
RCM1534	BL21(DE3) (pMC1052)	This Study
RCM1535	DH5α (pMC1053)	This Study
RCM1536	BL21(DE3) (pMC1053)	This Study
RCM1423	DH5α (pMC971)	This Study
RCM1537	DH5α (pMC1054)	This Study
RCM1538	BL21(DE3) (pMC1054)	This Study
RCM1539	DH5α (pMC1055)	This Study
RCM1540	BL21(DE3) (pMC1055)	This Study
RCM1424	DH5α (pMC972)	This Study
RCM1541	DH5α (pMC1056)	This Study
RCM1542	BL21(DE3) (pMC1056)	This Study
RCM1543	DH5α (pMC1057)	This Study
RCM1544	BL21(DE3) (pMC1057)	This Study
RCM1545	DH5α (pMC1058)	This Study
RCM1546	BL21(DE3) (pMC1058)	This Study
RCM1425	DH5α (pMC973)	This Study
RCM1547	DH5α (pMC1059)	This Study
RCM1548	BL21(DE3) (pMC1059)	This Study
RCM1426	DH5α (pMC974)	This Study
RCM1549	DH5α (pMC1060)	This Study
RCM1550	BL21(DE3) (pMC1060)	This Study
RCM1427	DH5α (pMC975)	This Study
RCM1551	DH5α (pMC1061)	This Study
RCM1552	BL21(DE3) (pMC1061)	This Study
RCM1553	DH5α (pMC1062)	This Study
RCM1554	BL21(DE3) (pMC1062)	This Study
RCM1428	DH5α (pMC976)	This Study
RCM1555	DH5α (pMC1063)	This Study
RCM1556	BL21(DE3) (pMC1063)	This Study
RCM1557	DH5α (pMC1064)	This Study
RCM1558	BL21(DE3) (pMC1064)	This Study
RCM1559	DH5α (pMC1065)	This Study
RCM1560	BL21(DE3) (pMC1065)	This Study
RCM1561	DH5α (pMC1066)	This Study
RCM1562	DH5α (pMC1067)	This Study
RCM1563	BL21(DE3) (pMC1067)	This Study
RCM1534	DH5α (pMC1068)	This Study
RCM1565	BL21(DE3) (pMC1068)	This Study
RCM1566	DH5α (pMC1069)	This Study
RCM1567	BL21(DE3) (pMC1069)	This Study
RCM1568	DH5α (pMC1070)	This Study
RCM1569	BL21(DE3) (pMC1070)	This Study
RCM1570	DH5α (pMC1071)	This Study

Strain	Description	Source/Reference
RCM1571	BL21(DE3) (pMC1071)	This Study
RCM1572	DH5α (pMC1072)	This Study
RCM1573	DH5α (pMC1073)	This Study
RCM1574	BL21(DE3) (pMC1073)	This Study
RCM1635	BL21(DE3) (βN-4)	This Study
RCM1636	BL21(DE3) (βN-2)	This Study
RCM1637	BL21(DE3) (βN)	This Study
RCM1639	BL21(DE3) (βN_2)	This Study
RCM1640	BL21(DE3) (β1-2)	This Study
RCM1774	BL21(DE3) (β5-9)	This Study
RCM1776	BL21(DE3) (β10-14)	This Study
RCM1778	BL21(DE3) (β15-C)	This Study
RCM1641	BL21(DE3) (α1-154)	This Study
RCM1780	BL21(DE3) (αN-5)	This Study
RCM1782	BL21(DE3) (α6-11)	This Study
RCM1784	BL21(DE3) (α12-16)	This Study
RCM1786	BL21(DE3) (α17-C)	This Study

Table A1. *E. coli* strains used in this Study

Appendix 2

Bacterial Plasmids

Plasmid	Description	Source/Reference
pUC18	Cloning Vector, 2.6kb, lacZ', ColE1 origin	(Yanisch-Perron *et al.*, 1985)
pMAL-c2	Expression Vector, Maltose-binding protein (MBP) C-terminal Tag, 6.6 kb, $lacI^q$, lacZα, M13 origin	(Ausubel *et al.*, 1994), New England Biolabs
pDONR201	Gateway vector, 4.5 kb, (Km, Cm)	Life Technologies
pMC629	pMAL-c2 with modified multiple cloning site with *Bam*HI in the first reading frame	J. Bettadapura, Unpublished
pMC910	pMAL-c2 vector with stop codon in multiple cloning site following the *Eco*RI site	This Study
pMC793	pMAL-c2 modified multiple cloning site with *Bam*HI in third reading frame	J. Bettadapura, Unpublished
pMC925	pMAL-c2 vector modified to gateway vector via ligation with cassette b, (Ap, Cm)	This Study
pMC754	PfEMP3 fragment FI amplified by PCR from 3D7 genomic DNA with p766 and p767. Cloned into *Bam*HI/*Eco*RI pMC629	V. Gatzigiannis, Unpublished Results
pMC798	PfEMP3 fragment FIa amplified by PCR from 3D7 genomic DNA with p768 and p769. Cloned into *Bgl*II/*Eco*RI pMC793	J. Bettadapura, Unpublished Results
pMC839	PfEMP3 fragment FIa.1 amplified by PCR from pMC789 with p766 and p994 and cloned into *Sma*I pUC18	This Study
pMC840	PfEMP3 fragment FIa.1 cut from pMC839 and transferred to *Bam*HI/*Eco*RI pMC629	This Study
pMC841	PfEMP3 fragment FIa.2 amplified by PCR from pMC789 with p995 and p996 and cloned into *Sma*I pUC18	This Study
pMC842	PfEMP3 fragment FIa.2 cut from pMC841 and transferred to *Bam*HI/*Eco*RI pMC629	This Study
pMC843	PfEMP3 fragment FIa.3 amplified by PCR from pMC789 with p997 and p998 and cloned into *Sma*I pUC18	This Study
pMC844	PfEMP3 fragment FIa.3 cut from pMC843 and transferred to *Bam*HI/*Eco*RI pMC629	This Study
pMC845	PfEMP3 fragment FIa.4 amplified by PCR from pMC789 with p999 and p942 and cloned into *Sma*I pUC18	This Study
pMC846	PfEMP3 fragment FIa.4 cut from pMC845 and transferred to *Bam*HI/*Eco*RI pMC629	This Study
pMC799	PfEMP3 fragment FIb amplified by PCR from 3D7 genomic DNA with p943 and p767. Cloned into *Bam*HI/*Eco*RI pMC793	J. Bettadapura, Unpublished
pMC624	PfEMP3 fragment FII amplified by PCR from 3D7 genomic DNA with p768 and p769. Cloned into *Bam*HI/*Eco*RI pGEX-4T-1	J. Bettadapura, Unpublished
pMC755	PfEMP3 fragment FII cut from pMC624 and cloned into *Bam*HI/*Eco*RI pMC629	V. Gatzigiannis, Unpublished
pMC616	PfEMP3 fragment FIII amplified by PCR from 3D7 genomic DNA with p776 and p773. Cloned into *Bam*HI/*Eco*RI pGEX-4T-1	J. Bettadapura, Unpublished
pMC756	PfEMP3 fragment FIII amplified by PCR from pMC616 with p350 and p350a. Cloned into *Bam*HI/*Sal*I pMAL-c2	V. Gatzigiannis, Unpublished

Plasmid	Description	Source/Reference
pMC751	PfEMP3 fragment FIV amplified by PCR from 3D7 genomic DNA with p774 and p775. Cloned into *Bam*HI/*Eco*RI pGEX-4T-1	J. Bettadapura, Unpublished
pMC757	PfEMP3 fragment FIV cut from pMC751 and cloned into *Bam*HI/*Eco*RI pMC629	V. Gatzigiannis, Unpublished
pMC617	PfEMP3 fragment FV amplified by PCR from 3D7 genomic DNA with p799 and p797. Cloned into *Bam*HI/*Eco*RI pGEX-4T-1	J. Bettadapura, Unpublished
pMC758	PfEMP3 fragment FV from pMC617 cloned into *Bam*HI/SalI pMAL-c2	V. Gatzigiannis, Unpublished
pMC902	PfEMP3 fragment F1a with F1a.1 deleted (F1aΔF1a.1) amplified by PCR from 3D7 gDNA with p995 and p942 cloned blunt end into *Sma*I pUC18	This Study
pMC903	PfEMP3 F1aΔF1a.1 from pMC902 cloned into *Eco*RI/*Bam*HI pMC629	This Study
pMC932	PfEMP3 deletion of 15 aa from N-terminal (F1aΔ15) amplified by PCR from pMC798 with *att*B oligonucleotides p1107 and p1110. Cloned via a BP reaction into pDONR201 (pENTR201-F1aΔ15) (Km)	This Study
pMC941	F1aΔ15 from pMC932 transferred by the 'one tube protocol' into pMC1342 via the LR reaction (pEXPMAL-FIaΔ15)	This Study
pMC933	PfEMP3 deletion of 29 aa from N-terminal (F1aΔ29) amplified by PCR from pMC798 with *att*B oligonucleotides p1108 and p1110. Cloned via a BP reaction into pDONR201 (pENTR201-F1aΔ29) (Km)	This Study
pMC942	FIaΔ29 from pMC933 transferred by the 'one tube protocol' into pMC1342 via the LR reaction (pEXPMAL-FIaΔ29)	This Study
pMC934	PfEMP3 deletion of 45 aa from the N-terminal (F1aΔ45) amplified by PCR from pMC798 with *att*B oligonucleotides p1109 and p1110. Cloned via a BP reaction into pDONR201 (pENTR201-F1aΔ45) (Km)	This Study
pMC943	FIaΔ45 from pMC934 transferred by the 'one tube protocol' into pMC1342 via the LR reaction (pEXPMAL-FIaΔ45).	This Study
pMC990	PfEMP3 second exon residues 16-29 created by annealing of p1211 and p1212. Cloned into *Eco*RI/*Bam*HI pMAL-c2	This Study
pMC1009	PfEMP3 second exon residues 16-45 PCR amplified from pMC798 with p1236 and p1237 cloned into *Eco*RI/*Hin*dIII pMAL-c2	This Study
pMC1010	PfEMP3 second exon residues 16-60 PCR amplified from pMC798 with p1236 and p1238 cloned into *Eco*RI/*Hin*dIII pMAL-c2	This Study
pMC1011	PfEMP3 second exon residues 1-16 PCR amplified from pMC798 with p1245 and p1246 cloned into *Eco*RI/*Hin*dIII pMAL-c2	This Study
pMC1189	Pf332 Exon1 Fragment 1 amplified by PCR from 3D7 genomic DNA with p1353 and p1354 and cloned into *Bam*HI/*Xho*I pMC629	This Study
pMC1191	Pf332 Exon1 Fragment 2 amplified by PCR from 3D7 genomic DNA with p1354 and p1438 and cloned into *Bam*HI/*Xho*I pMC629	This Study
pMC1192	Pf332 Exon1 Fragment 3 amplified by PCR from 3D7 genomic DNA with p1439 and p1365 and cloned into *Bam*HI/*Xho*I pMC629	This Study

Plasmid	Description	Source/Reference
pMC970	Pf332 Fragment 1 amplified by PCR with *att*B oligonucleotides p1159 and p1180 from 3D7 genomic DNA. Cloned via a BP reaction into pDONR201 (pENTR201-Pf332-frag1) (Km)	This Study
pMC1052	Pf332 Fragment 1 from pMC970 cloned into *Eco*RI pMC910	This Study
pMC1053	Pf332 Fragment 2 amplified by PCR with p1160 and p1181 and cloned into *Eco*RI pMC910	This Study
pMC971	Pf332 Fragment 3 amplified by PCR with *att*B oligonucleotides p1161 and p1182 from 3D7 genomic DNA. Cloned via a BP reaction into pDONR201 (pENTR201-Pf332-Frag3) (Km)	This Study
pMC1054	Pf332 Fragment 3 from pMC971 cloned into *Eco*RI pMC910	This Study
pMC1055	Pf332 Fragment 4 amplified by PCR with p1162 and p1183 and cloned into *Eco*RI pMC910	This Study
pMC972	Pf332 Fragment 5 amplified by PCR with *att*B oligonucleotides p1163 and p1184 from 3D7 genomic DNA. Cloned via a BP reaction into pDONR201 (pENTR201-Pf332-Frag5) (Km)	This Study
pMC1056	Pf332 Fragment 5 from pMC972 cloned into *Eco*RI pMC910	This Study
pMC1057	Pf332 Fragment 6 amplified by PCR from 3D7 genomic DNA with p1164 and p1185. Cloned into *Eco*RI pMC910	This Study
pMC1058	Pf332 Fragment 7 amplified by PCR from 3D7 genomic DNA with p1165 and p1186. Cloned into *Eco*RI pMC910	This Study
pMC973	Pf332 Fragment 8 amplified by PCR with *att*B oligonucleotides p1166 and p1187 from 3D7 genomic DNA. Cloned via a BP reaction into pDONR201 (pENTR201-Pf332-Frag8) (Km)	This Study
pMC1059	Pf332 Fragment 8 from pMC973 cloned into *Eco*RI pMC910	This Study
pMC974	Pf332 Fragment 9 amplified by PCR with *att*B oligonucleotides p1167 and p1188 from 3D7 genomic DNA. Cloned via a BP reaction into pDONR201 (pENTR201-Pf332-Frag9) (Km)	This Study
pMC1060	Pf332 Fragment 9 from pMC974 cloned into *Eco*RI pMC910	This Study
pMC975	Pf332 Fragment 10 amplified by PCR with *att*B oligonucleotides p1168 and p1189 from 3D7 genomic DNA. Cloned via a BP reaction into pDONR201 (pENTR201-Pf332-Frag10) (Km)	This Study
pMC1061	Pf332 Fragment 10 from pMC975 cloned into *Eco*RI pMC910	This Study
pMC1062	Pf332 Fragment 11 amplified by PCR from 3D7 genomic DNA with p1169 and p1190. Cloned into *Eco*RI pMC910	This Study
pMC976	Pf332 Fragment 12 amplified by PCR with *att*B oligonucleotides p1170 and p1191 from 3D7 genomic DNA. Cloned via BP reaction into pDONR201 (pENTR201-Pf332-Frag12) (Km)	This Study
pMC1063	Pf332 Fragment 12 from pMC976 cloned into *Eco*RI pMC910	This Study

Plasmid	Description	Source/Reference
pMC1064	Pf332 Fragment 13 amplified by PCR from 3D7 genomic DNA with p1171 and p1192. Cloned into *Eco*RI pMC910	This Study
pMC1065	Pf332 Fragment 14 amplified by PCR from 3D7 genomic DNA with p1172 and p1193. Cloned into *Eco*RI pMC910	This Study
pMC1066	Pf332 Fragment 15 amplified by PCR from 3D7 genomic DNA with p1173 and p1194. Cloned into *Sma*1 pUC18	This Study
pMC1067	Pf332 Fragment 15 from pMC1066 cloned into *Eco*RI pMC910	This Study
pMC1068	Pf332 Fragment 16 amplified by PCR from 3D7 genomic DNA with p1174 and p1195 Cloned into *Eco*RI pMC910	This Study
pMC1069	Pf332Fragment 17 amplified by PCR from 3D7 genomic DNA with p1175 and p1196. Cloned into *Eco*RI pMC910	This Study
pMC1070	Pf332 Fragment 18 amplified by PCR from 3D7 genomic DNA with p1176 and p1197. Cloned into *Eco*RI pMC910	This Study
pMC1071	Pf332 Fragment 19 amplified by PCR from 3D7 genomic DNA with p1177 and p1198. Cloned into *Eco*RI pMC910	This Study
pMC1072	Pf332 Fragment 20 amplified by PCR from 3D7 genomic DNA with p1178 and p1199. Cloned into *Sma*1 pUC18	This Study
pMC1073	Pf332 Fragment 20 from pMC1072 cloned into *Eco*RI pMC910	This Study
βN-4	β-spectrin N-terminal plus repeats 1-4 cloned *Bam*HI/*Eco*RI into pGEX-3X	X. An, New York Blood Center
βN-2	β-spectrin N-terminal plus repeats 1 and 2 (residues 1-527) cloned *Bam*HI/*Eco*RI into pGEX-3X	X. An, New York Blood Center
βN	β-spectrin N-terminal (residues 1-301) cloned *Bam*HI/*Eco*RI into pGEX-3X	X. An, New York Blood Center
$\beta_{191\text{-}301}$	β-spectrin residues 191-301 cloned *Bam*HI/*Eco*RI into pGEX-3X	X. An, New York Blood Center
β1-2	β-spectrin repeats 1 and 2 cloned *Bam*HI/*Eco*RI into pGEX-3X	X. An, New York Blood Center
β5-9	β-spectrin repeats 5-9 cloned *Eco*RI/*Not*I into pGEX-4T-2	X. An, New York Blood Center
β10-14	β-spectrin repeats 10-14 cloned *Bam*HI/*Eco*RI into pGEX-3X	X. An, New York Blood Center
β15-C	β-spectrin repeats 15-17 plus C-terminal cloned *Bam*HI/*Eco*RI into pGEX-3X	X. An, New York Blood Center
$\alpha_{1\text{-}154}$	α-spectrin residues 1-154 cloned *Bam*HI/*Eco*RI into pGEX-3X	X. An, New York Blood Center
αN-5	α-spectrin N-terminal plus repeats 1-5 cloned into *Sma*I/*Not*I pGEX-4T-2	X. An, New York Blood Center
α6-11	α-spectrin repeats 6-11 cloned into *Sma*I/*Not*I pGEX-4T-2	X. An, New York Blood Center
α12-16	α-spectrin repeats 12-16 cloned into *Sma*I/*Not*I pGEX-4T-2	X. An, New York Blood Center
α17-C	α-spectrin repeats 17-22 plus C-terminal cloned into *Sma*I/*Not*I pGEX-4T-2	X. An, New York Blood Center

Table A2. Bacterial Plasmids used in this Study
All plasmids confer Ampicillin resistance unless otherwise stated to confer Kanamycin (Km) or Chloramphenicol (Cm) resistance.

Appendix 3
Oligonucleotide Primers

Oligonucleotide	Nucteotide sequence (5' → 3')	Use
p823	GGT CGT CAG ACT GTC GAT GAA GCC	Forward sequencing oligonucleotide for pMAL vectors
p1047	GGT GCG GGC CTC TTC GCT ATT ACG	Reverse sequencing oligonucleotide for pMAL vectors
p804	ATT TCA GGA TCC GAG CTC GAG ATC TGG TAC CAT GGA ATT CGA	Forward oligonucleotide for the modification of pMAL-c2 to pMC629
p824	AGC TTC GAA TCC CAT GGT ACC AGA TCT CGA GCT CGG ATC CTG AAA T	Reverse oligonucleotide for the modification of pMAL-c2 to pMC629
p766	ccg aga tct TTT ACG GTT GTT AAG AAT	Forward oligonucleotide for amplification of PfEMP3 fragments FI, FIa and FIa.1
p767	cga gaa ttc tta TGG TTC ATG TTC TAA T	Reverse oligonucleotide for amplification of PfEMP3 fragments FI and FIb
p768	cgc gga tcc CCA ACC AAA TTA CCT GAA	Forward oligonucleotide for amplification of PfEMP3 fragment FII
p769	cga gaa ttc tta TCT AGA TTT TCG CGT GC	Reverse oligonucleotide for amplification of PfEMP3 fragment FII
p776	cga gga ttc TCT GAT GGA TTAAAA GAA	Forward oligonucleotide for amplification of PfEMP3 fragment FIII
p773	cgc gaa ttc tta CAT GTT TCC TAT ACT T	Reverse oligonucleotide for amplification of PfEMP3 fragment FIII
p774	cga gga tcc ATA GGA AAC ATG GAA CAA	Forward oligonucleotide for amplification of PfEMP3 fragment FIV
p775	ccg gaa ttc tta TCC TTC ATT AGG TGT AT	Reverse oligonucleotide for amplification of PfEMP3 fragment FIV
p799	cga gga tcc GAT TTA AAG AAT AAA GCT A	Forward oligonucleotide for amplification of PfEMP3 fragment FV
p797	cgc gaa ttc tta ATT TTT TTT TCC TCT CAA	Reverse oligonucleotide for amplification of PfEMP3 fragment FV
p942	ccg gaa ttc tta TAG TTC ATT TAT AGC AC	Reverse oligonucleotide for amplification of PfEMP3 fragments FIa, FIa.4 and FIaΔFIa.1
p943	caa tgg atc cAA TGA ACT AAA AGA AAG G	Forward oligonucleotide for amplification of PfEMP3 fragments FIb
p994	ccg gaa ttc tta CTC TTT TCT TTT ATG ATC CCT G	Reverse oligonucleotide for amplification of PfEMP3 fragment FIa.1
p995	cgc gga ttc GCT TTA AAA CAG AAA ACT	Forward oligonucleotide for amplification of PfEMP3 fragments FIa.2 and FIaΔFIa.1
p996	ccg gaa ttc tta CTT TAA TGC TTC TCC ATT ATT TA	Reverse oligonucleotide for amplification of PfEMP3 fragment FIa.2
p997	cgc gga tcc GAA AAA GAA AAT AAA GAA ACA	Forward oligonucleotide for amplification of PfEMP3 fragment FIa.3
p998	ccg gaa ttc tta TTT CAA ATC CTT TTC TAC	Reverse oligonucleotide for amplification of PfEMP3 fragment FIa.3
p999	cgc gga tcc GAA ATG GAA TTG AAA GAG AAG	Forward oligonucleotide for amplification of PfEMP3 fragment FIa.4

Oligonucleotide	Nucteotide sequence (5' → 3')	Use
p1110	ggg gac cac ttt gta caa gaa agc tgg gtc TAG TTC ATT TAT AGC AC	Reverse oligonucleotide for amplification of PfEMP3 fragments FIaΔ15, FIaΔ29 and FIaΔ45
p1107	gggg aca agt ttg tac aaa aaa gca ggc tta ATA TTT GAA ATA AGA CTT AAA AG	Forward oligonucleotide for amplification of PfEMP3 fragment FIaΔ15
p1108	gggg aca agt ttg tac aaa aaa gca ggc tta GGG AAT ACA AGG TTA AGC	Forward oligonucleotide for amplification of PfEMP3 fragment FIaΔ29
p1109	gggg aca agt ttg tac aaa aaa gca ggc tta GAG GCA TTA AAA GAA AAG C	Forward oligonucleotide for amplification of PfEMP3 fragment FIaΔ45
p1236	ccg gaa ttc ATA TTT GAA ATA AGA CTT AAA AG	Forward oligonucleotide for amplification of PfEMP3 fragments 16-45 and 16-60
p1237	ccc aag ctt tta CTT AGT TCT AGG ATC CCT TAC	Reverse oligonucleotide for amplification of PfEMP3 fragment 16-45
p1238	ccc aag ctt tta CTC TTT TCT TTT ATG ATC CCT G	Reverse oligonucleotide for amplification of PfEMP3 fragment 16-60
p1212	aa ttc ATA TTT GAA ATA AGA CTT AAA AGA TCA TTA GCC CAG GTT TTG taa g	Forward oligonucleotide for construction of PfEMP3 fragment 16-29
p1211	ga tcc tta CAA AAC CTG GGC TAA TGA TCT TTT AAG TCT TAT TTC AAA TAT g	Reverse oligonucleotide for construction of PfEMP3 fragment 16-29
p1245	ccg gaa ttc TTT ACG GTT GTT AAG AAT	Forward oligonucleotide for amplification of PfEMP3 fragments 1-16
p1246	ccc aag ctt tta ATT ATA CAC ATT GAC A	Reverse oligonucleotide for amplification of PfEMP3 fragment 1-16
p1353	cgc gga tcc ATG TCT AAT ATA AAT AAC AAA	Forward oligonucleotide for amplification of Pf332 exon 1 fragment 1
p1354	ccg ctc gag tta ACT AAC AAT ACC ATC CTT ATC	Reverse oligonucleotide for amplification of Pf332 exon 1 fragment 1
p1365	cgc gga tcc GAA TCA TAT AAA GCT ACT AAA	Forward oligonucleotide for amplification of Pf332 exon 1 fragment 2
p1356	ccg ctc gag tta CTT ATA TAC CAA GAC CCA TAT AAT	Reverse oligonucleotide for amplification of Pf332 exon 1 fragment 3
p1438	ccg ctc gag tta TTC TTC ATA AGT AGG CTT AAT	Reverse oligonucleotide for amplification of Pf332 exon 1 fragment 2
p1439	cgc gga tcc AAT GAT GAA GAC AAA AGC AAG	Forward oligonucleotide for amplification of Pf332 exon 1 fragment 3

Oligonucleotide	Nucteotide sequence (5'→ 3')	Use
p1159	gggg aca agt ttg tac aaa aaa gca ggc tta gaa ttc CAT TCT TTG ATT GAT CGT GTT C	Forward oligonucleotide for amplification of Pf332 exon 2 fragment 1
p1160	gggg aca agt ttg tac aaa aaa gca ggc tta gaa ttc TTT AAA GGT CAA TTA ATT AAC GA	Forward oligonucleotide for amplification of Pf332 exon 2 fragment 2
p1161	gggg aca agt ttg tac aaa aaa gca ggc tta gaa ttc AAC GAT GAC GTT CGA GAC AAA	Forward oligonucleotide for amplification of Pf332 exon 2 fragment 3
p1162	gggg aca agt ttg tac aaa aaa gca ggc tta gaa ttc ATA GTA GAA GAT GAA GCA TCA GTC	Forward oligonucleotide for amplification of Pf332 exon 2 fragment 4
p1163	gggg aca agt ttg tac aaa aaa gca ggc tta gaa ttc AAA GAA GAA TTA ATT ACT GAA ATG	Forward oligonucleotide for amplification of Pf332 exon 2 fragment 5
p1164	gggg aca agt ttg tac aaa aaa gca ggc tta gaa ttc CCA TTA GAA GAA ACG AAA ATT G	Forward oligonucleotide for amplification of Pf332 exon 2 fragment 6
p1165	gggg aca agt ttg tac aaa aaa gca ggc tta gaa ttc GTT AAA GAT ATT GGA TGA GTT AG	Forward oligonucleotide for amplification of Pf332 exon 2 fragment 7
p1166	gggg aca agt ttg tac aaa aaa gca ggc tta gaa ttc ACA GAA GAA GCT GTA CAG TAT G	Forward oligonucleotide for amplification of Pf332 exon 2 fragment 8
p1167	gggg aca agt ttg tac aaa aaa gca ggc tta gaa ttc GGA GAA GGA TCG ATT ACG	Forward oligonucleotide for amplification of Pf332 exon 2 fragment 9
p1168	gggg aca agt ttg tac aaa aaa gca ggc tta gaa ttc GAA ATA GTG GAC GAA GTG TCT C	Forward oligonucleotide for amplification of Pf332 exon 2 fragment 10
p1169	gggg aca agt ttg tac aaa aaa gca ggc tta gaa ttc TCT GAA TCC GTT AAT GGG	Forward oligonucleotide for amplification of Pf332 exon 2 fragment 11
p1170	gggg aca agt ttg tac aaa aaa gca ggc tta gaa ttc AAA GAA ATA ATT GAC GAA AAA TCA C	Forward oligonucleotide for amplification of Pf332 exon 2 fragment 12
p1171	gggg aca agt ttg tac aaa aaa gca ggc tta gaa ttc AAT GTA TGG ATT GAG AAA GAA	Forward oligonucleotide for amplification of Pf332 exon 2 fragment 13
p1172	gggg aca agt ttg tac aaa aaa gca ggc tta gaa ttc CAG GAA GAA TCT CAT GTT GAA A	Forward oligonucleotide for amplification of Pf332 exon 2 fragment 14

Oligonucleotide	Nucteotide sequence (5' → 3')	Use
p1173	gggg aca agt ttg tac aaa aaa gca ggc tta gaa ttc AAA ATC GAA TCA ATT ACT GAA GAT	Forward oligonucleotide for amplification of Pf332 exon 2 fragment 15
p1174	gggg aca agt ttg tac aaa aaa gca ggc tta gaa ttc GAA ATA ATA CAA GGT GGA TAT T	Forward oligonucleotide for amplification of Pf332 exon 2 fragment 16
p1175	gggg aca agt ttg tac aaa aaa gca ggc tta gaa ttc GTA GAA GAA GGA TCA GAT ACG	Forward oligonucleotide for amplification of Pf332 exon 2 fragment 17
p1176	gggg aca agt ttg tac aaa aaa gca ggc tta gaa ttc GAT AAA GCC CTT AAT GAG	Forward oligonucleotide for amplification of Pf332 exon 2 fragment 18
p1177	gggg aca agt ttg tac aaa aaa gca ggc tta gaa ttc AAT GAT ACT GTA ATG GTT AT	Forward oligonucleotide for amplification of Pf332 exon 2 fragment 19
p1178	gggg aca agt ttg tac aaa aaa gca ggc tta gaa ttc AAA TAT GCT AAG AAA AGA TTT	Forward oligonucleotide for amplification of Pf332 exon 2 fragment 20
p1180	ggg gac cac ttt gta caa gaa agc tgg gtc gaa ttc AAT TAA TTG ACC TTT AAA TGT A	Reverse oligonucleotide for amplification of Pf332 exon 2 fragment 1
p1181	ggg gac cac ttt gta caa gaa agc tgg gtc gaa ttc ATT TTC TTT GTC TCG AAC GTC A	Reverse oligonucleotide for amplification of Pf332 exon 2 fragment 2
p1182	ggg gac cac ttt gta caa gaa agc tgg gtc gaa ttc TGC TCC TTC TTC TTC TAC AAC TTC C	Reverse oligonucleotide for amplification of Pf332 exon 2 fragment 3
p1183	ggg gac cac ttt gta caa gaa agc tgg gtc gaa ttc TTC ATT GTC TTC ATT AAT CAA ACC	Reverse oligonucleotide for amplification of Pf332 exon 2 fragment 4
p1184	ggg gac cac ttt gta caa gaa agc tgg gtc gaa ttc TGG AGT ATG TTC ATT AAT AAT ATC	Reverse oligonucleotide for amplification of Pf332 exon 2 fragment 5
p1185	ggg gac cac ttt gta caa gaa agc tgg gtc gaa ttc GCT AAC TGA TCC AAT ATC TTT	Reverse oligonucleotide for amplification of Pf332 exon 2 fragment 6
p1186	ggg gac cac ttt gta caa gaa agc tgg gtc gaa ttc TCC TTC ATA CTG TAC AGC	Reverse oligonucleotide for amplification of Pf332 exon 2 fragment 7
p1187	ggg gac cac ttt gta caa gaa agc tgg gtc gaa ttc CGT AAT CGA TCC TTC TCC A	Reverse oligonucleotide for amplification of Pf332 exon 2 fragment 8

Oligonucleotide	Nucteotide sequence (5'→ 3')	Use
p1188	ggg gac cac ttt gta caa gaa agc tgg gtc gaa ttc TAC GAC TTC TTC AGT TAC TGT TG	Reverse oligonucleotide for amplification of Pf332 exon 2 fragment 9
p1189	ggg gac cac ttt gta caa gaa agc tgg gtc gaa ttc TTC CCC ATT AAC GGA TTC AGA	Reverse oligonucleotide for amplification of Pf332 exon 2 fragment 10
p1190	ggg gac cac ttt gta caa gaa agc tgg gtc gaa ttc TAT TTT TTC AGT AAG TGA TTT TTC G	Reverse oligonucleotide for amplification of Pf332 exon 2 fragment 11
p1191	ggg gac cac ttt gta caa gaa agc tgg gtc gaa ttc TTT CTC AAT CCA TAC ATT TTC	Reverse oligonucleotide for amplification of Pf332 exon 2 fragment 12
p1192	ggg gac cac ttt gta caa gaa agc tgg gtc gaa ttc TGA TCC TTG TTG TAC AAC TTT	Reverse oligonucleotide for amplification of Pf332 exon 2 fragment 13
p1193	ggg gac cac ttt gta caa gaa agc tgg gtc gaa ttc AAT ATC TTC AGT AAT TGA TTC G	Reverse oligonucleotide for amplification of Pf332 exon 2 fragment 14
p1194	ggg gac cac ttt gta caa gaa agc tgg gtc gaa ttc AGT AAA AGA TCC ACC TTG TAT	Reverse oligonucleotide for amplification of Pf332 exon 2 fragment 15
p1195	ggg gac cac ttt gta caa gaa agc tgg gtc gaa ttc ATT AAA AGA CCC TTC TTC TAA	Reverse oligonucleotide for amplification of Pf332 exon 2 fragment 16
p1196	ggg gac cac ttt gta caa gaa agc tgg gtc gaa ttc CAT AAT TTT ATA ATT AAG GGC	Reverse oligonucleotide for amplification of Pf332 exon 2 fragment 17
p1197	ggg gac cac ttt gta caa gaa agc tgg gtc gaa ttc GTC ATT GGC AGA TTT ATT TG	Reverse oligonucleotide for amplification of Pf332 exon 2 fragment 18
p1198	ggg gac cac ttt gta caa gaa agc tgg gtc gaa ttc AAG TTC ATC GTA CTT AAA TTG	Reverse oligonucleotide for amplification of Pf332 exon 2 fragment 19
p1199	ggg gac cac ttt gta caa gaa agc tgg gtc gaa ttc GTT CTC ATT TAC ACT AAA TTC	Reverse oligonucleotide for amplification of Pf332 exon 2 fragment 20

Table A3. Oligonucleotide Primers used in this Study

Appendix 4
Antibodies and Antisera

Antibody / antiserum	Characteristics and uses	Dilution used	Source
Anti-rabbit Ig, Affinity Isolated, Raised in sheep, Conjugated to HRP	Secondary antibody for detection of rabbit antibodies used in immunoblot analysis	1/2000	Silenus, AMRAD, Melbourne, Australia
S43	Polyclonal anti-HSP70 antiserum Primary antiserum for detection of *P. falciparum* HSP70 protein	1/10000	The Walter and Eliza Hall Institute
S44	S25 R501 polyclonal rabbit anti-MESA antiserum Primary antiserum for detection of MESA protein	1/2000	The Walter and Eliza Hall Institute
S55	Polyclonal rabbit anti-spectrin antiserum Primary antiserum for detection of Spectrin protein	1/200	M. Foley, Department of Biochemistry, LaTrobe University
S56	Polyclonal rabbit anti-GST antiserum Primary antiserum for detection of GST fusion proteins	1/5000	R. Coppel, previously The Walter and Eliza Hall Institute
S901	R162 rabbit anti-Pf332 antiserum Primary antiserum for detection of Pf332 protein	1/300	K. Berzins, Department of Immunology, Stockholm University, Sweden
S904	Polyclonal rabbit anti protein 4.1 antiserum Primary antiserum for detection of protein 4.1 protein	1/200	N. Mohandas, Lawrence Berkeley National Laboratory, University of California, USA
S1302	Polyclonal rabbit anti-MBP antiserum Preabsorbed to *E. coli* lysate Primary antiserum for detection of MBP fusion proteins	1/1000	J. Bettadapura, Department of Microbiology, Monash University
S1339	Polyclonal rabbit anti-His-KAHRP antiserum Primary antiserum for detection of KAHRP protein	1/500	K. L. Waller, Department of Microbiology, Monash University
S4659	Monoclonal anti-PfEMP3 antiserum Primary antiserum for detection of PfEMP3 protein	1/200	The Walter and Eliza Hall Institute
6H1-1	Monoclonal anti-conserved PfEMP1 cytoplasmic domain antiserum Primary antiserum for detection of PfEMP1	1/100	The Walter and Eliza Hall Institute

Table A4. Antibodies and Antisera used in this Study

References

Ahlborg, N., Berzins, K. and Perlmann, P. (1991) Definition of the epitope recognised by the *Plasmodium falciparum*-reactive human monoclonal antibody 33G2. *Molecular and Biochemical Parasitology*, **46**, 89-95.

Ahlborg, N., Flyg, B.W., Iqbal, J., Perlmann, P. and Berzins, K. (1993) Epitope specificity and capacity to inhibit parasite growth *in vitro* of human antibodies to repeat sequences of the *Plasmodium falciparum* antigen Ag332. *Parasite Immunology*, **15**, 391-400.

Ahlborg, N., Iqbal, J., Bjork, L., Stahl, S., Perlmann, P. and Berzins, K. (1996) *Plasmodium falciparum*: differential parasite growth inhibition mediated by antibodies to the antigens Pf332 and Pf155/RESA. *Experimental Parasitology*, **82**, 155-163.

Allen, S.J., O'Donnell, A., Alexander, N.D., Mgone, C.S., Peto, T.E., Clegg, J.B., Alpers, M.P. and Weatherall, D.J. (1999) Prevention of cerebral malaria in children in Papua New Guinea by southeast Asian ovalocytosis band 3. *The American Journal of Tropical Medicine and Hygiene*, **60**, 1056-1060.

Alloisio, N., Dalla Venezia, N., Rana, A., Andrabi, K., Texier, P., Gilsanz, F., Cartron, J.P., Delaunay, J. and Chishti, A.H. (1993) Evidence that red blood cell protein p55 may participate in the skeleton-membrane linkage that involves protein 4.1 and glycophorin C. *Blood*, **82**, 1323-1327.

Altschul, S.F., Madden, T.L., Schaffer, A.A., Zhang, J., Zhang, Z., Miller, W. and Lipman, D.J. (1997) Gapped BLAST and PSI-BLAST: a new generation of protein database search programs. *Nucleic Acids Research*, **25**, 3389-3402.

al-Yaman, F., Genton, B., Mokela, D., Raiko, A., Kati, S., Rogerson, S., Reeder, J. and Alpers, M. (1995) Human cerebral malaria: lack of significant association between erythrocyte rosetting and disease severity. *Transactions of the Royal Society of Tropical Medicine & Hygiene*, **89**, 55-58.

An, X., Lecomte, M.C., Chasis, J.A., Mohandas, N. and Gratzer, W. (2002) Shear-response of the spectrin dimer-tetramer equilibrium in the red blood cell membrane. *The Journal of Biological Chemistry*, **277**, 31796-31800.

An, X.L., Takakuwa, Y., Nunomura, W., Manno, S. and Mohandas, N. (1996) Modulation of band 3-ankyrin interaction by protein 4.1. Functional implications in regulation of erythrocyte membrane mechanical properties. *The Journal of Biological Chemistry*, **271**, 33187-33191.

Anderson, R.A. and Lovrien, R.E. (1984) Glycophorin is linked by band 4.1 protein to the human erythrocyte membrane skeleton. *Nature*, **307**, 655-658.

Anderson, R.A. and Marchesi, V.T. (1985) Regulation of the association of membrane skeletal protein 4.1 with glycophorin by polyphosphoinositide. *Nature*, **318**, 295-298.

Ausubel, F.M., Brend, R., Kingston, R.E., Moore, D.D., Seidman, J.G., Smith, J.A. and Struhl, K. (1994) *Current Protocols in Molecular Biology*. Greene Publishing Associate and Willey Interscience, New York.

Azim, A.C., Knoll, J.H., Beggs, A.H. and Chishti, A.H. (1995) Isoform cloning, actin binding, and chromosomal localization of human erythroid dematin, a member of the villin superfamily. *The Journal of Biological Chemistry*, **270**, 17407-17413.

Banumathy, G., Singh, V. and Tatu, U. (2002) Host Chaperones are recruiter in membrane-bound complexes by *Plasmodium falciparum*. *The Journal of Biological Chemistry*, **277**, 3902-3912.

Barragan, A., Spillmann, D., Kremsner, P.G., Wahlgren, M. and Carlson, J. (1999) *Plasmodium falciparum*: molecular background to strain-specific rosette disruption by glycosaminoglycans and sulfated glycoconjugates. *Experimental Parasitology*, **91**, 133-143.

Barragan, A., Fernandez, V., Chen, Q., von Euler, A., Wahlgren, M. and Spillmann, D. (2000) The duffy-binding-like domain 1 of *Plasmodium falciparum* erythrocyte membrane protein 1 (PfEMP1) is a heparan sulfate ligand that requires 12 mers for binding. *Blood*, **95**, 3594-3599.

Baruch, D.I., Pasloske, B.L., Singh, H.B., Bi, X., Ma, X.C., Feldman, M., Taraschi, T.F. and Howard, R.J. (1995) Cloning the *P. falciparum* gene encoding PfEMP1, a malarial variant antigen and adherence receptor on the surface of parasitized human erythrocytes. *Cell*, **82**, 77-87.

Baruch, D.I., Gormely, J.A., Ma, C., Howard, R.J. and Pasloske, B.L. (1996) *Plasmodium falciparum* erythrocyte membrane protein 1 is a parasitized erythrocyte receptor for adherence to CD36, thrombospondin, and intercellular adhesion molecule 1. *Proceedings of the National Academy of Sciences USA*, **93**, 3497-3502.

Baruch, D.I., Ma, X.C., Singh, H.B., Bi, X., Pasloske, B.L. and Howard, R.J. (1997) Identification of a region of PfEMP1 that mediates adherence of *Plasmodium falciparum* infected erythrocytes to CD36: conserved function with variant sequence. *Blood*, **90**, 3766-3775.

Becker, P.S., Schwartz, M.A., Morrow, J.S. and Lux, S.E. (1990) Radiolabel-transfer cross-linking demonstrates that protein 4.1 binds to the N-terminal region of beta spectrin and to actin in binary interactions. *European Journal of Biochemistry*, **193**, 827-836.

Begg, G.E., Harper, S.L., Morris, M.B. and Speicher, D.W. (2000) Initiation of spectrin dimerization involves complementary electrostatic interactions between paired triple-helical bundles. *The Journal of Biological Chemistry*, **275**, 3279-3287.

Benedetti, C.E., Kobarg, J., Pertinhez, T.A., Gatti, R.M., de Souza, O.N., Spisni, A. and Meneghini, R. (2003) *Plasmodium falciparum* histidine-rich protein II binds to actin, phosphatidylinositol 4,5-bisphosphate and erythrocyte ghosts in a pH dependent manner and undergoes coil-to-helix transitions in anionic micelles. *Molecular and Biochemical Parasitology*, **128**, 157-166.

Bennett, B.J., Mohandas, N. and Coppel, R.L. (1997) Defining the Minimal Domain of the *Plasmodium falciparum* Protein MESA Involved in the Interaction with the Red Cell Membrane Skeletal Protein 4.1. *The Journal of Biological Chemistry*, **272**, 15299-15306.

Bennett, V. and Branton, D. (1977) Selective association of spectrin with the cytoplasmic surface of human erythrocyte plasma membranes. Quantitative determination with purified (32P)spectrin. *The Journal of Biological Chemistry*, **252**, 2753-2763.

Bennett, V. and Stenbuck, P.J. (1979) Identification and partial purification of ankyrin, the high affinity membrane attachment site for human erythrocyte spectrin. *The Journal of Biological Chemistry*, **254**, 2533-2541.

Bennett, V. and Stenbuck, P.J. (1980a) Association between ankyrin and the cytoplasmic domain of band 3 isolated from the human erythrocyte membrane. *The Journal of Biological Chemistry*, **255**, 6424-6432.

Bennett, V. and Stenbuck, P.J. (1980b) Human Erythrocyte Ankyrin. Purification and Properties. *The Journal of Biological Chemistry*, **255**, 2540-2548.

Bennett, V. (1985) The membrane skeleton of human erythrocytes and its implications for more complex cells. *Annual Review of Biochemistry*, **54**, 273-304.

Bhattacharyya, R., Das, A.K., Moitra, P.K., Pal, B., Mandal, I. and Basu, J. (1999) Mapping of a palmitoylatable band 3-binding domain of human erythrocyte membrane protein 4.2. *The Biochemical Journal*, **340**, 505-512.

Blisnick, T., Morales Betoulle, M.E., Barale, J.C., Uzureau, P., Berry, L., Desroses, S., Fujioka, H., Mattei, D. and Braun Breton, C. (2000) Pfsbp1, a Maurer's cleft *Plasmodium falciparum* protein, is associated with the erythrocyte skeleton. *Molecular and Biochemical Parasitology*, **111**, 107-121.

Bork, P., Sander, C., Valencia, A. and Bukau, B. (1992) A module of the DnaJ heat shock proteins found in malaria parasites. *Trends in Biochemical Science*, **17**, 129.

Bowman, S., Lawson, D., Basham, D., Brown, D., Chillingworth, T., Churcher, C.M., Craig, A., Davies, R.M., Devlin, K., Feltwell, T., Gentles, S., Gwilliam, R., Hamlin, N., Harris, D., Holroyd, S., Hornsby, T., Horrocks, P., Jagels, K., Jassal, B., Kyes, S., McLean, J., Moule, S., Mungall, K., Murphy, L., Oliver, K., Quail, M.A., Rajandream, M.-A., Rutter, S., Skelton, J., Squares, S., Sulston, J.E., Whitehead, S., Woodward, J.R., Newbold, C. and Barrell, B.G. (1999) The complete nucleotide sequence of chromosome 3 of *Plasmodium falciparum*. *Nature*, **400**, 532-538.

Branton, D., Cohen, C.M. and Tyler, J. (1981) Interaction of Cytoskeletal Proteins on the Human Erythrocyte Membrane. *Cell*, **24**, 24-32.

Breman, J.G. (2001) The ears of the hippopotamus: manifestations, determinants, and estimates of the malaria burden. *The American Journal of Tropical Medicine and Hygiene*, **64**, 1-11.

Broderick, M.J. and Winder, S.J. (2002) Towards a complete atomic structure of spectrin family proteins. *Journal of Structural Biology*, **137**, 184-193.

Brown, G.V., Culvenor, J.G., Crewther, P.E., Bianco, A.E., Coppel, R.L., Saint, R.B., Stahl, H.D., Kemp, D.J. and Anders, R.F. (1985) Localization of the ring-infected erythrocyte surface antigen (RESA) of *Plasmodium falciparum* in merozoites and ring-infected erythrocytes. *The Journal of Experimental Medicine*, **162**, 774-779.

Bruce, L.J., Ring, S.M., Anstee, D.J., Reid, M.E., Wilkinson, S. and Tanner, M.J. (1995) Changes in the blood group Wright antigens are associated with a mutation at amino acid 658 in human erythrocyte band 3: a site of interaction between band 3 and glycophorin A under certain conditions. *Blood*, **85**, 541-547.

Buffet, P.A., Gamain, B., Scheidig, C., Baruch, D., Smith, J.D., Hernandez-Rivas, R., Pouvelle, B., Oishi, S., Fujii, N., Fusai, T., Parzy, D., Miller, L.H., Gysin, J. and Scherf, A. (1999) *Plasmodium falciparum* domain mediating adhesion to chondroitin sulfate A: a receptor for human placental infection. *Proceedings of the National Academy of Sciences USA*, **96**, 12743-12748.

Byers, T.J. and Branton, D. (1985) Visualization of the protein associations in the erythrocyte membrane skeleton. *Proceedings of the National Academy of Sciences USA*, **82**, 6153-6157.

Carlson, J., Holmquist, G., Taylor, D.W., Perlmann, P. and Wahlgren, M. (1990) Antibodies to a histidine-rich protein (PfHRP1) disrupt spontaneously formed *Plasmodium falciparum* erythrocyte rosettes. *Proceedings of the National Academy of Sciences USA*, **87**, 2511-2515.

Carlson, J., Ekre, H.P., Helmby, H., Gysin, J., Greenwood, B.M. and Wahlgren, M. (1992a) Disruption of *Plasmodium falciparum* erythrocyte rosettes by standard heparin and heparin devoid of anticoagulant activity. *The American Journal of Tropical Medicine and Hygiene*, **46**, 595-602.

Carlson, J., Helmby, H., Hill, A.V., Brewster, D., Greenwood, B.M. and Wahlgren, M. (1992b) Human cerebral malaria: association with erythrocyte rosetting and lack of anti-rosetting antibodies. *Lancet*, **336**, 1457-1460.

Carlson, J. and Wahlgren, M. (1992) *Plasmodium falciparum* erythrocyte rosetting is mediated by promiscuous lectin-like interactions. *The Journal of Experimental Medicine*, **176**, 1311-1317.

Casey, J.R. and Reithmeier, R.A. (1991) Analysis of the oligomeric state of Band 3, the anion transport protein of the human erythrocyte membrane, by size exclusion high performance liquid chromatography. Oligomeric stability and origin of heterogeneity. *The Journal of Biological Chemistry*, **266**, 15726-15737.

Castresana, J. and Saraste, M. (1995) Does Vav bind to F-actin through a CH domain? *FEBS Letters*, **374**, 149-151.

Chang, S.H. and Low, P.S. (2003) Identification of a critical ankyrin-binding loop on the cytoplasmic domain of erythrocyte membrane band 3 by crystal structure analysis and site-directed mutagenesis. *The Journal of Biological Chemistry*, **278**, 6879-6884.

Chasis, J.A., Agre, P. and Mohandas, N. (1988) Decreased Membrane Mechanical Stability and *in vivo* Loss of Surface Area Reflect Spectrin Deficiencies in Hereditary Spherocytosis. *Journal of Clinical Investigation*, **82**, 617-623.

Chasis, J.A., Knowles, D., Winardi, R., George, E. and Mohandas, N. (1991) Conformational changes in cytoplasmic domains of Band 3 and Glycophorin-A affect red cell membrane properties. *Blood*, **78**, 252.

Chasis, J.A. and Mohandas, N. (1992) Red blood cell glycophorins. *Blood*, **80**, 1869-1879.

Chen, Q., Barragan, A., Fernandez, V., Sundstrom, A., Schlichtherle, M., Sahlen, A., Carlson, J., Datta, S. and Wahlgren, M. (1998) Identification of *Plasmodium falciparum* erythrocyte membrane protein 1 (PfEMP1) as the rosetting ligand of the malaria parasite *P. falciparum*. *The Journal of Experimental Medicine*, **187**, 15-23.

Chen, Q., Heddini, A., Barragan, A., Fernandez, V., Pearce, S.F. and Wahlgren, M. (2000) The semiconserved head structure of *Plasmodium falciparum* erythrocyte membrane protein 1 mediates binding to multiple independent host receptors. *The Journal of Experimental Medicine*, **192**, 1-10.

Chishti, A.H., Maalouf, G.J., Marfatia, S., Palek, J., Wang, W., Fisher, D. and Liu, S.C. (1994) Phosphorylation of protein 4.1 in *Plasmodium falciparum*-infected human red blood cells. *Blood*, **83**, 3339-3345.

Chishti, A.H., Palek, J., Fisher, D., Maalouf, G.J. and Liu, S.C. (1996) Reduced invasion and growth of *Plasmodium falciparum* into elliptocytic red blood cells with a combined deficiency of protein 4.1, glycophorin C, and p55. *Blood*, **87**, 3462-3469.

Chotivanich, K.T., Dondorp, A.M., White, N.J., Peters, K., Vreeken, J., Kager, P.A. and Udomsangpetch, R. (2000) The resistance to physiological shear stresses of the erythrocytic rosettes formed by cells infected with *Plasmodium falciparum*. *Annals of Tropical Medicine and Parasitology*, **94**, 219-226.

Clough, B., Atilola, F.A., Black, J. and Pasvol, G. (1998a) *Plasmodium falciparum*: the importance of IgM in the rosetting of parasite-infected erythrocytes. *Experimental Parasitology*, **89**, 129-132.

Clough, B., Atilola, F.A. and Pasvoi, G. (1998b) The role of rosetting in the multiplication of *Plasmodium falciparum*: rosette formation neither enhances nor targets parasite invasion into uninfected red cells. *British Journal of Haematology*, **100**, 99-104.

Cohen, C.M., Tyler, J.M. and Branton, D. (1980) Spectrin-actin associations studied by electron microscopy of shadowed preparations. *Cell*, **21**, 875-883.

Cohen, C.M. and Foley, S.F. (1982) The role of band 4.1 in the association of actin with erythrocyte membranes. *Biochimica et Biophysica Acta*, **688**, 691-701.

Conboy, J.G., Chan, J., Mohandas, N. and Kan, Y.W. (1988) Multiple protein 4.1 isoforms produced by alternative splicing in human erythroid cells. *Proceedings of the National Academy of Sciences USA*, **85**, 9062-9065.

Cooke, B.M., Morris-Jones, S., Greenwood, B.M. and Nash, G.B. (1993) Adhesion of parasitized red blood cells to cultured endothelial cells: a flow-based assay of isolates from Gambian children with falciparum malaria. *Parasitiology*, **107**, 359-368.

Cooke, B.M., Rogerson, S.J., Brown, G.V. and Coppel, R.L. (1996) Adhesion of malaria-infected red blood cells to chondroitin sulfate A under flow conditions. *Blood*, **88**, 4040-4044.

Cooke, B.M., Nicoll, C.L., Baruch, D.I. and Coppel, R.L. (1998) A recombinant peptide based on *Pf*EMP-1 blocks and reverses adhesion of malaria-infected red blood cells to CD36 under flow. *Molecular Microbiology*, **30**, 83-90.

Cooke, B.M., Mohandas, N. and Coppel, R.L. (2001) The malaria-infected red blood cell: structural and functional changes. *Advances in Parasitology*, **50**, 1-86.

Cooke, B.M., Glenister, F.K., Mohandas, N. and Coppel, R.L. (2002) Assignment of functional roles to parasite proteins in malaria-infected red blood cells by competitive flow-based adhesion assay. *British Journal of Haematology*, **117**, 203-211.

Coppel, R.L., Culvenor, J.G., Bianco, A.E., Crewther, P.E., Stahl, H.D., Brown, G.V., Anders, R.F. and Kemp, D.J. (1986) Variable antigen associated with the surface of erythrocytes infected with mature stages of *Plasmodium falciparum*. *Molecular and Biochemical Parasitology*, **20**, 265-277.

Coppel, R.L., Lustigman, S., Murray, L. and Anders, R.F. (1988) MESA is a *Plasmodium falciparum* phosphoprotein associated with the erythrocyte membrane skeleton. *Molecular and Biochemical Parasitology*, **31**, 223-231.

Coppel, R.L. (1992) Repeat structures in a *Plasmodium falciparum* protein (MESA) that binds human erythrocyte protein 4.1. *Molecular and Biochemical Parasitology*, **50**, 335-347.

Coppel, R.L., Davern, K.M. and McConville, M.J. (1994) Immunochemistry of Parasite Antigens. In van Oss, C.J. and van Regenmortel, M.H.V. (eds.), *Immunochemistry*. Marcel Dekker, Inc, New York, pp. 475-531.

Coppel, R.L. and Black, C.G. (1998) Malaria Parasite DNA. In Serman, I.W. (ed.), *Malaria: Parasite Biology, Pathogenesis, and Protection*. American Society for Microbiology, Washington, pp. 185-202.

Coppel, R.L., Cooke, B.M., Magowan, C. and Mohandas, N. (1998) Malaria and the erythrocyte. *Current Opinion in Haematology*, **5**, 132-138.

Correas, I., Leto, T.L., Speicher, D.W. and Marchesi, V.T. (1986) Identification of the functional site of erythrocyte protein 4.1 involved in spectrin-actin associations. *The Journal of Biological Chemistry*, **261**, 3310-3315.

Cortes, G.T., Winograd, E. and Wiser, M.F. (2003) Characterisation of proteins localised to a subcellular compartment associated with an alternate secretory pathway of the malaria parasite. *Molecular and Biochemical Parasitology*, **129**, 127-135.

Crabb, B., Cooke, B.M., Reeder, J.C., Waller, R.F., Caruana, S.R., Davern, K.M., Wickham, M.E., Brown, G.V., Coppel, R.L. and Cowman, A.F. (1997) Targeted Gene Disruption Shows That Knobs Enable Malaria-Infected Red Cells to Cytoadhere under Physiological Shear Stress. *Cell*, **89**, 287-296.

Crandall, I. and Sherman, I.W. (1991) *Plasmodium falciparum* (human malaria)-induced modifications in human erythrocyte band 3 protein. *Parasitology*, **102 Pt 3**, 335-340.

Crandall, I., Collins, W.E., Gysin, J. and Sherman, I.W. (1993) Synthetic peptides based on motifs present in human band 3 protein inhibit cytoadherence/sequestration of the malaria parasite *Plasmodium falciparum*. *Proceedings of the National Academy of Sciences USA*, **90**, 4703-4707.

Crandall, I., Land, K.M. and Sherman, I.W. (1994) *Plasmodium falciparum*: pfalhesin and CD36 form an adhesin/receptor pair that is responsible for the pH-dependent portion of cytoadherence/sequestration. *Experimental Parasitology*, **78**, 203-209.

Crandall, I. and Sherman, I.W. (1994) Cytoadherence-related neoantigens on *Plasmodium falciparum* (human malaria)-infected human erythrocytes result from the exposure of normally cryptic regions of the band 3 protein. *Parasitology*, **108**, 257-267.

Cranmer, S.L., Magowan, C., Liang, J., Coppel, R.L. and Cooke, B.M. (1997) An alternative to serum for cultivation of *Plasmodium falciparum in vitro*. *Transactions of the Royal Society of Tropical Medicine and Hygiene*, **91**, 363-365.

Cranston, H.A., Boylan, C.W., Carroll, G.L., Sutera, S.P., Williamson, J.R., Gluzman, I.Y. and Krogstad, D.J. (1984) *Plasmodium falciparum* maturation abolishes physiologic red cell deformability. *Science*, **223**, 400-403.

Culvenor, J.G., Langford, C.J., Crewther, P.E., Saint, R.B., Coppel, R.L., Kemp, D.J., Anders, R.F. and Brown, G.V. (1987) *Plasmodium falciparum*: Identification and Localization of a Knob Protein Antigen Expressed by a cDNA Clone. *Experimental Parasitology*, **63**, 58-67.

Cush, R., Cronin, J.M., Stewart, W.J., Maule, C.H., Molloy, J. and Goddard, N.J. (1993) The resonant mirror: A novel optical biosensor for direct sensing of biomolecular interactions. Part I: Principle of operation and associated instrumentation. *Biosensors and Bioelectronics*, **8**, 347-353.

Da Silva, E., Foley, M., Dluzewski, A.R., Murray, L.J., Anders, R.F. and Tilley, L. (1994) The *Plasmodium falciparum* protein RESA interacts with the erythrocyte cytoskeleton and modifies erythrocyte thermal stability. *Molecular and Biochemical Parasitology*, **66**, 59-69.

Danilov, Y.N., Fennell, R., Ling, E. and Cohen, C.M. (1990) Selective modulation of band 4.1 binding to erythrocyte membranes by protein kinase C. *The Journal of Biological Chemistry*, **265**, 2556-2562.

Davis, L.H. and Bennett, V. (1990) Mapping the binding sites of human erythrocyte ankyrin for the anion exchanger and spectrin. *The Journal of Biological Chemistry*, **265**, 10589-10596.

Davis, L.H., Davis, J.Q. and Bennett, V. (1992) Ankyrin regulation: an alternatively spliced segment of the regulatory domain functions as an intramolecular modulator. *The Journal of Biological Chemistry*, **267**, 18966-18972.

Degen, R., Weiss, N. and Beck, H.P. (2000) *Plasmodium falciparum*: cloned and expressed CIDR domains of PfEMP1 bind to chondroitin sulfate A. *Experimental Parasitology*, **95**, 113-121.

Deguercy, A., Hommel, M. and Schrevel, J. (1990) Purification and characterization of 37-kilodalton proteases from and *Plasmodium berghei* which cleave erythrocyte cytoskeletal components. *Molecular and Biochemical Parasitology*, **38**, 233-244.

Delaunay, J. (2002) Molecular basis of red cell membrane disorders. *Acta haematologica*, **108**, 210-218.

Derick, L.H., Liu, S.C., Chishti, A.H. and Palek, J. (1992) Protein immunolocalization in the spread erythrocyte membrane skeleton. *European Journal of Cell Biology*, **57**, 317-320.

DeSilva, T.M., Peng, K.C., Speicher, K.D. and Speicher, D.W. (1992) Analysis of human red cell spectrin tetramer (head-to-head) assembly using complementary univalent peptides. *Biochemistry*, **31**, 10872-10878.

Dhawan, S., Dua, M., Chishti, A.H. and Hanspal, M. (2003) Ankyrin peptide blocks falcipain-2-mediated malaria parasite release from red blood cells. *The Journal of Biological Chemistry*, **in press**.

Dhermy, D. (1991) The spectrin super-family. *Biology of the Cell*, **71**, 249-254.

Discher, D., Parra, M., Conboy, J.G. and Mohandas, N. (1993) Mechanochemistry of the alternatively spliced spectrin-actin binding domain in membrane skeletal protein 4.1. *The Journal of Biological Chemistry*, **268**, 7186-7195.

Dluzewski, A.R., Zicha, D., Dunn, G.A. and Gratzer, W.B. (1995) Origins of the parasitophorous vacuole membrane of the malaria parasite: surface area of the parasitized red cell. *European Journal of Cell Biology*, **68**, 446-449.

Dolan, S.A., Proctor, J.L., Alling, D.W., Okubo, Y., Wellems, T.E. and Miller, L.H. (1994) Glycophorin B as an EBA-175 independent *Plasmodium falciparum* receptor of human erythrocytes. *Molecular and Biochemical Parasitology*, **64**, 55-63.

Dua, M., Raphael, P., Sijwali, P.S., Rosenthal, P.J. and Hanspal, M. (2001) Recombinant falcipain-2 cleaves erythrocyte membrane ankyrin and protein 4.1. *Molecular and Biochemical Parasitology*, **116**, 95-99.

Eda, S., Lawler, J. and Sherman, I.W. (1999) *Plasmodium falciparum*-infected erythrocyte adhesion to the type 3 repeat domain of thrombospondin-1 is mediated by a modified band 3 protein. *Molecular and Biochemical Parasitology*, **100**, 195-205.

Eder, P.S., Soong, C.J. and Tao, M. (1986) Phosphorylation reduces the affinity of protein 4.1 for spectrin. *Biochemistry*, **25**, 1764-1770.

Elford, B.C., Cowan, G.M. and Ferguson, D.J. (1995) Parasite-regulated membrane transport processes and metabolic control in malaria-infected erythrocytes. *The Biochemical Journal*, **308**, 361-374.

Ellis, J., Irving, D.O., Wellems, T.E., Howard, R.J. and Cross, G.A.M. (1987) Structure and expression of the knob-associated histidine-rich protein of *Plasmodium falciparum*. *Molecular and Biochemical Parasitology*, **26**, 203-214.

Elmendorf, H.G., Bangs, J.D. and Haldar, K. (1992) Synthesis and secretion of proteins by released malarial parasites. *Molecular and Biochemical Parasitology*, **52**, 215-230.

Elmendorf, H.G. and Haldar, K. (1994) *Plasmodium falciparum* exports the Golgi marker sphingomyelin synthase into a tubovesicular network in the cytoplasm of mature erythrocytes. *Journal of Cell Biology*, **124**, 449-462.

Endo, M., Nunomura, W., Takakuwa, Y., Hatakeyama, M. and Higashi, T. (1998) A novel epitope (pentapeptide) in the human hemoglobin beta chain. *Hemoglobin*, **22**, 321-331.

Facer, C.A. (1995) Erythrocytes carrying mutations in spectrin and protein 4.1 show differing sensitivities to invasion by *Plasmodium falciparum*. *Parasitology Research*, **81**, 52-57.

Fandeur, T., Mercereau-Puijalon, O. and Bonnemains, B. (1996) *Plasmodium falciparum*: genetic diversity of several strains infectious for the squirrel monkey (*Saimiri sciureus*). *Experimental Parasitology*, **84**, 1-15.

Favaloro, J.M., Coppel, R.L., Corcoran, L.M., Foote, S.J., Brown, G.V., Anders, R.F. and Kemp, D.J. (1986) Structure of the RESA gene of *Plasmodium falciparum*. *Nucleic Acids Research*, **14**, 8265-8277.

Fernandez, V., Hommel, M., Chen, Q., Hagblom, P. and Wahlgren, M. (1999) Small, clonally variant antigens expressed on the surface of the *Plasmodium falciparum*-infected erythrocyte are encoded by the *rif* gene family and are the target of human immune responses. *The Journal of Experimental Medicine*, **190**, 1393-1404.

Fischer, K., Horrocks, P., Preuss, M., Wiesner, J., Wunsch, S., Camargo, A.A. and Lanzer, M. (1997) Expression of var genes located within polymorphic subtelomeric domains of *Plasmodium falciparum* chromosomes. *Molecular and Cellular Biology*, **17**, 3679-3686.

Foley, M., Tilley, L., Sawyer, W.H. and Anders, R.F. (1991) The ring-infected erythrocyte surface antigen of *Plasmodium falciparum* associates with spectrin in the erythrocyte membrane. *Molecular and Biochemical Parasitology*, **46**, 137-147.

Foley, M., Corcoran, L., Tilley, L. and Anders, R. (1994) *Plasmodium falciparum*: mapping the membrane-binding domain in the ring-infected erythrocyte surface antigen. *Experimental Parasitology*, **79**, 340-350.

Foley, M. and Tilley, L. (1998) Protein trafficking in malaria-infected erythrocytes. *International Journal for Parasitology*, **28**, 1671-1680.

Fowler, V.M. and Bennett, V. (1984) Erythrocyte Membrane Tropomyosin. Purification and Properties. *The Journal of Biological Chemistry*, **259**, 5978-5989.

Fowler, V.M. (1987) Identification and Purification of a Novel Mr 43,000 Tropomyosin- binding Protein from Human Erythrocyte Membranes. *The Journal of Biological Chemistry*, **262**, 12792-12800.

Fowler, V.M. (1990) Tropomodulin: A Cytoskeletal Protein that Binds to the End of Erythrocyte Tropomyosin and Inhibits Tropomyosin Binding to Actin. *Journal of Cell Biology*, **111**, 471-481.

Fowler, V.M., Sussmann, M.A., Miller, P.G., Flucher, B.E. and Daniels, M.P. (1993) Tropomodulin is associated with the free (pointed) ends of the thin filaments in rat skeletal muscle. *Journal of Cell Biology*, **120**, 411-420.

Gardiner, D.L., Holt, D.C., Thomas, E.A., Kemp, D.J. and Trenholme, K.R. (2000) Inhibition of *Plasmodium falciparum clag9* gene function by antisense RNA. *Molecular and Biochemical Parasitology*, **110**, 33-41.

Gardner, K. and Bennett, V. (1986) A New Erythrocyte Membrane-associated Protein with Calmodulin Binding Activity. Identification and purification. *The Journal of Biological Chemistry*, **261**, 1339-1348.

Gardner, K. and Bennett, V. (1987) Modulation of spectrin-actin assembly by erythrocyte adducin. *Nature*, **328**, 359-362.

Gardner, M.J., Tettelin, H., Carucci, D.J., Cummings, L.M., Aravind, L., Koonin, E.V., Shallom, S., Mason, T., Yu, K., Fujii, C., Pederson, J., Shen, K., Jing, J., Aston, C., Lai, Z., Schwartz, D.C., Pertea, M., Salzberg, S., Zhou, L., Sutton, G.G., Clayton, R., White, O., Smith, H.O., Fraser, C.M., Adams, M.D., Venter, J.C. and Hoffman, S.L. (1998) Chromosome 2 sequence of the human malaria parasite *Plasmodium falciparum*. *Science*, **282**, 1126-1132.

Gardner, M.J., Hall, N., Fung, E., White, O., Berriman, M., Hyman, R.W., Carlton, J.M., Pain, A., Nelson, K.E., Bowman, S., Paulsen, I.T., James, K., Eisen, J.A., Rutherford, K., Salzberg, S.L., Craig, A., Kyes, S., Chan, M.-S., Nene, V., Shallom, S.J., Suh, B., Peterson, J., Angiuoli, S., Pertea, M., Allen, J., Selengut, J., Haft, D., Mather, M.W., Vaidya, A.B., Martin, D.M.A., Fairlamb, A.H., Fraunholz, M.J., Roos, D.S., Ralph, S.A., McFadden, G.I., Cummings, L.M., Subramanian, G.M., Mungall, C., Venter, J.C., Carucci, D.J., Hoffman, S.L., Newbold, C., Davis, R.W., Fraser, C.M. and Barrell, B. (2002) Genome sequence of the human malaria parasite *Plasmodium falciparum*. *Nature*, **419**, 498-511.

Gatzigiannis, V. (1999) Study of Protein-Protein Interactions in Malaria: Interactions of *P. falciparum* Erythrocyte Membrane Protein 3 (PfEMP3) with Parasitic Proteins and Red Blood Cell Cytoskeletal Proteins. Department of Microbiology. Monash University, Melbourne.

George, A.J., French, R.R. and Glennie, M.J. (1995) Measurement of kinetic binding constants of a panel of anti-saporin antibodies using a resonant mirror biosensor. *Journal of Immunological Methods*, **183**, 51-63.

Gilligan, D.M. and Bennett, V. (1993) The Junctional Complex of the Membrane Skeleton. *Seminars in Hematology*, **30**, 74-83.

Gimm, J.A., An, X., Nunomura, W. and Mohandas, N. (2002) Functional characterization of spectrin-actin-binding domains in 4.1 family of proteins. *Biochemistry*, **41**, 7275-7282.

Glenister, F.K., Coppel, R.L., Cowman, A.F., Mohandas, N. and Cooke, B.M. (2002) Contribution of parasite proteins to altered mechanical properties of malaria-infected red blood cells. *Blood*, **99**, 1060-1063.

Gluzman, I.Y., Francis, S.E., Oksman, A., Smith, C.E., Duffin, K.L. and Goldberg, D.E. (1994) Order and specificity of the *Plasmodium falciparum* hemoglobin degradation pathway. *Journal of Clinical Investigation*, **93**, 1602-1608.

Goebl, M.G. (1992) Is the erythrocyte protein p55 a membrane-bound guanylate kinase? *Trends in Biochemical Science*, **17**, 99.

Goel, V.K., Li, X., Chen, H., Liu, S., Chishti, A.H. and Oh, S.S. (2003) Band 3 is a host receptor binding merozoite surface protein 1 during the *Plasmodium falciparum* invasion of erythrocytes. *Proceedings of the National Academy of Sciences USA*, **100**, 5164-5169.

Golan, D.E., Corbett, J.D., Korsgren, C., Thatte, H.S., Hayette, S., Yawata, Y. and Cohen, C.M. (1996) Control of band 3 lateral and rotational mobility by band 4.2 in intact erythrocytes: release of band 3 oligomers from low-affinity binding sites. *Biophysical Journal*, **70**, 1534-1542.

Goodyer, I.D., Johnson, J., Eisenthal, R. and Hayes, D.J. (1994) Purification of mature-stage *Plasmodium falciparum* by gelatine flotation. *Annual Journal of Tropical Medicine and Parasitology*, **88**, 209-211.

Gray, C., McCormick, C., Turner, G. and Craig, A. (2003) ICAM-1 can play a major role in mediating *P. falciparum* adhesion to endothelium under flow. *Molecular and Biochemical Parasitology*, **128**, 187-193.

Gritzmacher, C.A. and Reese, R.T. (1984) Reversal of Knob Formation on *Plasmodium falciparum*-Infected Erythrocytes. *Science*, **226**, 65-67.

Gruenberg, J., Allred, D.R. and Sherman, I.W. (1983) Scanning Electron Microscope-Analysis of the Protrusions (Knobs) Present on the Surface of *Plasmodium falciparum*-infected Erythrocytes. *Journal of Cell Biology*, **97**, 795-802.

Gruner, A.C., Brahimi, K., Eling, W., Konings, R., Meis, J., Aikawa, M., Daubersies, P., Guerin-Marchand, C., Mellouk, S., Snounou, G. and Druilhe, P. (2001) The *Plasmodium falciparum* knob-associated PfEMP3 antigen is also expressed at pre-erythrocytic stages and induces antibodies which inhibit sporozoite invasion. *Molecular and Biochemical Parasitology*, **112**, 253-261.

Guan, K.L. and Dixon, J.E. (1991) Eukaryotic proteins expressed in *Escherichia coli*: an improved thrombin cleavage and purification procedure of fusion proteins with glutathione S-transferase. *Analytical Biochemistry*, **192**, 262-267.

Gysin, J. (1998) Animal Models: Primates. In Sherman, I.W. (ed.), *Malaria. Parasite Biology, Pathogenesis and Protection*. ASM Press, Washington.

Haldar, K., Samuel, B.U., Mohandas, N., Harrison, T. and Hiller, N.L. (2001) Transport mechanisms in *Plasmodium*-infected erythrocytes: lipid rafts and a tubovesicular network. *International Journal for Parasitology*, **31**, 1393-1401.

Han, B.G., Nunomura, W., Takakuwa, Y., Mohandas, N. and Jap, B.K. (2000) Protein 4.1R core domain structure and insights into regulation of cytoskeletal organization. *Nature Structural Biology*, **7**, 871-875.

Hanahan, D. (1985) Techniques for transformation of *E. coli*. In Glover, D.M. (ed.), *DNA cloning: a practical approach*. IRL Press Ltd., Oxford, pp. 109-135.

Hanspal, M., Dua, M., Takakuwa, Y., Chishti, A.H. and Mizuno, A. (2002) *Plasmodium falciparum* cysteine protease falcipain-2 cleaves erythrocyte membrane skeletal proteins at late stages of parasite development. *Blood*, **100**, 1048-1054.

Hargreaves, W.R., Giedd, K.N., Verkleij, A. and Branton, D. (1980) Reassociation of ankyrin with band 3 in erythrocyte membranes and in lipid vesicles. *The Journal of Biological Chemistry*, **255**, 11965-11972.

Harper, S.L., Begg, G.E. and Speicher, D.W. (2001) Role of Terminal Nonhomologous Domains in Initiation of Human Red Cell Spectrin Dimerization. *Biochemistry*, **40**, 9935-9943.

Harris, H.W., Jr. and Lux, S.E. (1980) Structural characterization of the phosphorylation sites of human erythrocyte spectrin. *The Journal of Biological Chemistry*, **255**, 11512-11520.

Hassoun, H., Hanada, T., Lutchman, M., Sahr, K.E., Palek, J., Hanspal, M. and Chishti, A.H. (1998) Complete deficiency of glycophorin A in red blood cells from mice with targeted inactivation of the band 3 (AE1) gene. *Blood*, **91**, 2146-2151.

Haynes, J. (1993) Erythrocytes and malaria. *Current Opinion in Hematology*, 79-89.

Helmby, H., Cavelier, L., Pettersson, U. and Wahlgren, M. (1993) Rosetting *Plasmodium falciparum*-infected erythrocytes express unique strain-specific antigens on their surface. *Infection and Immunity*, **61**, 284-288.

Hemming, N.J., Anstee, D.J., Staricoff, M.A., Tanner, M.J. and Mohandas, N. (1995) Identification of the membrane attachment sites for protein 4.1 in the human erythrocyte. *The Journal of Biological Chemistry*, **270**, 5360-5366.

Herrera, S., Werner, R., Herrera, M., Clavijo, P., Mancilla, L., de Plata, C., Matile, H. and Certa, U. (1993) A conserved region of the MSP-1 surface protein of *Plasmodium falciparum* contains a recognition sequence for erythrocyte spectrin. *The EMBO Journal*, **12**, 1607-1614.

Hinterberg, K., Scherf, A., Gysin, J., Toyoshima, T., Aikawa, M., Mazie, J.C., da Silva, L.P. and Mattei, D. (1994) *Plasmodium falciparum*: the Pf332 antigen is secreted from the parasite by a brefeldin A-dependent pathway and is translocated to the erythrocyte membrane via the Maurer's clefts. *Experimental Parasitology*, **79**, 279-291.

Hirawake, H., Kita, K. and Sharma, Y.D. (1997) Variations in the C-terminal repeats of the knob-associated histidine-rich protein of *Plasmodium falciparum*. *Biochimcia et Biophysica Acta*, **1360**, 105-108.

Holt, D.C., Gardiner, D.L., Thomas, E.A., Mayo, M., Bourke, P.F., Sutherland, C.J., Carter, R., Myers, G., Kemp, D.J. and Trenholme, K.R. (1999) The cytoadherence linked asexual gene family of *Plasmodium falciparum*: are there roles other than cytoadherence? *International Journal of Parasitology*, **29**, 939-944.

Horne, W.C., Huang, S.C., Becker, P.S., Tang, T.K. and Benz, E.J., Jr. (1993) Tissue-specific alternative splicing of protein 4.1 inserts an exon necessary for formation of the ternary complex with erythrocyte spectrin and F-actin. *Blood*, **82**, 2558-2563.

Hougard, J.M., Fontenille, D., Chandre, F., Darriet, F., Carnevale, P. and Guillet, P. (2002) Combating malaria vectors in Africa: current directions of research. *Trends in Parasitology*, **18**, 283-286.

Howard, R.J. and Gilladoga, A.D. (1989) Molecular studies related to the pathogenesis of cerebral malaria. *Blood*, **74**, 2603-2618.

Hughes, C.A. and Bennett, V. (1995) Adducin: a physical model with implications for function in assembly of spectrin-actin complexes. *The Journal of Biological Chemistry*, **270**, 18990-18996.

Husain-Chishti, A., Levin, A. and Branton, D. (1988) Abolition of actin-bundling by phosphorylation of human erythrocyte protein 4.9. *Nature*, **334**, 718-721.

Husain-Chishti, A., Faquin, W., Wu, C.C. and Branton, D. (1989) Purification of Erythrocyte Dematin (protein 4.9) Reveals an Endogenous Protein Kinase That Modulates Actin-bundling Activity. *The Journal of Biological Chemistry*, **264**, 8985-8991.

Inaba, M., Gupta, K.C., Kuwabara, M., Takahashi, T., Benz, E.J., Jr. and Maede, Y. (1992) Deamidation of human erythrocyte protein 4.1: possible role in aging. *Blood*, **79**, 3355-3361.

Jarolim, P., Palek, J., Amato, D., Hassan, K., Sapak, P., Nurse, G.T., Rubin, H.L., Zhai, S., Sahr, K.E. and Liu, S.C. (1991) Deletion in erythrocyte band 3 gene in malaria-resistant Southeast Asian ovalocytosis. *Proceedings of the National Academy of Sciences USA*, **88**, 11022-11026.

Jin, L. and Harrison, S.C. (2002) Crystal structure of human calcineurin complexed with cyclosporin A and human cyclophilin. *Proceedings of the National Academy of Sciences USA*, **99**, 13522-13526.

Jons, T. and Drenckhahn, D. (1992) Identification of the binding interface involved in linkage of cytoskeletal protein 4.1 to the erythrocyte anion exchanger. *The EMBO Journal*, **11**, 2863-2867.

Joshi, R. and Bennett, V. (1990) Mapping the domain structure of human erythrocyte adducin. *The Journal of Biological Chemistry*, **265**, 13130-13136.

Joshi, R., Gilligan, D.M., Otto, E., McLaughlin, T. and Bennett, V. (1991) Primary structure and domain organization of human alpha and beta adducin. *Journal of Cell Biology*, **115**, 665-675.

Kaneko, O., Tsuboi, T., Ling, I., Howell, S., Shirano, M., Tachibana, M., Cao, Y., Holder, A.A. and Torii, M. (2001) The high molecular mass rhoptry protein, RhopH1, is encoded by members of the *clag* multigene family in *Plasmodium falciparum* and *Plasmodium yoelii*. *Molecular and Biochemical Parasitology*, **118**, 223-231.

Kant, R. and Sharma, Y.D. (1996) Allelic forms of the knob associated histidine-rich protein gene of *Plasmodium falciparum*. *FEBS Letters*, **380**, 147-151.

Karinch, A.M., Zimmer, W.E. and Goodman, S.R. (1990) The Identification and Sequence of the Actin-binding Domain of Human Red Blood Cell b-Spectrin. *The Journal of Biological Chemistry*, **265**, 11833-11840.

Kennedy, S.P., Warren, S.L., Forget, B.G. and Morrow, J.S. (1991) Ankyrin binds to the 15th repetitive unit of erythroid and nonerythroid β-spectrin. *Journal of Cell Biology*, **115**, 267-277.

Kilejian, A. (1979) Characterization of a protein correlated with the production of knob-like protrusions on membranes of erythrocytes infected with *Plasmodium falciparum*. *Proceedings of the National Academy of Sciences USA*, **76**, 4650-4653.

Kilejian, A. (1984) The biosynthesis of the knob protein and a 65 000 dalton histidine-rich polypeptide of *Plasmodium falciparum*. *Molecular and Biochemical Parasitology*, **12**, 185-194.

Kilejian, A., Rashid, M.A., Aikawa, M., Aji, T. and Yang, Y.F. (1991) Selective association of a fragment of the knob protein with spectrin, actin and the red cell membrane. *Molecular and Biochemical Parasitology*, **44**, 175-182.

Kim, A.C., Metzenberg, A.B., Sahr, K.E., Marfatia, S.M. and Chishti, A.H. (1996) Complete genomic organization of the human erythroid p55 gene (MPP1), a membrane-associated guanylate kinase homologue. *Genomics*, **31**, 223-229.

Kopito, R.R. and Lodish, H.F. (1985) Primary structure and transmembrane orientation of the murine anion exchange protein. *Nature*, **316**, 234-238.

Korsgren, C. and Cohen, C.M. (1986) Purification and Properties of Human Erythrocyte Band 4.2. Association with the Cytoplasmic Domain of Band 3. *The Journal of Biological Chemistry*, **261**, 5536-5543.

Korsgren, C. and Cohen, C.M. (1988) Associations of Human Erythrocyte Band 4.2. Binding to ankyrin and to the cytoplasmic domain of band 3. *The Journal of Biological Chemistry*, **263**, 10212-12028.

Korsgren, C. and Cohen, C.M. (1991) Organization of the gene for human erythrocyte membrane protein 4.2: Structural similarities with the gene for the a subunit of factor XIII. *Proceedings of the National Academy of Sciences USA*, **88**, 4840-4844.

Kotula, L., Laury-Kleintop, L.D., Showe, L., Sahr, K., Linnenbach, A.J., Forget, B. and Curtis, P.J. (1991) The exon-intron organization of the human erythrocyte α-spectrin gene. *Genomics*, **9**, 131-140.

Kuhlman, P.A., Hughes, C.A., Bennett, V. and Fowler, V.M. (1996) A new function for adducin. Calcium/calmodulin-regulated capping of the barbed ends of actin filaments. *The Journal of Biological Chemistry*, **271**, 7986-7991.

Kun, J.F.J., Waller, K.L. and Coppel, R.L. (1999) *Plasmodium falciparum*: Structural and Functional Domains of the Mature-Parasite-Infected Erythrocyte Surface Antigen. *Experimental Parasitology*, **91**, 258-267.

Kushwaha, A., Perween, A., Mukund, S., Majumdar, S., Bhardwaj, D., Chowdhury, N.R. and Chauhan, V.S. (2002) Amino terminus of *Plasmodium falciparum* acidic basic repeat antigen interacts with the erythrocyte membrane through band 3 protein. *Molecular and Biochemical Parasitology*, **122**, 45-54.

Kyes, S.A., Rowe, J.A., Kriek, N. and Newbold, C.I. (1999) Rifins: a second family of clonally variant proteins expressed on the surface of red cells infected with *Plasmodium falciparum*. *Proceedings of the National Academy of Sciences USA*, **96**, 9333-9338.

Lambert, S., Yu, H., Prchal, J.T., Lawler, J., Ruff, P., Speicher, D., Cheung, M.C., Kan, Y.W. and Palek, J. (1990) cDNA sequence for human erythrocyte ankyrin. *Proceedings of the National Academy of Sciences USA*, **87**, 1730-1734.

Landau, I. and Gautret, P. (1998) Animal Models: Rodents. In Sherman, I.W. (ed.), *Malaria. Parasite Biology, Pathogenesis and Protection*. ASM Press, Washington.

Langreth, S.G., Jensen, J.B., Reese, R.T. and Trager, W. (1978) Fine structure of human malaria *in vitro*. *The Journal of Protozoology*, **25**, 443-452.

Langreth, S.G., Reese, R.T., Motyl, M.R. and Trager, W. (1979) *Plasmodium falciparum*: Loss of Knobs on the Infected Erythrocyte Surface after Long-Term Cultivation. *Experimental Parasitology*, **48**, 213-219.

Langreth, S.G. and Peterson, E. (1985) Pathogenicity, Stability, and Immunogenicity of a Knobless Clone of *Plasmodium falciparum* in Colombian Owl Monkeys. *Infection and Immunity*, **47**, 760-766.

Lanzer, M., de Bruin, D., Wertheimer, S.P. and Ravetch, J.V. (1994) Transcriptional and nucleosomal characterization of a subtelomeric gene cluster flanking a site of chromosomal rearrangements in *Plasmodium falciparum*. *Nucleic Acids Research*, **22**, 4176-4182.

Le Bonniec, S., Deregnaucourt, C., Redeker, V., Banerjee, R., Grellier, P., Goldberg, D.E. and Schrevel, J. (1999) Plasmepsin II, an acidic hemoglobinase from the *Plasmodium falciparum* food vacuole, is active at neutral pH on the host erythrocyte membrane skeleton. *The Journal of Biological Chemistry*, **274**, 14218-14223.

Le Bonniec, S.L., Fournier, C., Deregnaucourt, C., Grellier, P., Dhermy, D., Lecomte, M.C. and Schrevel, J. (1996) Human erythroid spectrin alpha subunit and its SH3 domain are sensitive to acidic *Plasmodium falciparum* proteolytic activity. *Comptes rendus de l'Academie des sciences. Serie III, Sciences de la vie*, **319**, 1011-1017.

Leech, J.H., Barnwell, J.W., Aikawa, M., Miller, L.H. and Howard, R.J. (1984a) *Plasmodium falciparum* Malaria: Association of Knobs on the Surface of Infected Erythrocytes with a Histidine-rich Protein and the Erythrocyte Skeleton. *The Journal of Cell Biology*, **98**, 1256-1264.

Leech, J.H., Barnwell, J.W., Miller, L.H. and Howard, R.J. (1984b) Identification of a strain-specific malarial antigen exposed on the surface of *Plasmodium falciparum*-infected erythrocytes. *The Journal of Experimental Medicine*, **159**, 1567-1575.

Leto, T.L. and Marchesi, V.T. (1984) A structural model of human erythrocyte protein 4.1. *The Journal of Biological Chemistry*, **259**, 4603-4608.

Li, F., Dluzewsk, A., Coley, A.M., Thomas, A., Tilley, L., Anders, R.F. and Foley, M. (2002) Phage-displayed peptides bind to the malarial protein apical membrane antigen-1 and inhibit the merozoite invasion of host erythrocytes. *The Journal of Biological Chemistry*, **277**, 50303-50310.

Li, X. and Bennett, V. (1996) Identification of the spectrin subunit and domains required for formation of spectrin/adducin/actin complexes. *The Journal of Biological Chemistry*, **271**, 15695-15702.

Ling, E., Gardner, K. and Bennett, V. (1986) Protein kinase C phosphorylates a recently identified membrane skeleton- associated calmodulin-binding protein in human erythrocytes. *The Journal of Biological Chemistry*, **261**, 13875-13878.

Ling, E., Danilov, Y.N. and Cohen, C.M. (1988) Modulation of Red Cell Band 4.1 Function by cAMP-dependent Kinase and Protein Kinase C Phosphorylation. *The Journal of Biological Chemistry*, **263**, 2209-2216.

Liu, S.C., Windisch, P., Kim, S. and Palek, J. (1984) Oligomeric States of Spectrin in Normal Erythrocyte Membranes: Biochemical and Electron Microscopic Studies. *Cell*, **37**, 587-594.

Liu, S.C., Derick, L.H. and Palek, J. (1987) Visualization of the hexagonal lattice in the erythrocyte membrane skeleton. *Journal of Cell Biology*, **104**, 527-536.

Lobo, C., Rodriguez, M., Reid, M. and Lustigman, S. (2003) Glycophorin C is the receptor for the *Plasmodium falciparum* erythrocyte binding ligand PfEBP-2 (baebl). *Blood*, **101**, 4628-4631.

Lofvenberg, L. and Backman, L. (2001) High-performance liquid chromatography analysis of spectrin oligomerization. *Analytical Biochemistry*, **292**, 222-227.

Lombardo, C.R., Willardson, B.M. and Low, P.S. (1992) Localization of the protein 4.1-binding site on the cytoplasmic domain of erythrocyte membrane band 3. *The Journal of Biological Chemistry*, **267**, 9540-9546.

Low, P.S., Westfall, M.A., Allen, D.P. and Appell, K.C. (1984) Characterization of the reversible conformational equilibrium of the cytoplasmic domain of erythrocyte membrane band 3. *The Journal of Biological Chemistry*, **259**, 13070-13076.

Lucas, J.Z. and Sherman, I.W. (1998) *Plasmodium falciparum*: thrombospondin mediates parasitized erythrocyte band 3-related adhesin binding. *Experimental Parasitology*, **89**, 78-85.

Luna, E.J., Kidd, G.H. and Branton, D. (1979) Identification by peptide analysis of the spectrin-binding protein in human erythrocytes. *The Journal of Biological Chemistry*, **254**, 2526-2532.

Lustigman, S., Anders, R.F., Brown, G.V. and Coppel, R.L. (1990) The mature-parasite-infected erythrocyte surface antigen (MESA) of *Plasmodium falciparum* associates with the erythrocyte membrane skeletal protein, band 4.1. *Molecular and Biochemical Parasitology*, **38**, 261-270.

Lux, S.E., John, K.M., Kopito, R.R. and Lodish, H.F. (1989) Cloning and characterization of band 3, the human erythrocyte anion-exchange protein (AE1). *Proceedings of the National Academy of Sciences USA*, **86**, 9089-9093.

Lux, S.E., John, K.M. and Bennett, V. (1990) Analysis of cDNA for human erythrocyte ankyrin indicates a repeated structure with homology to tissue-differentiation and cell-cycle control proteins. *Nature*, **344**, 36-42.

Lux, S.E. and Palek, J. (1995) Disorders of the red cell membrane. In Handin, R.I., Lux, S.E. and Stossel, T.P. (eds.), *Blood: Principles and Practice of Hematology*. JB Lippincott Co., Philidelphia, pp. 1701-1818.

MacPherson, G.G., Warrell, M.J., White, N.J., Looareesuwan, S. and Warrell, D.A. (1985) Human cerebral malaria. A quantitative ultrastructural analysis of parasitized erythrocyte sequestration. *American Journal of Pathology*, **119**, 385-401.

Magowan, C., Coppel, R.L., Lau, A.O.T., Moronne, M.M., Tchernia, G. and Mohandas, N. (1995) Role of the *Plasmodium falciparum* Mature-Parasite-Infected Erythrocyte Surface Antigen (MESA/PfEMP-2) in Malarial Infection of Erythrocytes. *Blood*, **86**, 3196-3204.

Magowan, C., Brown, J.T., Liang, J., Heck, J., Coppel, R.L., Mohandas, N. and Meyer-Ilse, W. (1997) Intracellular structures of normal and aberrant *Plasmodium falciparum* malaria parasites imaged by soft x-ray microscopy. *Proceedings of the National Academy of Sciences USA*, **94**, 6222-6227.

Magowan, C., Liang, J., Yeung, J., Takakuwa, Y., Coppel, R.L. and Mohandas, N. (1998) *Plasmodium falciparum*: influence of malarial and host erythrocyte skeletal protein interactions on phosphorylation in infected erythrocytes. *Experimental Parasitology*, [illegible] 40-49.

Magowan, C., Nunomura, W., Waller, K.L., Yeung, J., Liang, J., Van Dort, H., Low, P.S., Coppel, R.L. and Mohandas, N. (2000) *Plasmodium falciparum* histidine-rich protein 1 associates with the band 3 binding domain of ankyrin in the infected red cell membrane. *Biochimica et Biophysica Acta*, **1502**, 461-470.

Maier, A.G., Duraisingh, M.T., Reeder, J.C., Patel, S.S., Kazura, J.W., Zimmerman, P.A. and Cowman, A.F. (2003) *Plasmodium falciparum* erythrocyte invasion through glycophorin C and selection for Gerbich negativity in human populations. *Nature Medicine*, **9**, 87-92.

Mak, A.S., Roseborough, G. and Baker, H. (1987) Tropomyosin from human erythrocyte membrane polymerizes poorly but binds F-actin effectively in the presence and absence of spectrin. *Biochimica et Biophysica Acta*, **912**, 157-166.

Mandal, D., Moitra, P.K. and Basu, J. (2002) Mapping of a spectrin-binding domain of human erythrocyte membrane protein 4.2. *The Biochemical Journal*, **364**, 841-847.

Manno, S., Takakuwa, Y., Nagao, K. and Mohandas, N. (1995) Modulation of Erythrocyte Membrane Mechanical Function by b-Spectrin Phosphorylation and Dephosphorylation. *The Journal of Biological Chemistry*, **270**, 5659-5665.

Marchesi, V.T. (1974) Isolation of Spectrin from Erythrocyte Membranes. *Methods in Enzymology*, **32**, 275-277.

Marfatia, S.M., Lue, R.A., Branton, D. and Chishti, A.H. (1994) *In vitro* binding studies suggest a membrane-associated complex between erythroid p55, protein 4.1, and glycophorin C. *The Journal of Biological Chemistry*, **269**, 8631-8634.

Marfatia, S.M., Leu, R.A., Branton, D. and Chishti, A.H. (1995) Identification of the protein 4.1 binding interface on glycophorin C and p55, a homologue of the Drosophila discs-large tumor suppressor protein. *The Journal of Biological Chemistry*, **270**, 715-719.

Marfatia, S.M., Morais-Cabral, J.H., Kim, A.C., Byron, O. and Chishti, A.H. (1997) The PDZ domain of human erythrocyte p55 mediates its binding to the cytoplasmic carboxyl terminus of glycophorin C. Analysis of the binding interface by *in vitro* mutagenesis. *The Journal of Biological Chemistry*, **272**, 24191-24197.

Matsuoka, Y., Hughes, C.A. and Bennett, V. (1996) Adducin regulation. Definition of the calmodulin-binding domain and sites of phosphorylation by protein kinases A and C. *The Journal of Biological Chemistry*, **271**, 25157-25166.

Mattei, D. and Scherf, A. (1992a) The *Pf332* gene of *Plasmodium falciparum* codes for a giant protein that is translocated from the parasite to the membrane of infected erythrocytes. *Gene*, **110**, 71-79.

Mattei, D. and Scherf, A. (1992b) The Pf332 gene codes for a megadalton protein of *Plasmodium falciparum* asexual blood stages. *Memórias do Instituto Oswaldo Cruz*, **87**, 163-168.

McCormick, C.J., Craig, A., Roberts, D., Newbold, C.I. and Berendt, A.R. (1997) Intercellular adhesion molecule-1 and CD36 synergize to mediate adherence of *Plasmodium falciparum*-infected erythrocytes to cultured human microvascular endothelial cells. *Journal of Clinical Investigation*, **100**, 2521-2529.

McGough, A.M. and Josephs, R. (1990) On the structure of erythrocyte spectrin in partially expanded membrane skeletons. *Proceedings of the National Academy of Sciences USA*, **87**, 5208-5212.

Mehboob, S., Luo, B.H., Patel, B.M. and Fung, L.W. (2001) αβ Spectrin coiled coil association at the tetramerization site. *Biochemistry*, **40**, 12457-12464.

Mgone, C.S., Koki, G., Paniu, M.M., Kono, J., Bhatia, K.K., Genton, B., Alexander, N.D. and Alper, M.P. (1996) Occurrence of the erythrocyte band 3 (AE1) gene deletion in relation to malaria endemicity in Papua New Guinea. *Transactions of the Royal Society of Tropical Medicine & Hygiene*, **90**, 228-231.

Michaely, P. and Bennett, V. (1995) The ANK repeats of erythrocyte ankyrin form two distinct but cooperative binding sites for the erythrocyte anion exchanger. *The Journal of Biological Chemistry*, **270**, 22050-22057.

Miller, L.H., Fremount, H.N. and Luse, S.A. (1971) Deep vascular schizogony of *Plasmodium knowlesi* in *Macaca mulatta*. Distribution in organs and ultrastructure of parasitized red cells. *The American Journal of Tropical Medicine and Hygiene*, **20**, 816-824.

Mische, S.M., Mooseker, M.S. and Morrow, J.S. (1987) Erythrocyte adducin: a calmodulin-regulated actin-bundling protein that stimulates spectrin-actin binding. *Journal of Cell Biology*, **105**, 2837-2845.

Mohandas, N. and Chasis, J.A. (1993) Red blood cell deformability, membrane material properties and shape: regulation by transmembrane, skeletal and cytosolic proteins and lipids. *Seminars in Hematology*, **30**, 171-192.

Mohandas, N. (1994). Mechanical properties of the red cell membrane in relation to molecular structure and genetic defects. *Annual Review of Biophysics and Biomolecular Structure* **23**: 787-818.

Morgan, C.L., Newman, D.J., Cohen, S.B.A., Lowe, P. and Price, C.P. (1998) Real-time analysis of cell surface HLA class I interactions. *Biosensors and Bioelectronics*, **13**, 1099-1105.

Morris, M.B. and Lux, S.E. (1995) Characterization of the binary interaction between human erythrocyte protein 4.1 and actin. *European Journal of Biochemistry*, **231**, 644-650.

Murray, M.C. and Perkins, M.E. (1989) Phosphorylation of erythrocyte membrane and cytoskeleton proteins in cells infected with *Plasmodium falciparum*. *Molecular and Biochemical Parasitology*, **34**, 229-236.

Nacer, A., Berry, L., Slomianny, C. and Mattei, D. (2001) *Plasmodium falciparum* signal sequences: simply sequences or special signals? *International Journal for Parasitology*, **31**, 1371-1379.

Nagao, E., Kaneko, O. and Dvorak, J.A. (2000) *Plasmodium falciparum*-infected erythrocytes: qualitative and quantitative analyses of parasite-induced knobs by atomic force microscopy. *Journal of Structural Biology*, **130**, 34-44.

Nagel, R.L. and Roth, E.F., Jr. (1989) Malaria and red cell genetic defects. *Blood*, **74**, 1213-1221.

Nagel, R.L. (1990) Innate resistance to malaria: the intraerythrocytic cycle. *Blood Cells*, **16**, 321-339.

Nakashima, K. and Beutler, E. (1979) Comparison of structure and function of human erythrocyte and human muscle actin. *Proceedings of the National Academy of Sciences USA*, **76**, 935-938.

Nash, G.B., O'Brien, E., Gordon-Smith, E.C. and Dormandy, J.A. (1989) Abnormalities in the mechanical properties of red blood cells caused by *Plasmodium falciparum*. *Blood*, **74**, 855-861.

Nash, G.B., Cooke, B.M., Carlson, J. and Wahlgren, M. (1992) Rheological properties of rosettes formed by red blood cells parasitized by *Plasmodium falciparum*. *British Journal of Haematology*, **82**, 757-763.

Nigg, E.A., Bron, C., Girardet, M. and Cherry, R.J. (1980) Band 3-glycophorin A association in erythrocyte membrane demonstrated by combining protein diffusion measurements with antibody-induced cross-linking. *Biochemistry*, **19**, 1887-1893.

Nunomura, W., Takakuwa, Y., Tokimitsu, R., Krauss, S.W., Kawashima, M. and Mohandas, N. (1997) Regulation of CD44-protein 4.1 interaction by Ca^{2+} and calmodulin. Implications for modulation of CD44-ankyrin interaction. *The Journal Biological Chemistry*, **272**, 30322-30328.

Nunomura, W., Takakuwa, Y., Parra, M., Conboy, J. and Mohandas, N. (2000a) Regulation of protein 4.1R, p55, and glycophorin C ternary complex in human erythrocyte membrane. *The Journal of Biological Chemistry*, **275**, 24540-24546.

Nunomura, W., Takakuwa, Y., Parra, M., Conboy, J.G. and Mohandas, N. (2000b) Ca^{2+}-dependent and Ca^{2+}-independent calmodulin binding sites in erythrocyte protein 4.1. Implications for regulation of protein 4.1 interactions with transmembrane proteins. *The Journal of Biological Chemistry*, **275**, 6360-6367.

Oh, S.S., Chishti, A.H., Palek, J. and Liu, S.C. (1997) Erythrocyte membrane alterations in *Plasmodium falciparum* malaria sequestration. *Current Opinion in Hematology*, **4**, 148-154.

Oh, S.S., Voigt, S., Fisher, D., Yi, S.J., LeRoy, P.J., Derick, L.H., Liu, S. and Chishti, A.H. (2000) *Plasmodium falciparum* erythrocyte membrane protein 1 is anchored to the actin-spectrin junction and knob-associated histidine-rich protein in the erythrocyte skeleton. *Molecular and Biochemical Parasitology*, **108**, 237-247.

Ohanian, V., Wolfe, L.C., John, K.M., Pinder, J.C., Lux, S.E. and Gratzer, W.B. (1984) Analysis of the ternary interaction of the red cell membrane skeletal proteins spectrin, actin, and 4.1. *Biochemistry*, **23**, 4416-4420.

Ohanian, V. and Gratzer, W. (1984) Preparation of red-cell-membrane cytoskeletal constituents and characterisation of protein 4.1. *European Journal of Biochemistry*, **144**, 375-379.

Pasloske, B.L., Baruch, D.I., van Schravendijk, M.R., Handunnetti, S.M., Aikawa, M., Fujioka, H., Taraschi, T.F., Gormley, J.A. and Howard, R.J. (1993) Cloning and characterization of a *Plasmodium falciparum* gene encoding a novel high-molecular weight host membrane-associated protein, PfEMP3. *Molecular and Biochemical Parasitology*, **59**, 59-72.

Pasloske, B.L., Baruch, D.I., Ma, C., Taraschi, T.F., Gormley, J.A. and Howard, R.J. (1994) PfEMP3 and HRP1: co-expressed genes localized to chromosome 2 of *Plasmodium falciparum*. *Gene*, **144**, 131-136.

Pasternack, G.R., Anderson, R.A., Leto, T.L. and Marchesi, V.T. (1985) Interactions between protein 4.1 and band 3. An alternative binding site for an element of the membrane skeleton. *The Journal of Biological Chemistry*, **260**, 3676-3683.

Patel, S.S., Mehlotra, R.K., Kastens, W., Mgone, C.S., Kazura, J.W. and Zimmerman, P.A. (2001) The association of the glycophorin C exon 3 deletion with ovalocytosis and malaria susceptibility in the Wosera, Papua New Guinea. *Blood*, **98**, 3489-3491.

Pekrun, A., Pinder, J.C., Morris, S.A. and Gratzer, W.B. (1989) Composition of the ternary protein complex of the red cell membrane cytoskeleton. *European Journal of Biochemistry*, **182**, 713-717.

Petersen, C., Nelson, R., Magowan, C., Wollish, W., Jensen, J. and Leech, J. (1989) The mature erythrocyte surface antigen of *Plasmodium falciparum* is not required for knobs or cytoadherence. *Molecular and Biochemical Parasitology*, **36**, 61-65.

Pinder, J.C. and Gratzer, W.B. (1983) Structural and dynamic states of actin in the erythrocyte. *Journal of Cell Biology*, **96**, 768-775.

Platt, O.S., Lux, S.E. and Falcone, J.F. (1993) A highly conserved region of human erythrocyte ankyrin contains the capacity to bind spectrin. *The Journal of Biological Chemistry*, **268**, 24421-24426.

Pongponratn, E., Riganti, M., Punpoowong, B. and Aikawa, M. (1991) Microvascular sequestration of parasitized erythrocytes in human falciparum malaria: a pathological study. *The American Journal of Tropical Medicine and Hygiene*, **44**, 168-175.

Ralston, G., Dunbar, J. and White, M. (1977) The temperature-dependent dissociation of spectrin. *Biochimica et Biophysica Acta*, **491**, 345-348.

Raphael, P., Takakuwa, Y., Manno, S., Liu, S.C., Chishti, A.H. and Hanspal, M. (2000) A cysteine protease activity from *Plasmodium falciparum* cleaves human erythrocyte ankyrin. *Molecular and Biochemical Parasitology*, **110**, 259-272.

Raventos-Suarez, C., Kaul, D.K., Macaluso, F. and Nagel, R.L. (1985) Membrane knobs are required for the microcirculatory obstruction induced by *Plasmodium falciparum*-infected erythrocytes. *Proceedings of the National Academy of Sciences USA*, **82**, 3829-3833.

Reed, M.B., Caruana, S.R., Batchelor, A.H., Thompson, J.K., Crabb, B.S. and Cowman, A.F. (2000) Targeted disruption of an erythrocyte binding antigen in *Plasmodium falciparum* is associated with a switch toward a sialic acid-independent pathway of invasion. *Proceedings of the National Academy of Sciences USA*, **97**, 7509-7514.

Reeder, J.C., Cowman, A.F., Davern, K.M., Beeson, J.G., Thompson, J.K., Rogerson, S.J. and Brown, G.V. (1999) The adhesion of *Plasmodium falciparum*-infected erythrocytes to chondroitin sulfate A is mediated by *P. falciparum* erythrocyte membrane protein 1. *Proceedings of the National Academy of Sciences USA*, **96**, 5198-5202.

Ringwald, P., Peyron, F., Lepers, J.P., Rabarison, P., Rakotomalala, C., Razanamparany, M., Rabodonirina, M., Roux, J. and Le Bras, J. (1993) Parasite virulence factors during falciparum malaria: rosetting, cytoadherence, and modulation of cytoadherence by cytokines. *Infection and Immunity*, **61**, 5198-5204.

Roberts, D.J., Pain, A., Kai, O., Kortok, M. and Marsh, K. (2000) Autoagglutination of malaria-infected red blood cells and malaria severity. *Lancet*, **355**, 1427-1428.

Rosenthal, P.J. (2002) Hydrolysis of erythrocyte proteins by proteases of malaria parasites. *Current Opinion in Hematology*, **9**, 140-145.

Rowe, A., Berendt, A.R., Marsh, K. and Newbold, C.I. (1994) *Plasmodium falciparum*: a family of sulphated glycoconjugates disrupts erythrocyte rosettes. *Experimental Parasitology*, **79**, 506-516.

Rowe, A., Obeiro, J., Newbold, C.I. and Marsh, K. (1995) *Plasmodium falciparum* rosetting is associated with malaria severity in Kenya. *Infection and Immunity*, **63**, 2323-2326.

Rowe, J.A., Moulds, J.M., Newbold, C.I. and Miller, L.H. (1997) *P. falciparum* rosetting mediated by a parasite-variant erythrocyte membrane protein and complement-receptor 1. *Nature*, **388**, 292-295.

Rubio, J.P., Thompson, J.K. and Cowman, A.F. (1996) The var genes of *Plasmodium falciparum* are located in the subtelomeric region of most chromosomes. *The EMBO Journal*, **15**, 4069-4077.

Ruff, P., Speicher, D.W. and Husain-Chishti, A. (1991) Molecular identification of a major palmitoylated erythrocyte membrane protein containing the *src* homology 3 motif. *Proceedings of the National Academy of Sciences USA*, **88**, 6595-6599.

Rybicki, A.C., Musto, S. and Schwartz, R.S. (1995a) Decreased content of protein 4.2 in ankyrin-deficient normoblastosis (nb/nb) mouse red blood cells: evidence for ankyrin enhancement of protein 4.2 membrane binding. *Blood*, **86**, 3583-3589.

Rybicki, A.C., Musto, S. and Schwartz, R.S. (1995b) Identification of a band-3 binding site near the N-terminus of erythrocyte membrane protein 4.2. *Biochemical Journal*, **15**, 677-681.

Rybicki, A.C., Schwartz, R.S., Hustedt, E.J. and Cobb, C.E. (1996) Increase rotational mobility and extractability of band 3 from protein 4.2-deficient erythrocyte membranes: evidence of a role for protein 4.2 in strengthening the band 3-cytoskelton linkage. *Blood*, **88**, 2745-2753.

Sahr, K.E., Laurila, P., Kotula, L., Scarpa, A.L., Coupal, E., Leto, T.L., Linnenbach, A.J., Winkelmann, J.C., Speicher, D.W., Marchesi, V.T., Curtis, P.J. and Forget, B.G. (1990) The Complete cDNA and Polypeptide Sequences of Human Erythroid α- spectrin. *The Journal of Biological Chemistry*, **265**, 4434-4443.

Sambrook, J., Fritsch, E.F. and Maniatis, T. (1989) *Molecular Cloning: A Laboratory Manual*. Cold Springs Harbor Press, Cold Springs Harbor, New York.

Sanderson, A., Walliker, D. and Molez, J.F. (1981) Enzyme typing of *Plasmodium falciparum* from African and some other Old World countries. *Transactions of the Royal Society Tropical Medicine and Hygiene*, **75**, 263-267.

Schischmanoff, P.O., Winardi, R., Discher, D.E., Parra, M.K., Bicknese, S.E., Witkowska, H.E., Conboy, J.G. and Mohandas, N. (1995) Defining of the minimal domain of protein 4.1 involved in spectrin-actin binding. *The Journal of Biological Chemistry*, **270**, 21243-21250.

Schulman, S., Roth, E.F., Jr., Cheng, B., Rybicki, A.C., Sussman, II, Wong, M., Wang, W., Ranney, H.M., Nagel, R.L. and Schwartz, R.S. (1990) Growth of *Plasmodium falciparum* in human erythrocytes containing abnormal membrane proteins. *Proceedings of the National Academy of Sciences USA*, **87**, 7339-7343.

Serjeanson, S.W., White, B.S., Bhatia, K. and Trent, R.J. (1994) A 3.5 kb deletion in the glycophorin C gene accounts for the Gerbich-negative blood group in Melanesians. *Immunology and Cell Biology*, **72**, 23-27.

Shahbakhti, F. and Gratzer, W.B. (1986) Analysis of the self-association of human red cell spectrin. *Biochemistry*, **25**, 5969-5975.

Sharma, Y.D. and Kilejian, A. (1987) Structure of the knob protein (KP) gene of *Plasmodium falciparum*. *Molecular and Biochemical Parasitology*, **26**, 11-16.

Shenai, B.R., Sijwali, P.S., Singh, A. and Rosenthal, P.J. (2000) Characterization of native and recombinant falcipain-2, a principal trophozoite cysteine protease and essential hemoglobinase of *Plasmodium falciparum*. *The Journal of Biological Chemistry*, **275**, 29000-29010.

Shotton, D.M., Burke, B.E. and Branton, D. (1979) The molecular structure of human erythrocyte spectrin. Biophysical and electron microscopic studies. *Journal of Molecular Biology*, **131**, 303-329.

Siegel, D.L. and Branton, D. (1985) Partial Purification and Characterization of an Actin-bundling Protein, Band 4.9, from Human Erythrocytes. *Journal of Cell Biology*, **100**, 775-785.

Sim, B.K., Chitnis, C.E., Wasniowska, K., Hadley, T.J. and Miller, L.H. (1994) Receptor and ligand domains for invasion of erythrocytes by *Plasmodium falciparum*. *Science*, **264**, 1941-1944.

Smith, J.D., Chitnis, C.E., Craig, A.G., Roberts, D.J., Hudson-Taylor, D.E., Peterson, D.S., Pinches, R., Newbold, C.I. and Miller, L.H. (1995) Switches in expression of *Plasmodium falciparum var* genes correlate with changes in antigenic and cytoadherent phenotypes of infected erythrocytes. *Cell*, **82**, 101-110.

Smith, J.D., Kyes, S., Craig, A.G., Fagan, T., Hudson-Taylor, D., Miller, L.H., Baruch, D.I. and Newbold, C.I. (1998) Analysis of adhesive domains from the A4VAR *Plasmodium falciparum* erythrocyte membrane protein-1 identifies a CD36 binding domain. *Molecular and Biochemical Parasitology*, **97**, 133-148.

Somner, E.A., Black, J. and Pasvol, G. (2000) Multiple human serum components act as bridging molecules in rosette formation by *Plasmodium falciparum*-infected erythrocytes. *Blood*, **95**, 674-682.

Speicher, D.W. and Marchesi, V.T. (1984) Erythrocyte spectrin is comprised of many homologous triple helical segments. *Nature*, **311**, 177-180.

Speicher, D.W., Weglarz, L. and DeSilva, T.M. (1992) Properties of human red cell spectrin heterodimer (side-to-side) assembly and identification of an essential nucleation site. *The Journal of Biological Chemistry*, **267**, 14775-14782.

Speicher, D.W., DeSilva, T.M., Speicher, K.D., Ursitti, J.A., Hembach, P. and Weglarz, L. (1993) Location of the Human Red Cell Spectrin Tetramer Binding Site and Detection of a Related "Closed" Hairpin Loop Dimer using Proteolytic Footprinting. *The Journal of Biological Chemistry*, **268**, 4227-4235.

Spycher, C., Klonis, N., Spielmann, T., Kump, E., Steiger, S., Tilley, L. and Beck, H.P. (2003) MAHRP-1, a novel *Plasmodium falciparum* histidine-rich protein, binds ferriprotoporphyrin IX and localises to the Maurer's clefts. *The Journal of Biological Chemistry*, **in press**.

Steck, T.L. and Kant, J.A. (1974) Preparation of impermeable ghosts and inside-out vesicles from human erythrocyte membranes. *Methods in Enzymology*, **31**, 172-180.

Steck, T.L. (1978) The band 3 protein of the human red cell membrane: a review. *Journal of Supramolecular Structure*, **8**, 311-324.

Su, X.Z., Heatwole, V.M., Wertheimer, S.P., Guinet, F., Herrfeldt, J.A., Peterson, D.S., Ravetch, J.A. and Wellems, T.E. (1995) The large diverse gene family *var* encodes proteins involved in cytoadherence and antigenic variation of *Plasmodium falciparum*-infected erythrocytes. *Cell*, **82**, 89-100.

Subrahmanyam, G., Bertics, P.J. and Anderson, R.A. (1991) Phosphorylation of protein 4.1 on tyrosine-418 modulates its function *in vitro*. *Proceedings of the National Academy of Sciences USA*, **88**, 5222-5226.

Tanaka, T., Kadowaki, K., Lazarides, E. and Sobue, K. (1991) Ca^{2+}-dependent regulation of the spectrin/actin interaction by calmodulin and protein 4.1. *The Journal of Biological Chemistry*, **266**, 1134-1140.

Taraschi, T.F., Trelka, D., Martinez, S., Schneider, T. and O'Donnell, M.E. (2001) Vesicle-mediated trafficking of parasite proteins to the host cell cytosol and erythrocyte surface membrane in *Plasmodium falciparum* infected erythrocytes. *International Journal for Parasitology*, **31**, 1381-1391.

Tellez, M., Matesanz, F. and Alcina, A. (2003) The C-terminal domain of the *Plasmodium falciparum* acyl-CoA sythetases PfACS1 and PfACS3 functions as ligand for ankyrin. *Molecular and Biochemical Parasitology*, **129**, 191-198.

Thevenin, B.J. and Low, P.S. (1990) Kinetics and regulation of the ankyrin-band 3 interaction of the human red blood cell membrane. *The Journal of Biological Chemistry*, **265**, 16166-16172.

Thevenin, B.J., Periasamy, N., Shohet, S.B. and Verkman, A.S. (1994) Segmental dynamics of the cytoplasmic domain of erythrocyte band 3 determined by time-resolved fluorescence anisotrophy: Sensitivity to pH and ligand binding. *Proceedings of the National Academy of Sciences USA*, **91**, 1741-1745.

Tilney, L.G. and Detmers, P. (1975) Actin in erythrocyte ghosts and its association with spectrin. Evidence for a nonfilamentous form of these two molecules *in situ*. *Journal of Cell Biology*, **66**, 508-520.

Trager, W., Rudzinska, M.A. and Bradbury, P.C. (1966) The fine structure of *Plasmodium falciparum* and its host erythrocytes in natural malarial infections in man. *Bulletin of the World Health Organization*, **35**, 883-885.

Trager, W. and Jensen, J. (1976) Human malaria parasites in continuous culture. *Science*, **193**, 673-675.

Trager, W. and Jensen, J.B. (1978) Cultivation of malarial parasites. *Nature*, **273**, 621-622.

Trenholme, K.R., Gardiner, D.L., Holt, D.C., Thomas, E.A., Cowman, A.F. and Kemp, D.J. (2000) *clag9*: A cytoadherence gene in *Plasmodium falciparum* essential for binding of parasitized erythrocytes to CD36. *Proceedings of the National Academy of Sciences USA*, **97**, 4029-4033.

Treutiger, C.J., Scholander, C., Carlson, J., McAdam, K.P., Raynes, J.G., Falksveden, L. and Wahlgren, M. (1999) Rouleaux-forming serum proteins are involved in the rosetting of *Plasmodium falciparum*-infected erythrocytes. *Experimental Parasitology*, **93**, 215-224.

Trigg, P.I. and Kondrachine, A.V. (1998) The Current Global Malaria Situation. In Sherman, I.W. (ed.), *Malaria. Parasite Biology, Pathogenesis and Protection*. ASM Press, Washington.

Triglia, T., Stahl, H.D., Crewther, P.E., Scanlon, D., Brown, G.V., Anders, R.F. and Kemp, D.J. (1987) The complete sequence of the gene for the knob-associated histidine-rich protein from *Plasmodium falciparum*. *The EMBO Journal*, **6**, 1413-1419.

Tse, W.T. and Lux, S.E. (1999) Red blood cell membrane disorders. *British Journal of Haematology*, **104**, 2-13.

Tyler, J.M., Reinhardt, B.N. and Branton, D. (1980) Associations of Erythrocyte Membrane Proteins. Binding of purified bands 2.1 and 4.1 to spectrin. *The Journal of Biological Chemistry*, **255**, 7034-7039.

Udomsangpetch, R., Carlsson, J., Wahlin, B., Holmquist, G., Ozaki, L.S., Scherf, A., Mattei, D., Mercereau-Puijalon, O., Uni, S., Aikawa, M. and et al. (1989a) Reactivity of the human monoclonal antibody 33G2 with repeated sequences of three distinct *Plasmodium falciparum* antigens. *The Journal of Immunology*, **142**, 3620-3626.

Udomsangpetch, R., Wahlin, B., Carlson, J., Berzins, K., Torii, M., Aikawa, M., Perlmann, P. and Wahlgren, M. (1989b) *Plasmodium falciparum*-infected erythrocytes form spontaneous erythrocyte rosettes. *The Journal of Experimental Medicine*, **169**, 1835-1840.

Udomsangpetch, R., Brown, A.E., Smith, C.D. and Webster, H.K. (1991) Rosette formation by *Plasmodium coatneyi*-infected red blood cells. *The American Journal of Tropical Medicine and Hygiene*, **44**, 399-401.

Udomsangpetch, R., Webster, H.K., Pattanapanyasat, K., Pitchayangkul, S. and Thaithong, S. (1992) Cytoadherence characteristics of rosette-forming *Plasmodium falciparum*. *Infection and Immunity*, **60**, 4483-4490.

Udomsangpetch, R., Thanikkul, K., Pukrittayakamee, S. and White, N.J. (1995) Rosette Formation By *Plasmodium vivax*. *Transactions of the Royal Society of Tropical Medicine & Hygiene*, **89**, 635-637.

Ungewickell, E. and Gratzer, W. (1978) Self-association of human spectrin. A thermodynamic and kinetic study. *European Journal of Biochemistry*, **88**, 379-385.

Ungewickell, E., Bennett, P.M., Calvert, R., Ohanian, V. and Gratzer, W.B. (1979) *In vitro* formation of a complex between cytoskeletal proteins of the human erythrocyte. *Nature*, **280**, 811-814.

Ursitti, J.A. and Fowler, V.M. (1994) Immunolocalization of tropomodulin, tropomyosin and actin in spread human erythrocyte skeletons. *Journal of Cell Science*, **107**, 1633-1639.

Vertessy, B.G. and Steck, T.L. (1989) Elasticity of the human red cell membrane skeleton. Effects of temperature and denaturants. *Biophysical Journal*, **55**, 255-262.

Viel, A. and Branton, D. (1994) Interchain binding at the tail end of the Drosophila spectrin molecule. *Proceedings of the National Academy of Sciences USA*, **91**, 10839-10843.

Voigt, S., Hanspal, M., LeRoy, P.J., Zhao, P.S., Oh, S.S., Chishti, A.H. and Liu, S.C. (2000) The cytoadherence ligand *Plasmodium falciparum* erythrocyte membrane protein 1 (PfEMP1) binds to the *P. falciparum* knob-associated histidine- rich protein (KAHRP) by electrostatic interactions. *Molecular and Biochemical Parasitology*, **110**, 423-428.

von Ruckmann, B., Jons, T., Dolle, F., Drenckhahn, D. and Schubert, D. (1997) Cytoskeleton-membrane connections in the human erythrocyte membrane: band 4.1 binds to tetrameric band 3 protein. *Biochimica et Biophysica Acta*, **1325**, 226-234.

Walder, J.A., Chatterjee, R., Steck, T.L., Low, P.S., Musso, G.F., Kaiser, E.T., Rogers, P.H. and Arnone, A. (1984) The interaction of hemoglobin with the cytoplasmic domain of band 3 of the human erythrocyte membrane. *The Journal of Biological Chemistry*, **259**, 10238-10246.

Waller, K.L., Cooke, B.M., Nunomura, W., Mohandas, N. and Coppel, R.L. (1999) Mapping the binding domains involved in the interaction between the *Plasmodium falciparum* knob-associated histidine-rich protein (KAHRP) and the cytoadherence ligand *P. falciparum* erythrocyte membrane protein 1 (PfEMP1). *The Journal of Biological Chemistry*, **274**, 23808-23813.

Waller, K.L. (2000) Investigation of Protein-Protein Interactions at the Cytoskeleton of *Plasmodium falciparum*-infected Red Blood Cells. Department of Microbiology. Monash University, Melbourne.

Waller, K.L., Nunomura, W., Cooke, B.M., Mohandas, N. and Coppel, R.L. (2002) Mapping the domains of the cytoadherence ligand *Plasmodium falciparum* erythrocyte membrane protein 1 (PfEMP1) that bind to the knob-associated histidine-rich protein (KAHRP). *Molecular and Biochemical Parasitology*, **119**, 125-129.

Waller, K.L., Nunomura, W., An, X., Cooke, B., Mohandas, N. and Coppel, R.L. (2003) The mature parasite-infected erythrocyte surface antigen (MESA) of *Plasmodium falciparum* binds to the 30 kDa domain of protein 4.1 in malaria-infected red blood cells. *Blood*, **102**, 1911-1914.

Walliker, D., Quakyi, I.A., Wellems, T.E., McCutchan, T.F., Szarfman, A., London, W.T., Corcoran, L.M., Burkot, T.R. and Carter, R. (1987) Genetic analysis of the human malaria parasite *Plasmodium falciparum*. *Science*, **236**, 1661-1666.

Walsh, M., Lutz, R.J., Cotter, T.G. and O'Connor, R. (2002) Erythrocyte survival is promoted by plasma and suppressed by a Bak-derived BH3 peptide that interacts with membrane-associated Bcl-X_L. *Blood*, **99**, 3439-3448.

Waseem, A. and Palfrey, H.C. (1988) Erythrocyte adducin. Comparison of the α- and β-subunits and multiple-site phosphorylation by protein kinase C and cAMP-dependent protein kinase. *European Journal of Biochemistry*, **178**, 563-573.

Waterkeyn, J.G., Wickham, M.E., Davern, K.M., Cooke, B.M., Coppel, R.L., Reeder, J.C., Culvenor, J.G., Waller, R.F. and Cowman, A.F. (2000) Targeted mutagenesis of *Plasmodium falciparum* erythrocyte membrane protein 3 (PfEMP3) disrupts cytoadherence of malaria-infected red blood cells. *The EMBO Journal*, **19**, 2813-2823.

Waterkeyn, J.G., Cowman, A.F. and Cooke, B.M. (2001) *Plasmodium falciparum*: gelatin enrichment selects for parasites with full-length chromosome 2. Implications for cytoadhesion assays. *Experimental Parasitology*, **97**, 115-118.**Watts, H.J., Lowe, C.R. and Pollard-Knight, D.V.** (1994) *Analytical Chemistry*, **66**, 2465-2470.

Weber, A., Pennise, C.R., Babcock, G.G. and Fowler, V.M. (1994) Tropomodulin caps the pointed ends of actin filaments. *Journal of Cell Biology*, **127**, 1627-1635.

White, N.J. and Ho, M. (1992) The pathophysiology of malaria. *Advances in Parasitology*, **31**, 83-173.

Wickert, H., Rohrbach, P., Scherer, S.J., Krohne, G. and Lanzer, M. (2003) A putative Sec23 homologue of *Plasmodium falciparum* is located in Maurer's clefts. *Molecular and Biochemical Parasitology*, **129**, 209-213.

Wickham, M.E., Rug, M., Ralph, S.A., Klonis, N., McFadden, G.I., Tilley, L. and Cowman, A.F. (2001) Trafficking and assembly of the cytoadherence complex in *Plasmodium falciparum*-infected human erythrocytes. *The EMBO Journal*, **20**, 5636-5649.

Wiesner, J., Mattei, D., Scherf, A. and Lanzer, M. (1998) Biology of Giant Proteins of *Plasmodium*: Resolution of Polyacrylamide-Agarose Composite Gels. *Parasitology Today*, **14**, 38-40.

Willardson, B.M., Thevenin, B.J., Harrison, M.L., Kuster, W.M., Benson, M.D. and Low, P.S. (1989) Localization of the ankyrin-binding site on erythrocyte membrane protein, band 3. *The Journal of Biological Chemistry*, **264**, 15893-15899.

Winkelmann, J.C., Chang, J.G., Tse, W.T., Scarpa, A.L., Marchesi, V.T. and Forget, B.G. (1990) Full-length Sequence of the cDNA for Human Erythroid b-Spectrin. *The Journal of Biological Chemistry*, **265**, 11827-11832.

Winkelmann, J.C. and Forget, B.G. (1993) Erythroid and nonerythroid spectrins. *Blood*, **81**, 3173-3185.

Winograd, E. and Sherman, I.W. (1989) Characterization of a modified red cell membrane protein expressed on erythrocytes infected with the human malaria parasite *Plasmodium falciparum*: possible role as a cytoadherent mediating protein. *Journal of Cell Biology*, **108**, 23-30.

Winograd, E., Hume, D. and Branton, D. (1991) Phasing the conformational unit of spectrin. *Proceedings of the National Academy of Sciences USA*, **88**, 10788-10791.

Winstanley, P.A. (2000) Chemotherapy for falciparum malaria: the armoury, the problems and the prospects. *Parasitology Today*, **16**, 146-153.

Wiser, M.F., Lanners, H.N., Bafford, R.A. and Favaloro, J.M. (1997) A novel alternate secretory pathway for the export of *Plasmodium* proteins into the host erythrocyte. *Proceedings of the National Academy of Sciences USA*, **94**, 9108-9113.

Wiser, M.F., Lanners, H.N. and Bafford, R.A. (1999) Export of *Plasmodium* proteins via a novel secretory pathway. *Parasitology Today*, **15**, 194-198.

Workman, R.F. and Low, P.S. (1998) Biochemical analysis of potential sites for protein 4.1-mediated anchoring of the spectrin-actin skeleton to the erythrocyte membrane. *The Journal of Biological Chemistry*, **273**, 6171-6176.

Wunsch, S., Sanchez, C., Gekle, M., Kersting, U., Fischer, K., Horrocks, P. and Lanzer, M. (1997) A method to measure the cytoplasmic pH of single, living *Plasmodium falciparum* parasites. *Behring Institute Mitteilungen*, **99**, 44-50.

Yan, Y., Winograd, E., Viel, A., Cronin, T., Harrison, S.C. and Branton, D. (1993) Crystal structure of the repetitive segments of spectrin. *Science*, **262**, 2027-2030.

Yanisch-Perron, C., Vieira, J. and Messing, J. (1985) Improved M13 phage cloning vectors and host strains: nucleotide sequences of the M13mp18 and pUC19 vectors. *Gene*, **33**, 103-119.

Young, M.T., Beckman, R., Toye, A.M. and Tanner, M.J.A. (2000) Red-cell glycophorin A-band 3 interactions associated with the movement of band 3 to the cell surface. *Biochemical Journal*, **350**, 53-60.

Young, M.T. and Tanner, M.J.A. (2003) Distinct regions of human glycophorin A enhance human red cell anion exchanger (band 3; AE1) transport function and surface trafficking. *The Journal of Biological Chemistry*, **278**, 32954-32961.

Yu, J. and Goodman, S.R. (1979) Syndeins: the spectrin-binding protein(s) of the human erythrocyte membrane. *Proceedings of the National Academy of Sciences USA*, **76**, 2340-2344.

Zhang, D., Kiyatkin, A., Bolin, J.T. and Low, P.S. (2000) Crystallographic structure and functional interpretation of the cytoplasmic domain of erythrocyte membrane band 3. *Blood*, **96**, 2925-2933.